

Cationic surfactant based coatings for protein separations and control of
electroosmotic flow in capillary electrophoresis

by

Mahmoud Farouk Mahmoud Bahnasy

A thesis submitted in partial fulfillment of the requirements for the degree of

Doctor of Philosophy

Department of Chemistry
University of Alberta

© Mahmoud Farouk Mahmoud Bahnasy, 2014

Abstract

Capillary electrophoresis (CE) is a fast and high efficiency separation technique based on the differential migration of charged species in an electric field. CE is useful for the separation of a wide range of analytes from small ions to large biomolecules. However, CE separations of proteins are challenging due to the adsorption of protein onto the capillary silica surface. Capillary coatings are the most common way to minimize this adsorption. This thesis focuses on the use of two-tailed cationic surfactant based coatings as means of preventing protein adsorption.

Factors affecting the stability of two-tailed cationic surfactant coatings have been investigated. The impact of small i.d. capillaries (5-25) μm on enhanced stability of surfactant bilayer cationic coatings and on the efficiency of separation of basic proteins was studied. Using a dioctadecyldimethylammonium bromide (DODAB) coated 5 μm i.d capillary, exceptional short term stability (210 consecutive runs) and long term stability (300 runs over a 30 day period) were achieved. The average separation efficiency of four basic model proteins was 1.4-2 millions plates/m. DODAB coatings were stable over a pH range of 3-8 as demonstrated by strong anodic magnitude of electroosmotic flow (EOF) and good EOF reproducibility. Surprisingly, at $\text{pH} \geq 9$, EOF became less anodic and even became suppressed cathodic. The reason is unclear. Chemical degradation of DODAB at high pH was excluded. Increased vesicle size at high pH and/or accelerated desorption may be involved.

A surfactant bilayer/diblock copolymer coating was developed to tune the EOF and prevent protein adsorption. The coating consisted of a DODAB bilayer which served as a strong anchor to the capillary wall and polyoxyethylene (POE) stearate to suppress the EOF. The coating has been applied successfully to the capillary zone electrophoretic separation of basic, acidic and histone proteins, and to capillary isoelectric focusing. The ability to tune the EOF enabled both single-step capillary isoelectric focusing (cIEF) and two-step cIEF to be performed. A strongly suppressed EOF coating provided a linear pH gradient and allowed for the separation of two hemoglobin variants HbA and HbS. Factors affecting the stability and EOF of the developed surfactant bilayer/diblock copolymer coating were studied. The magnitude of the anodic EOF can be tuned by varying the hydrophilic block POE chain length. The hydrophobic block of the diblock copolymer accounts for stability of the coating, with a longer (stearate) block giving the best stability. The sequential coating provided a stable and suppressed EOF over a broad range of pH 3.0-11.5. The EOF was suppressed and anodic at low pH. As the pH increases, the EOF was still suppressed but became cathodic. This reversal in EOF of the sequential coating is consistent with the reported applications of the sequential coating, and the behavior of the underlying DODAB bilayer. The sequential coating shows a good stability in buffers containing up to 20% v/v acetonitrile.

Preface

This dissertation is submitted for the degree of Doctor of Philosophy at the University of Alberta. All the work was conducted in the Department of Chemistry, University of Alberta under the supervision of Prof. Charles A. Lucy. The thesis consists of seven chapters. Chapter One is an introduction. I am a co-author of the work in Chapters Two and Three. The work in Chapters Four, Five and Six is my original work. Chapter Seven represents a summary of the work in the thesis and possible future projects.

Chapter Two of this thesis has been published as Makedonka D. Gulcev, Teague McGinitie, Mahmoud F. Bahnasy and Charles A. Lucy, "Surfactant bilayer coatings in narrow-bore capillaries in capillary electrophoresis ", *Analyst*, 135 (10), 2688-2693, 2010. Makedonka D. Gulcev was a former PhD student who initiated the project. She was involved in concept formation, experimental work with DDAB-coated capillaries and writing of the manuscript. Teague McGinitie was an undergraduate student who performed some preliminary experiments. I did the experimental work for the short and long-term stability studies of DODAB-coated capillaries and the separation of the neurotransmitters. I was in charge of addressing reviewers' comment after submission of the manuscript. Charles A. Lucy was the supervisory author and was involved with concept formation and manuscript composition.

Chapter Three of this thesis has been published as Amy M. MacDonald, Mahmoud F. Bahnasy and Charles A. Lucy, "A Modified Supported Bilayer/Diblock Copolymer – Working Towards a Tunable Coating for Capillary

Electrophoresis", *J. Chromatogr. A*, 1218 (1), 178-184, 2011. Amy M. MacDonald was a former PhD student who initiated the project. Amy did part of the experimental work and graduated in 2008 before finishing the project. I completed the experimental work. I was in charge of writing the manuscript and addressing reviewers' comments. Charles A. Lucy was the supervisory author.

Chapter Four of this thesis has been published as Mahmoud F. Bahnasy and Charles A. Lucy, "A versatile semi-permanent coating for capillary isoelectric focusing", *J. Chromatogr. A*, 1267, 89-95, 2012. I was responsible for concept formation, did all experimental work, was in charge of manuscript composition, submission and addressing reviewers' comment under the supervision of Prof. Charles A. Lucy.

Chapter Five of this thesis is my original work and is currently unpublished. I was responsible for all areas of concept formation, data collection and analysis, as well as Chapter composition. Nathan R. Paisley, CHEM 299 and summer undergraduate student did part of the experimental work in Sections 5.3.1, 5.3.3 and 5.3.5 under my supervision.

Chapter Six of this thesis is my original work and is currently unpublished.

Acknowledgements

I would like to express my profound gratitude and sincere thanks to my supervisor Dr. Charles A. Lucy for his valuable supervision, continuous guidance, constructive suggestions and patience throughout my graduate career.

Thanks to Lucy group members for the informative discussions and friendly experience. Thanks to Dr. Donna Gulcev for her guidance and valuable technical advice during my first year of graduate studies. Thanks to the CE guys; Lei Pei and Bob Stanley for their help and enjoyable time in the lab. Special thanks to dear friends and labmates Dr. Mohammed Ibrahim and Dr. Farooq Wahab for their endless support.

I would like to thank to Kim Do from the electronics shop for her help with maintenance of CE instruments. Thanks to Dr. Mark Lies from Beckman Coulter for providing cIEF gel polymer solution and the pI Marker Kit.

This work was sponsored by the Natural Sciences and Engineering Research Council of Canada (NSERC) and the University of Alberta. The financial support of Queen Elizabeth II scholarship is highly appreciated. Thanks to Faculty of graduate studies, graduate student's association and CE in the Biotechnology & Pharmaceutical Industries symposium for travel grants which allowed my to attend conferences in Orlando and Arizona.

Finally, I would like to express my heart felt gratitude to my great parents and my wife for their encouragement and endless support.

Table of Contents

Chapter One: Introduction	1
1.1 History.....	1
1.2 Modes of Capillary Electrophoresis.....	2
1.2.1 Capillary Zone Electrophoresis (CZE).....	3
1.2.2 Electrokinetic Chromatography (EKC).....	3
1.2.3 Capillary Isoelectric Focusing (cIEF).....	4
1.2.4 Capillary Gel Electrophoresis (CGE).....	4
1.2.5 Capillary Isotachopheresis (CITP).....	5
1.2.6 Capillary electrochromatography (CEC).....	5
1.3 Fundamentals of CE.....	6
1.3.1 Instrumentation.....	6
1.3.2 Electroosmotic flow (EOF).....	10
1.3.3 Electrophoretic and apparent mobilities.....	16
1.4 Band broadening in CE.....	20
1.4.1 Longitudinal diffusion.....	22
1.4.2 Joule heating.....	24
1.4.3 Electromigration dispersion.....	25
1.4.4 Injector band broadening.....	27
1.4.5 Detector band broadening.....	28
1.4.6 Solute-wall interaction.....	30
1.5 Protein adsorption.....	31
1.5.1 Background.....	31
1.5.2 Monitoring protein adsorption.....	33
1.5.3 Preventing protein adsorption in CE.....	34
1.5.3.1 Surfactant coatings.....	36
1.6 Thesis Overview.....	42
1.7 References.....	43

Chapter Two: Surfactant bilayer coatings in narrow-bore capillaries in capillary electrophoresis.....	47
2.1 Introduction.....	47
2.2 Experimental.....	49
2.2.1 Apparatus.....	49
2.2.2 Chemicals.....	49
2.2.3 Surfactant Preparation.....	50
2.2.4 Coating Procedure.....	51
2.2.5 Protein Separations.....	51
2.2.6 Durability and Reproducibility of DODAB in 5 μm capillaries	52
2.2.7 Separation of Neurotransmitters.....	53
2.3 Results and Discussion.....	53
2.3.1 Effect of inner diameter (i.d.) on DDAB coating performance	54
2.3.2 DODAB coatings in narrow capillaries.....	61
2.3.3 Separation of neurotransmitters on a DODAB-coated 5 μm i.d. capillary.....	68
2.4 Conclusions.....	71
2.5 References.....	72
Chapter Three: A modified supported bilayer/diblock copolymer – working towards a tunable coating for capillary electrophoresis.....	75
3.1 Introduction.....	75
3.2 Experimental.....	79
3.2.1 Apparatus.....	79
3.2.2 Chemicals.....	79
3.2.3 Preparation of and coating with the surfactant/copolymer solution.....	80
3.2.4 EOF Measurements.....	81
3.2.5 Protein Separations.....	82
3.3 Results and Discussion.....	83
3.3.1 EOF of sequential DODAB/POE stearate coatings.....	84

3.3.2	Temporal coating studies.....	86
3.3.3	Adjustable EOF with DODAB/POE stearate coatings.....	92
3.3.4	Protein Separations.....	94
3.3.4.1	Separation of basic proteins.....	94
3.3.4.2	Histone Separations.....	97
3.3.4.3	Separation of acidic proteins.....	101
3.4	Conclusions.....	103
3.5	References.....	104
Chapter Four: A versatile semi-permanent sequential bilayer/diblock copolymer coating for capillary isoelectric focusing.....		107
4.1	Introduction.....	107
4.2	Experimental.....	111
4.2.1	Apparatus.....	111
4.2.2	Chemicals.....	112
4.2.3	Methods.....	112
4.3	Results and Discussion.....	114
4.3.1	Preliminary optimization of ampholyte concentration.....	115
4.3.2	Single-step cIEF.....	117
4.3.3	Two-step cIEF.....	127
4.3.4	Linearity of pH gradient.....	133
4.3.5	Separation of hemoglobin variants.....	136
4.4	Conclusions.....	139
4.5	References.....	140
Chapter Five: Polyoxyethylene diblock copolymer coatings for capillary electrophoresis.....		143
5.1	Introduction.....	143
5.2	Experimental.....	146
5.2.1	Apparatus.....	146
5.2.2	Chemicals.....	146

5.2.3	Buffer preparation.....	147
5.2.4	Coating procedure.....	147
5.2.5	Coating stability.....	148
5.3	Results and Discussion.....	149
5.3.1	Effect of the hydrophobic block.....	150
5.3.2	Effect of the hydrophilic block.....	152
5.3.3	Ionic retention characteristics of POE.....	155
5.3.4	Effect of pH on the coating performance.....	158
5.3.5	Stability of the coating under mixed aqueous-organic conditions.....	162
5.4	Conclusions.....	165
5.5	References.....	166

Chapter Six: Cationic surfactant bilayer capillary coatings under alkaline conditions.....	169	
6.1	Introduction.....	169
6.2	Experimental.....	171
6.2.1	Apparatus.....	171
6.2.2	Chemicals.....	172
6.2.3	Surfactant preparation and coating procedure.....	172
6.2.4	Coating stability.....	173
6.2.5	ESI-MS.....	173
6.2.6	Dynamic light scattering measurements.....	174
6.3	Results and Discussion.....	174
6.3.1	DODAB stability at pH 3-7.....	174
6.3.2	DODAB stability at pH ≥ 7.0	176
6.3.3	pH switching of DODAB coated capillaries.....	181
6.3.4	Alkaline reactions of DODAB.....	184
6.3.5	Aggregation behavior of DODAB under alkaline conditions....	187
6.3.6	Protein separation.....	190
6.4	Conclusions.....	193

6.5	References.....	194
	Chapter Seven: Summary and Future work.....	196
7.1	Summary.....	196
7.1.1	Chapter Two.....	196
7.1.2	Chapter Three.....	197
7.1.3	Chapter Four.....	198
7.1.4	Chapter Five.....	199
7.1.5	Chapter Six.....	200
7.2	Future work.....	201
7.2.1	Gemini cationic surfactants as capillary coatings.....	201
7.2.2	Capillary coatings for in-capillary derivatization.....	205
7.3	References.....	210
	Bibliography.....	211

List of Tables

Table 1.1	Physico-chemical properties of two-tailed cationic surfactants used as capillary coatings.....	39
Table 2.1	Migration time reproducibilities (% RSD) and protein efficiencies on various i.d. capillaries coated with 2 Mm DDAB.....	59
Table 3.1	EOF Mobility, Rate Constant and Correlation Coefficient for sequential DODAB then POE stearate coatings.....	91
Table 3.2	Efficiency ranges and EOF values for basic proteins separated on sequential 0.1 mM DODAB then POE 40 stearate coatings.....	96
Table 6.1	Buffers used to study pH stability of DODAB coated capillaries.....	177
Table 6.2	DODAB vesicle size behavior in water, NaOH and NaCl.....	189

List of Figures

Figure 1.1	Schematic of capillary electrophoresis instrumentation.....	7
Figure 1.2	Schematic of the electric double layer and the potential profile as a function of distance from the capillary wall.....	12
Figure 1.3	Comparison of EOF and pressure driven flow profiles and corresponding peak shapes.....	15
Figure 1.4	Migration order within a capillary under an applied electric field and the resultant electropherogram.....	19
Figure 1.5	Schematic of Electromigration Dispersion (EMD) as a result of mismatched conductivity between the sample zone and the buffer.....	26
Figure 1.6	Aggregate structures of (A) single-tailed surfactant and (B) two-tailed surfactant.....	38
Figure 1.7	Structure of two-tailed cationic surfactants used as capillary coatings.....	39
Figure 1.8	Separation of five basic proteins at pH 3 using (A) bare capillary; (B) CTAB-coated capillary; and (C) DDAB-coated capillary.....	40
Figure 2.1	Separation of cationic proteins on 25 μm i.d. capillary using 2 mM DDAB coating.....	56
Figure 2.2	Separation of cationic proteins on 10 μm i.d. capillary using 2 mM DDAB coating.....	57
Figure 2.3	Separation of cationic proteins on 5 μm i.d. capillary using 2 mM DDAB coating.....	58
Figure 2.4	Reproducibility Studies of 0.5 mM DODAB on a 5 μm i.d. capillary.....	63
Figure 2.5	Cationic protein reproducibility studies using 5 μm i.d. capillary coated with 0.5 mM DODAB.....	65
Figure 2.6	Cationic protein reproducibility studies using 10 μm i.d. capillary coated with 0.5 mM DODAB.....	67
Figure 2.7	Separation of neurotransmitters on 0.5 mM DODAB-coated 5 μm i.d. capillary.....	69
Figure 2.8	Separation of the neurotransmitters on a 5 μm bare capillary.....	70

Figure 3.1	Schematic of the A) mixed and B) sequential coating methods.....	77
Figure 3.2	EOF stability for mixed and sequential coating methods using 0.1 mM DODAB/POE 40 stearate.....	85
Figure 3.3	Effect of POE 8 stearate concentration on the intercalation rate into the DODAB bilayer.....	88
Figure 3.4	Effect of POE 40 stearate concentration on the intercalation rate into the DODAB bilayer.....	89
Figure 3.5	Effect of POE 100 stearate concentration on the intercalation rate into the DODAB bilayer.....	90
Figure 3.6	EOF vs. POE 40 stearate concentration on a capillary first coated with 0.1 mM DODAB followed by coating with a mixture of 0.01% POE 8 stearate and POE 40 stearate.....	93
Figure 3.7	Representative separations of basic proteins on a sequential 0.1 mM DODAB then 0.075% POE 40 stearate coating with no recoating between 30 runs.....	95
Figure 3.8	Histone type III-S separation on a 0.1 mM DODAB then 0.075% POE 40 stearate sequentially coated capillary.....	99
Figure 3.9	Histone type III-S separation on a 0.1 mM DODAB/0.075% POE 40 stearate mixed coated capillary...	100
Figure 3.10	Separation of two acidic proteins on a 0.1 mM DODAB then 0.01% POE 8 stearate sequentially coated capillary.....	102
Figure 4.1	Schematic of single-step and two-step cIEF procedures.....	109
Figure 4.2	cIEF separation of 6 peptide markers on a 0.1 mM DODAB /0.075% POE 40 stearate coated capillary using: a) 1.25% v/v; or b) 2.5% v/v carrier ampholytes.....	116
Figure 4.3	Single-step cIEF separation of 6 peptide markers on a 0.1 mM DODAB /0.075% POE 40 stearate sequentially coated capillary using 2.5% v/v of the carrier ampholytes pI 3-10..	119
Figure 4.4	Single-step cIEF separation of 5 peptide markers on a 0.1 mM DODAB /0.075% POE 40 stearate a) 50 μ m i.d. and b) 25 μ m i.d. coated capillaries using 2.5% v/v of the carrier ampholytes pI 5-8.....	120
Figure 4.5	Single-step cIEF separation of 5 peptide markers on a 0.1 mM DODAB /0.075% POE 40 stearate coated capillary monitored at: a) 280 nm; and b) 420 nm.....	123

Figure 4.6	Single-step cIEF separation of 5 peptide markers on a 0.1 mM DODAB /0.075% POE 40 stearate a) 32 (23.5) cm, b) 48.5 (40) cm and 65 (56.5) cm coated capillaries using 2.5% v/v of the carrier ampholytes pI 5-8.....	125
Figure 4.7	Single-step cIEF separation of 6 peptide markers on a 0.1 mM DODAB /0.075% POE 40 stearate a) 32 (23.5) cm; and b) 48.5 (40) cm coated capillaries using 2.5% v/v of the carrier ampholytes pI 3-10.....	126
Figure 4.8	Two-step cIEF separation of 6 peptide markers on a) 0.1 mM DODAB /0.075% POE 40 stearate and b) 0.1 mM DODAB /0.001% POE 100 stearate sequentially coated capillaries using 2.5% v/v of the carrier ampholytes pI 3-10	129
Figure 4.9	Two-step cIEF separations of 6 peptide markers using different ampholyte concentrations and different POE stearate chain lengths.....	131
Figure 4.10	Two-step cIEF separation of 5 peptide markers on a 0.1 mM DODAB /0.075% POE 40 stearate coated capillary using 2.5% v/v of the carrier ampholytes pI 5-8.....	132
Figure 4.11	Linearity of the pH gradient established on a 0.1 mM DODAB /0.075% POE 40 stearate coated capillary using 2.5% v/v carrier ampholytes.....	135
Figure 4.12	Two-step cIEF separation of two hemoglobin variants; HbA ₀ and HbS on a 0.1 mM DODAB/0.075% POE 40 stearate sequentially coated capillary.....	137
Figure 4.13	Two-step cIEF separation of two hemoglobin variants; HbA ₀ and HbS on a commercially coated capillary.....	138
Figure 5.1	Stability of DODAB/POE diblock copolymer constructs vs. POE diblock copolymer alone coating.....	151
Figure 5.2	Structure of diblock copolymers used to study the effect of A) hydrophobic block and B) hydrophilic block.....	153
Figure 5.3	Effect of hydrophobic chain length of the diblock copolymer on EOF.....	154
Figure 5.4	Effect of buffer anion on EOF of DODAB/diblock copolymer coatings.....	157
Figure 5.5	Effect of pH on the EOF of DODAB/POE diblock copolymer coated capillaries.....	159
Figure 5.6	EOF stability of the DODAB/POE diblock copolymers vs. pH.....	161

Figure 5.7	Stability of the coating under mixed aqueous-organic conditions.....	164
Figure 6.1	Stability of 0.1 mM DODAB coated capillaries at pH 3-7 in various buffers of constant (44 mM) ionic strength.....	178
Figure 6.2	Stability of 0.1 mM DODAB coated capillaries at pH \geq 7.0.....	180
Figure 6.3	EOF of 0.1 mM DODAB coated capillary switched between pH 3.0 and pH 9.0.....	182
Figure 6.4	EOF of 0.1 mM DODAB coated capillary switched between pH 3.0 and pH 11.5.....	183
Figure 6.5	ESI Mass spectra of DODAB and DODAB treated with ammonia.....	186
Figure 6.6	Separation of two basic proteins on 0.1 mM DODAB coated capillaries: a) before, b) after one cycle and c) after two cycles of switching between pH 3.0 and 9.0.....	192
Figure 7.1	General structure of gemini surfactants.....	202
Figure 7.2	Examples for di-quaternary cationic gemini surfactants a) with amino substituted spacer group and b) with non-substituted spacer group.....	204
Figure 7.3	Derivatization of an amino acid with Fmoc-Cl.....	208
Figure 7.4	The structure (A) and the polymerization reaction (B) of 1,2-bis(10,12-tricosadiynoyl)-sn-glycero-3-phosphocholine (Diyne PC).....	208
Figure 7.5	Schematic for the proposed in-capillary derivatization of amino acid mixture with Fmoc.....	209

List of Abbreviations

Abbreviation	Full name
2D-CE	two-dimensional capillary electrophoresis
ACN	acetonitrile
AFM	atomic force microscopy
BGE	background electrolyte
α -chymo A	α -chymotrypsinogen A
CAC	critical aggregation concentration
CE	capillary electrophoresis
CGE	capillary gel electrophoresis
CIEF	capillary isoelectric focusing
CITP	capillary isotachopheresis
CMC	critical micelle concentration
CTAB	cetyltrimethylammonium bromide
CVC	critical vesicle concentration
cyto c	cytochrome c
CZE	Capillary zone electrophoresis
DDAB	Didodecyldimethylammonium bromide
Diyne PC	1,2-bis(10,12-tricosadiynoyl)-sn-glycero-3-phosphocholine
DLS	Dynamic light scattering
DNA	deoxyribonucleic acid
DODAB	dioctadecyldimethylammonium bromide

EKC	electrokinetic chromatography
EMD	electromigration dispersion
EOF	electroosmotic flow
HPLC	High performance liquid chromatography
i.d.	inner diameter
IHP	inner Helmholtz plane
lyso	lysozyme
LOD	Limit of detection
LOQ	limit of quantification
o.d.	outer diameter
OHP	outer Helmholtz plane
PDI	polydispersity index
PDMA	polydimethylacrylamide
PEG	polyethylene glycol
PEO	polyethyleneoxide
POE	polyoxyethylene
psi	Pound per square inch
RNase A	ribonuclease A
RSD	relative standard deviation
SDS	sodium dodecyl sulfate
SMIL	successive multiple ionic layer
SN ²	Nucleophilic substitution

SUV	smaller unilamellar vesicles
Tris	tris(hydroxymethyl) aminomethane
UV-Vis	ultraviolet-visible

List of Symbols

Symbol	Full name
a_h	cross sectional area of surfactant headgroup
b	pathlength
k	retention factor
k_b	Boltzman constant
k_d	desorption rate constant
l_c	length of the hydrophobic region of the surfactant
l_{det}	length of detection window
l_{inj}	length of injection plug
pI	isoelectric point
pK_a	negative logarithm of acid dissociation constant
q	electric charge
m	slope of linear calibration curve
n_m	number of moles in the mobile phase
n_s	number of moles in the stationary phase
r	capillary radius
r_h	hydrated radius of ion
t_{EOF}	migration time of neutral marker
t_{inj}	injection time
t_M	migration time
t_{M_1}	migration time of first peak

t_{M_2}	migration time of second peak
$t_{\text{rise,max}}$	maximum rise time of detector
w_b	baseline peak width
w_{b_1}	baseline width of first peak
w_{b_2}	baseline width of second peak
$w_{1/2}$	peak width at its half height
v	velocity
A	absorbance
C	concentration
D	diffusion coefficient
E	electric field
F	faraday constant
F_E	electric force
F_F	frictional force
H	plate height
I	current
I_s	ionic strength
K_d	equilibrium distribution coefficient
L_d	capillary length to detector
L_t	total length of capillary
N	number of theoretical plates or efficiency
P	power

P_o	light intensity in absence of absorption
P_t	light intensity transmitted through analyte
P_f	Packing factor
ΔP	pressure difference across the capillary
R	resistance
R_g	gas constant
R_s	resolution
R^2	correlation coefficient
T	temperature in Kelvin
V	applied voltage
V_c	volume of the hydrophobic region of the surfactant
V_{inj}	Injection volume
V_m	volume of the mobile phase
V_s	volume of the stationary phase
β	Phase ratio
ϵ	dielectric constant
ϵ_λ	molar absorptivity coefficient at wavelength λ
ζ	zeta potential
η	viscosity
λ	wavelength
K^{-1}	electrical double layer thickness
μ_{app}	apparent mobility

μ_e	electrophoretic mobility
μ_{EOF}	electroosmotic mobility
$\Delta\mu_{app}$	Difference in apparent mobilities
μ_{avg}	average electrophoretic mobility
σ	standard deviation
σ_{tot}^2	total variance
σ_{diff}^2	variance due to longitudinal diffusion
σ_{temp}^2	variance due to temperature non uniformities
σ_{EMD}^2	variance due to electromigration dispersion
σ_{inj}^2	variance due to injection broadening
σ_{det}^2	variance due to detector broadening
σ_{ads}^2	variance due to adsorption on capillary wall
Ψ_0	surface potential at capillary wall
Ψ_{OHP}	potential at outer Helmholtz plane
Ω_T	temperature coefficient for electrophoretic mobilities

Chapter One: Introduction

1.1 History

Electrophoresis is the differential movement of charged species in the presence of an electric field. Many biological molecules such as enzymes and proteins display electrophoretic characteristics [1]. In 1937, Tiselius introduced electrophoresis as a separation technique when he separated a mixture of serum proteins using a quartz tube filled with buffer solution [2]. Sample components migrated into broad, partially resolved bands according to their charge and size to the electrode of opposite charge. He was awarded the Nobel Prize in chemistry in 1948 for this work. The “moving boundary electrophoresis” separation technique performed by Tiselius was limited by Joule heating. Joule heating is the heat generated due to passage of current in a solution. The resultant thermal convection limited the separation efficiency and resulted in incomplete separation of the analytes. For this reason, anti-convective media like polyacrylamide or agarose gel has been used to perform electrophoresis. In 1959, Raymond and Weintraub used polyacrylamide gels for the separation of proteins [3]. Although these gels effectively reduced thermal convection, they still resulted in some limitations. To avoid gel degradation, only hundreds of volts could be applied, which resulted in long analysis times and low efficiencies. Other limitations and technical problems of gel electrophoresis include gel preparation, sample loading, poor reproducibility and gel staining.

In 1967, Hjerten took the initial step towards open tubular electrophoresis. He used a 3 mm diameter gel-free quartz tube to separate inorganic ions [4]. The tube was rotated to reduce thermal convection. In the 1970s, Virtanen performed electrophoresis in 200 μm inner diameter (i.d.) glass capillary which reduced convection problems [5]. Mikkers *et al.* used 200 μm i.d. capillary to reduce dispersion caused by thermal convection [6]. The potential of electrophoresis as a separation technique was fully realized when Jorgenson and Lukacs used narrower 75 μm i.d. capillaries [7]. The use of a smaller capillary i.d. greatly advanced the technique by eliminating the need to use gel as anti-convective media. The high surface to volume ratio of narrow i.d. capillaries allows rapid and efficient heat dissipation and reduces Joule heating to a negligible level. In turn, this allows the application of voltages up to 30 kV, resulting in fast analysis times and high separation efficiencies.

Since then, CE has become a popular and efficient technique for the separation of a wide range of analytes - from small ions to large biomolecules. The most prominent achievement for CE as a separation technique was the sequencing of DNA in the human genome project [8]. The applications of CE have expanded to include proteomics [9], metabolomics [10], pharmaceutical analysis [11], biological analysis [12], forensics [13] and food analysis [14].

1.2 Modes of Capillary Electrophoresis

Capillary electrophoresis is a highly versatile technique. It can be operated under many different formats or modes. These different modes utilize different

mechanisms of separation which provide orthogonal and complementary information. Many two-dimensional capillary electrophoresis (2D-CE) applications are based on the integration of different modes of CE [15, 16].

1.2.1 Capillary Zone Electrophoresis (CZE)

CZE is the most widely used CE mode due to its simplicity and versatility. The separation is based on the differential migration of charged analyte species in a capillary filled only with a buffer solution (also called background electrolyte, BGE). Thus the technique can also be called free-solution electrophoresis. The separated analyte species move inside the capillary in discrete zones according to their charge/size ratios. The technique can be used to separate a wide range of analytes including inorganic ions, carbohydrates, peptides and proteins. Due to its popularity, CZE will be the main focus of this chapter.

1.2.2 Electrokinetic Chromatography (EKC)

One drawback of CZE (Section 1.2.1) is that it cannot separate neutral molecules, as their charge is zero. EKC is as an electrophoretic mode which enables the separation of neutral molecules [17]. As its name suggests, EKC is a hybrid of electrophoresis and chromatography. An ionic pseudo-stationary phase in the running buffer (e.g. micelle, vesicle, microemulsions, etc.) interacts with solutes in a chromatographic manner. A neutral species partitions in and out of the micelle and gains an apparent electrophoretic mobility due to the mobility of the ionic micelle. The differential interaction between neutral species with the pseudo-stationary phase enables their separation.

1.2.3 Capillary Isoelectric Focusing (cIEF)

cIEF is a special high resolution mode of capillary electrophoresis used for the separation of amphoteric compounds such as protein isoforms [18]. A capillary is filled with a mixture of proteins and carrier ampholytes, a mixture of amphoteric compounds with variable pIs and possessing a good buffering capacity. Upon application of a high electric field across the capillary, a pH gradient is established along the length of the capillary due to migration of the ampholytes to their isoelectric point (pI). The charge of the protein decreases as it moves along the pH gradient until the protein reaches a region where the pH matches its pI and its mobility becomes zero. Thus, amphoteric sample components are focused at different points along the capillary according to their pI. cIEF can be used for the separation of proteins variants, determination of impurities within therapeutic proteins and determination of the isoelectric point of proteins [19]. cIEF will be the focus of Chapter Four in this thesis. A more detailed description of cIEF is deferred until then.

1.2.4 Capillary Gel Electrophoresis (CGE)

Macromolecules such as sodium dodecyl sulfate (SDS)-saturated proteins and DNA possess constant mass/charge ratios. As such, they exhibit a constant mobility under CZE conditions and elute in a single peak. To separate such molecules based on size, CGE adds a sieving matrix to the separation medium. Traditionally, polyacrylamide or agarose have been used as molecular sieving matrices to perform CGE [20]. The capillary format offers several advantages to CGE over the traditional slab gel format. The capillary format allows application

of higher voltages, faster separations, online detection and ease of automation. CGE has been applied to SDS- protein separations [20] and DNA separations [21]. CGE is not explored in this thesis.

1.2.5 Capillary Isotachophoresis (CITP)

CITP is a moving boundary electrophoresis where the separated analyte zones move at constant velocity between two electrolytes. The leading electrolyte has the highest effective mobility and the terminating electrolyte has the lowest effective mobility. Once an electric field is applied, the leading ion moves the fastest followed by adjacent zones of the analyte ions in decreasing order of their effective mobilities and latest comes the terminating ion. CITP has been used as an effective pre-concentration tool prior to CE separations e.g. CITP-CZE. This is useful for enhanced detection sensitivity, enhanced limit of detection and sample cleanup [22]. CITP is not studied in this thesis, and so will not be discussed further.

1.2.6 Capillary Electrochromatography (CEC)

Capillary electrochromatography (CEC) combines the high separation efficiency of CZE and the variety of parameters that can be manipulated in HPLC, particularly the selection of stationary phase. CEC utilizes an electric field rather than a pressure pump resulting in high efficiency separations due to the flat flow profile of electroosmotic flow (EOF). Since, there is no pressure drop, smaller particles can be used for packing, resulting in higher efficiency. The dual separation mechanism of partitioning and electrophoretic migration can offer

unique selectivities. However, the technique also suffers from some limitations. A minor change in the pH or ionic strength can alter the EOF which affects reproducibility of the technique. Joule heating affects the viscosity of the mobile phase and the partitioning of the analyte. In addition, bubble formation in the capillary leads to current breakdown and reduced flow [23]. CEC will not be discussed further in this thesis.

1.3 Fundamentals of CE

1.3.1 Instrumentation

The basic components of a CE instrument are shown in Figure 1.1. A CE instrument consists of a separation capillary, two buffer vials into which the two capillary ends are placed, a sample vial, a high voltage power supply, an online detection system and a data analysis system [24, 25]. Capillaries are mostly made of fused silica with an outer protective polyimide coating to enhance their strength and flexibility. Typically capillaries with i.d of 25-75 μm and lengths of 20-100 cm are used. An efficient cooling system either air-based or coolant-based is needed to thermostat the capillary. The high voltage power supply is capable of delivering up to 30 kV. The stability of the power supply is important for reproducibility of migration times. The polarity can be switched in order to facilitate the analysis of positively charged or negatively charged analytes or mixture of both analytes.

To perform a separation, the bare fused silica capillary is preconditioned with NaOH to deprotonate silanols on the fused silica surface, followed by water

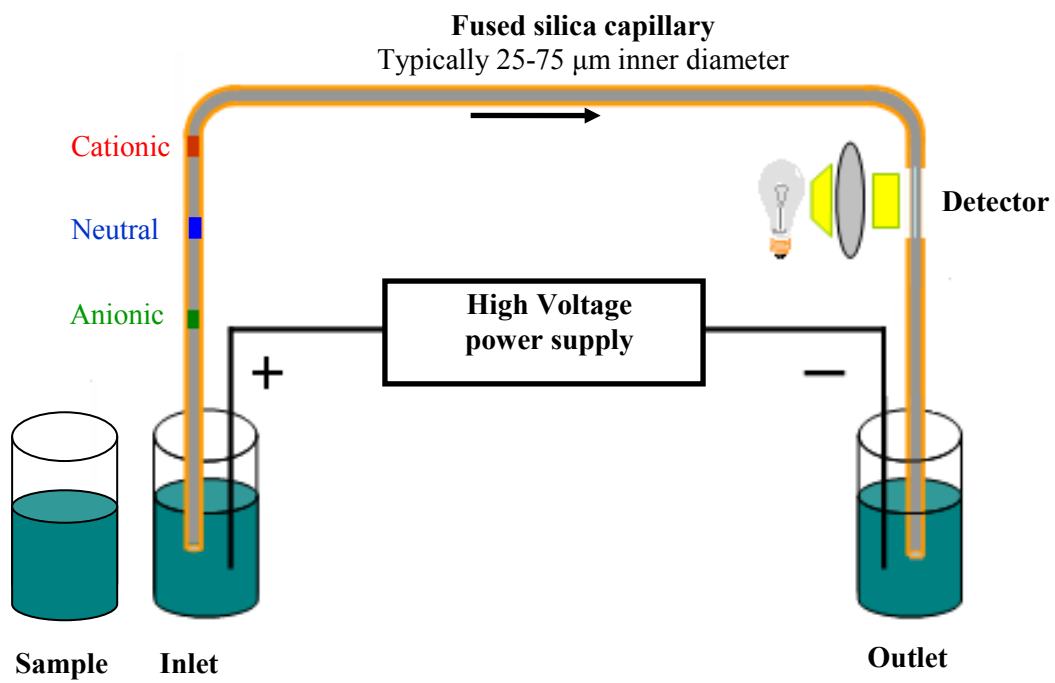


Figure 1.1: Schematic of capillary electrophoresis instrumentation.

and then the separation buffer. The inlet end of the buffer-filled capillary is placed into the sample vial and a small plug (a few nanoliters) of sample is injected into the capillary either by applying a voltage (electrokinetic injection) or a pressure (hydrodynamic injection). For electrokinetic injection, the amount of sample injected is dependent on both the electroosmotic flow (EOF) and electrophoretic mobility of the analyte. This dependence on the EOF may result in poor reproducibility of the electrokinetic injection. The dependence on the electrophoretic mobility results in biasing of the amount of each analyte injected due to the difference in their electrophoretic mobilities. Thus, hydrodynamic injection is the preferred method of injection as it is independent on the EOF and electrophoretic mobilities of the analytes [25]. Hydrodynamic injection is performed by applying a pressure at the injection end or a vacuum at the detection end of the capillary. The injected sample volume can be calculated using the Poiseuille Equation [24, 25]:

$$\text{Volume} = \frac{\pi r^4 \Delta P t_{\text{inj}}}{8 \eta L_t} = \frac{\pi d^2 \Delta P t_{\text{inj}}}{128 \eta L_t} \quad (1.1)$$

where ΔP is the applied pressure across the capillary in pascals (Pa), r is the capillary inner radius, d is the capillary inner diameter in meters, t_{inj} is the injection time in seconds, η is the viscosity of the sample solution (Pa·s), and L_t is the total length of the capillary in meters.

After the sample injection, the capillary inlet is placed back into the inlet buffer vial and a high voltage is applied across the capillary through two platinum

electrodes inserted into the two buffer vials (configuration shown in Figure 1.1). The EOF results in bulk flow of the solution inside the capillary. The charged sample components also possess electrophoretic mobilities related to their charge/size ratios and thus can be separated. The separated analytes pass through an optical window created by removing the polyimide coating near the capillary outlet and thus are detected on-capillary.

Detection methods for CE include UV-Vis absorbance, fluorescence and electrochemical measurements [26]. Optical detection methods are more common, with UV-Vis absorption detection being most common. The absorbance measurement is governed by Beer-Lambert's law [27]:

$$\log (P_o /P_t)= A = \epsilon_{\lambda} bC \quad (1.2)$$

where P_o is the intensity of the light in the absence of absorption, P_t is the intensity of light transmitted by the solution, A is the absorbance, ϵ_{λ} is the molar absorptivity of the analyte, b is the detection pathlength and C is the concentration of the analyte. One of the main drawbacks of UV-VIS detection is the low sensitivity since the pathlength is defined by the capillary inner diameter. Limits of detection range from 10^{-5} to 10^{-8} M. The use of larger capillary i.d. to enhance the sensitivity increases Joule heating due to the decrease in the surface-volume ratio. Some capillary modifications have been used to increase the pathlength at the detection zone like Z-type [28, 29] and bubble cells [29, 30]. The use of a Z-cell greatly enhance the optical pathlength, however it results in increased band broadening and limited resolution [28]. In addition, the increased noise level

partly offsets the signal gain from the pathlength extension [29]. The bubble cell offers a 3-5 fold increase in sensitivity with minimal loss in resolution as long as the slit length of the detection window is reduced appropriately [29].

In this work, two commercially available CE instruments have been used. First, the P/ACE 5500 system (Beckman Instruments, Fullerton, CA, USA) equipped with a UV absorbance detector was used in Chapter Three. The optical window was 7 cm from the capillary outlet end. A liquid coolant system was used to thermostat the capillary. Second, a Hewlett Packard ^{3D}CE instrument (now sold by Agilent) equipped with a photodiode array detector was used in Chapters 2, 4, 5 and 6. The optical window was made 8.5 cm from the capillary outlet end. An air cooling system is used to thermostat the capillary.

1.3.2 Electroosmotic flow (EOF)

EOF is the bulk flow of the solution inside the capillary under the influence of an applied electric field as a result of the surface charge on the inner surface of the capillary. The silanol groups (SiOH) on the inner surface of the capillary are weakly acidic with a pK_a value of 5.3 [31]. At low pH, the ionization of the surface silanol groups is suppressed and the electroosmotic flow approaches zero. Increasing the pH deprotonates the silanol groups and results in higher EOF.

The driving force of EOF is the negative charge on the inner surface of fused silica capillaries. The positive counterions in the liquid phase will compensate the negative charge of the wall so that an electrical double layer is

created at the solid-liquid interface. To understand the origin of EOF, we need to have a look into the electrical double layer formed at the capillary surface in contact with a buffer solution (Figure 1.2). The electrical double layer consists of an immobilized compact inner layer and an outer mobile diffuse layer [32]. The inner layer is called the Stern layer or Helmholtz layer. The Helmholtz layer is divided into two sublayers. The first one extends from the negatively charged capillary wall to the inner Helmholtz plane (IHP) which is defined by the center of the non-solvated cations that are strongly bound to the capillary surface. The second sublayer extends from the IHP to the outer Helmholtz plane (OHP) which is defined by the centre of the immobilized solvated counter ions that are electrostatically adsorbed to the capillary wall. The plane of shear is formed at the outer edge of the Stern compact layer (i.e. slightly behind the OHP). Any ions within the plane of shear are stationary. Beyond the plane of shear is the diffuse double layer.

Figure 1.2 shows also the potential profile as a function of the distance from the capillary surface. The potential at the capillary wall is Ψ_0 . The potential decreases linearly through the Stern layer. But the counter ions in the compact Stern layer do not fully neutralize the negative charge on the capillary surface, and so the potential at the outer Helmholtz plane (Ψ_{OHP}) is still negative. The excess negative charge at the plane of shear is compensated by the excessive positive charge in the diffuse double layer that extends to the bulk solution. Thus beyond the OHP, the potential decreases in magnitude exponentially through the diffuse layer until it becomes zero in the bulk solution. The potential at the plane

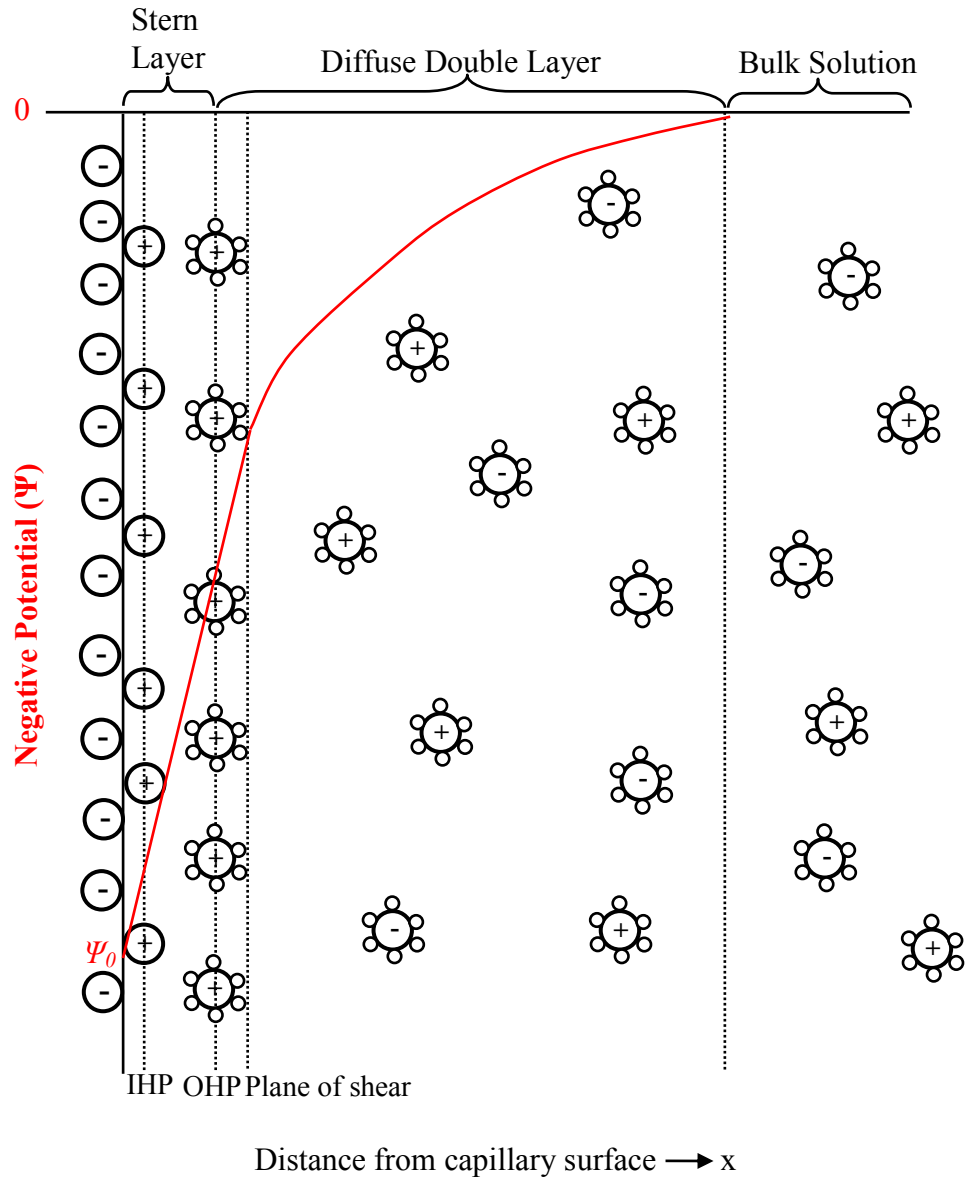


Figure 1.2: Schematic of the electric double layer and the **potential profile** as a function of distance from the capillary wall. Adapted from reference [32].

of shear is called the zeta potential (ζ), a term commonly associated with the electrical double layer and related to the EOF mobility.

When an electric field is applied across the bare capillary, the cations within the diffuse double layer are drawn towards the cathode. As these cations are solvated, they drag the bulk movement of the solution inside the capillary towards the cathode. The magnitude of the EOF can be described by the von Smoluchowski equation [33, 34]:

$$\mu_{\text{eof}} = \frac{\varepsilon \zeta}{\eta} \quad (1.3)$$

where μ_{eof} is the EOF mobility, ε is the dielectric constant of the solution, ζ is the zeta potential and η is the viscosity. A higher pH results in greater deprotonation of the silanols which yields a higher negative charge on the capillary wall (Ψ_0), and hence a larger zeta potential and a higher EOF. A higher ionic strength of the buffer compresses the electrical double layer, decreases the zeta potential and hence decreases the EOF. The relationship between the ionic strength and electrical double layer thickness (κ^{-1}) is obtained from the following equation [33]:

$$\kappa^{-1} = \frac{1}{F} \cdot \sqrt{\frac{\varepsilon R_g T}{2000 I_s}} \quad (1.4)$$

where F is the Faraday constant, ε is the dielectric constant of the solvent, R_g is the universal gas constant, T is the temperature in Kelvin, and I_s is the ionic strength of the bulk solution. The double layer thickness for an aqueous solution

of a uni-univalent electrolyte ranges from approximately 10 nm for a dilute bulk solution (0.001 mM) to 1 nm for a concentrated electrolyte solution (100 mM) [35].

EOF can be considered as an electric field-driven pump analogous to the mechanical pump used in HPLC. A unique feature of EOF is the flat flow profile (Figure 1.3) as the negative charge is uniformly distributed along the capillary wall. Since the EOF is generated along the entire capillary length and there is no pressure drop, a uniform velocity and flat flow profile exists across the capillary diameter except for very close (< 100 nm) to the wall where the velocity approaches zero. This flat flow profile minimizes band broadening, increases peak efficiency and improves the resolution. The flat flow profile of EOF is independent of the capillary i.d. as long as the capillary i.d. is 10-50 times greater than the double layer thickness [36]. On the other hand, the mechanical pump in HPLC results in a laminar or parabolic flow (Figure 1.3) due to the pressure drop across the separation column as a result of the shear force at the wall. In turn, this result in increased band broadening and decreased peak efficiency compared to CE.

In the presence of an applied electric field, a neutral compound will migrate across the capillary only driven by EOF. Thus, a neutral compound (also called a neutral marker) can be used to measure the magnitude of the EOF. Examples of neutral markers include benzyl alcohol (detection λ , 214 nm) or

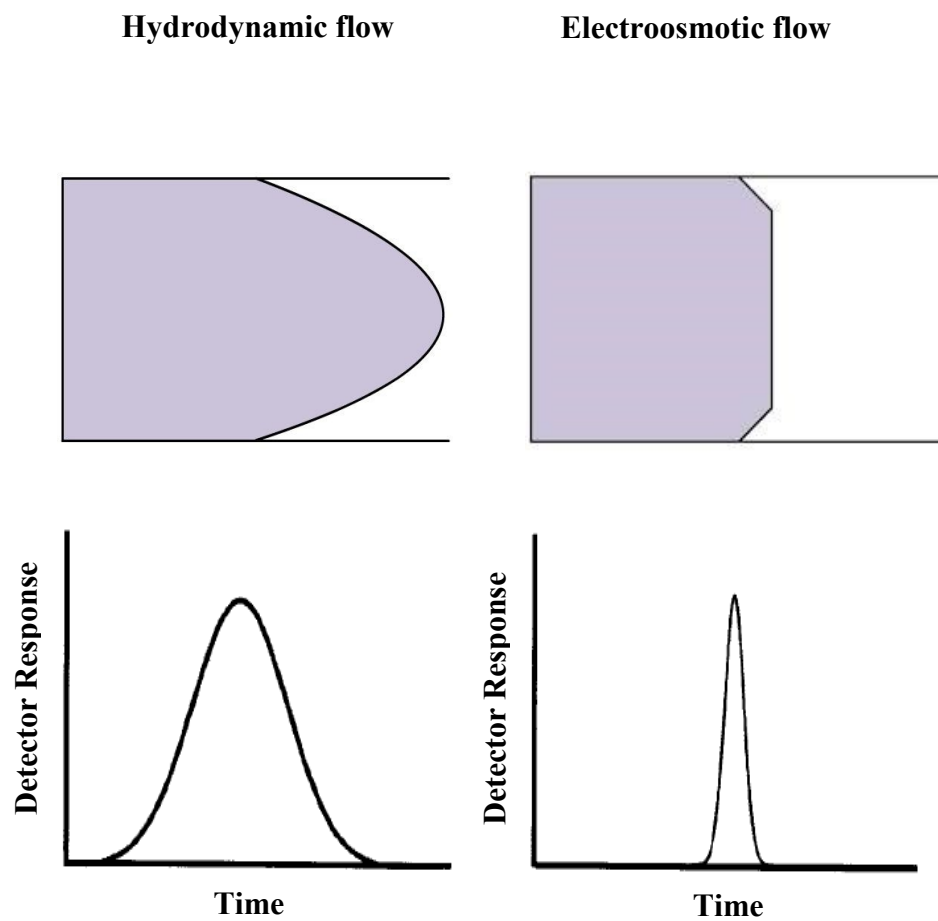


Figure 1.3: Comparison of EOF and pressure driven flow profiles and corresponding peak shapes. Adapted from reference [25].

mesityl oxide (detection λ , 254 nm). For on-capillary detection as used in this thesis, the EOF can be calculated as:

$$\mu_{\text{eof}} = \frac{L_d L_t}{V t_{\text{EOF}}} \quad (1.5)$$

where L_t and L_d are the total length of the capillary and the capillary length to the detector, respectively, V is the voltage applied, and t_{EOF} is the migration time of the neutral marker.

1.3.3 Electrophoretic and apparent mobilities

The velocity of a charged particle is dependent upon the applied electric field as well as its inherent electrophoretic mobility.

$$v = \mu_e E \quad (1.6)$$

where v is the velocity of the ion, μ_e is the electrophoretic mobility and E is the applied electric field (V/cm). The electrophoretic mobility of an ionic species in a given medium is a constant inherent property of this ion. This mobility is governed by the electric force that the molecule experiences, balanced by its frictional drag through the medium [24, 25]. The electrical force (F_E) is given by:

$$F_E = qE \quad (1.7)$$

where q is the charge of the ion. As the ion begins to move under the influence of this electric force, it experiences a frictional force in the opposite direction to its

motion due to the frictional drag of the solvent. The frictional force (F_F) on a spherical ion is given by:

$$F_F = -6\pi\eta r_h v \quad (1.8)$$

where η is the solution viscosity, r_h is the hydrated radius of the ion and v is its velocity. When a steady state is reached during the electrophoretic process, the driving electric force and the retarding frictional force are balanced.

$$qE = 6\pi\eta r_h v \quad (1.9)$$

By rearranging and substituting Equation 1.6 into Equation 1.9, the Hückel equation for the electrophoretic mobility of a spherical ion is obtained [25]:

$$\mu_e = q/6\pi\eta r_h \quad (1.10)$$

Based on this equation, ions with a high charge and a small hydrodynamic radius will have high mobilities. The separation mechanism in CZE is based on the difference in the electrophoretic mobilities which results from different charge /size ratios of the analyte ions. However, the Hückel equation, assuming a spherical molecule, is not an accurate predictor of electrophoretic mobility [37]. Empirical expressions possessing dependences on molecular volume to a power other than the $-1/3$ suggested by the Hückel equation are better predictors of electrophoretic mobilities [37].

When an electric field is applied in capillary electrophoresis, a charged ion migrates under the influence of both its electrophoretic mobility and the EOF. Therefore, the apparent mobility (μ_{app}) of an ion is given by [25]:

$$\mu_{\text{app}} = \mu_e + \mu_{\text{EOF}} \quad (1.11)$$

The apparent mobility of an ion in the presence of an electric field can be calculated using the following equation:

$$\mu_{\text{app}} = \frac{L_d L_t}{V t_M} \quad (1.12)$$

where L_t , L_d and V are defined as above for Equation 1.5, and t_M is the migration time of the analyte.

The effective electrophoretic mobility of an ionic species can be calculated experimentally from the migration time of the ion t_M and the migration time of a neutral marker t_{EOF} using:

$$\mu_{\text{eof}} = \frac{L_d L_t}{V} \left(\frac{1}{t_M} - \frac{1}{t_{\text{EOF}}} \right) \quad (1.13)$$

Figure 1.4 shows an idealized separation of a mixture of anions, cations and neutral species under the influence of an electric field in a bare fused silica capillary. All neutral species do not possess electrophoretic mobility and migrate only driven by EOF. Thus, all neutrals are co-eluted as a single peak with a migration time of t_{EOF} that can be used to calculate the magnitude of EOF. Cationic species have their electrophoretic mobilities in the same direction

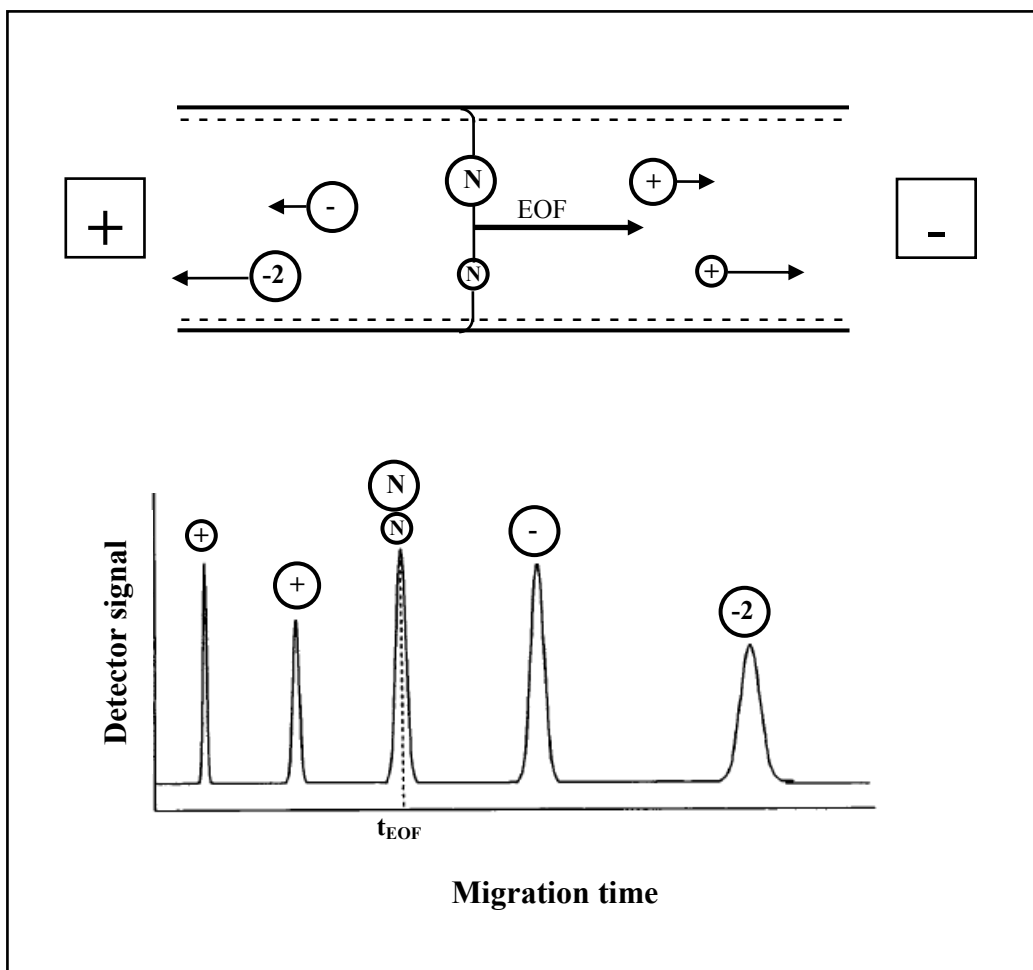


Figure 1.4: Migration order within a capillary under an applied electric field and the resultant electropherogram.

of EOF (co-EOF, towards the detector in Figure 1.1) and so they migrate ahead of the EOF peak. Anionic species have their electrophoretic mobilities in opposite direction to the EOF (counter EOF) but the magnitude of EOF of a bare capillary is strong enough to sweep these anionic species toward the detector. As a result, the anionic peaks will migrate after the EOF peak. If the electrophoretic mobility of an anion (e.g., Cl^- and SO_4^{2-}) is greater than the magnitude of the EOF, this anion will migrate towards the anode in the direction opposite to the detector and no peaks will be detected for this anion.

1.4 Band broadening in CE

Band broadening in CE is the result of multiple dispersive processes that occur during the electrophoretic separation. An important measure of the band broadening is the separation efficiency. It measures how narrow is the peak and is expressed in the number of theoretical plates (N) as follows:

$$N = \frac{L_d^2}{\sigma_{\text{tot}}^2} \quad (1.14)$$

where L_d is the capillary length to the detector and σ_{tot}^2 is the total peak variance.

N can be calculated experimentally using:

$$N = 5.54 \left(\frac{t_M}{w_{1/2}} \right)^2 \quad (1.15)$$

where t_M is the migration time of the peak and $w_{1/2}$ is the peak width at its half height.

Resolution is a quantitative measure of how well two components are separated. Thus, resolution can be related to the peak standard deviations by the following equation:

$$R_s = \frac{(t_{M_2} - t_{M_1})}{2(\sigma_1 + \sigma_2)} \quad (1.16)$$

where t_{M_1} and t_{M_2} are the migration times of two adjacent peaks numbered 1 and 2, σ_1 and σ_2 are their standard deviations. Two peaks are considered to be baseline resolved when $R_s \geq 1.5$. For a Gaussian peak, the baseline peak width w_b equals four times the standard deviation of the peak σ . Thus, resolution can be calculated from the difference in migration times of two peaks relative to their peak widths according to the following equation:

$$R_s = \frac{2(t_{M_2} - t_{M_1})}{(w_{b_1} + w_{b_2})} \quad (1.17)$$

where w_{b_1} and w_{b_2} are the baseline peak widths. The relationship between the resolution and the number of theoretical plates (N) in CE is:

$$R_s = \frac{1}{4} \cdot \frac{\Delta\mu_{app}}{\mu_{avg,app}} \cdot \sqrt{N} \quad (1.18)$$

where $\Delta\mu_{app}$ is the difference in the apparent electrophoretic mobilities of the two components and $\mu_{avg,app}$ is the average of their apparent electrophoretic mobilities. Equation 1.18 shows that the resolution R_s is directly proportional to the square

root of the separation efficiency N . Thus, it is important to minimize band broadening to enhance the separation efficiencies and hence the resolution. Under ideal conditions in CE, longitudinal diffusion is the fundamental source of band broadening. In a real system, other sources of band broadening may exist, such that the total peak variance (σ_{tot}^2) is:

$$\sigma_{\text{tot}}^2 = \sigma_{\text{diff}}^2 + \sigma_{\text{temp}}^2 + \sigma_{\text{EMD}}^2 + \sigma_{\text{inj}}^2 + \sigma_{\text{det}}^2 + \sigma_{\text{ads}}^2 \quad (1.19)$$

where σ_{diff}^2 is the variance due to longitudinal diffusion band broadening, σ_{temp}^2 is temperature induced band broadening, σ_{EMD}^2 is electromigration dispersion band broadening, σ_{inj}^2 is the injection band broadening, σ_{det}^2 is the detector band broadening and σ_{ads}^2 is solute wall adsorption band broadening. A brief discussion of these sources of band broadening with a greater focus on solute wall adsorption band broadening will be presented in the following sections.

1.4.1 Longitudinal diffusion

Under ideal electrophoretic separation, longitudinal diffusion is the sole source of band broadening in CE. Longitudinal diffusion is the spreading of the analyte along the capillary axis as a result of a concentration gradient. This spreading results in a Gaussian peak with the highest concentration at the centre and its width is determined by extent of diffusion that occurs [38]. The variance caused by the longitudinal diffusion can be described by:

$$\sigma_{\text{diff}}^2 = 2Dt_M = 2D \frac{L_d L_t}{\mu_{\text{app}} V} \quad (1.20)$$

where D is the diffusion coefficient of the analyte and t_M is the migration time of the analyte. According to Equation 1.20, a large diffusion coefficient and a longer migration time result in broader peaks. Large molecules such as proteins have small diffusion coefficients and experience less longitudinal diffusion than smaller molecules. The use of higher electric field decreases the time spent by the analyte in the capillary (t_M) and thus decreases longitudinal diffusion band broadening. However, the high voltage approach is limited by Joule heating (Section 1.4.2).

Substitution of Equation 1.20 into Equation 1.14 gives an expression of N in terms of the applied voltage:

$$N = \frac{\mu_{\text{app}} V L_d}{2DL_t} \quad (1.21)$$

The separation efficiency is directly proportional to the applied voltage. N in the above equation represents the maximum theoretical efficiency that can be achieved during an electrophoretic separation assuming that longitudinal diffusion is the sole contributor to band broadening. In a real system, the experimental N will be lower than that described in Equation 1.21 due to other sources of band broadening (Equation 1.19).

1.4.2 Joule heating

As described above, the use of a higher field strength is advantageous for separation. A higher voltage reduces the separation time, reduces longitudinal diffusion band broadening due to decreased time spent in the capillary (Equation 1.20) and increases the separation efficiency (Equation 1.21). However, the voltage applied may be limited by Joule heating which is a contributor to band broadening. Joule heating results from the heat generated by the passage of an electric current (I) through a solution when a potential difference is applied. Joule heating can be explained using Ohm's law as follows:

$$V = IR \quad (1.22)$$

which can be also expressed as:

$$P = I^2R \quad (1.23)$$

where V is the voltage across the capillary, I is the electrical current, R is the resistance to the current flow and P is the applied power. When the heat generation exceeds the heat dissipation through the capillary wall, the temperature will increase at the capillary center at a higher rate compared to the capillary wall. The presence of a temperature gradient (radial temperature difference) in the BGE results in viscosity differences across the capillary. Analytes move faster in the warmer, lower viscosity zone near the axis of the capillary than in the cooler

zones near the capillary wall. This results in a parabolic electrophoretic mobility profile and increased band broadening.

Ohm's plots (current vs. voltage) are commonly used to monitor Joule heating. The voltage at which the curve shows positive deviation from linearity is designated the maximum operating potential after which Joule heating will occur. An efficient cooling system is required to thermostat the capillary. This is important for consistent migration times and minimal Joule heating.

The variance caused by thermal gradient can be expressed as [39]:

$$\sigma_{\text{temp}}^2 = \frac{r^6 E^6 \kappa^2 \Omega_T^2 \mu_{\text{app}}^2 t_M}{1536 D k_b^2} \quad (1.24)$$

where r is the capillary radius, E is the applied electric field, κ is the electric conductivity of BGE, Ω_T is the temperature coefficient for electrophoretic mobilities, μ_{app} is the apparent mobility, t_M is the migration time, D is the diffusion coefficient and k_b is the Boltzmann constant. From Equation 1.24, the use of a narrower capillary, a lower applied electric field or a lower conductivity buffer will reduce Joule heating band broadening.

1.4.3 Electromigration dispersion

Electromigration dispersion (EMD) occurs when there is a significant mismatch between the conductivity of the sample zone and the surrounding buffer. Figure 1.5.a shows an example for a sample with a higher conductivity compared to the surrounding buffer. A sample with higher mobility than the surrounding buffer will experience higher conductivity and a lower electric field

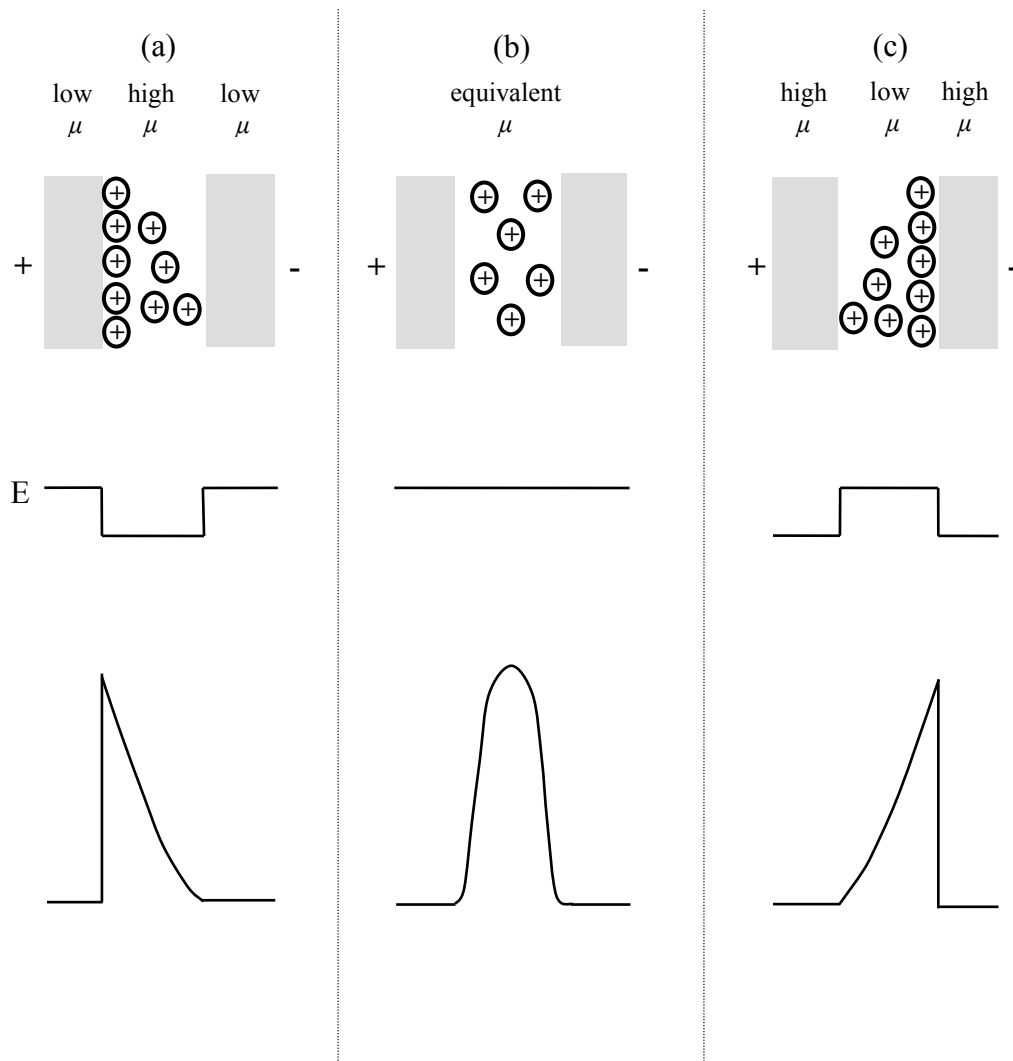


Figure 1.5: Schematic of Electromigration Dispersion (EMD) as a result of mismatched conductivity between the sample zone and the buffer. Adapted from reference [25].

strength. Ions in the sample zone move at lower velocity because the electric field is low. When the ions diffuse out of the sample zone to the surrounding buffer at left, they encounter a higher electric field strength and accelerate back into the sample zone – thus keeping the trailing edge of the peak sharp. Sample ions that diffuse out of the sample zone to the buffer at the right of Figure 1.5.a will encounter a higher electric field strength and accelerate in the direction of migration away from sample zone resulting in broad front. Alternately, a sample zone with lower conductivity than the surrounding buffer will experience a higher electric field strength. This results in a sharp front and broad trailing edge (Figure 1.5.c). A matched conductivity between the sample zone and the buffer (Figure 1.5.b) results in neither fronting nor tailing of the sample zone. EMD can be minimized by decreasing the field strength, injection length, sample concentration, and the mobility difference between the sample and buffer ions, or by increasing the buffer concentration [40, 41].

1.4.4 Injector band broadening

A large injection plug can cause band broadening. The variance caused by a rectangular injection plug can be expressed as [42]:

$$\sigma_{inj}^2 = \frac{V_{inj}^2}{12} = \frac{l_{inj}^2}{12} \quad (1.26)$$

where V_{inj}^2 is the volume injected in cm^3 and l_{inj}^2 is the length of the injected sample zone in cm. Thus, it is important to minimize the injection length to enhance separation efficiency. However, detection limit difficulties may

necessitate longer injection plugs. An ideal injection plug length should be less than the standard deviation caused by longitudinal diffusion, $(2Dt_M)^{1/2}$ [25]. Assuming that injection does not decrease efficiency by more than 10 %, the maximum length of an injection plug is given by [43-45]:

$$l_{inj} = \sqrt{2.4Dt_M} \quad (1.27)$$

where l_{inj} is the length of the sample plug and D is the diffusion coefficient. It is clear from Equation 1.27 that injection plug length band broadening affects large molecules (lower diffusion coefficients) and fast migrating peaks (shorter migration times) the most.

1.4.5 Detector band broadening

Online UV-visible detection is the most commonly used method of detection in CE and it has been used throughout this thesis. An optical detection window can be created by burning off the polyimide coating near the capillary outlet end. The length of the detection window is set by the cartridge aperture. Detector band broadening can be significant when the length of the sample zone is comparable to the length of detection window [44]. The variance resulting from detector band broadening can be expressed as:

$$\sigma_{det}^2 = \frac{l_{det}^2}{12} \quad (1.28)$$

where l_{det} is the length of the detection window. Broadening due to detection can be reduced by reducing the slit aperture but this may be limited if the radiant power reaching the detector becomes low enough to increase the detector noise [46]. The maximum length of the detection window that does not decrease efficiency by more than 10% is given by:

$$l_{\text{det}} = \sqrt{2.4Dt_M} \quad (1.29)$$

For a large molecule like a protein with a diffusion coefficient of $1 \times 10^{-6} \text{ cm}^2/\text{s}$, the maximum detection window is 380 μm when t_M is 10 min and 273 μm when t_M is 5 min. All work in this thesis was carried out with a cartridge aperture (slit width) of 200 μm .

Another source of band broadening that is related to detection is the speed of the detector electronics. The detector rise time (the time required for the detector output to increase from 10% to 90%) should be minimal to guarantee a sufficiently quick response to not broaden the peak. However, too fast of a rise time can lead to increased baseline noise. The maximum detector rise time that does not decrease efficiency by more than 10% is given by [44]:

$$t_{\text{rise,max}} = \sqrt{\frac{0.2Dt_M^3}{L_d^2}} \quad (1.30)$$

In addition, the data acquisition rate (Hz) should be fast enough to yield an actual representation of the peak, *i.e.* must sample the detector signal rapidly to

have enough data points so as to not distort the peak shape, height or area [47]. A good guideline is to acquire roughly 10 data points across one peak width at half height [47].

1.4.6 Solute-wall interaction

Adsorption of an analyte onto the capillary wall causes band broadening and deteriorates the separation efficiency. This adsorption introduces a chromatographic like retention and C-term band broadening which decreases the inherent high efficiency of CE. Analytes adsorb to the capillary wall through different mechanisms including electrostatic interactions with the negatively charged silanol groups, hydrogen bonding with protonated silanol groups and hydrophobic interactions [48]. The variance due to adsorption onto the capillary wall is given by [49]:

$$\sigma_{\text{ads}}^2 = \left[\frac{K^2 r^3}{(r + 2K)^3 D} + \frac{4r^2 K}{(r + 2K)^3 k_d} \right] \cdot v^2 t \quad (1.31)$$

where K is the equilibrium distribution coefficient of the analyte between the wall and the solution, r is the capillary radius, D is the diffusion coefficient, k_d is the desorption rate constant, v is the migration velocity of the analyte and t is the migration time of the analyte. The first term in the bracket on the right-hand side in Equation 1.31 is the broadening arising from the radial diffusion of the analyte to the capillary wall and the second term arises from the slow desorption kinetics. Extremely slow desorption kinetics can cause irreversible adsorption and total loss of the analyte.

The equilibrium distribution coefficient of the analyte is given by :

$$K = \frac{n_s}{n_m} \cdot \frac{V_m}{V_s} = k \cdot \beta \quad (1.32)$$

where n_s and n_m are the number of analyte moles in the stationary and mobile phases, V_s and V_m are the volumes of the stationary and mobile phases, k is retention factor of the analyte and β is the phase ratio. Both terms in Equation 1.31 are dependent on the equilibrium distribution coefficient and consequently the retention factor. Green and Jorgenson found that k values as low as 0.05 can decrease plate numbers for protein separations by 20 fold [50]. A decrease in the capillary i.d. increases the capillary surface/volume ratio resulting in lower β , higher k and increased adsorption interactions between the analyte and the capillary wall. The effect of capillary i.d. will be studied in Chapter Two.

Approaches that decrease the interaction between the analyte and the capillary wall will reduce the retention factor and thus reduce solute-wall adsorption band broadening. The work in this thesis focuses on the development of surfactant based coatings to minimize protein adsorption in CE.

1.5 Protein adsorption

1.5.1 Background

Large biomolecules like proteins suffer from extensive adsorption to the capillary wall. The main driving forces for protein adsorption are electrostatic and hydrophobic interactions as proteins possess large number of charged and

hydrophobic moieties [51]. The amino acid sequence of the protein determines its overall charge, its isoelectric point (pI) and its hydrophobic property. Electrostatic interactions are highly influenced by the pI of the protein and the pH of the buffer. Proteins with high pI > 7 (e.g. lysozyme, pI=11.3) possess an overall positive charge over the wide range of pH $< pI$. Such basic proteins experience strong electrostatic interactions with the negatively charged silica capillary wall. Acidic proteins (e.g. ovalbumin, pI =4.7) carry an overall negative charge when pH $> pI$. Despite the columbic repulsion between the anionic proteins and the silica surface, acidic proteins may still experience adsorption to the capillary wall but to a lesser extent than basic proteins [52]. Both the net charge of the protein and its charge localization influence the adsorption of a protein to the capillary surface. Protein configurations that bring more local positive charges close to the negatively charged capillary surface contribute more to the adsorption process [53].

Hydrophobic interaction is another important driving force for the adsorption of proteins to the capillary surface. Hydrophobic interactions occur between the hydrophobic patches of proteins represented by non polar amino acids and a hydrophobic surface. An increase in the hydrophobicity of the surface leads to increased protein adsorption [54].

The adsorption of proteins onto the capillary wall leads to degraded separations, including peak band broadening [55], migration time irreproducibility [56] and low sample recovery [52]. Lucy *et al.* wrote a review on theory of

protein adsorption, methods used to monitor protein adsorption and non-covalent capillary coatings used to minimize protein adsorption in CE [57]. Methods used to monitor protein adsorption are discussed in brief below.

1.5.2 Monitoring protein adsorption

Peak efficiency measures how narrow is the peak and is expressed in the number of theoretical plates (N) as detailed in Section 1.4. Peak efficiency is the most common method of monitoring protein adsorption and the effectiveness of capillary coatings used to minimize this adsorption. An experimentally determined efficiency (Equation 1.15) lower than the maximum theoretical limit based on longitudinal diffusion (Equation 1.21) indicates other sources of band broadening are occurring (*i.e.*, typically adsorption). Peak efficiency is generally an indicator of reversible adsorption [57]. However, peak asymmetry is also an indicator of adsorption. For instance, a peak tail that never returns back to the initial baseline level is an indicative of irreversible adsorption.

EOF measurements: Adsorption of protein onto the capillary surface alters the electroosmotic flow by altering the zeta potential within the capillary [52]. The EOF on a bare capillary can be determined by injecting a neutral marker. After protein samples have been injected, the EOF is again determined. A decrease in the EOF is an indicator of an altered zeta potential due to protein adsorption. If the EOF magnitude does not return to its original value after consecutive injections of the neutral marker (in the absence of proteins), this is an indicator of irreversible adsorption of the protein onto the capillary surface [58].

Migration time: The change in EOF caused by protein adsorption will lead to changes in the migration times of analytes. In addition, protein adsorbed on the capillary surface may introduce chromatographic like retention which would increase the migration time [50, 59] and broaden the peak.

Protein recovery: Towns and Regnier [60] developed the first method to quantify the protein loss inside the capillary as a measure of irreversible adsorption. A custom instrument with two online detectors positioned 50 cm apart along the capillary was used. The decrease in the peak area from the first to the second detector was considered a measure of irreversible adsorption. Yeung and Lucy [61] modified the previous technique for a one detector system compatible with commercial instruments. Triplicate separations of a protein sample were performed on a 47 cm capillary. The capillary was then cut to a length of 27 and another three separations were performed (injection conditions are adjusted to keep the injected volume constant). The decrease in the peak area from the short to the long capillary is a measure of irreversible adsorption.

The measures detailed above to monitor protein adsorption are useful to determine the effectiveness of approaches used for preventing protein adsorption. The following section will discuss in brief some of the approaches used to prevent protein adsorption.

1.5.3 Preventing protein adsorption in CE

Numerous approaches have been employed to minimize protein adsorption in CE. Extremely low pH buffers [62] have been used to fully protonate the

silanols so that the electrostatic interactions between the capillary wall and proteins are reduced. However, some proteins aggregate and precipitate under acidic conditions. At extremely high pH values, both proteins and the silica surface exhibit high negative charge density, and adsorption should be reduced due to electrostatic repulsion [56].

High ionic strength buffers compete with proteins for electrostatic adsorption sites on the silica surface, thus decreasing protein adsorption [50]. However, the resulting increase in conductivity requires the use of lower voltages and capillaries of smaller diameter to allow for efficient heat dissipation.

Small molecule buffer additives have been used to minimize protein adsorption. Zwitterionic additives (*e.g.* betaine) have been used with the advantage of not increasing the Joule heating but they yielded low efficiency separations [63]. Polyamines have been used to reduce protein adsorption under buffer conditions where amines are protonated [64].

Presently, the most common method to prevent adsorption is to coat the capillary surface. An ideal coating for CE should be stable, low cost, regenerable, prevent solute-wall interaction, maintain high separation efficiency and does not interfere with detection [57]. Coatings can be classified as covalently bonded phases, physically adsorbed static coatings, or dynamic coatings. Covalent coatings have high stability and are very effective at preventing protein adsorption [65]. However, drawbacks associated with covalent coatings include long preparation time, higher cost, lack of regeneration and limited pH stability.

Particularly of interest are “static” or “semipermanent” adsorbed coatings where the adsorbed material need not be in the run buffer [57]. Physically adsorbed coatings are easy to prepare, regenerable, and cost effective. Static adsorbed coatings based on surfactant bilayers will be the main focus of this thesis.

1.5.3.1 Surfactant coatings

Surfactants are amphiphilic molecules possessing both a hydrophobic tail and a hydrophilic head group. A surfactant concentration in solution higher than its critical aggregation concentration (CAC) results in aggregation of the free surfactant monomers to form micelles or vesicles. The packing factor of the surfactant determines the shape of the aggregate [66]. The packing factor is given by [67]:

$$P_f = \frac{V_c}{l_c a_h} \quad (1.33)$$

where V_c and l_c are the volume and length of the hydrophobic region of the surfactant and a_h is the cross sectional area of the head group. When the packing factor is $<1/3$ (e.g. sodium dodecyl sulfate, SDS), the surfactant molecule is conical in shape and packs as a spherical micelle (Figure 1.6.A). When the packing factor is $1/3-1/2$ (e.g. cetyltrimethylammonium bromide, CTAB), the surfactant has a truncated cone shape and forms spherical or cylindrical micelles depending on the solution conditions. When the packing factor is $1/2-1$ (e.g. didodecyldimethylammonium bromide, DDAB), the surfactant is cylindrical in shape and vesicles and bilayers are favored over micelles (Figure 1.6.B).

Two-tailed cationic surfactants (Figure 1.7) have the correct packing (i.e. cylindrical geometry) factor to form a bilayer on the inner surface of capillaries [68]. Formation of a bilayer rather than hemi-micelles such as formed by CTAB results in a more effective coating [68]. Fig 1.8 shows the separation of five basic proteins in bare, CTAB coated and DDAB coated capillaries [68]. In the bare capillary, two of the five proteins were irreversibly adsorbed and did not elute. Peaks of the other 3 proteins are broad and tailed, indicative of wall adsorption. In CTAB coated capillaries, three out of five proteins were separated with a recovery of 80 % but the other two proteins never eluted. Using a DDAB coated capillary, all five proteins were separated with recoveries ranging from 85% to 100%. The enhanced coating performance and protein recoveries with DDAB were attributed to the increased capillary surface coverage with DDAB bilayer whereas the hemi-micelle surface structure of CTAB leaves significant gaps in the surface coating.

Single-tailed cationic surfactants such as CTAB form dynamic coatings, i.e. the surfactant must be present in the BGE to maintain the coating. The presence of free surfactant molecules in the BGE may interfere with the detection scheme. For instance, dynamic coatings or small-molecule additives may complicate online MS analysis of proteins separated by CE. Coating material entering the mass spectrometer may lead to suppression of analyte signals and/or contamination of the ion source [69]. An added benefit of two-tailed cationic surfactants is that they form static or semipermanent coatings, i.e., the surfactant does not have to be in the running buffer. The enhanced stability results from the bilayer structure at the capillary surface [68].

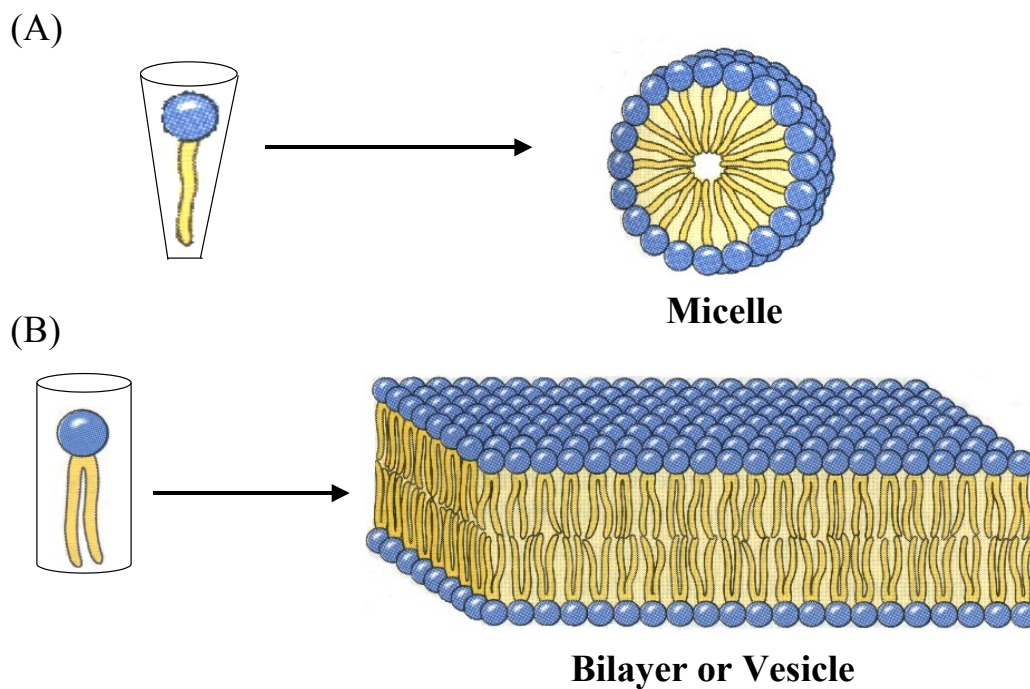
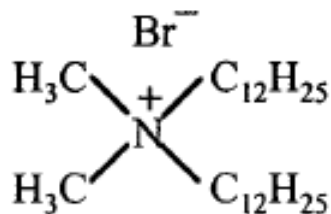
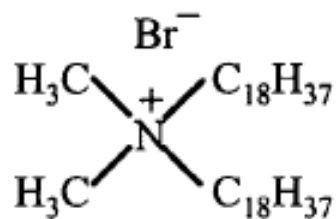


Figure 1.6: Aggregate structures of (A) single-tailed surfactant and (B) two-tailed surfactant. Reprinted with permission from reference [66]. Copyright (2000) American Chemical Society.



Didodecyldimethylammonium
bromide (**DDAB**)



Diocetadecyldimethylammonium
bromide (**DODAB**)

Figure 1.7: Structure of two-tailed cationic surfactants used as capillary coatings

Table 1.1: Physico-chemical properties of two-tailed cationic surfactants used as capillary coatings

Surfactant	CMC ^a (10 ⁻³ mM)	Chain melting temperature T _m (° C)
DDAB	35	16 [70]
DODAB	0.0037	45 [70]

^a Calculated based on reference [71].

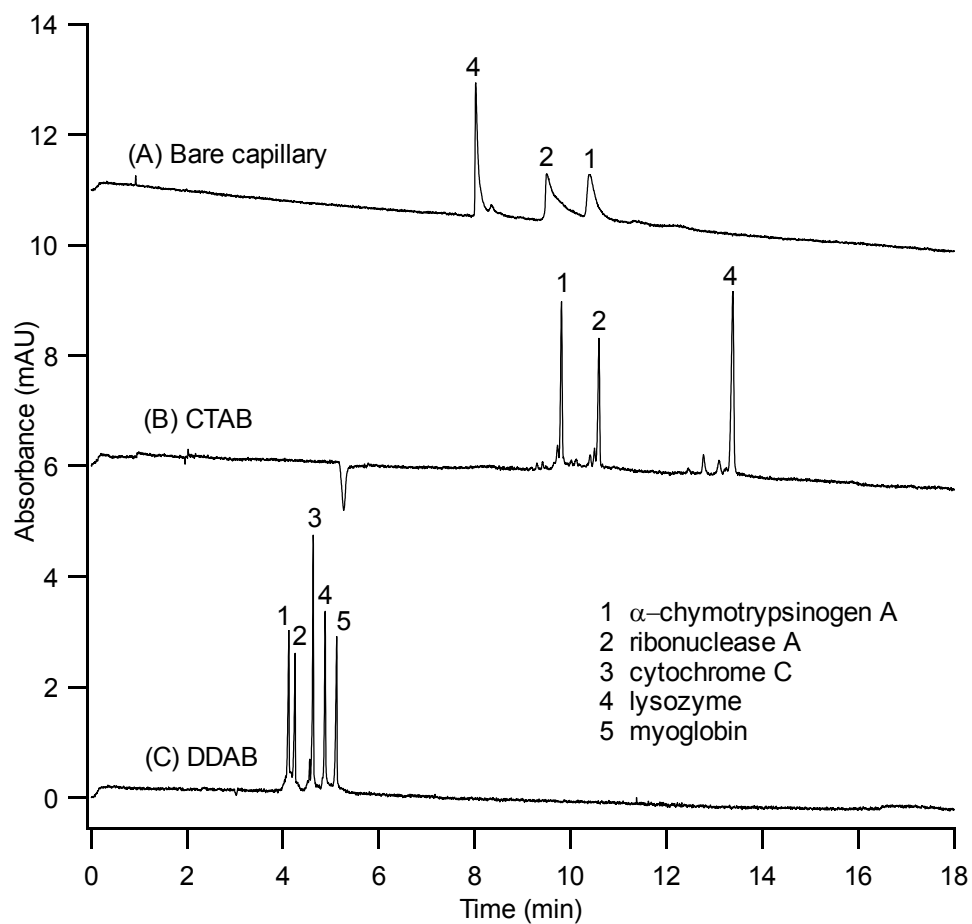


Figure 1.8: Separation of five basic proteins at pH 3 using (A) bare capillary; (B) CTAB-coated capillary; and (C) DDAB-coated capillary. Reprinted with permission from reference [68]. Copyright (2001) American Chemical Society.

Experimental conditions: 50-cm capillary (40 cm to detector); UV detection at 214 nm; +15 kV applied voltage (A), -15 kV applied voltage (B, C); buffer, 25 mM phosphate buffer at pH 3.0 containing (A) no surfactant, (B) 0.5 mM CTAB, or (C) 0.1 mM DDAB. Note that the myoglobin peak was not observed after a 40-min run time in (B).

A longer alkyl chain analogue of DDAB is dioctadecyldimethyl ammonium bromide (DODAB). The longer alkyl chain results in lower critical vesicle concentration (CVC) (Table 1.1) [71]. Yassine and Lucy demonstrated that the use of longer alkyl chain surfactants enhanced stability of semipermanent bilayer coatings [72] as a direct consequence of the lower CVC. Using a DODAB coated capillary, 60 successive high efficiency separations of proteins could be performed without any regeneration of the coating [72].

Only capillary coatings based on two-tailed cationic surfactants and particularly DODAB will be studied in this thesis. My coatings will be characterized based on migration time reproducibility, EOF stability and protein separation efficiency.

1.6 Thesis Overview

Adsorption of protein onto the capillary silica surface leads to degraded CE separations. Capillary coatings are the most common way to minimize this adsorption. Two-tailed cationic surfactants are of interest since they form semipermanent physically adsorbed capillary coatings which are easy to prepare, stable and cost effective. The aims of this thesis are: to investigate factors that affect the stability of two-tailed cationic surfactant coatings, to generate a series of tailored coatings based on two-tailed cationic surfactants, and to investigate new application of the developed coatings. Chapter Two studies the impact of small i.d. capillaries (5-25) μm on the stability of surfactant bilayer cationic coatings and on the efficiency of separation of basic proteins. In Chapter Three, a surfactant bilayer/diblock copolymer coating is developed to tune the EOF and minimize protein adsorption. The coating has been applied to the separation of basic, acidic and histone proteins. In Chapter Four, the surfactant bilayer/diblock copolymer coating is applied to a different mode of CE; capillary isoelectric focusing (cIEF). The ability to tune the EOF enabled both single-step cIEF and two-step cIEF to be performed. Chapter Five explores the use of a series of POE diblock copolymers as capillary coatings. Factors affecting the stability and the EOF of these coatings have been studied. The effects of the hydrophilic and hydrophobic chain lengths, buffer counter ions, pH and mixed organic-aqueous conditions were all studied. Chapter Six investigates the stability of DODAB under alkaline conditions. Chapter Seven summarizes studies performed in this thesis and suggests further areas of investigation.

1.7 References

- [1] Hardy, W. B., *J. Physiol.* 1905, 33, 251-337.
- [2] Tiselius, A., *Trans. Faraday Soc.* 1937, 33, 524-530.
- [3] Raymond, S. and Weintraub, L., *Science* 1959, 130, 711.
- [4] Hjertén, S., *Chromatogr. Rev.* 1967, 9, 122-219.
- [5] Virtanen, R., *Acta Polytech. Scand.* 1974, 123, 1-67.
- [6] Mikkers, F. E. P., Everaerts, F. M. and Verheggen, T., *J. Chromatogr.* 1979, 169, 11-20.
- [7] Jorgenson, J. W. and Lukacs, K. D., *Anal. Chem.* 1981, 53, 1298-1302.
- [8] Dovichi, N. J. and Zhang, J. Z., *Angew. Chem., Int. Ed.* 2000, 39, 4463-4468.
- [9] Desiderio, C., Rossetti, D. V., Iavarone, F., Messina, I. and Castagnola, M., *J. Pharm. Biomed. Anal.* 2010, 53, 1161-1169.
- [10] Kami, K., Fujimori, T., Sato, H., Sato, M., Yamamoto, H., Ohashi, Y., Sugiyama, N., Ishihama, Y., Onozuka, H., Ochiai, A., Esumi, H., Soga, T. and Tomita, M., *Metabolomics* 2013, 9, 444-453.
- [11] Altria, K., Marsh, A. and Sanger-van de Griend, C., *Electrophoresis* 2006, 27, 2263-2282.
- [12] Elbashir, A. A. and Aboul-Enein, H. Y., *Biomed. Chromatogr.* 2010, 24, 1038-1044.
- [13] Cruces-Blanco, C., Gamiz-Gracia, L. and Garcia-Campana, A. M., *TrAC, Trends Anal. Chem.* 2007, 26, 215-226.
- [14] Pinero, M. Y., Bauza, R. and Arce, L., *Electrophoresis* 2011, 32, 1379-1393.
- [15] Dickerson, J. A., Ramsay, L. M., Dada, O. O., Cermak, N. and Dovichi, N. J., *Electrophoresis* 2010, 31, 2650-2654.
- [16] Zhang, Z. X., Du, X. Z. and Li, X. M., *Anal. Chem.* 2011, 83, 1291-1299.
- [17] Terabe, S., Otsuka, K., Ichikawa, K., Tsuchiya, A. and Ando, T., *Anal. Chem.* 1984, 56, 111-113.
- [18] Lin, J., Tan, Q. and Wang, S., *J. Sep. Sci.* 2011, 34, 1696-1702.

- [19] Cooper, J. W., Wang, Y. J. and Lee, C. S., *Electrophoresis* 2004, 25, 3913-3926.
- [20] Zhu, Z., Lu, J. J. and Liu, S., *Anal. Chim. Acta* 2012, 709, 21-31.
- [21] Barron, A. E. and Blanch, H. W., *Sep. Purif. Methods* 1995, 24, 1-118.
- [22] Malá, Z., Gebauer, P. and Boček, P., *Electrophoresis* 2013, 34, 19-28.
- [23] Simal-Gandara, J., *Crit. Rev. Anal. Chem.* 2004, 34, 85-94.
- [24] Landers, J. P. (Ed.), *Handbook of Capillary and Microchip Electrophoresis and Associated Microtechniques*, CRC Press, Boca Raton 2008.
- [25] Heiger, D. (Ed.), *An Introduction High Performance Capillary Electrophoresis*, Agilent Technologies, Germany 2000.
- [26] Swinney, K. and Bornhop, D. J., *Electrophoresis* 2000, 21, 1239-1250.
- [27] Harris, D. C. (Ed.), *Quantitative Chemical Analysis* New York 2007.
- [28] Chervet, J. P., Vansoest, R. E. J. and Ursem, M., *J. Chromatogr.* 1991, 543, 439-449.
- [29] Heiger, D. N., Kaltenbach, P. and Sievert, H. J. P., *Electrophoresis* 1994, 15, 1234-1247.
- [30] Xue, Y. J. and Yeung, E. S., *Anal. Chem.* 1994, 66, 3575-3580.
- [31] Schwer, C. and Kenndler, E., *Anal. Chem.* 1991, 63, 1801-1807.
- [32] Bard, A. J. and Faulkner, L. R., *Electrochemical Methods : Fundamentals and Applications*, John Wiley & Sons, Inc., New York 2001.
- [33] Zhou, M. X. and Foley, J. P., *Anal. Chem.* 2006, 78, 1849-1858.
- [34] Smoluchowski, M. V., *Bull. Int. Acad. Sci. Cracovie* 1903, 184.
- [35] Gas, B., Stedry, M. and Kenndler, E., *J. Chromatogr. A* 1995, 709, 63-68.
- [36] Knox, J. H. and Grant, I. H., *Chromatographia* 1987, 24, 135-143.
- [37] Fu, S. L. and Lucy, C. A., *Anal. Chem.* 1998, 70, 173-181.
- [38] Huang, X. H., Coleman, W. F. and Zare, R. N., *J. Chromatogr.* 1989, 480, 95-110.

- [39] Grossman, P. D. and Colburn, J. C., *Capillary Electrophoresis Theory and Practice*, Academic Press, Inc., San Diego, CA 1992.
- [40] Yassine, M. M. and Lucy, C. A., *Electrophoresis* 2006, 27, 3066-3074.
- [41] Macdonald, A. M., *Ph.D. Thesis* 2008, Chemistry, University of Alberta, Edmonton.
- [42] Sternberg, J. C., *Adv. Chromatogr.* 1966, 2, 206-270.
- [43] Grushka, E. and McCormick, R. M., *J. Chromatogr. A* 1989, 471, 421-428.
- [44] Lucy, C. A., Yeung, K. K. C., Peng, X. J. and Chen, D. D. Y., *LC-GC* 1998, 16, 26-32.
- [45] Otsuka, K. and Terabe, S., *J. Chromatogr.* 1989, 480, 91-94.
- [46] Walbroehl, Y. and Jorgenson, J. W., *J. Chromatogr.* 1984, 315, 135-143.
- [47] Hinshaw, J. V., *Lc Gc North America* 2001, 19, 1136.
- [48] Ermakov, S. V., Zhukov, M. Y., Capelli, L. and Righetti, P. G., *J. Chromatogr. A* 1995, 699, 297-313.
- [49] Minarik, M., Gas, B., Rizzi, A. and Kenndler, E., *J. Cap. Elec.* 1995, 2, 89-96.
- [50] Green, J. S. and Jorgenson, J. W., *J. Chromatogr.* 1989, 478, 63-70.
- [51] Norde, W. and Haynes, C. A., *Proteins at Interfaces II: Fundamentals and Applications*, American Chemical Society, Washington, DC 1995.
- [52] Towns, J. K. and Regnier, F. E., *Anal. Chem.* 1992, 64, 2473-2478.
- [53] Yao, Y. and Lenhoff, A. M., *Anal. Chem.* 2004, 76, 6743-6752.
- [54] Zhao, Z. X., Malik, A. and Lee, M. L., *Anal. Chem.* 1993, 65, 2747-2752.
- [55] Schure, M. R. and Lenhoff, A. M., *Anal. Chem.* 1993, 65, 3024-3037.
- [56] Lauer, H. H. and McManigill, D., *Anal. Chem.* 1986, 58, 166-170.
- [57] Lucy, C. A., MacDonald, A. M. and Gulcev, M. D., *J. Chromatogr. A* 2008, 1184, 81-105.

- [58] Graf, M., Garcia, R. G. and Watzig, H., *Electrophoresis* 2005, 26, 2409-2417.
- [59] Fang, N., Zhang, H., Li, J. W., Li, H. W. and Yeung, E. S., *Anal. Chem.* 2007, 79, 6047-6054.
- [60] Towns, J. K. and Regnier, F. E., *Anal. Chem.* 1991, 63, 1126-1132.
- [61] Yeung, K. K. C. and Lucy, C. A., *Anal. Chem.* 1997, 69, 3435-3441.
- [62] McCormick, R. M., *Anal. Chem.* 1988, 60, 2322-2328.
- [63] Bushey, M. M. and Jorgenson, J. W., *J. Chromatogr.* 1989, 480, 301-310.
- [64] Corradini, D., Bevilacqua, L. and Nicoletti, I., *Chromatographia* 2005, 62, S43-S50.
- [65] Doherty, E. A. S., Meagher, R. J., Albarghouthi, M. N. and Barron, A. E., *Electrophoresis* 2003, 24, 34-54.
- [66] Melanson, J. E., Baryla, N. E. and Lucy, C. A., *Anal. Chem.* 2000, 72, 4110-4114.
- [67] Israelachvili, J. N., *Intermolecular and Surface Forces*, Academic Press, London 1992.
- [68] Baryla, N. E., Melanson, J. E., McDermott, M. T. and Lucy, C. A., *Anal. Chem.* 2001, 73, 4558-4565.
- [69] Rundlett, K. L. and Armstrong, D. W., *Anal. Chem.* 1996, 68, 3493-3497.
- [70] Feitosa, E., Jansson, J. and Lindman, B., *Chem. Phys. Lipids* 2006, 142, 128-132.
- [71] Svitova, T. F., Smirnova, Y. P., Pisarev, S. A. and Berezina, N. A., *Colloids Surf., A* 1995, 98, 107-115.
- [72] Yassine, M. M. and Lucy, C. A., *Anal. Chem.* 2005, 77, 620-625.

Chapter Two: Surfactant bilayer coatings in narrow-bore capillaries in capillary electrophoresis*

2.1 Introduction

Capillary electrophoresis is a technique commonly utilized in the analysis of various analytes due to its speed and efficiency. Typically, CE capillaries with inner diameters (i.d.) ranging from 25 to 75 μm are used. However, electrophoretic separations have been performed with capillary i.d. ranging from 2 to 10 μm [1-9]. These capillaries have been commonly used as a means to study biological microenvironments such as intracellular contents [1, 2, 4-8, 10]. Investigation of cellular response through single cell analysis may provide insight in proteomics as well as other biological systems [11]. Further, capillaries with small i.d. ($< 25 \mu\text{m}$) are comparable in size to microchip channel depths.

Analyte adsorption in CE and microfluidics results in reduced efficiency, poor migration time reproducibility and irreversible loss of analyte [12]. Methods traditionally employed to reduce adsorption include: extreme pH buffers [13-15], high salt concentrations [14-16] and buffer additives [15, 16]. High ionic strength buffers and the zwitterionic additive betaine were used to reduce the protein-wall interactions, which resulted in improved resolution, protein efficiency and migration time reproducibility [16]. Presently, the most common method to

* A version of this chapter has been published as Makedonka D. Gulcev, Teague McGinitie, Mahmoud F. Bahnasy and Charles A. Lucy, "Surfactant bilayer coatings in narrow-bore capillaries in capillary electrophoresis", *Analyst*, 135 (10), 2688-2693, 2010.

prevent adsorption is to coat the surface [12, 17]. Coatings can be covalently bonded phases [18-23], physically adsorbed polymer coatings [23-32] or dynamic coatings [33-35].

Surfactants can form capillary coatings which enable efficient protein separations [36-39]. Two-tailed surfactants such as didodecyldimethylammonium bromide (DDAB) and dioctadecyldimethylammonium bromide (DODAB) possess the correct packing factor (i.e., a cylindrical geometry) to form a supported bilayer on a flat surface [34]. Formation of a bilayer rather than hemimicelles (such as formed by cetyltrimethylammonium bromide, CTAB) results in better coating of the surface as reflected by near quantitative recovery of protein (85-100% vs. 0-81% for CTAB) [34]. The formation of a bilayer also increases the stability of the surfactant coating such that surfactant does not need to be present in the separation buffer. Using 25 μm i.d. DODAB-coated capillary, sixty separations of model cationic proteins were performed over a 12 day period with efficiencies of 300 000-400 000 plates/m without regeneration of the coating [37].

Previous studies have observed that the i.d. of the capillary can influence the efficiency and stability of the surfactant bilayer coatings. Westerlund and co-workers noted enhanced protein efficiencies in 25 μm i.d. capillaries coated with DDAB compared to 50 μm i.d. capillaries (980 000 – 1 140 000 plates/m vs. 490 000-530 000 million plates/m, respectively) [39]. Using DDAB, Yassine and Lucy observed increased stability for the bilayer coating as the capillary i.d. was

decreased from 100 to 25 μm [36]. Thus, there appear to be advantages to using surfactant based coatings in narrow channel domains.

Herein, the previous studies are extended to investigate the impact of narrow capillary diameters ($\leq 25 \mu\text{m}$) on the stability of surfactant bilayer coatings and on the efficiency of separations of model cationic proteins. To illustrate the applicability of the proposed coatings in smaller i.d. capillaries, the separation of cationic neurotransmitters was performed on a DODAB-coated 5 μm i.d. capillary.

2.2 Experimental

2.2.1 Apparatus

All capillary electrophoresis experiments were conducted on a Hewlett Packard ^{3D}CE instrument equipped with a UV absorbance detector. Detection of proteins was performed at 214 nm. Detection of neurotransmitters was performed at 200 nm. Data acquisition at 10 Hz was carried out on a Pentium II HP personal computer running HP ^{3D}CE ChemStation. Untreated fused-silica capillaries (Polymicro Technologies, Phoenix, AZ, USA) of total length 32 cm (23 cm to the detector) with i.d. of 25, 10 and 5 μm and o.d of 365 μm were used. An external N₂ source (connected using HP attachments) was used for high pressure rinses (up to 8 bar) and injections. The capillary temperature was maintained at 25°C.

2.2.2 Chemicals

All solutions were prepared using Nanopure 18-M Ω ultrapure water (Barnstead, Dubuque, IA, USA). Lithium acetate buffers were prepared from

lithium acetate dihydrate (Aldrich, Milwaukee, WI, USA) and adjusted to pH 5.0 using glacial acetic acid (Anachemia Canada Inc., Montreal, QC, Canada). Tris-phosphate buffers were prepared from phosphoric acid and adjusted to pH 5.0 using Tris(hydroxymethyl) aminomethane, 99.9+% (Aldrich). The cationic surfactants DDAB and DODAB and cationic proteins α -chymotrypsinogen A – α -chymo A (bovine pancreas), cytochrome *c* – cyto *c* (bovine heart), lysozyme - lyso (chicken egg white) and ribonuclease A – RNase A (bovine pancreas) were used as received from Sigma (Oakville, ON, Canada). Protein standards were dissolved in Nanopure water to a final concentration of 0.2 mg/mL. The neurotransmitters epinephrine, dopamine, ephedrine and serotonin were used as received from Sigma. Neurotransmitter standards were dissolved in Nanopure water to a final concentration of 0.1 mg/mL for epinephrine, dopamine and serotonin and 0.2 mg/mL for ephedrine.

2.2.3 Surfactant Preparation

DDAB solutions (2 mM) were prepared by dissolving the surfactant in lithium acetate buffer. The surfactant buffer mixtures were sonicated for 30 min at 25°C and then stirred for 15 min. This sonication/stir cycle was repeated until a clear solution was obtained. Typically 2 cycles were needed. The same procedure was followed for the 0.5 mM DODAB coating solution except that the bath sonicator temperature used was 60°C. The surfactant solution was then allowed to cool to room temperature before use. Fresh surfactant solutions were prepared daily.

2.2.4 Coating Procedure

The number of capillary volumes of coating solution flushed through the capillary was held constant for the various i.d. capillaries by varying the pressure and time used for rinses. All new capillaries were pretreated with 1.0 M sodium hydroxide (EMD Chemicals Inc., Gibbstown, NJ, USA) followed by Nanopure water and afterwards coated with the surfactant solution (either 2 mM DDAB or 0.5 mM DODAB). Finally, the capillaries were flushed with buffer (void of surfactant) to remove any non-adsorbed surfactant. The capillaries were not recoated between runs.

2.2.5 Protein Separations

New capillaries were used for capillary-to-capillary studies. New capillaries were preconditioned and coated as outlined in Section 2.2.4 above. Protein solutions were injected hydrodynamically and separated using -10 kV. The injection volume was held constant at 0.007 capillary volumes regardless of the capillary i.d. by varying the injection time.

Under ideal conditions in CE, peak broadening is governed solely by longitudinal diffusion; the plate number (N) under this condition is:

$$N = \frac{\mu_{\text{app}} V L_d}{2D L_t} \quad (2.1)$$

where μ_{app} is the apparent mobility of the proteins, V is the applied voltage, L_d and L_t are the capillary length to detector and total length, and D is the diffusion coefficient (0.9×10^{-6} cm²/s for α -chymo A; 1.1×10^{-6} cm²/s for RNase A; 1.4×10^{-6} cm²/s for cyto *c*; 1.1×10^{-6} cm²/s for lyso) [38]. Peak efficiencies were

calculated using the HP ChemStation software using the peak width at half height method, and are reported as the average of ten successive runs. However, the presence of wall adsorption in CE introduces a C-term to the broadening behavior [12, 40]. Thus, plates/m are commonly reported in the literature for protein separations by CE. Both plates and plates/m will be used throughout this chapter to allow comparison to theory and the literature.

The limit of detection (LOD) of the four standard cationic proteins on a 5 μm DODAB-coated capillary was determined. For each protein, the peak height was measured for a series of concentrations of 0.2, 0.4, 0.6, 0.8 and 1 mg/mL. The LOD was determined using:

$$\text{LOD} = \frac{3s_{\text{blank}}}{m} \quad (2.2)$$

where s_{blank} is the standard deviation for replicate determinations of peak height of the blank (50 mM Li Acetate pH 5.0) and m is the slope of linear calibration curve for the peak height measurements of the protein.

2.2.6 Durability and Reproducibility of DODAB in 5 μm capillaries

The performance of the DODAB coating on a 5 μm i.d. capillary was evaluated for: 1) short term stability by performing repetitive consecutive injections of the cationic proteins α -chymo A, cyto *c*, lyso, and RNase A without any regeneration or recoating of the capillary during the experiment; 2) long-term stability by performing 10 successive injections per day for 30 consecutive days without regenerating or refreshing the capillary; and 3) comparing the capillary-to-capillary reproducibility.

2.2.7 Separation of Neurotransmitters

New capillaries were used for the neurotransmitter work. Capillary preconditioning and coating procedures were identical to those outlined in Section 2.2.4. Neurotransmitters were injected hydrodynamically and separated using -30 kV. The separation buffer was 150 mM Tris-phosphate pH 5.0. The neurotransmitters separated (and their respective concentrations) were: epinephrine (0.1 mg/mL), dopamine (0.1 mg/mL), ephedrine (0.2 mg/mL), and serotonin (0.1 mg/mL).

2.3 Results and Discussion

The use of narrow bore capillaries is common in the analysis of biological microenvironments such as the contents of a single cell [1, 2, 4-8]. Biomolecules such as proteins and neurotransmitters may adsorb onto the surface of the bare capillaries leading to reduced efficiency, poor migration time reproducibility and low recovery [12]. Such adsorption is more significant in narrow capillaries.

As the capillary diameter decreases, the surface-to-volume ratio increases. In the presence of adsorption, an increase in the surface-to-volume ratio leads to increase in the retention factor of the analyte (Equation 1.32 in Chapter One). This leads to an increase in the adsorptive interactions between the solutes and the capillary resulting in increased C-term band broadening [2, 4, 5, 41, 42]. Moreover, such broadening can be so severe that in their seminal theoretical study, Schure and Lenhoff concluded there is little benefit to using smaller i.d. capillaries for large biomolecules if adsorption occurs [43].

Thus, performing separations in narrow capillaries is a rigorous test of the effectiveness of a capillary coating. In this study we evaluate the efficiency achieved in the separation of four standard cationic proteins as the capillary diameter is decreased. Also, for semi-permanent coatings such as surfactant bilayers, the stability of the coating is an additional important factor [36]. Previously it was observed that increased bilayer stability was achieved by decreasing the capillary i.d. from 100 to 25 μm [36]. To determine whether this trend extends to smaller i.d. capillaries, the reproducibility of both the migration time and peak efficiencies for the protein separations were also monitored in long-term studies using 5 μm capillaries.

2.3.1 Effect of inner diameter (i.d.) on DDAB coating performance

In the following study, 2 mM DDAB was used to coat the capillary. The capillary was coated at the start of the study, after which the excess DDAB was rinsed from the capillary. Following this, 40 successive injections of protein (200 min) were performed without regenerating the coating. Figures 2.1, 2.2 and 2.3 summarize the results of this experiment. In all of the capillaries, the migration times increase from run to run. In the absence of surfactant in the separation buffer, some of the bilayer dissolves to saturate the separation buffer, resulting in a gradual degradation of the coating [37]. The decrease in the anodic EOF results in an increase in migration time from run to run, and reflects the instability of the coating. Table 2.1 presents the migration time RSDs for the initial and final 10 runs (run-to-run for runs 1-10 and 31-40) of the various i.d. capillaries studied. Efficiencies are also reported in Table 2.1.

Figure 2.1 shows the performance of the 2 mM DDAB coating in a 25 μm i.d. capillary. The protein efficiencies for the first 10 consecutive injections (900 000-1 000 000 plates/m, Table 2.1) are comparable to those achieved by Yassine and Lucy (750 000- 1 050 000 plates/m) [36] and Westerlund and co-workers (980 000-1 140 000 plates/m) [39]. Further, Westerlund and co-workers demonstrated that the DDAB coating was stable in 25 μm capillaries for 14 consecutive runs (at least 100 min) without any recoating [39]. The results in Table 2.1 confirm this observation. However, as continued injections are performed without regenerating the coating, the peak efficiencies decrease from 900 000-1 000 000 plates/m (210 000-240 000 plates) for the initial 10 runs to 300 000-400 000 plates/m (70 000-90 000 plates) for the 31st-40th runs (Table 2.1). There is also drift in migration time (t_M) of the proteins (1.6-1.9% over the first 10 runs (Table 2.1) and 5.5-6.4% RSD over the entire 40 runs). The early reproducibility is comparable to that of Westerlund and co-workers, who observed protein migration time RSDs of 1.8-2.9 % (n=10) [39].

Figure 2.2 displays separations performed in a DDAB-coated 10 μm i.d. capillary. The protein efficiencies observed for the first 10 runs were 1 900 000-2 300 000 plates/m (440 000-540 000 plates) given in Table 2.1. Efficiencies decreased over the 40 consecutive runs (200 min), but remained much higher (1 500 000-2 000 000 plates/m, 360 000-470 000 plates) for runs 31-40 than for analogous runs in the 25 μm capillary case (300 000-400 000 plates/m). Similarly, the migration time reproducibility in the 10 μm i.d. capillary (3.8-4.6% RSD, n=40) were much improved over that observed for the 25 μm i.d.

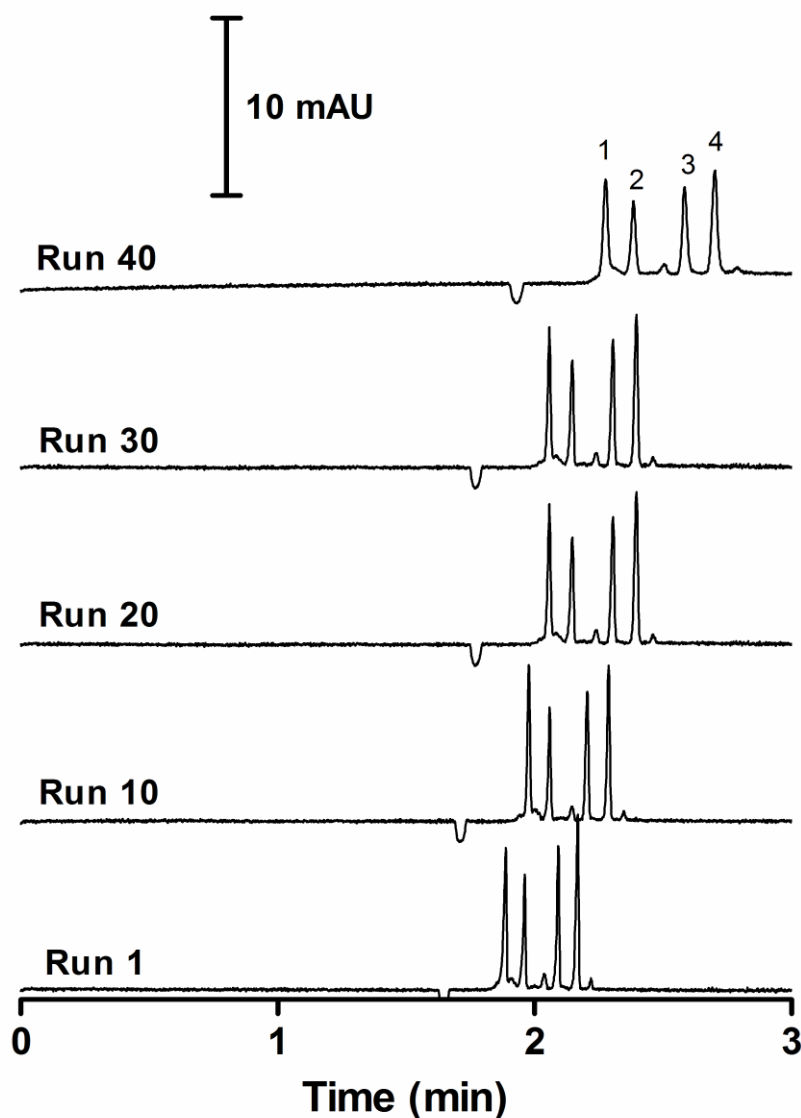


Figure 2.1: Separation of cationic proteins on 25 μm i.d. capillary using a 2 mM DDAB coating. The electropherograms have been offset along the y-axis to show successive runs. Proteins labeled: (1) α -chymotrypsinogen A, (2) ribonuclease A, (3) cytochrome *c* and (4) lysozyme.

Experimental conditions: Cationic surfactant coating was reconstituted in 50 mM Li acetate pH 5.0 buffer. Applied voltage, -10 kV; capillary, 32 cm (23 cm to detector); separation buffer, 50 mM Li acetate pH 5.0; λ (nm), 214; 0.2 mg/mL protein sample dissolved in water and injected hydrodynamically at 5 kPa for 6.6 s.

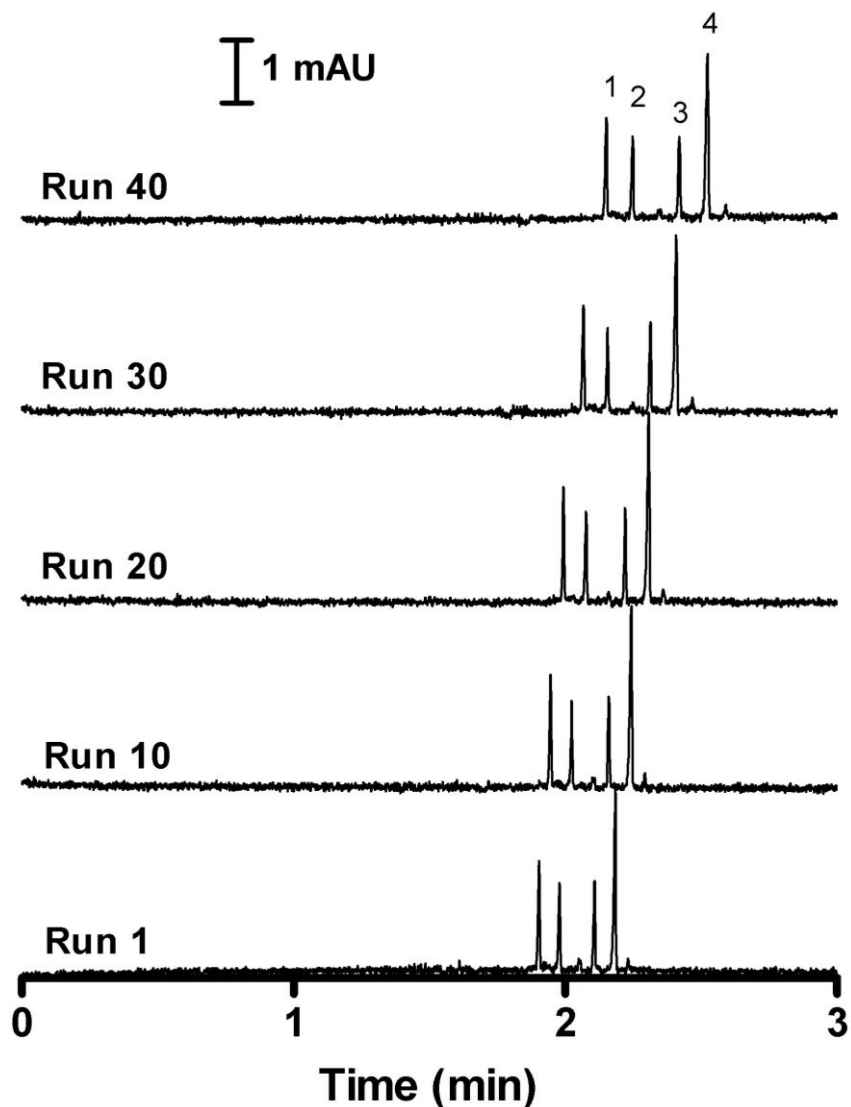


Figure 2.2: Separation of cationic proteins on 10 μm i.d. capillary using a 2 mM DDAB coating. The electropherograms have been offset along the y-axis to show successive runs. Proteins labeled: (1) α -chymotrypsinogen A, (2) ribonuclease A, (3) cytochrome *c* and (4) lysozyme.

Experimental conditions: Cationic surfactant coating was reconstituted in 50 mM Li acetate pH 5.0 buffer. Applied voltage, -10 kV; capillary, 32 cm (23 cm to detector); separation buffer, 50 mM Li acetate pH 5.0; λ (nm), 214; 0.2 mg/mL protein sample dissolved in water and injected hydrodynamically at 5 kPa for 45 s.

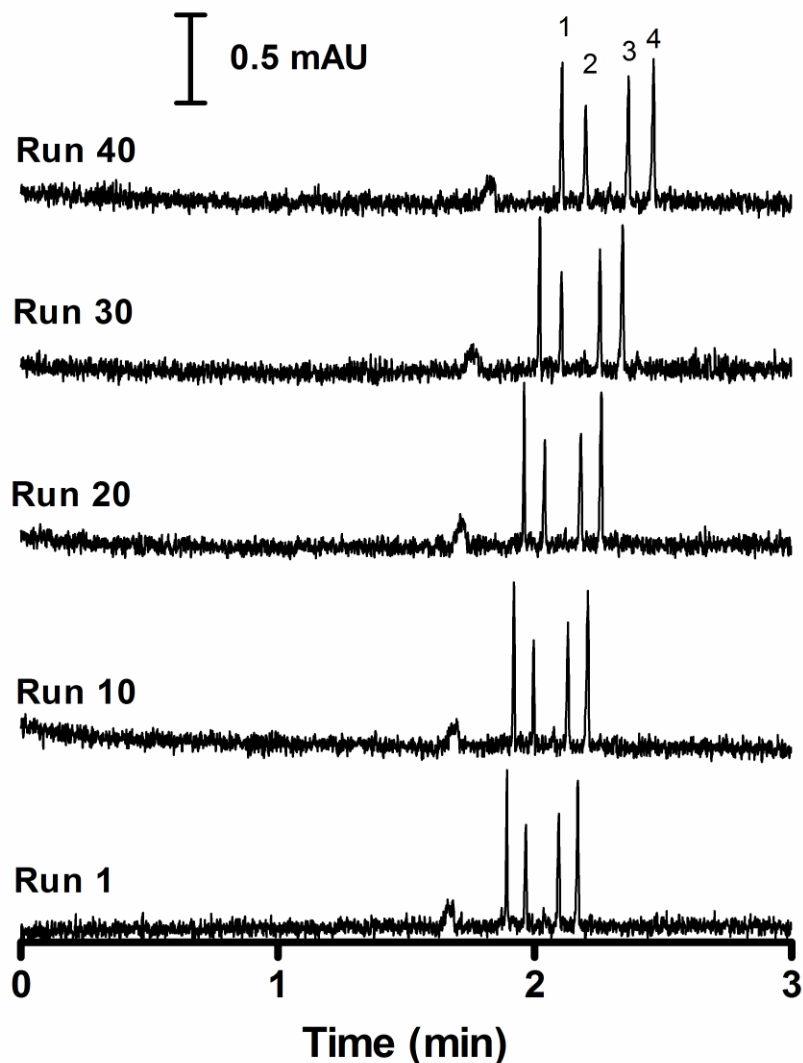


Figure 2.3: Separation of cationic proteins on 5 μm i.d. capillary using a 2 mM DDAB coating. The electropherograms have been offset along the y-axis to show successive runs. Proteins labeled: (1) α -chymotrypsinogen A, (2) ribonuclease A, (3) cytochrome *c* and (4) lysozyme.

Experimental conditions: Cationic surfactant coating was reconstituted in 50 mM Li acetate pH 5.0 buffer. Applied voltage, -10 kV; capillary, 32 cm (23 cm to detector); separation buffer, 50 mM Li acetate pH 5.0; λ (nm), 214; 0.2 mg/mL protein sample dissolved in water and injected hydrodynamically at 5 kPa for 180 s.

Table 2.1: Migration Times Reproducibility (%RSD) and Protein Efficiencies on various i.d. capillaries coated with 2 mM DDAB

Runs	Capillary (i.d) μm	α -Chymotryp. A		Ribonuclease A		Cytochrome c		Lysozyme	
		%RSD t_m	Plates/m ($\times 10^3$)	%RSD t_m	Plates/m ($\times 10^3$)	%RSD t_m	Plates/m ($\times 10^3$)	%RSD t_m	Plates/m ($\times 10^3$)
1-10	25	1.5	910	1.9	930	1.6	1 000	1.7	990
	10	0.92	2 100	0.78	2 200	0.85	2 300	1.6	1 900
	5	0.47	2 200	0.48	2 000	0.53	1 900	0.54	2 000
31-40	25	1.4	300	1.5	300	1.6	400	1.7	400
	10	1.2	1 800	1.2	2 000	1.2	2 000	1.4	1 500
	5	1.3	2 100	1.3	2 000	1.4	1 600	1.5	1 900

Experimental Conditions: Cationic surfactant coating was prepared in 50 mM lithium acetate (pH 5.0). Applied voltage, -10 kV; capillary, 32 cm in total length and 23 cm to detector; separation buffer, 50 mM lithium acetate pH 5.0; λ (nm), 214; injection, 0.007 capillary volumes of 0.2 mg/mL of each protein in water introduced hydrodynamically.

capillary (5.5-6.4 %RSD, n=40). Nonetheless, there is still noticeable drift in the migration times in Figure 2.2. (5.5-6.4 %RSD, n=40).

Finally, Figure 2.3 demonstrates the stability of DDAB coating in a 5 μm i.d. capillary. Throughout the 40 runs the protein efficiencies remained constant: 1 900 000-2 200 000 (450 000-510 000 plates) for the first 10 runs and 1 600 000-2 100 000 plates/m (370 000-480 000 plates) for the 31st-40th runs (Table 2.1) and are comparable to those observed for the 10 μm i.d. capillary. The migration time reproducibility for these 40 consecutive runs was 3.2-3.8 %RSD, which is an improvement over the 10 μm i.d. capillary case discussed above.

The improved migration time RSDs observed with decreasing the capillary i.d. (Figures 2.1, 2.2, 2.3 and Table 2.1) is indicative of enhanced coating stability. Desorption of surfactant from the bilayer occurs when the bulk surfactant concentration is less than the CVC. Decreasing the capillary i.d. results in a decrease in the volume-to-surface ratio. Consequently, less DDAB must desorb from the bilayer to saturate the smaller bulk solution volume in the smaller i.d. capillary. Thus, capillary diameters should be kept narrow to maximize the bilayer stability.

In spite of the high protein efficiencies and improved protein migration time RSDs observed with the smaller capillary i.d., an obvious drawback was the decreased S/N ratio. When the capillary diameter was decreased from 25 μm to 10 μm there was a 5-fold decrease in the S/N ratio. Additionally, on decreasing

the capillary i.d. further from 10 μm to 5 μm a 2-fold decrease in S/N ratio was noted.

At high sample concentrations, efficiencies are governed by electromigration dispersion [44]. In both the 5 and 25 μm DDAB-coated capillaries the efficiency decreased to 500 000 plates/m (fronting) when 1.0 mg/mL RNase A was injected. This indicates that sample capacity in concentration units is independent of capillary diameter, but that the mass sample capacity will decrease proportional to capillary volume.

In all the 5, 10 and 25 μm DDAB-coated capillaries; the migration times for the separated proteins are the same for fresh DDAB coatings independent of the capillary diameter (Figures 2.1, 2.2 and 2.3). This is to be expected as the capillary inner diameter is greater than 10-50 times the double layer thickness (hence the EOF is constant) [45] and there is no protein adsorption on the capillary wall (which would add a chromatographic retention that would depend on the surface area-to-volume of the capillary). The consistency of the migration times indicate that a similar charge density non-adsorptive coating is formed regardless of the inner diameter of the capillary.

2.3.2 DODAB coatings in narrow capillaries

Yassine and Lucy demonstrated that the stability of surfactant bilayer coatings improves as the critical vesicle concentration (CVC) of the surfactant used to form the coating decreases [36]. The decrease in the CVC enables the equilibrium between the bilayer and the free surfactant monomers in the bulk

solution to be achieved with less desorption of the bilayer since fewer DODAB monomers are required to reach the CVC value in the bulk solution. The CVC can be reduced by using a longer-tailed homologue of DDAB such as dioctadecyldimethylammonium bromide (DODAB) [37]. Using a DODAB-coated 25 μm i.d. capillary, Yassine and Lucy performed 60 successive protein separations over a 12 day period without regenerating or refreshing the coating [37].

In the following study, protein separations were performed on DODAB-coated 5 μm i.d. capillaries. Preliminary studies found that when 0.1 mM DODAB was used as the coating solution, an efficiency of 1 200 000 plates/m (280 000 plates, for $n=120$) and an efficiency reproducibility of 12 %RSD was achieved after an hour of coating. Coating the 5 μm i.d. capillary with 0.5 mM DODAB for 30 min yielded an efficiency of 1 800 000 plates/m (430 000 plates, for $n=120$) and an efficiency reproducibility of 7.1 %RSD. The low separation efficiency RSDs show that little protein is irreversibly retained on the 0.5 mM DODAB-coated capillaries in keeping with the high recoveries previously obtained for their DDAB-coated counterparts [34, 46]. Therefore, a 30 min coating with 0.5 mM DODAB was used in the following performance studies.

Figure 2.4 shows the separation efficiencies over the 210 consecutive runs (total of 17.5 h) performed without coating regeneration. Since the standard deviation for efficiencies was high, the average efficiency for all four proteins over 10 runs are plotted. Like the DDAB coating above, $\sim 2\,000\,000$ plates/m

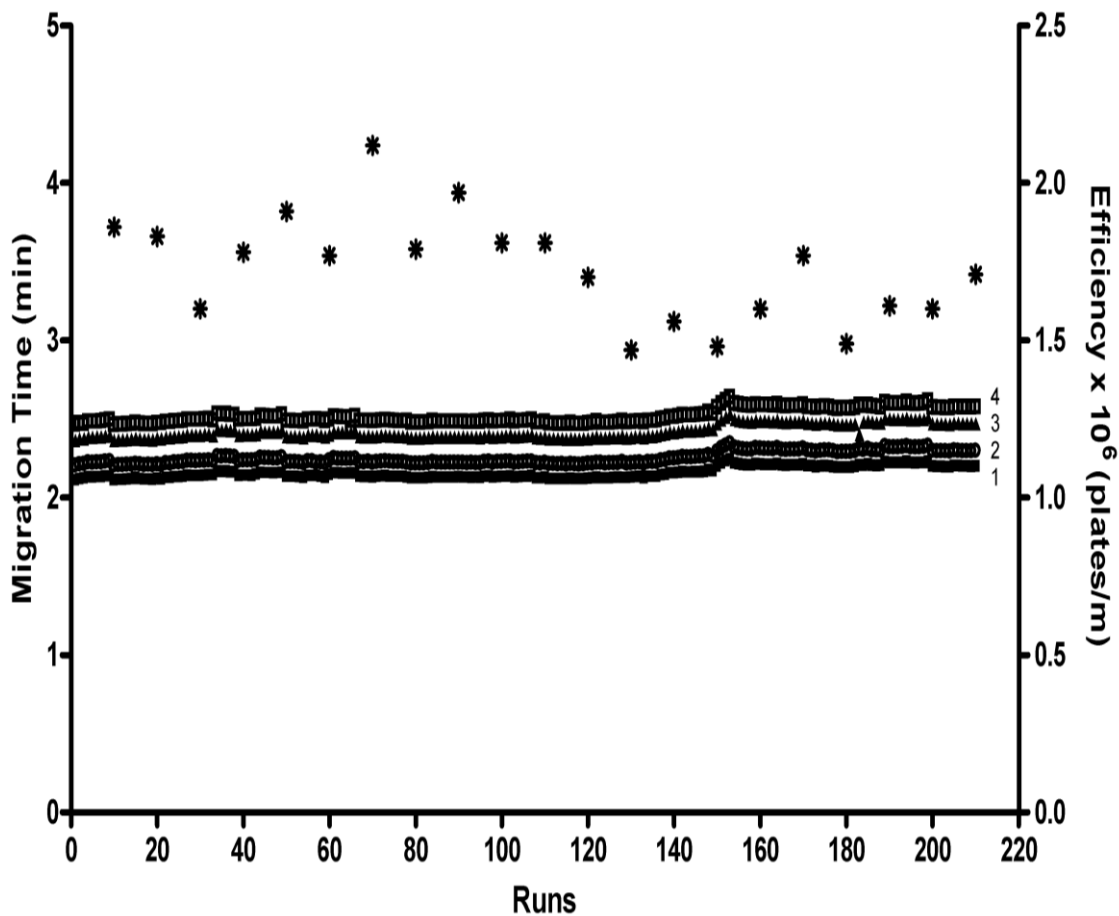


Figure 2.4: Reproducibility studies of 0.5 mM DODAB on a 5 μm i.d. capillary. Migration times of proteins studied: (1- \blacksquare) α -chymo A; (2- \circ) RNase A; (3- \blacktriangle) cyto *c*; (4- \square) lyso. Efficiency (*) is reported as the average protein efficiency for the 4 proteins (for $n=10$ runs) over 210 consecutive runs.

Experimental conditions: same as in Figure 2.3.

(430 000 plates) were observed for the first 120 runs and $\geq 1\,400\,000$ plates/m ($> 340\,000$ plates) thereafter. The efficiencies (cited as plates) are less than the theoretical limit based in longitudinal diffusion (2 000 000- 3 500 000 plates). The decreased efficiencies (in plates) observed for the 5 μm i.d. is due to extra-column band broadening due to the injection plug length (Section 1.4.4, necessitated by the low S/N in the 5 μm) and detector rise times (Section 1.4.5, limited by the instrument).

Figure 2.4 also shows migration times for each of the four cationic proteins over the 210 consecutive runs. The migration time reproducibility was $\leq 1.9\%$, which is much better than observed for DDAB above. This improved stability is consistent with Yassine and Lucy's work where the stability of the coating increased with increasing chain length of the surfactant [37]. The cause of the abrupt shift in the migration times after 150 runs (12.5 h) in Figure 2.4 is unknown. If only the first 150 runs are considered, the migration time RSD was $\leq 0.80\%$.

A new capillary was coated to confirm the long term stability of the DODAB coating in 5 μm capillaries. Ten separations were performed daily without recoating or refreshing the coating. A total of three hundred successive runs were performed over this 30 day period without ever regenerating or refreshing the capillary (Figure 2.5). The studies were intended to conclude upon complete failure of the coating but as the coating remained stable for 30 days, the experiment was concluded at this point.

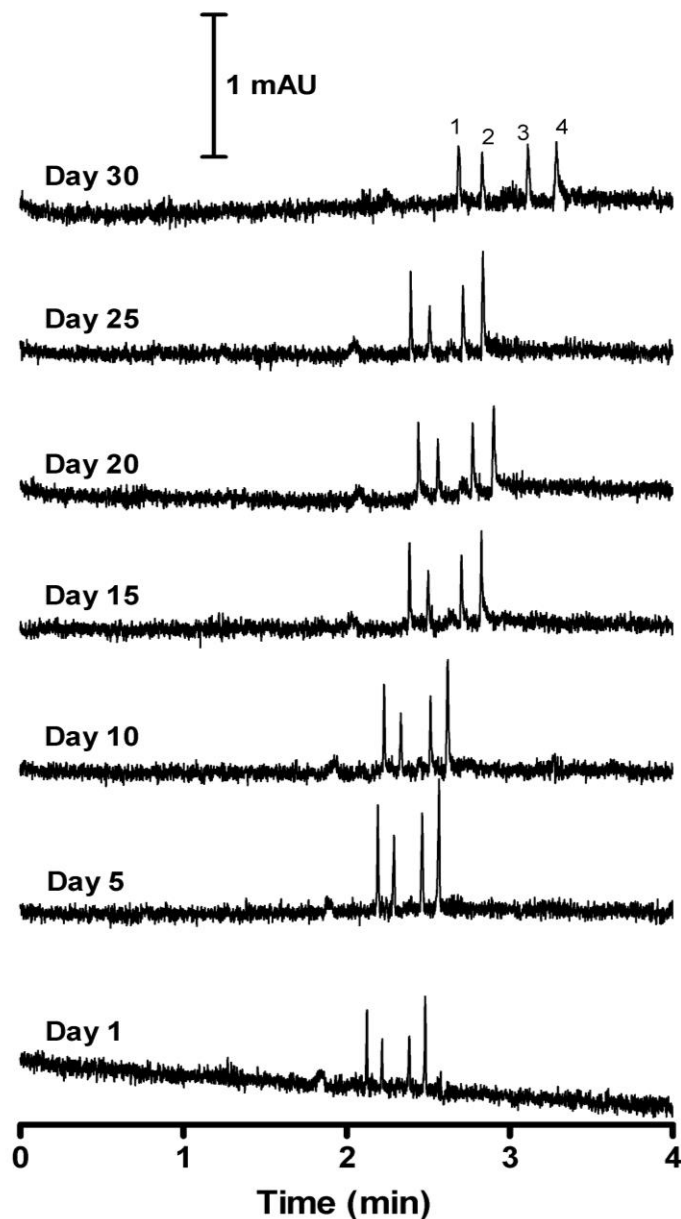


Figure 2.5: Cationic protein reproducibility studies using 5 μm i.d. capillary coated with 0.5 mM DODAB. The electropherograms have been offset along the y-axis to show days. Proteins labeled: (1) α -chymotrypsinogen, (2) ribonuclease A, (3) cytochrome *c*, and (4) lysozyme. For each day ten consecutive runs were performed.

Experimental conditions: Cationic surfactant coating was reconstituted in 50 mM Li acetate pH 5.0 buffer. Applied voltage, -10 kV; capillary, 32 cm x 5 μm i.d. (23 cm to detector); separation buffer, 50 mM Li Acetate pH 5.0; λ (nm), 214; 0.2 mg/mL protein sample dissolved in water and injected hydrodynamically at 5 kPa for 180 s.

Average protein efficiencies of 1 600 000 plates/m (380 000 plates) were obtained over the 30 day period. The protein efficiencies were around ~2 000 000 plates/m (~400 000 plates) for the first 15 days and varied randomly, after which they dropped to 1 500 000-1 600 000 plates/m (320 000-380 000 plates) by day 25. Finally, by day 30, the average protein efficiency had decreased and was between 870 000-1 400 000 plates/m (204 000-330 000 plates).

Protein migration time RSDs were 0.16-3.7% run-to-run and 6.8% day-to-day (n = 30 days). An eventual increase in %RSD for the protein migration times was observed (shown by the drift in protein migration times in Figure 2.5).

The long-term stability study was also performed with a 10 μm i.d. DODAB-coated capillary (Figure 2.6). Efficiencies comparable to the 5 μm i.d. DODAB-coated capillary were obtained for the first 6 days. By day 7, protein efficiencies decreased ~3-fold. The average protein efficiencies decreased from 2 100 000 plates/m on day 1 to 650 000 plates/m on day 7. The coating failed after day 7 and the long-term study for the 10 μm i.d. capillary was concluded.

The limit of detection (LOD) of the four standard cationic proteins on a 5 μm DODAB-coated capillary ranged from 2.7×10^{-6} M (α -chymo A) to 7.6×10^{-6} M (RNaseA), corresponding to limit of quantification (LOQ) of 9×10^{-6} M (α -chymo A) to 2.3×10^{-5} M (RNaseA).

The capillary-to-capillary migration time RSDs of the model cationic proteins investigated using 5 μm i.d. capillaries (ten successive runs, for n=3

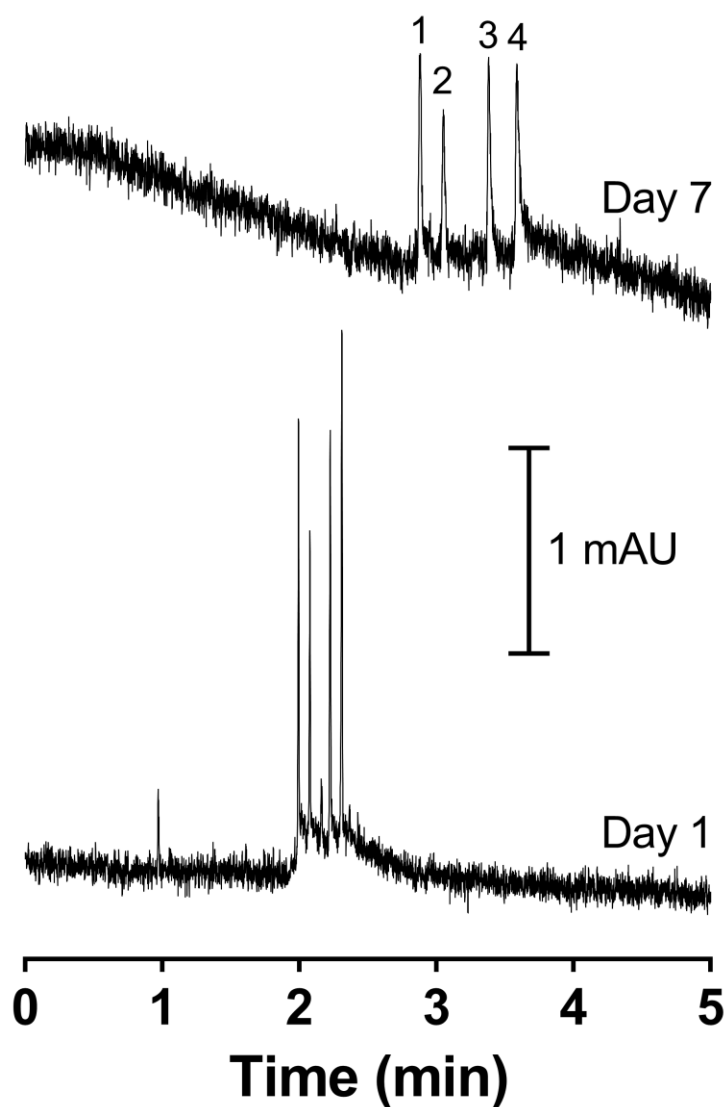


Figure 2.6: Cationic protein reproducibility studies using a 10 μm i.d. capillary coated with 0.5 mM DODAB. The electropherograms have been offset along the y-axis to show days. Proteins labeled: (1) α -chymotrypsinogen, (2) ribonuclease A, (3) cytochrome *c*, and (4) lysozyme. For each day ten consecutive runs were performed.

Experimental conditions: Cationic surfactant coating was reconstituted in 50 mM Li acetate pH 5.0 buffer. Applied voltage, -10 kV; capillary, 32 cm x 5 μm i.d. (23 cm to detector); separation buffer, 50 mM Li Acetate pH 5.0; λ (nm), 214; 0.2 mg/mL protein sample dissolved in water and injected hydrodynamically at 5 kPa for 45 s.

capillaries) were 1.0-1.3 %. In conclusion, the high degree of reproducibility suggests that capillaries are effectively coated with 0.5 mM DODAB.

2.3.3 Separation of neurotransmitters on a DODAB-coated 5 μm i.d. capillary

Separation and determination of neurotransmitters are important in life sciences and clinical diagnoses [47]. Neurotransmitters undergo adsorption on bare capillaries resulting in poor peak efficiencies. This adsorption can be more significant in narrow capillaries. Woods et al. found that peak efficiencies for neurotransmitters decreased as the capillary i.d. decreased from 12 μm to 770 nm i.d. [4] along with noticeable peak tailing [4, 5].

Herein, the separation of a mixture of cationic neurotransmitters was performed on a 5 μm i.d. DODAB-coated capillary using 150 mM Tris phosphate separation buffer. Figure 2.7 shows the separation of dopamine, ephedrine, serotonin and epinephrine. These are baseline resolved (Figure 2.7) using our cationic surfactant coating. The peak efficiencies range from 470 000-610 000 plates/m (110 000-140 000 plates). Separation of the same mixture on a bare 5 μm i.d. capillary under the same buffer conditions resulted in an unresolved mixture and a substantial baseline shift and tailing for over 1 min (Figure 2.8). At pH 5, the neurotransmitters are positively charged. Electrostatic repulsion between the cationic surfactant coating and the positively charged neurotransmitters decreases the adsorption of the neurotransmitters resulting in better peak efficiencies and resolution.

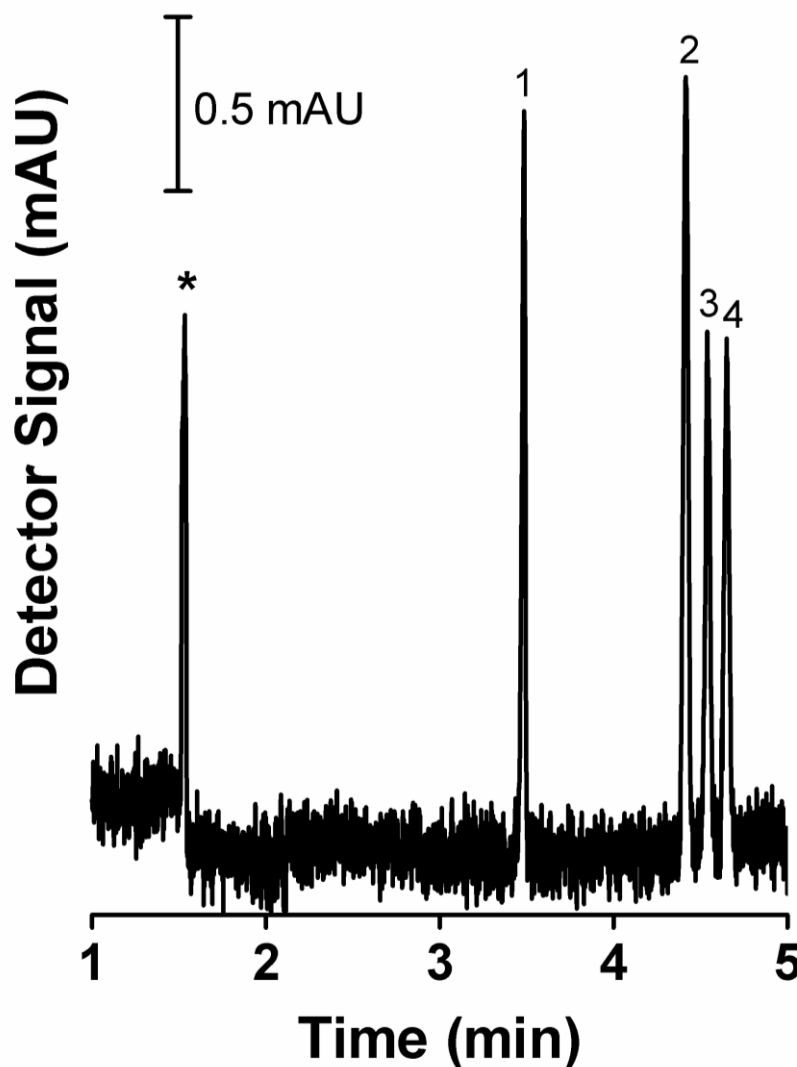


Figure 2.7: Separation of neurotransmitters on a 0.5 mM DODAB-coated 5 μm i.d. capillary. Neurotransmitters labeled: (1) epinephrine, (2) dopamine, (3) ephedrine, and (4) serotonin. The water dip is denoted by (*).

Experimental conditions: Cationic surfactant coating was reconstituted in 50 mM Li acetate pH 5 buffer. Applied voltage, -30 kV; capillary, 32 cm x 5 μm i.d. (23 cm to detector); separation buffer, 150 mM Tris-phosphate pH 5; λ (nm), 200; 0.1 mg/mL for all neurotransmitters except ephedrine which was 0.2 mg/mL; neurotransmitters were dissolved in water and injected hydrodynamically at 5 kPa for 180 s.

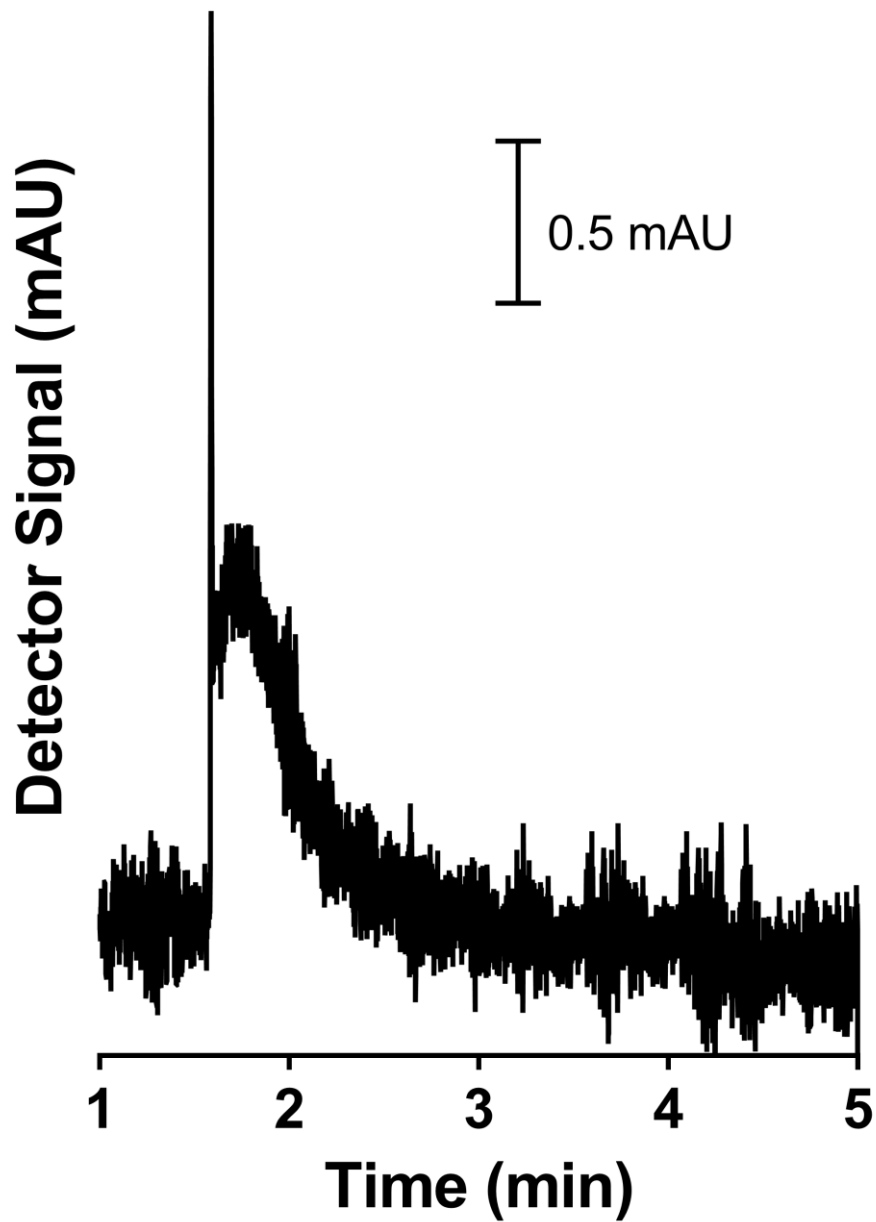


Figure 2.8: Separation of the neurotransmitters on a 5 μm bare capillary.

Experimental conditions: Applied voltage, +30 kV; capillary, 32 cm x 5 μm i.d. (23 cm to detector); separation buffer, 150 mM Tris-phosphate pH 5; λ (nm), 200; 0.1 mg/mL for all neurotransmitters except ephedrine which was 0.2 mg/mL; neurotransmitters were dissolved in water and injected hydrodynamically at 5 kPa for 180 s.

2.4 Conclusions

Cationic surfactants such as DDAB and DODAB readily form semi-permanent bilayer coatings in CE capillaries. The use of narrower capillary diameters ($\leq 25 \mu\text{m}$) results in enhanced stability of surfactant bilayer coatings and higher efficiency of separations of model cationic proteins and neurotransmitters. The bilayer stability is further enhanced by increasing the length of the surfactant alkyl chain. The DODAB-coated $5 \mu\text{m}$ capillary offered both high short-term and long-term stabilities. The capillary maintained high performance for 300 injections performed over a 30 day period without any regeneration of the coating with a migration time reproducibility of 6.8% RSD. Efficiencies of ~ 2 million plates/m were observed for proteins and $>470\ 000$ plates/m for cationic neurotransmitters.

2.5 References

- [1] Olefirowicz, T. M. and Ewing, A. G., *Anal. Chem.* 1990, *62*, 1872-1876.
- [2] Sloss, S. and Ewing, A. G., *Anal. Chem.* 1993, *65*, 577-581.
- [3] Gilman, S. D., Jeremy, J. P. and Andrew, G. E., *J. Microcol. Sep.* 1994, *6*, 373-384.
- [4] Woods, L. A., Roddy, T. P., Paxon, T. L. and Ewing, A. G., *Anal. Chem.* 2001, *73*, 3687-3690.
- [5] Woods, L. A. and Ewing, A. G., *Chem Phys Chem* 2003, *4*, 207-211.
- [6] Bergquist, J., Tarkowski, A., Ekman, R. and Ewing, A., *Proc. Natl. Acad. Sci. U. S. A.* 1994, *91*, 12912-12916.
- [7] Hogan, B. L. and Yeung, E. S., *Anal. Chem.* 1992, *64*, 2841-2845.
- [8] Gostkowski, M. L., McDoniel, J. B., Wei, J., Curey, T. E. and Shear, J. B., *J. Am. Chem. Soc.* 1998, *120*, 18-22.
- [9] Lindberg, P., Stjernström, M. and Roeraade, J., *Electrophoresis* 1997, *18*, 1973-1979.
- [10] Gostkowski, M. L., Wei, J. and Shear, J. B., *Anal. Biochem.* 1998, *260*, 244-250.
- [11] Greif, D., Galla, L., Ros, A. and Anselmetti, D., *J. Chromatogr. A* 2008, *1206*, 83-88.
- [12] Lucy, C. A., MacDonald, A. M. and Gulcev, M. D., *J. Chromatogr. A* 2008, *1184*, 81-105.
- [13] McCormick, R. M., *Anal. Chem.* 1988, *60*, 2322-2328.
- [14] Green, J. S. and Jorgenson, J. W., *J. Chromatogr.* 1989, *478*, 63-70.
- [15] Bushey, M. M. and Jorgenson, J. W., *J. Chromatogr.* 1989, *480*, 301-310.
- [16] Liu, Y., Foote, R. S., Culbertson, C. T., Jacobson, S. C., Ramsey, R. S. and Ramsey, J. M., *J. Microcol. Sep.* 2000, *12*, 407-411.
- [17] Doherty, E. A. S., Meagher, R. J., Albarghouthi, M. N. and Barron, A. E., *Electrophoresis* 2003, *24*, 34-54.
- [18] Hjertén, S., *J. Chromatogr.* 1985, *347*, 191-198.

- [19] Liu, S., Gao, L., Pu, Q., Lu, J. J. and Wang, X., *J. Proteome Res.* 2006, 5, 323-329.
- [20] Liu, S., Pu, Q., Gao, L. and Lu, J., *Talanta* 2006, 70, 644-650.
- [21] Jacobson, S. C., Moore, A. W. and Ramsey, J. M., *Anal. Chem.* 2002, 67, 2059-2063.
- [22] Waters, L. C., Jacobson, S. C., Krutchinina, N., Khandurina, J., Foote, R. S. and Ramsey, J. M., *Anal. Chem.* 1998, 70, 158-162.
- [23] McClain, M. A., Culbertson, C. T., Jacobson, S. C., Allbritton, N. L., Sims, C. E. and Ramsey, J. M., *Anal. Chem.* 2003, 75, 5646-5655.
- [24] Ullsten, S., Zuberovic, A., Wetterhall, M., Hardenborg, E., Markides, K., E. and Bergquist, J., *Electrophoresis* 2004, 25, 2090-2099.
- [25] Simo, C., Elvira, C., González, N., San Román, J., Barbas, C. and Cifuentes, A., *Electrophoresis* 2004, 25, 2056-2064.
- [26] Sakai-Kato, K., Kato, M., Nakajima, T., Toyo'oka, T., Imai, K. and Utsunomiya-Tate, N., *J. Chromatogr. A* 2006, 1111, 127-132.
- [27] Puerta, A., Axén, J., Söderberg, L. and Bergquist, J., *J. Chromatogr. B* 2006, 838, 113-121.
- [28] Runmiao, Y., Ronghua, S., Shuhua, P., Dan, Z., Hang, L. and Yanmei, W., *Electrophoresis* 2008, 29, 1460-1466.
- [29] Sanders, J. C., Breadmore, M. C., Kwok, Y. C., Horsman, K. M. and Landers, J. P., *Anal. Chem.* 2003, 75, 986-994.
- [30] Phillips, K. S., Kottegoda, S., Kang, K. M., Sims, C. E. and Allbritton, N. L., *Anal. Chem.* 2008, 80, 9756-9762.
- [31] Mellors, J. S., Gorbounov, V., Ramsey, R. S. and Ramsey, J. M., *Anal. Chem.* 2008, 80, 6881-6887.
- [32] Garza, S., Chang, S. and Moini, M., *J. Chromatogr. A* 2007, 1159, 14-21.
- [33] Giordano, B. C., Muza, M., Trout, A. and Landers, J. P., *J. Chromatogr. B* 2000, 742, 79-89.
- [34] Barylá, N. E., Melanson, J. E., McDermott, M. T. and Lucy, C. A., *Anal. Chem.* 2001, 73, 4558-4565.
- [35] Wei, W. and Ju, H., *Electrophoresis* 2005, 26, 586-592.
- [36] Yassine, M. M. and Lucy, C. A., *Anal. Chem.* 2004, 76, 2983-2990.

- [37] Yassine, M. M. and Lucy, C. A., *Anal. Chem.* 2005, 77, 620-625.
- [38] Mohabbati, S. and Westerlund, D., *J. Chromatogr. A* 2006, 1121, 32-39.
- [39] Mohabbati, S., Hjerten, S. and Westerlund, D., *Anal. Bioanal. Chem.* 2008, 390, 667-678.
- [40] Gas, B., Stedry, M. and Kenndler, E., *Electrophoresis* 1997, 18, 2123-2133.
- [41] Liu, J., Dolnik, V., Hsieh, Y. Z. and Novotny, M., *Anal. Chem.* 1992, 64, 1328-1336.
- [42] Deyl, Z., Miksik, I., Charvátová, J. and Eckhardt, A., *J. Chromatogr. A* 2003, 1013, 233-238.
- [43] Schure, M. R. and Lenhoff, A. M., *Anal. Chem.* 1993, 65, 3024-3037.
- [44] Xu, X., Kok, W. T. and Poppe, H., *J. Chromatogr. A* 1996, 742, 211-227.
- [45] Knox, J. H. and Grant, I. H., *Chromatographia* 1987, 24, 135-143.
- [46] Melanson, J. E., Barylá, N. E. and Lucy, C. A., *Anal. Chem.* 2000, 72, 4110-4114.
- [47] Schwarz, M. A. and Hauser, P. A., *Anal. Chem.* 2003, 75, 4691.

Chapter Three: A modified supported bilayer/diblock copolymer – working towards a tunable coating for capillary electrophoresis*

3.1 Introduction

A common challenge in capillary electrophoresis (CE) separations of proteins and biomolecules is their adsorption onto the surface of the capillary [1, 2]. Adsorption can lead to undesirable effects such as band broadening [3], poor migration time repeatability [4] and low sample recovery [5]. The most common method of minimizing adsorption is to coat the capillary wall. Such coatings can be broadly classified as covalently bonded polymers [6-8], physically adsorbed polymers [9-11] and dynamic coatings [5, 12, 13]. Covalent coatings are very effective at preventing protein adsorption [14]. However, covalent coatings are more time consuming to prepare and cannot be easily regenerated. Physically adsorbed polymers and surfactant coatings are easy to prepare, regenerable and cost effective [15].

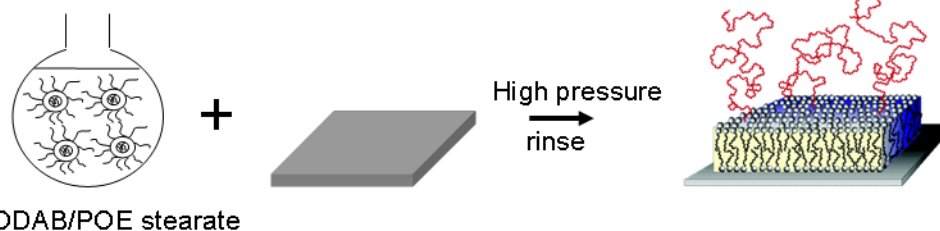
Coatings prepared from two-tailed cationic surfactants are easy to form and produce stable semi-permanent coatings [12, 16-18]. However, the strong anodic EOF [12, 16, 19] overwhelms the differences in electrophoretic mobilities of most proteins, such that the resolution can be limited. A reduced EOF enables the mobility of the proteins to come to the forefront so that better resolution can

* A version of this chapter has been published as Amy M. MacDonald, Mahmoud F. Bahnasy and Charles A. Lucy, "A Modified Supported Bilayer/Diblock Copolymer – Working Towards a Tunable Coating for Capillary Electrophoresis", *J. Chromatogr. A*, 1218 (1), 178-184, 2011.

be achieved. The suppressed EOF of zwitterionic surfactants [20, 21] and phospholipids [22, 23] allows the separation of both acidic and basic proteins. However such coatings lack the strong electrostatic attraction of the cationic surfactants. As a consequence the performance of phospholipid coatings is strongly dependent on factors such as the size and lamellarity of the vesicle, the phospholipid concentration and the ionic strength and buffer type of the solution in which the vesicles are prepared [22].

Previously, we reported a coating procedure which combined the stability of a cationic bilayer coating with a suppressed EOF [24]. This coating was formed by flushing the capillary with a mixture of the surfactant dioctadecyldimethylammonium bromide (DODAB) and polyoxyethylene stearate (POE). In this thesis POE stearate will be described as a diblock copolymer with a hydrophilic polyoxyethylene (POE) block and a hydrophobic (stearate) block. POE stearate can also be considered to be a chain-end functionalized polymer where the POE polymer is end-functionalized with alkyl stearate chain. POE is also known as polyethylene glycol (PEG) or polyethyleneoxide (PEO). The DODAB forms a bilayer on the surface of the capillary. The hydrophobic portion of the diblock copolymer inserts into the DODAB bilayer, leaving the hydrophilic POE moieties protruding into the surrounding solution. A schematic of this can be seen in the rightmost diagram in Figure 3.1A where the bilayer structure is adapted from Figure 10 of reference [25]. The suppressed EOF allows for high resolution of either acidic or basic proteins [24]. The ability to tune this suppressed EOF is important in maximizing the resolution of analytes with

A) Mixed method



B) Sequential method

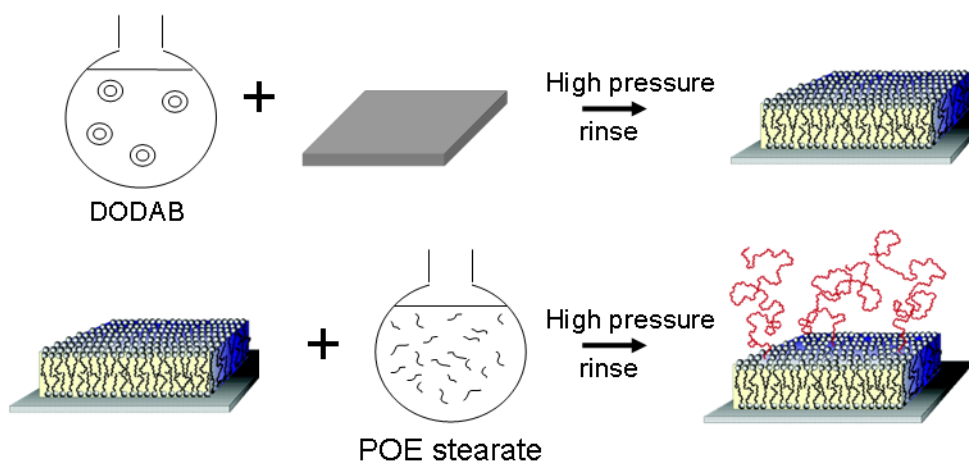


Figure 3.1: Schematic of the A) mixed and B) sequential coating methods.

For the mixed method (A), DODAB and POE stearate are added to a flask, sonicated and stirred, and then rinsed through the capillary. For the sequential method (B), a DODAB solution is first rinsed through the capillary to form a bilayer on the wall. A POE stearate solution is then rinsed through the capillary and the stearate chains intercalate into the bilayer. Bilayer structures adapted from Figure 10 of reference [25].

similar electrophoretic mobilities. However control of the EOF through variation of the DODAB to POE stearate concentration using the mixed method proved complex and unpredictable [26].

For this reason, a coating with similar properties to the one previously developed, but with an EOF that can be easily tuned is developed herein. In the Sequential method (Figure 3.1B) a DODAB solution is first flowed through the capillary to form the bilayer on the capillary wall through electrostatic interactions between the DODAB vesicles and the fused silica wall. This is followed by a flow of POE stearate solution, which forms a hydrophilic neutral coating on the surface of the cationic bilayer, through hydrophobic interactions between the surfactant hydrocarbon chains and the stearate tail, yielding a suppressed EOF.

With many tunable coatings the adjustable EOF is in response to changes in the buffer pH [27-30]. However, pH is an important variable in the optimization of a protein separation. Having both the EOF and separation selectivity governed by the same variable restricts method development. The EOF can also be tuned using additives such as diethylaminetriamine [31], hexamethonium bromide [32], polarizable anions with zwitterionic surfactants [21, 33] and surfactant mixtures [20, 34, 35]. However, the addition of additives to the buffer may also alter the protein mobility and overall separation.

In this chapter we develop semi-permanent DODAB/POE stearate sequential coatings for which the EOF can be controlled. The stability, ease of

preparation and efficiency of separations of model proteins are used to assess the coatings. The ability to control the EOF enabled the separation of histone protein subtypes.

3.2 Experimental

3.2.1 Apparatus

All CE experiments were performed using a P/ACE 2100 system (Beckman Instruments, Fullerton, CA, USA) equipped with a UV absorbance detector upgraded to 5000 series optics, or a P/ACE 5500 system with an on-column diode array UV absorbance detector (Beckman). Detection was performed at 214 nm. The data acquisition rate was 5 Hz (P/ACE 2100) or 4 Hz (P/ACE 5500) and the detector time constant was 0.5 s (P/ACE 2100). Instrument control and data acquisition were controlled using P/ACE station software for Windows 95 (Beckman). Untreated fused silica capillaries (Polymicro Technologies, Phoenix, AZ, USA) with an i.d. of 50 μm , o.d. of 360 μm , and total length of 67, 47 or 27 cm (60, 40 or 20 cm to the detector, respectively) were used unless otherwise stated. The capillary was thermostated at 25°C.

3.2.2 Chemicals

All solutions were prepared in Nanopure 18 M Ω water (Barnstead, Chicago, IL, USA). Buffers were prepared from stock solutions of sodium dihydrogen phosphate (BDH, Toronto, ON, Canada), Ultrapure tris (hydroxymethyl) aminomethane (Tris; Schwarz/Mann Biotech, Cleveland, OH, USA), acetic acid (Caledon Laboratories LTD., ON, Canada) or formic acid (EM

Science, Gibbstown, NJ, USA). Buffer pH was measured using a Corning digital pH meter model 445 (Corning, Acton, MA, USA).

The cationic surfactant dioctadecyldimethylammonium bromide (DODAB) and diblock copolymers polyoxyethylene (POE) 8 stearate, POE 40 stearate and POE 100 stearate were used as received from Sigma (Oakville, ON, Canada). Two mM benzyl alcohol (Aldrich) was used as the neutral EOF marker. The proteins lysozyme (chicken egg white), cytochrome *c* (bovine heart), ribonuclease A (bovine pancreas), α -chymotrypsinogen A (bovine pancreas), trypsin inhibitor (soybean), α -lactalbumin (bovine milk) and histone type III-S (calf thymus) were used as received from Sigma.

3.2.3 Preparation of and coating with the surfactant/copolymer solution

Two different methods were used to prepare the DODAB/POE stearate solutions (Figure 3.1). Both are a variation of the sonicate/stir method used by Yassine and Lucy [12]. The first is essentially that described in [24] and is referred to as the *mixed method* herein. In the mixed method, the surfactant salt and the copolymer were added together in nanopure water and sonicated (Aquasonic 75 HT, VWR Scientific Products, West Chester, PA, USA) for 30 min at 75°C and then stirred at room temperature for 20 min. This process was repeated two to three times until a clear solution was obtained. A new 47 cm capillary was rinsed with 0.1 M NaOH for 10 min using high pressure (20 psi, 1 psi = 68.95 mbar). As depicted in Figure 3.1A, the DODAB/POE stearate mixture was then rinsed through the capillary for 20 min (20 psi) to form the coating.

Excess coating reagent was removed using a 0.5 min rinse with 50 mM sodium phosphate, pH 3 buffer (20 psi, ~1.6 capillary volumes).

In the second method (Figure 3.1B), referred to as the *sequential method*, a 0.1 mM solution of DODAB was prepared using the above sonication/stir procedure. POE 8, 40 and 100 stearate solutions of a range of concentrations (POE 8: 0.001 - 0.01% w/v; POE 40: 0.0004 - 1% w/v; POE 100: 0.0005 - 0.1% w/v) were prepared separately with no DODAB, also using the sonicate/stir method. New 47 cm capillaries were preconditioned with a 10 min rinse with 0.1 M NaOH (20 psi). The coating procedure was then (Figure 3.1B): a 10 min flow (20 psi) of 0.1 mM DODAB; followed by a 10 min (20 psi) rinse with a POE stearate solution of the concentration of interest. A 0.5 min 50 mM sodium phosphate, pH 3 buffer rinse was performed to remove unadsorbed coating solution from the capillary.

3.2.4 EOF Measurements

Fresh capillaries were used with each new buffer system to avoid hysteresis effects. The EOF was measured in two ways [36]. The direct voltage method was used to measure EOF whose magnitude was $> 1 \times 10^{-4} \text{ cm}^2/\text{Vs}$. A 3 s hydrodynamic injection of benzyl alcohol at 0.5 psi was followed by the application of voltage across the capillary. The EOF was calculated using:

$$\mu_{\text{eof}} = \frac{L_d L_t}{V t_M} \quad (3.1)$$

where L_t and L_d are the total length of the capillary and the capillary length to the detector, respectively, V is the voltage applied, and t_M is the migration time of the

neutral marker. Strongly suppressed EOF ($< 1 \times 10^{-4} \text{ cm}^2/\text{Vs}$) were measured using the 3 injection method of Williams and Vigh [37].

3.2.5 Protein Separations.

The coating procedure for separations using the mixed or the sequential coating methods are detailed in Section 3.2.3. Mixtures of 0.1 mg/mL each of lysozyme, cytochrome *c*, ribonuclease A and α -chymotrypsinogen A were injected for 3 s at 0.5 psi and separated using +17.5 kV. Efficiencies were calculated using the Foley-Dorsey method [38].

For histone separations a new capillary ($L_d=60 \text{ cm}$, $L_t=67 \text{ cm}$) was sequentially coated with 0.1 mM DODAB followed by 0.075% w/v POE 40 stearate. The capillary was then rinsed with 75 mM Tris formate pH 4.0. The rinse and coat times were adjusted from those in Section 3.2.3 based on the increased capillary length. A 0.25 mg/mL solution of the histone type III-S was injected hydrodynamically (0.5 psi) for 4 s and a voltage of +15 kV was applied. The width-at-half-height method was used for the histone separations as the baseline was not conducive to efficiency measurements using the Foley-Dorsey method.

For separation of acidic proteins, a new capillary ($L_d=20 \text{ cm}$, $L_t=27 \text{ cm}$) was sequentially coated with 0.1 mM DODAB followed by 0.01% POE 8 stearate. The capillary was then rinsed with 75 mM Tris-acetate with 20 mM CaCl_2 buffer (20 psi) to remove excess surfactant/copolymer. The rinse and coat times were adjusted from those in Section 3.2.3 based on the decreased capillary length. A mixture of 0.2 mg/mL trypsin and 0.05 mg/mL α -lactalbumin was injected hydrodynamically for 4 s at 0.5 psi and separated using -10 kV.

3.3 Results and Discussion

Coatings which prevent analyte adsorption while simultaneously allowing control of the EOF are highly desirable for protein separations in CE. A hydrophilic coating that yields a suppressed EOF can be generated by flushing a capillary with a mixture of the surfactant dioctadecyldimethylammonium bromide (DODAB) and the diblock copolymer polyoxyethylene stearate (Mixed method in Figure 3.1A) [24]. The resultant DODAB/POE 40 stearate coating resulted in a suppressed EOF and was effective for separating both acidic and basic proteins with efficiencies of up to 1 million plates/m [24]. However, while this coating was highly effective, the magnitude and direction of the suppressed EOF depends on the rinse time and the concentration of POE stearate [24]. For instance the open squares in Figure 3.2 show the effect of POE 40 stearate concentration mixed with 0.1 mM DODAB on the EOF at pH 3. Significant and unpredictable variation of the EOF is observed [26]. Coatings prepared using the mixed method showed similar unpredictable variation in EOF at pH 7.4 and pH 10. At all pH studied, POE 40 stearate concentrations of $\geq 0.75\%$ resulted in strong cathodic EOF. It is hypothesized that in mixtures of POE stearate and DODAB, the POE extends from the surface of the vesicle. As the concentration of the POE stearate increases, the POE interferes with adherence of the DODAB to the walls. Regardless of the cause, systematic control of the EOF was difficult using the mixed method [26].

3.3.1 EOF of sequential DODAB/POE stearate coatings

To improve control of the EOF a sequential coating method was developed (Figure 3.1B). First the capillary is rinsed with a DODAB solution to form a bilayer which results in a strongly anodic EOF [12, 16, 19]. The DODAB bilayer forms the anchor for the hydrophilic coating. Next the capillary is flushed with a solution of POE stearate. The hydrophobic stearate anchors into the hydrophobic interior of the bilayer. The hydrophilic POE block extends into solution above the bilayer yielding a strongly suppressed EOF [24]. Formation of the DODAB/POE stearate coating in this sequential manner (solid squares, Figure 3.2) results in a constant $-0.3 \times 10^{-4} \text{ cm}^2/\text{Vs}$ (i.e., suppressed) EOF for $> 0.01\%$ POE 40 stearate, independent of the concentration of POE 40 stearate.

The magnitude of the EOF from a DODAB/POE stearate coating formed in this sequential manner can be varied by changing the length of the POE block. Increasing the POE chain length from 8 to 40 units results in a weaker anodic EOF (Table 3.1). This decrease in EOF is consistent with the observation that as the maximum end-to-end distance of a linear polymer chain increases, the EOF within the capillary decreases significantly [39]. Similarly, EOF in the presence of a long chain polydimethylacrylamide (PDMA) coating was 10-fold more suppressed compared to a short chain PDMA coating [40, 41]. POE suppresses the EOF by shielding the capillary inner surface charge and/or increasing the viscosity of the solution [41, 42] in close proximity to the capillary wall (see Equation 1.3).

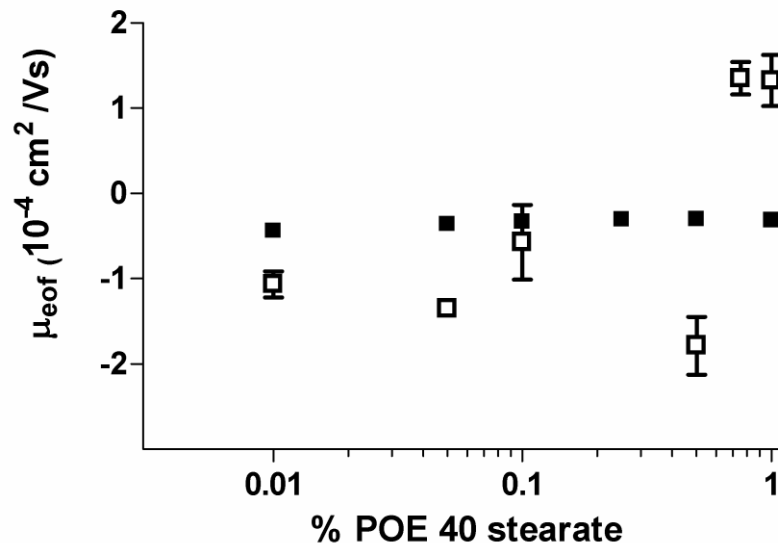


Figure 3.2: EOF stability for mixed and sequential coating methods using 0.1 mM DODAB/POE 40 stearate.

Experimental conditions: Applied voltage: -15 kV for sequential coating (■) and ±15 kV for the mixed coating (□); 47 cm × 50 μm i.d. capillary (40 cm to detector); 50 mM sodium phosphate buffer, pH 3.0; λ, 214 nm; 2 mM benzyl alcohol injected for 3 s at 0.5 psi; temperature, 25°C; . Error bars represent the standard deviation.

3.3.2 Temporal coating studies

Drummond et al. studied the interaction of a trimeric surfactant and POE 100 stearate with mica surfaces [43]. The exchange of the copolymer molecules with the cationic surfactant molecules was observed to be a slow process. Therefore, the kinetics of formation of a sequential DODAB then POE stearate coating was monitored in a similar fashion to that used in previous studies of the desorption of didodecyldimethylammonium bromide (DDAB) [44] and adsorption of phospholipids [22].

A new 47 cm capillary was coated with 0.1 mM DODAB for 10 min. POE stearate solution was flowed through the DODAB coated capillary for 0.5 min, followed by a 0.5 min 50 mM sodium phosphate pH 3 buffer rinse to remove any excess coating material. Benzyl alcohol was injected and the EOF was determined. Subsequent runs were carried out in which the capillary was rinsed for increasingly longer periods of time with copolymer followed by 0.5 min with buffer.

Figures 3.3 to 3.5 shows the results of the coat time studies for different concentrations of POE 8, POE 40 and POE 100 stearate sequentially coated on 0.1 mM DODAB coated capillaries. Prior to flowing POE stearate through the capillary (time = 0), the capillary possesses a DODAB bilayer coating, with a strongly anodic EOF ($\mu_{eof,DODAB}$). Upon rinsing the DODAB coated capillary with POE stearate, the EOF gradually becomes more attenuated until it reaches the suppressed EOF characteristic of a fully formed DODAB/POE stearate coating

($\mu_{eof, DODAB+POE\ stearate}$). The curves in Figures 3.3 to 3.5 were fit to the first order kinetic expression:

$$\mu_{eof} = \mu_{eof, DODAB} + ((\mu_{eof, DODAB+POE\ stearate} - \mu_{eof, DODAB}) * (1 - e^{-kt})) \quad (3.2)$$

using Prism (version 4.00, GraphPad Software Inc., San Diego, CA, USA) where μ_{eof} is the observed EOF and k is the rate constant for the decrease in magnitude of anodic EOF. As shown in Table 3.1, in all but one case Equation 3.2 fit the data with correlation coefficients (r^2) greater than 0.98. The EOF stabilizes more quickly with higher copolymer concentration (i.e., higher k in Table 3.1). The trend is similar to that observed for formation of phospholipid bilayer coatings [22].

Table 3.1 also shows that for a given concentration, EOF stabilizes more quickly with longer POE than their shorter chain counterparts. For example at 0.5×10^{-4} M POE stearate, the rate constant is almost two orders of magnitude greater for POE 40 stearate than POE 8 stearate. This is reflected in Figure 3.4 by the earlier stabilization of the EOF compared to Figure 3.3. When comparing 0.02×10^{-4} M POE 40 and POE 100 stearate, the EOF stabilized three times faster with POE 100 stearate. All further studies were conducted using POE stearate concentrations and rinse times that yield a saturated surface.

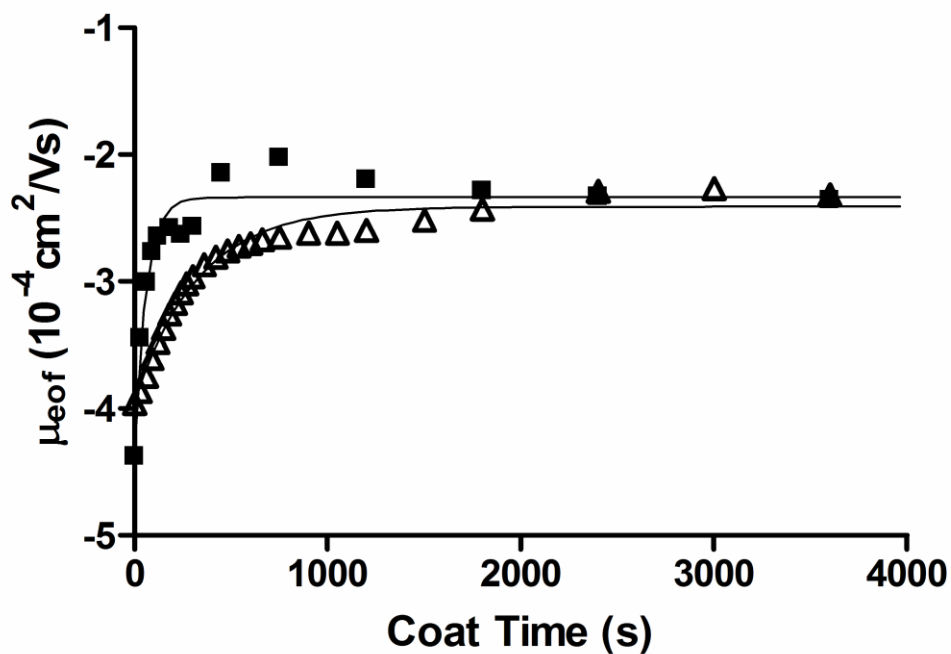


Figure 3.3: Effect of POE 8 stearate concentration on the intercalation rate into the DODAB bilayer. Concentrations used: 0.01% (1.6×10^{-4} M) (■) and 0.003% (0.5×10^{-4} M) (△).

Experimental conditions: DODAB concentration, 0.1 mM; applied voltage, -15 kV; 47 cm \times 50 μm i.d. capillary (40 cm to detector); 50 mM sodium phosphate buffer, pH 3.0; λ , 214 nm; 2 mM benzyl alcohol injected for 3 s at 0.5 psi; temperature, 25°C; data is fit to Equation 3.2.

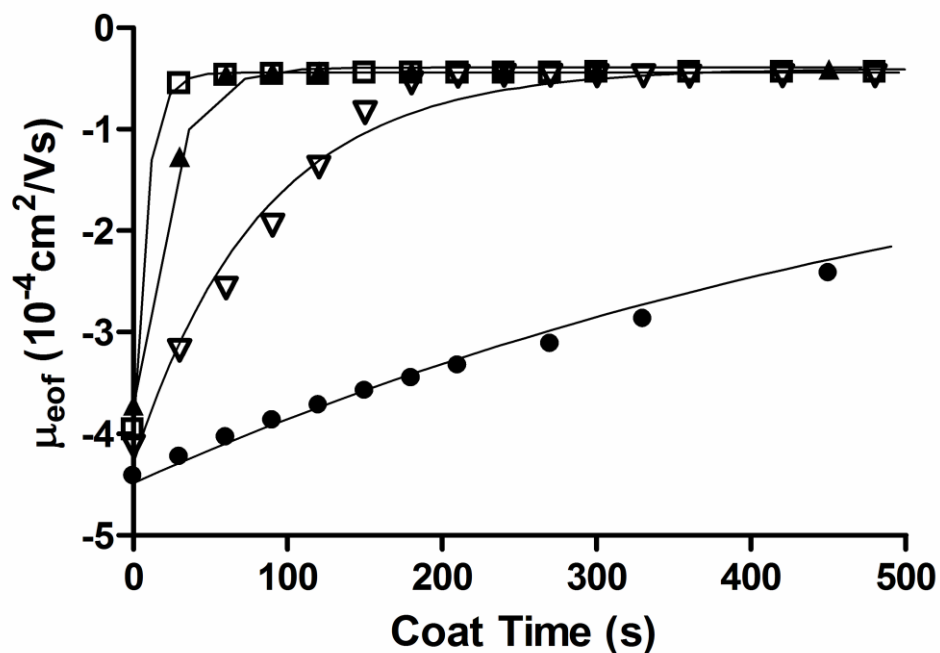


Figure 3.4: Effect of POE 40 stearate concentration on the intercalation rate into the DODAB bilayer. Concentrations used: 0.01% (0.5×10^{-4} M) (□), 0.006% (0.3×10^{-4} M) (▲), 0.002% (0.1×10^{-4} M) (▽), and 0.0004% (0.02×10^{-4} M) (●).

Experimental conditions: DODAB concentration, 0.1 mM; applied voltage, -15 or -17.5 kV; 47 cm \times 50 μ m i.d. capillary (40 cm to detector); 50 mM sodium phosphate buffer, pH 3.0; λ , 214 nm; 2 mM benzyl alcohol injected for 3 s at 0.5 psi; temperature, 25°C; data is fit to Equation 3.2.

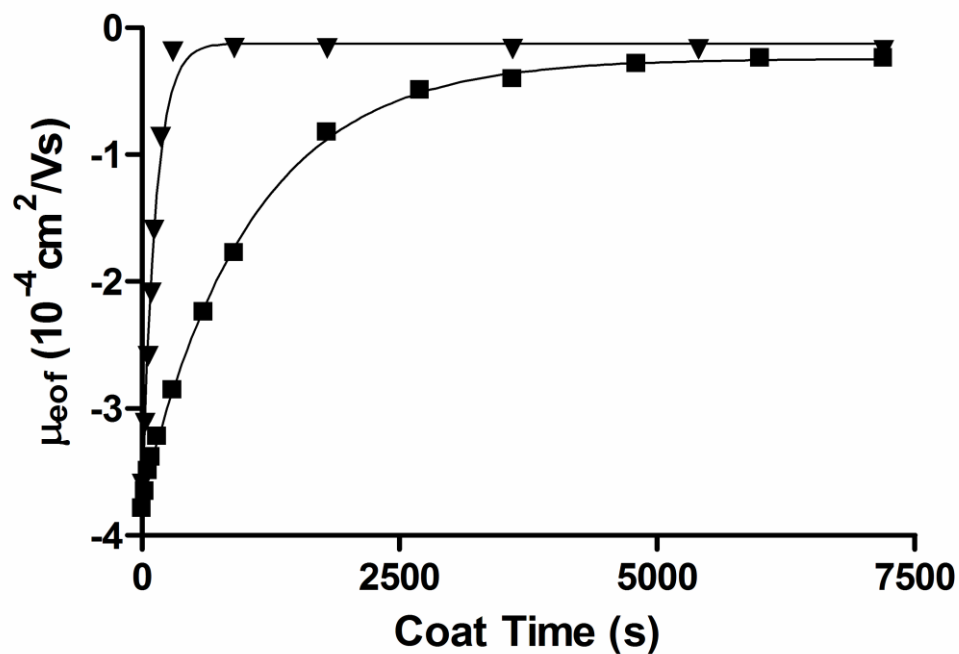


Figure 3.5: Effect of POE 100 stearate concentration on the intercalation rate into the DODAB bilayer. Concentrations used 0.0009% (0.02×10^{-4} M) (▼) and 0.0005% (0.01×10^{-4} M) (■) POE 100 stearate.

Experimental conditions: DODAB concentration, 0.1 mM; applied voltage, -15 kV; 47 cm \times 50 μm i.d. capillary (40 cm to detector); 50 mM sodium phosphate buffer, pH 3.0; λ , 214 nm; 2 mM benzyl alcohol injected for 3 s at 0.5 psi; temperature, 25°C; data is fit to Equation 3.2.

Table 3.1: EOF Mobility, Rate Constant and Correlation Coefficient for sequential DODAB then POE stearate coatings ^a

Stearate Copolymer	Copolymer Concentration % w/v, ($\times 10^{-4}$ M)	$\mu_{\text{eof,DODAB}}$ (10^{-4} cm ² /Vs)	$\mu_{\text{eof,DODAB + POE}}$ (10^{-4} cm ² /Vs) ^b	k (10^{-3} s ⁻¹) ^c	r^2
POE 8	0.003 (0.5)	-4.0	-2.40 (± 0.01)	3.1 (± 0.2)	0.980
POE 8	0.01 (1.6)	-4.4	-2.37 (± 0.01)	16.5 (± 2.4)	0.938
POE 40	0.0004 (0.02)	-4.4	-0.50 (± 0.01)	1.6 (± 0.1)	0.992
POE 40	0.002 (0.1)	-4.1	-0.47 (± 0.004)	12.0 (± 0.8)	0.981
POE 40	0.006 (0.3)	-3.7	-0.37 (± 0.002)	46.9 (± 1.7)	0.998
POE 40	0.01 (0.5)	-4.0	-0.44 (± 0.01)	116.2 (± 3.8)	0.999
POE 100	0.0005 (0.01)	-3.8	-0.24 (± 0.03)	0.9 (± 0.0)	0.999
POE 100	0.0009 (0.02)	-3.6	-0.17 (± 0.005)	7.7 (± 0.6)	0.988

^a All capillaries are first coated with 0.1 mM DODAB then POE Stearate; 50 mM sodium phosphate buffer, pH 3.0, 40/47 cm capillary.

^b Standard deviation in brackets

^c Standard error (i.e., standard deviation divided by square root of the number of replicates) in brackets

3.3.3 Adjustable EOF with DODAB/POE stearate coatings.

The ability to control the magnitude of the EOF is important in optimizing separations [21, 27, 29-31, 33-35, 45]. The EOF of the DODAB/POE stearate coating ($\mu_{eof, DODAB+POE\ stearate}$) is suppressed as the length of the POE block increases (Table 3.1). However, a discrete EOF is observed for each length of POE stearate. In theory very fine control of the EOF could be achieved using a series of POE stearate differing by one POE monomer unit. However, POE stearate is polydisperse. For example, the POE block of commercial POE 50 stearate ranges in size from 39 to 57 oxyethylene units [46]. Therefore, it is not feasible to vary the POE block size by one POE moiety.

Previous studies [33-35, 45] have achieved EOF control by mixing two discrete additives, each of which has an intrinsic and different EOF, e.g., anionic/cationic surfactant mixtures [34, 35, 45] and zwitterionic/cationic surfactant mixtures [33]. In a similar manner the EOF can be fine-tuned using mixtures of two POE stearate copolymers (Figure 3.6). The capillary was first coated with DODAB and then rinsed with a mixture of POE 8 and POE 40 stearate. The POE 8 stearate concentration was kept constant at 0.01% w/v and the POE 40 stearate concentration was varied.

A similar study was carried out using POE 40 and POE 100 stearate. However since both additives individually yield a strongly suppressed EOF, the EOF could only be varied from $-0.36 \times 10^{-4} \text{ cm}^2/\text{Vs}$ to $-0.25 \times 10^{-4} \text{ cm}^2/\text{Vs}$ over the POE 100 stearate range of 0.00002% to 0.1% w/v (POE 40 stearate constant at 0.001% w/v). The narrowness of this range precluded further study.

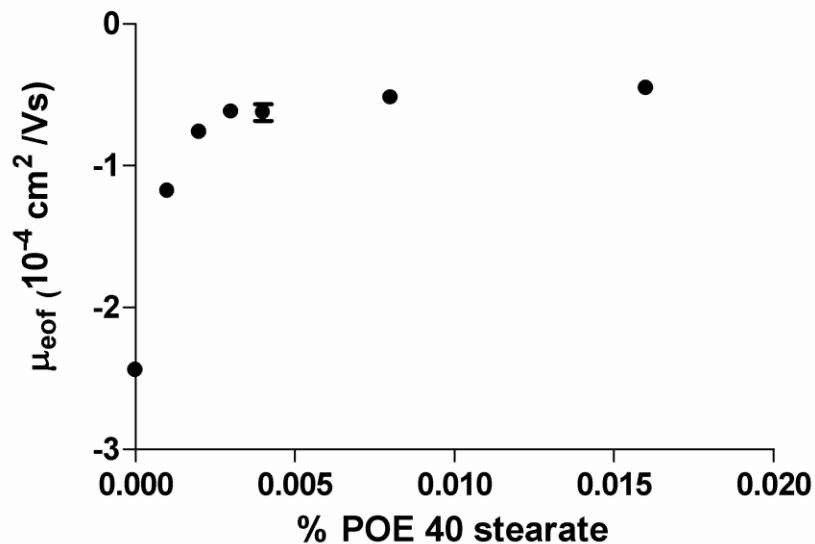


Figure 3.6: EOF vs. POE 40 stearate concentration on a capillary first coated with 0.1 mM DODAB followed by coating with a mixture of 0.01% POE 8 stearate and POE 40 stearate.

Experimental conditions: applied voltage, -15 kV; 47 cm \times 50 μm i.d. capillary (40 cm to detector); 50 mM sodium phosphate buffer, pH 3.0; λ , 214 nm; 2 mM benzyl alcohol injected for 3 s at 0.5 psi; temperature, 25°C. Error bars represent the standard deviation.

3.3.4 Protein Separations

3.3.4.1 Separation of basic proteins

The performance of coatings prepared using the sequential method was compared with similar coatings formed using the mixed method. The coating stability was monitored by successive injection of a sample of four basic proteins with no recoating performed between successive runs.

Figure 3.7 shows the separation of four basic proteins on a sequentially coated capillary. 0.1 mM DODAB was flowed through the capillary followed by 0.075% w/v POE 40 stearate (Sections 3.2.3 and 3.2.5). The average efficiencies of the sequential method (Table 3.2) were 30% higher than for a comparable mixed coating. Also, the sequential coating method resulted in greater coating stability than that of a comparable coating formed using the mixed method. Using the mixed method, a detectable drift in migration times was observed over 14 replicate runs without recoating, leading to migration time RSDs of 2.4-4.6%. For the sequential coating, migration time RSDs of 0.7-1.0% was observed over 30 replicate runs.

After performing 30 runs on the sequentially coated capillary, the coating was removed by flushing the capillary with methanol for 10 min at 20 psi. The sequential coating was regenerated using the procedure in Section 3.2.3. The regenerated sequential coating yielded migration times, peak areas and efficiencies that were the same to those obtained using first-time coated capillaries.

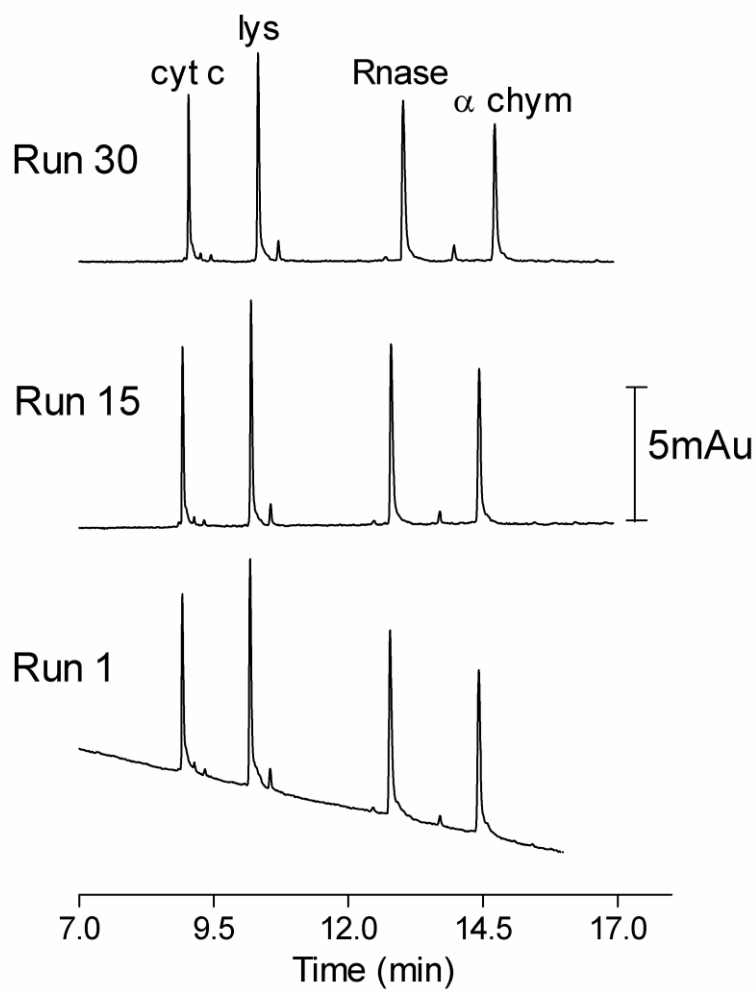


Figure 3.7: Representative separations of basic proteins on a sequential 0.1 mM DODAB then 0.075% POE 40 stearate coating with no recoating between 30 runs.

Experimental conditions: applied voltage, +17.5 kV; 47 cm \times 50 μ m i.d. capillary (40 cm to detector); 50 mM sodium phosphate buffer, pH 3.0; λ , 214 nm; 0.1 mg/mL protein sample injected for 3 s at 0.5 psi; temperature, 25°C.

Table 3.2: Efficiency ranges and EOF values for basic proteins separated on sequential 0.1 mM DODAB then POE 40 stearate coatings

Coating ^a	$\mu_{\text{eof,DODAB+POE}}$ ($\times 10^{-4} \text{ cm}^2/\text{Vs}$)	N, plates/m ($\times 10^3$) (Foley-Dorsey)			
		cyt <i>c</i>	lys	RNase A	α -chym
0.01% POE 40 stearate	-0.44 ± 0.01	310	1 200	580	680
0.05% POE 40 stearate	-0.36 ± 0.006	360	1 180	680	870
0.075% POE 40 stearate		800 ^b	760 ^b	820 ^b	940 ^b
0.1% POE 40 stearate	-0.33 ± 0.009	530 ^b	1 100	690	1 040
0.25% POE 40 stearate	-0.31 ± 0.004	430 ^b	1 020	720	910
0.5% POE 40 stearate	-0.30 ± 0.003	420 ^b	900	750	870
1% POE 40 stearate	-0.31 ± 0.005	320 ^b	1 040	680	850

^a All capillaries are first coated with 0.1 mM DODAB then POE 40 stearate; 50 mM sodium phosphate buffer, pH 3.0, 40/47 cm capillary, 0.1 mg/mL proteins

^b Calculated using width-at-half-height method.

The separation of the four standard basic proteins was carried out on coatings using a range of POE 40 stearate concentrations (0.01 - 1% w/v) prepared using the sequential coating method (Table 3.2). The efficiencies achieved are essentially independent of the POE stearate concentration. The efficiencies are consistently higher than those obtained from separations on a coating formed using the mixed method. These results indicate that better separations of basic proteins are obtained on the sequentially coated capillaries.

3.3.4.2 Histone Separations

Histones are the major structural proteins of chromatin, which packs DNA into higher order structures to accommodate the full genome [47, 48]. There are several different classes of histones, based on their lysine and arginine content. Within these classes there are several variants or subtypes, comprised of different amino acid sequences [49]. Histones are subject to an enormous number of posttranslational modifications, including acetylation and methylation [50]. Histone type III-S from calf thymus is studied in this work. This histone is lysine rich and mainly H1 in character [51]. CE can be a useful method to separate individual histones if an effective coating is used to prevent their adsorption onto the capillary wall [47, 52, 53]. Aguilar et al. separated histone type III-S from calf thymus on a hydroxypropylmethylcellulose (HPMC) coated capillary and observed one broad peak [47]. Thus resolution of the histone subtypes is a functional measure of the effectiveness of a CE coating. Recently, histone type III-S from calf thymus was separated into three H1 subtypes at pH 4.0 using a zwitterionic phospholipid coating [22]. Figure 3.8 shows resolution of nine

possible histone subtypes using a sequential 0.1 mM DODAB then 0.075% POE 40 stearate coating (Sections 3.2.3, 3.2.5). As noted previously, when the EOF is suppressed the protein mobilities are able to come to the forefront, enabling greater resolution. As the EOF on this coating was both suppressed and reversed, six more peaks were visible than on the phospholipid coating, which had a suppressed normal EOF.

The first run for all sets of histone separations had low peak areas. Similarly with the phospholipid coating poor resolution and low peak areas were observed on the first run of histones [22]. Subsequent runs on the sequential 0.1 mM DODAB then 0.075% POE 40 stearate coating resulted in efficiencies as high as 1.2 million plates/m. To determine whether this improvement in peak areas for the subsequent runs is due to voltage application or protein injection, voltage was applied as a pretreatment step before injection of the analytes. Peak areas for the separated proteins in first run after 100 min voltage application were equivalent to those without voltage application. Possibly, the first injection of the proteins blocks the few remaining active sites enabling subsequent runs to be performed with high recovery. The third, fifth and ninth runs are shown in Figure 3.8 as they are representative of all of the separations. The migration time RSDs were $\leq 0.5\%$ (n=9), which are comparable to those obtained on the phospholipid coating.

Comparable results were obtained for the histone separation using the mixed coating (Figure 3.9). Similar to the sequential method, low peak areas were observed for proteins in the first run. Subsequent runs on the mixed 0.1 mM

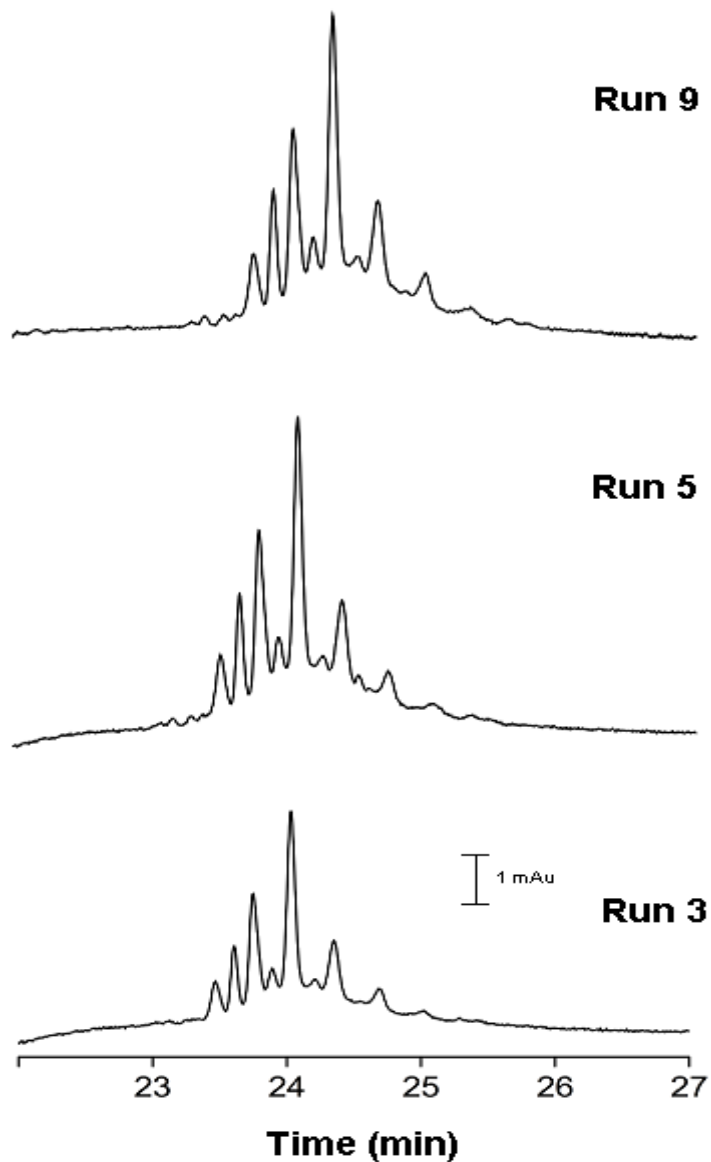


Figure 3.8: Histone type III-S separation on a 0.1 mM DODAB then 0.075% POE 40 stearate sequentially coated capillary.

Experimental conditions: applied voltage, +15 kV; 67 cm \times 50 μ m i.d. capillary (60 cm to detector); 75 mM Tris formate buffer, pH 4.0; λ , 200 nm; 0.25 mg/mL histone type III-S injected for 4 s at 0.5 psi; temperature, 25°C.

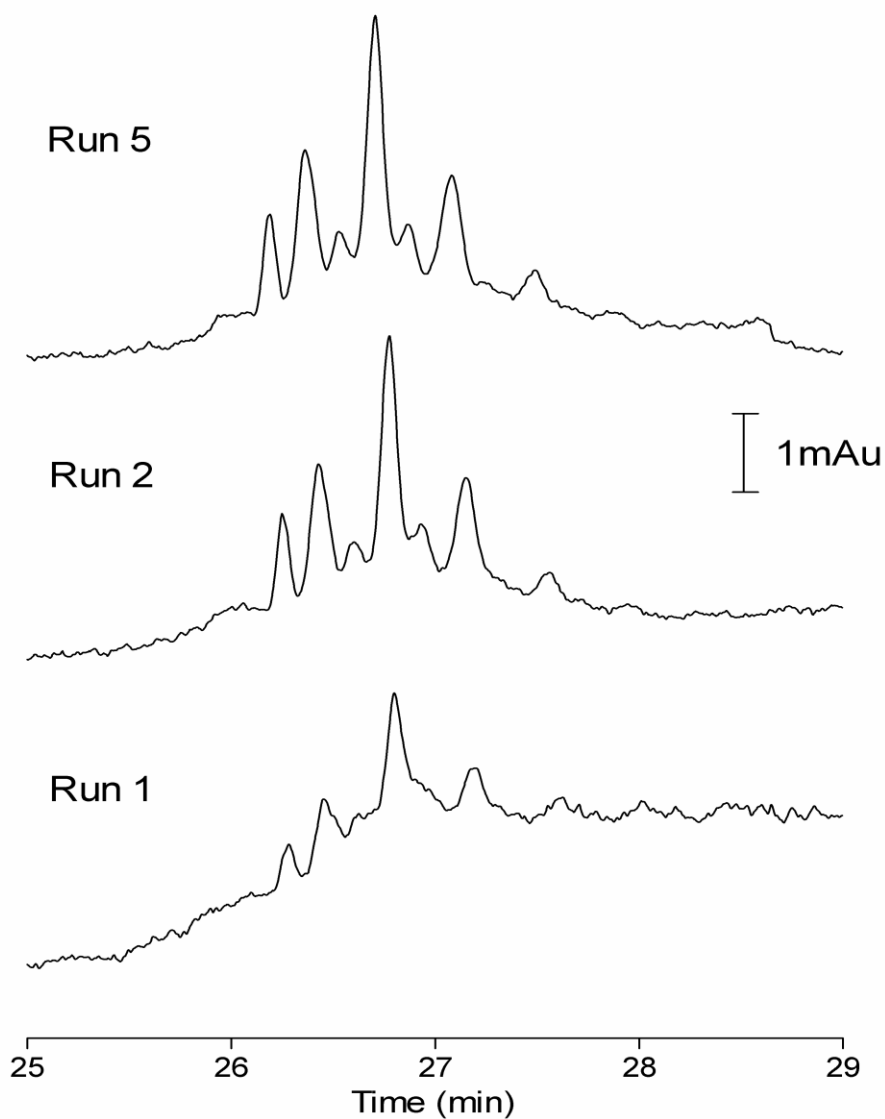


Figure 3.9: Histone type III-S separation on a 0.1 mM DODAB/0.075% POE 40 stearate mixed coated capillary.

Experimental conditions: applied voltage, +15 kV; 67 cm \times 50 μ m i.d. capillary (60 cm to detector); 75 mM Tris formate buffer, pH 4.0; λ , 200 nm; 0.25 mg/mL histone type III-S injected for 4 s at 0.5 psi; temperature, 25°C

DODAB/0.075% POE 40 stearate coating resulted in efficiencies of 1.1 million plates/m. The migration time RSDs were $\leq 0.2\%$ (n=5). While the performance of the two methods for the histones is comparable, the sequential method provides more predictable and stable EOF, and thus is more easily optimized.

3.3.4.3. Separation of acidic proteins

Figure 3.10 shows the separation of two acidic proteins on a sequentially coated capillary. DODAB (0.1 mM) was flowed through the capillary followed by 0.01% POE 8 stearate at pH 6.4 ($\mu_{\text{eof}} = -1.0 \times 10^{-4} \text{ cm}^2/\text{Vs}$). Calcium was added to the run buffer to reduce the electrostatic interaction of the acidic proteins with any exposed DODAB [26]. Trypsin and α -lactalbumin were separated with efficiency of 350 000 plates/m for α -lactalbumin.

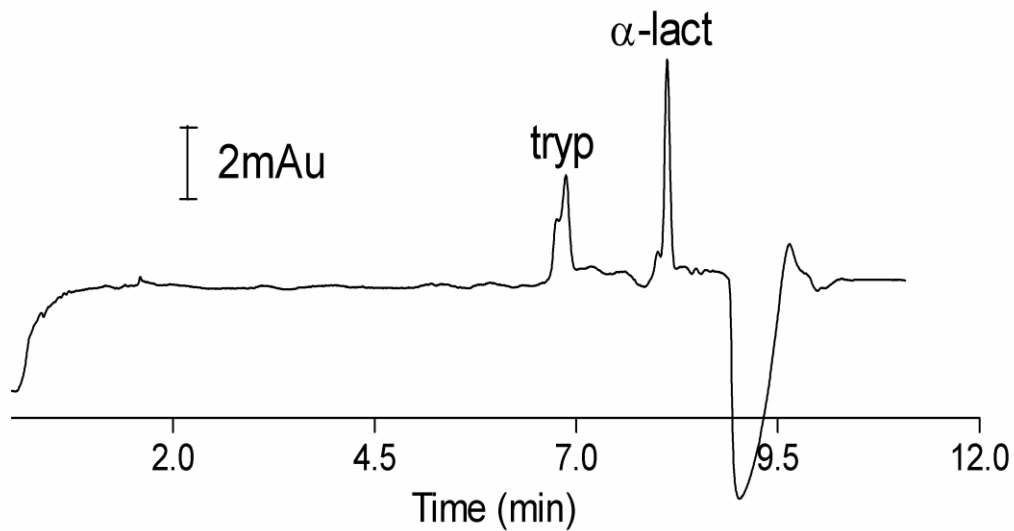


Figure 3.10: Separation of two acidic proteins on a 0.1 mM DODAB then 0.01% POE 8 stearate sequentially coated capillary.

Experimental conditions: applied voltage, -10 kV; 27 cm × 50 μm i.d. capillary (20 cm to detector); 75 mM Tris-acetate with 20 mM CaCl₂ buffer, pH 6.4; λ, 214 nm; 0.2 mg/mL trypsin and 0.05 mg/mL α-lactalbumin injected for 4 s at 0.5 psi; temperature, 25°C.

3.4 Conclusions

A coating prepared from DODAB and POE stearate was demonstrated to effectively prevent protein adsorption and tune the EOF. A sequential rather than mixed method for coating preparation produces a more predictable EOF and a more stable coating that can separate basic proteins with higher average efficiency. The EOF was tunable by varying the POE chain length, and by mixing copolymers of different POE lengths. A tunable EOF (-2.40 to -0.17×10^{-4} cm^2/Vs) was achieved by varying the POE chain length (8, 40 and 100 oxyethylene units). Mixtures of POE 8 and POE 40 stearate enabled continuous variation in EOF from -2.44 to -0.42×10^{-4} cm^2/Vs . Separations of basic proteins yielded efficiencies of 760 000 – 940 000 plates/m. Histone proteins can be separated with high efficiency into a nine subtypes on coatings formed using the sequential method. Acidic proteins are separated on a sequentially coated capillary at pH 6.4.

The sequential coating has also been applied successfully to capillary isoelectric focusing [54]. This will be discussed in Chapter Four. In addition, the sequential coating has been applied to kinetic CE analysis [55]. Interestingly, Krylov and coworkers observed moderately suppressed anodic EOF with a DODAB/POE 8 stearate coating at pH 3.0 and a moderately suppressed cathodic EOF using various buffers near physiological pH [55]. Similarly, Kawai et al. observed a steady transition in EOF for a DODAB/POE 40 stearate coating from suppressed anodic at pH 3.0 to suppressed cathodic at pH 7.0 using phosphate buffers [56]. This trend of EOF transition will be studied in Chapter Five.

3.5 References

- [1] Karger, B. L., Chu, Y. H. and Foret, F., *Annu. Rev. Biophys. Biomed.* 1995, 24, 579-610.
- [2] Quigley, W. W. C. and Dovichi, N. J., *Anal. Chem.* 2004, 76, 4645-4658.
- [3] Schure, M. R. and Lenhoff, A. M., *Anal. Chem.* 1993, 65, 3024-3037.
- [4] Lauer, H. H. and McManigill, D., *Anal. Chem.* 1986, 58, 166-170.
- [5] Towns, J. K. and Regnier, F. E., *Anal. Chem.* 1991, 63, 1126-1132.
- [6] Jiang, W., Awasum, J. N. and Irgum, K., *Anal. Chem.* 2003, 75, 2768-2774.
- [7] Towns, J. K. and Regnier, F. E., *J. Chromatogr.* 1990, 516, 69-78.
- [8] Cifuentes, A., Diez-Masa, J. C., Fritz, J., Anselmetti, D. and Bruno, A. E., *Anal. Chem.* 1998, 70, 3458-3462.
- [9] Gilges, M., Kleemiss, M. H. and Schomburg, G., *Anal. Chem.* 1994, 66, 2038-2046.
- [10] Chiu, R. W., Jimenez, J. C. and Monnig, C. A., *Anal. Chim. Acta* 1995, 307, 193-201.
- [11] Graul, T. W. and Schlenoff, J. B., *Anal. Chem.* 1999, 71, 4007-4013.
- [12] Yassine, M. M. and Lucy, C. A., *Anal. Chem.* 2005, 77, 620-625.
- [13] Cunliffe, J. M., Baryla, N. E. and Lucy, C. A., *Anal. Chem.* 2002, 74, 776-783.
- [14] Doherty, E. A. S., Meagher, R. J., Albarghouthi, M. N. and Barron, A. E., *Electrophoresis* 2003, 24, 34-54.
- [15] Lucy, C. A., MacDonald, A. M. and Gulcev, M. D., *J. Chromatogr. A* 2008, 1184, 81-105.
- [16] Melanson, J. E., Baryla, N. E. and Lucy, C. A., *Anal. Chem.* 2000, 72, 4110-4114.
- [17] Mohabbati, S. and Westerlund, D., *J. Chromatogr. A* 2006, 1121, 32-39.
- [18] Linden, M. V., Wiedmer, S. K., Hakala, R. M. S. and Riekkola, M. L., *J. Chromatogr. A* 2004, 1051, 61-68.
- [19] Mohabbati, S., Hjerten, S. and Westerlund, D., *Anal. Bioanal. Chem.* 2008, 390, 667-678.

- [20] Emmer, A. and Roeraade, J., *J. Liq. Chromatogr.* 1994, 17, 3831-3846.
- [21] Baryla, N. E. and Lucy, C. A., *Anal. Chem.* 2000, 72, 2280-2284.
- [22] Gulcev, M. D. and Lucy, C. A., *Anal. Chem.* 2008, 80, 1806-1812.
- [23] White, C. M., Luo, R., Archer-Hartmann, S. A. and Holland, L. A., *Electrophoresis* 2007, 28, 3049-3055.
- [24] MacDonald, A. M. and Lucy, C. A., *J. Chromatogr. A* 2006, 1130, 265-271.
- [25] Blom, A., Drummond, C., Wanless, E. J., Richetti, P. and Warr, G. G., *Langmuir* 2005, 21, 2779-2788.
- [26] Macdonald, A. M., *Ph.D. Thesis* 2008, Chemistry, University of Alberta, Edmonton.
- [27] Smith, J. T. and El Rassi, Z., *HRC-J. High Res. Chromatogr.* 1992, 15, 573-578.
- [28] Tien, P., Chau, L. K., Shieh, Y. Y., Lin, W. C. and Wei, G. T., *Chem. Mater.* 2001, 13, 1124-1130.
- [29] Hsieh, Y. Y., Lin, Y. H., Yang, J. S., Wei, G. T., Tien, P. and Chau, L. K., *J. Chromatogr. A* 2002, 952, 255-266.
- [30] Guo, Y., Imahori, G. A. and Colon, L. A., *J. Chromatogr. A* 1996, 744, 17-29.
- [31] Corradini, D., Bevilacqua, L. and Nicoletti, I., *Chromatographia* 2005, 62, S43-S50.
- [32] Buchberger, W. and Haddad, P. R., *J. Chromatogr. A* 1994, 687, 343-349.
- [33] Yeung, K. K. C. and Lucy, C. A., *J. Chromatogr. A* 1998, 804, 319-325.
- [34] Hult, E. L., Emmer and Roeraade, J., *J. Chromatogr. A* 1997, 757, 255-262.
- [35] Wang, C. Z. and Lucy, C. A., *Electrophoresis* 2004, 25, 825-832.
- [36] Yeung, K. K. C. and Lucy, C. A., *Anal. Chem.* 1997, 69, 3435.
- [37] Williams, B. A. and Vigh, C., *Anal. Chem.* 1996, 68, 1174-1180.
- [38] Foley, J. P. and Dorsey, J. G., *Anal. Chem.* 1983, 55, 730-737.
- [39] Doherty, E. A. S., Berglund, K. D., Buchholz, B. A., Kourkine, I. V., Przybycien, T. M., Tilton, R. D. and Barron, A. E., *Electrophoresis* 2002, 23, 2766-2776.

- [40] Cretich, M., Chiari, M., Pirri, G. and Crippa, A., *Electrophoresis* 2005, 26, 1913-1919.
- [41] Hellmich, W., Regtmeier, J., Duong, T. T., Ros, R., Anselmetti, D. and Ros, A., *Langmuir* 2005, 21, 7551-7557.
- [42] Grossman, P. D. and Colburn, J. C., *Capillary Electrophoresis, Theory and Practice*, Academic Press, Inc., San Diego, CA 1992.
- [43] Drummond, C., In, M. and Richetti, P., *Eur. Phys. J. E* 2004, 15, 159-165.
- [44] Yassine, M. M. and Lucy, C. A., *Anal. Chem.* 2004, 76, 2983-2990.
- [45] Liu, Q., Yang, Y. M. and Yao, S. Z., *J. Chromatogr. A* 2008, 1187, 260-266.
- [46] Robelin, C., Duval, F. P., Richetti, P. and Warr, G. G., *Langmuir* 2002, 18, 1634-1640.
- [47] Aguilar, C., Hofte, A. J. P., Tjaden, U. R. and van der Greef, J., *J. Chromatogr. A* 2001, 926, 57-67.
- [48] von Holt, C., *BioEssays* 1985, 3, 120-124.
- [49] Bossi, A., Gelfi, C., Orsi, A. and Righetti, P. G., *J. Chromatogr. A* 1994, 686, 121-128.
- [50] Peterson, C. L. and Laniel, M. A., *Curr. Biol.* 2004, 14, R546-R551.
- [51] Product Number H 5505, Product Information Sheet, Sigma Aldrich, St. Louis, MO, USA.
- [52] Gurley, L. R., London, J. E. and Valdez, J. G., *J. Chromatogr.* 1991, 559, 431-443.
- [53] Lindner, H., Helliger, W., Dirschlmaier, A., Talasz, H., Wurm, M., Sarg, B., Jaquemar, M. and Puschendorf, B., *J. Chromatogr.* 1992, 608, 211-216.
- [54] Bahnasy, M. F. and Lucy, C. A., *J. Chromatogr. A* 2012, 1267, 89-95.
- [55] de Jong, S., Epelbaum, N., Liyanage, R. and Krylov, S. N., *Electrophoresis* 2012, 33, 2584-2590.
- [56] Kawai, T., Ito, J., Sueyoshi, K., Kitagawa, F. and Otsuka, K., *J. Chromatogr. A* 2012, 1267, 65-73.

Chapter Four: A versatile semi-permanent sequential bilayer/diblock copolymer coating for capillary isoelectric focusing*

4.1 Introduction

Capillary Isoelectric Focusing (cIEF) is a high resolution electrophoretic technique used for the separation of protein variants [1-3], determination of impurities within therapeutic proteins, analysis of protein-ligand interaction [4], determination of the isoelectric point of proteins [5] and proteomic analyses [6]. The capillary format of IEF offers several advantages over traditional slab gel IEF including ease of automation, faster analysis time, smaller sample requirements and online detection [7-9]. One challenge to performing cIEF of proteins is their adsorption onto the silica capillary. Adsorption in CE results in broader peaks [10], poor migration time reproducibility [11] and low sample recovery [12]. Thus, the use of a coated capillary is necessary to minimize sample adsorption. In addition, the subtle differences in the pI values of protein variants require a suppressed and well tuned electroosmotic flow (EOF). Thus an ideal coating for cIEF should: (1) minimize solute-wall interactions; and (2) suppress the EOF to allow sufficient time for complete focusing.

*A version of this chapter has been published as Mahmoud F. Bahnasy and Charles A. Lucy, "A versatile semi-permanent coating for capillary isoelectric focusing", *J. Chromatogr. A*, 1267, 89-95, 2012.

cIEF may be performed in three ways: two-step; single-step; and whole-column imaging detection. Figure 4.1 shows a schematic for two-step and single-step cIEF procedures. In both cases, the capillary is filled with a mixture of the sample and ampholytes. Upon application of the voltage, a pH gradient is established inside the capillary and the sample components are focused along the capillary according to their isoelectric points. The EOF needs to be suppressed during the focusing step to allow for complete focusing. In order to be detected, the focused sample components need to be transported along the capillary to pass the online detection window. The traditional two-step cIEF was developed by Hjertén and co-workers [13]. Coated capillaries with strongly suppressed EOF ($0.05\text{-}0.20 \times 10^{-4} \text{ cm}^2/\text{Vs}$ [14, 15]) are required to ensure that the proteins do not migrate out of the capillary during the focusing step. Then, the focused proteins are mobilized towards the detector either hydrodynamically via pressure mobilization [16, 17] or electrokinetically using chemical mobilization [1]. In single-step cIEF, capillaries with a moderate EOF are used. This allows for simultaneous focusing and transport [18, 19]. Finally, in the whole-column imaging detection (WCID)-cIEF method the entire length of the capillary is detected, eliminating the need for the mobilization step [4, 20]. As WCID-cIEF requires custom instrumentation, this chapter will focus on the single-step and two-step focusing methodologies.

Bare silica capillaries cannot be used for cIEF separations since the strong EOF will flush the ampholytes and sample out of the capillary before

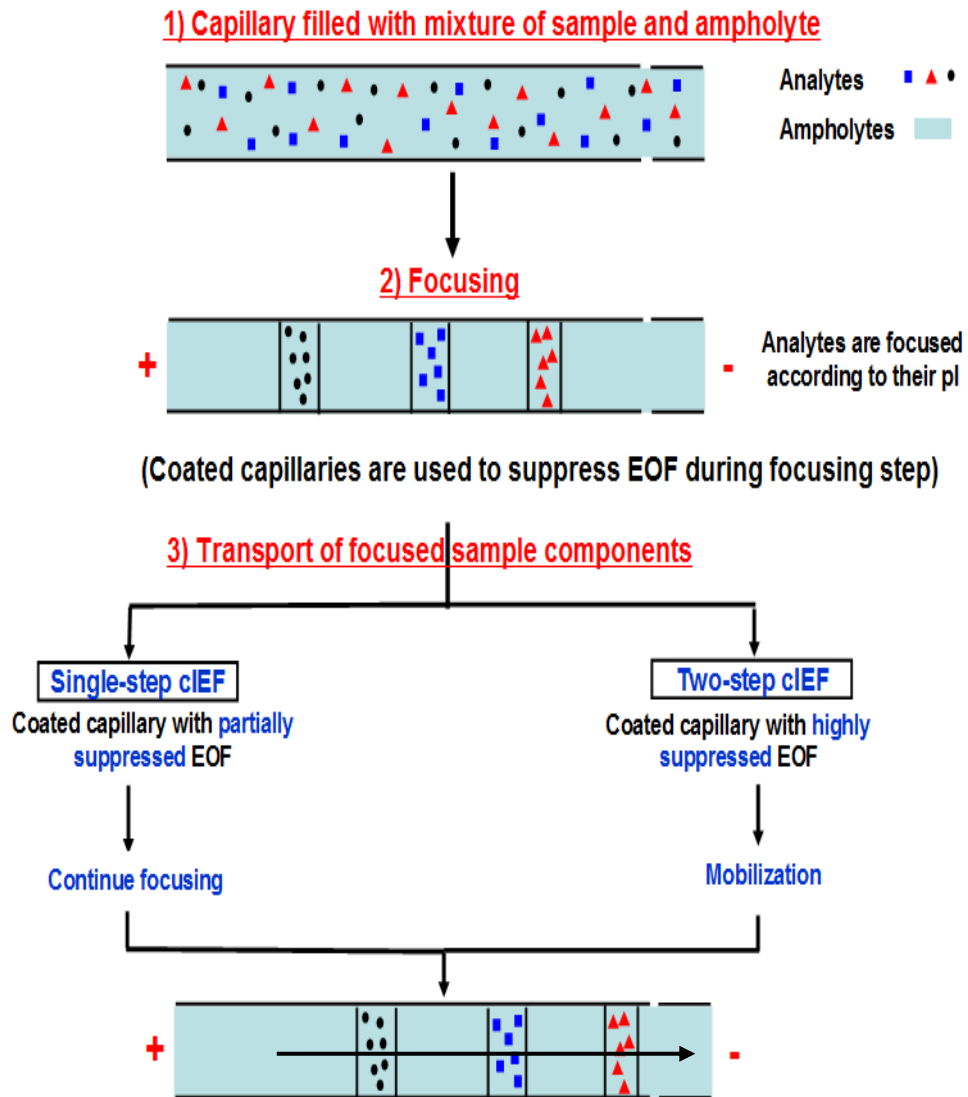


Figure 4.1: Schematic of single-step and two-step cIEF procedures.

focusing is complete. A variety of capillary coatings have used to suppress or eliminate the EOF for cIEF. Often, permanent covalent coatings [15, 16] are used but these are time consuming and labor intensive to prepare, expensive to purchase, and difficult to regenerate. The high cost of the commercial coated capillaries and the need for multiple capillaries due to protein precipitation and capillary clogging may lead to expensive analyses particularly during method development. In addition, one is limited to the dimensions of commercially coated capillaries (typically only available in 50 μm i.d.). These limitations call for the development of a versatile capillary coating compatible with cIEF separations. Dynamically coated capillaries [18, 21] have also been used for cIEF. Dynamic coatings are easy to prepare, but they lack the coating stability and consistent EOF of covalent coatings [8] and require extensive capillary conditioning to improve reproducibility [14].

Our group has recently developed a semi-permanent sequential hydrophilic coating (see Figure 3.1B) that yields a moderately suppressed to strongly suppressed EOF based on simply rinsing the capillary with two successive solutions [22, 23]. First, the capillary is rinsed with the cationic surfactant dioctadecyldimethylammonium bromide (DODAB) [22]. The DODAB has the correct packing factor to form a bilayer [24, 25] on the inner surface of the capillary. Next a solution of the neutral diblock copolymer polyoxyethylene (POE) stearate is flushed through the DODAB coated capillary. The hydrophobic portion of the diblock copolymer inserts into the DODAB bilayer, leaving the hydrophilic POE moieties protruding into the surrounding solution. A tunable

EOF (-2.40 to -0.17×10^{-4} cm^2/Vs) can be achieved by varying the POE chain length from 8, to 100 oxyethylene units [22]. A sequential coating rather than mixed coating (prepared by mixing DODAB and POE stearate in the same solution) resulted in more predictable EOF, better coating stability and higher separation efficiencies [22, 23]. The sequential coating has been used successfully for CZE of basic, acidic and histone proteins [22] and for kinetic CE analysis [26]. In this chapter, we investigate the application of the sequential DODAB-POE stearate coating to cIEF separations. The ease of control of the magnitude of the suppressed EOF makes this coating appropriate for both single-step and two-step cIEF.

4.2 Experimental

4.2.1 Apparatus

All capillary electrophoresis experiments were conducted on a Hewlett Packard ^{3D}CE instrument equipped with a UV absorbance detector. Data acquisition at 10 Hz was carried out on a computer running HP ^{3D}CE ChemStation. Untreated fused silica capillaries were obtained from Polymicro Technologies (Phoenix, AZ, USA). Unless otherwise stated, the capillaries were 50 μm i.d., 360 μm o.d., with a total length of 48.5 cm (40 cm to the detector). The cartridge aperture was 100 \times 200 μm , and the capillary was thermostated at 25°C. An external nitrogen tank was used for high pressure rinses and injections.

4.2.2 Chemicals

All solutions were prepared in Nanopure 18 M Ω water (Barnstead, Chicago, IL, USA). The cationic surfactant dioctadecyldimethylammonium bromide (DODAB) and diblock copolymers polyoxyethylene (POE) 40 stearate, and POE 100 stearate were used as received from Sigma (Oakville, ON, Canada). cIEF Gel Polymer solution; a mixture of ethylene glycol and poly-ethyleneoxide in water (p/n 477497) and pI Marker Kit (p/n A58481) were obtained from Beckman Coulter (Brea, CA, USA). This marker kit contains synthetic peptide markers with pI values of: 7.0 (Trp-Glu-His-Arg), 5.5 (Trp-Glu-His) and 4.1 (Trp-Asp-Asp-Arg); all contain tryptophan and are compatible with UV absorption at 280 nm [27]. Another set of pI markers with pI values of: 8.40, 7.65, 7.05 and 6.61 were obtained from Protein Simple (Toronto, Canada) of which the 7.65 and 6.61 pI markers absorb at both 280 nm and 420 nm which assists in tracking these markers. L-Arginine, iminodiacetic acid, sodium hydroxide, Ampholyte® 3-10 (10043), Ampholyte® 5-8 (10049) and the proteins Hemoglobin A (HbA₀, H0267), Hemoglobin S (HbS, H0392) were used as received from Sigma (St. Louis, MO, USA). Phosphoric acid and acetic acid were obtained from Caledon Laboratories Ltd. (Georgetown, ON, Canada).

4.2.3. Methods

DODAB and POE stearate coating solutions were prepared using the sonicate/stir method [28]. For the surfactant solution, DODAB was dissolved in water and sonicated for 30 min at 60 °C and then stirred for 15 min. Two sonication/stir cycles were used. The DODAB solution was then allowed to cool

to room temperature before use. POE stearate (POE 40 or POE 100) solutions were also dissolved in water, and treated using the same sonicate/stir procedure. Fresh solutions were prepared on the day of coating a new capillary. Capillaries are sequentially coated with DODAB then POE stearate of interest according to the procedure in Section 3.2.3 .

Based on the systematic studies performed to optimize cIEF method parameters in the work of S. Mack *et al.* [29] and [30], the anolyte was 200 mM phosphoric acid, the catholyte was 300 mM NaOH, and the chemical mobilizer was 350 mM acetic acid. Solutions of 0.5 M arginine and 0.2 M iminodiacetic acid were used as cathodic stabilizer and anodic stabilizer, respectively. Cathodic and anodic stabilizers are added as sacrificial ampholytes to minimize the effect of cathodic and anodic drift and to prevent the loss of carrier ampholytes or analytes of interest during sample focusing [29]. An applied voltage of +25 kV was used for both the focusing and mobilization steps.

Between successive runs, the capillary was rinsed at high pressure (2 bar) using 4.3 M urea for 5 min, followed by nanopure water for 5 min, and then finally with the cIEF gel for 5 min.

Samples contained 8 μ L of 0.2 M iminodiacetic acid, 36 μ L of 0.5 M L-arginine, 2-8 μ L of standard pI markers of interest and 1.25, 2.5 or 5% v/v of the carrier ampholytes. Samples were diluted to a final volume of 500 μ L using the cIEF gel polymer solution. Samples were injected at 3 bar pressure for 3 min. For samples containing hemoglobins, lyophilized HbA₀ and HbS were rehydrated

with 2.0 mL of water, and divided into several individual aliquots and stored at -20°C. As sample is needed, aliquots of both Hb isoforms were thawed and 3 μ L of each solution were mixed with the other components of the cIEF sample as stated above and diluted to a final volume of 500 μ L using the cIEF gel polymer solution.

4.3 Results and Discussion

cIEF is a special mode of capillary electrophoresis used for the separation of amphoteric compounds such as protein isoforms [1, 3, 31, 32]. A capillary is filled with a mixture of proteins and carrier ampholytes. Upon application of a high electric voltage across the capillary the ampholytes migrate to generate a pH gradient along the length of the capillary. The charge of the protein decreases as it moves along the pH gradient until the protein reaches a region where the pH matches its pI and its mobility becomes zero. Thus, amphoteric sample components are focused at different points along the capillary length according to their pI. Significant time is necessary for this focusing step, meaning that the EOF within the capillary needs to be suppressed. Capillary coatings are used to both suppress the EOF and to prevent protein adsorption. Once focusing is complete, either a single-step or two-step methodology can be used to move the focused sample zones toward the detector so that they can be measured and recorded. A moderately suppressed EOF is required for the single-step methodology while a strongly suppressed EOF is needed for the two-step cIEF method.

In this chapter we introduce a versatile semi-permanent coating that is compatible with both single-step and two-step cIEF separations. The sequential coating is easy to prepare, cost effective and provides the combined stability of cationic surfactant coatings and the suppressed EOF of neutral polymer coatings. A series of peptide markers whose pI values are distributed over the pH range 3-10 are used to assess the performance of the DODAB/POE stearate sequentially coated capillaries and track the linearity of the pH gradient.

4.3.1. Preliminary optimization of ampholyte concentration

A steady and stable pH gradient is critical during the focusing step. The pH gradient is stabilized by the presence of carrier ampholytes; a mixture of zwitterionic compounds that possess a good buffering capacity and conductivity. Resolution can be enhanced by increasing the number of carrier ampholytes focused between two analytes. This can be achieved by increasing the concentration of the carrier ampholytes [33]. However, a higher concentration of the carrier ampholytes increases the background signal, increases the initial current which causes Joule heating induced band broadening and can result in protein precipitation [33].

Here we studied the effect of varying the ampholyte concentration on the resolution of 6 peptide markers. Increasing the ampholyte concentration from 1.25 to 2.5% v/v resulted in more extended separation window for a DODAB/POE 40 coated capillary (Figure 4.2). The average peak width (at 50% of peak height) of the 6 peptide markers is 0.033 pH unit for 1.25% v/v ampholytes and 0.028 for

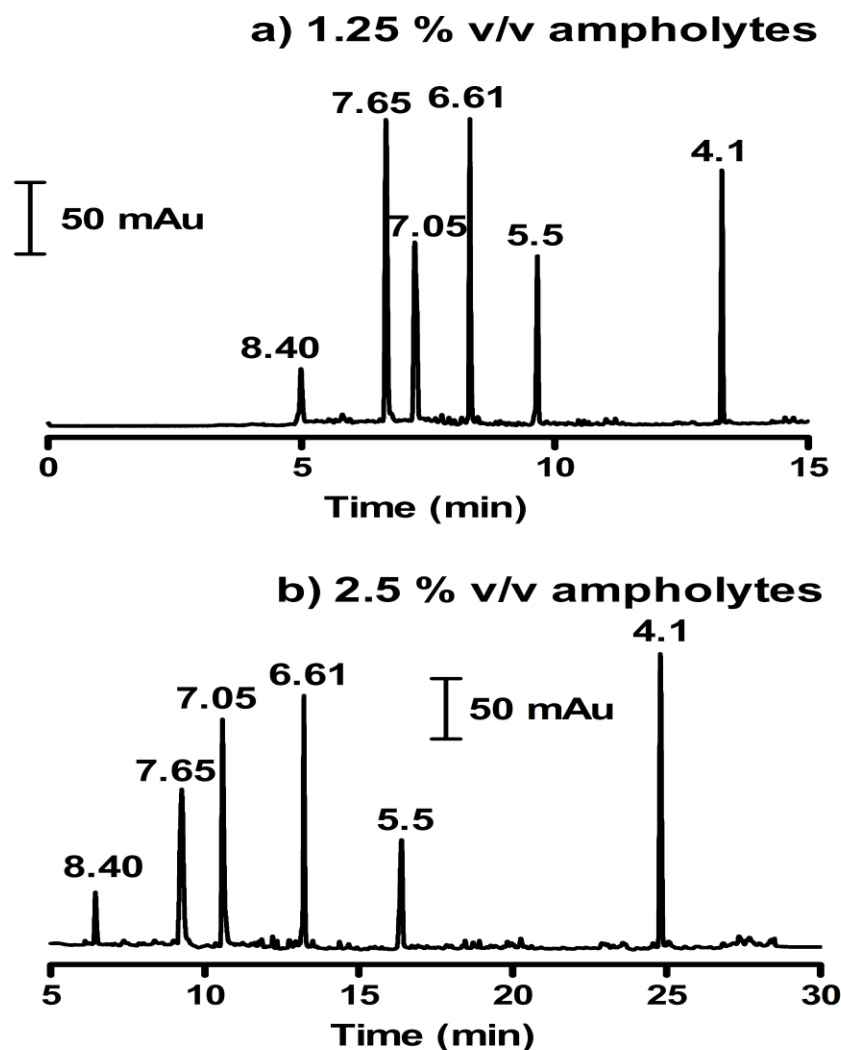


Figure 4.2: cIEF separation of 6 peptide markers on a 0.1 mM DODAB /0.075% POE 40 stearate coated capillary using: a) 1.25% v/v; or b) 2.5% v/v carrier ampholytes.

Experimental conditions: 48.5 cm \times 50 μ m i.d. capillaries (40 cm to detector); temperature, 25°C; λ , 280 nm. Samples contained 1.25 or 2.5% v/v of the carrier ampholytes pI 3-10; 8 μ L of 0.2 M iminodiacetic acid; 36 μ L of 0.5 M L-arginine and 6 peptide markers 8.40 (8 μ L), 7.65 (3 μ L), 7.05 (5 μ L), 6.61 (2 μ L), 5.5 (5 μ L) and 4.1 (5 μ L). Sample was diluted to a total volume of 500 μ L with cIEF gel and injected into the capillary at 3 bar pressure injection for 3 minutes. Sample was focused for 10 minutes at +25 kV using 200 mM phosphoric acid as anolyte 300 mM sodium hydroxide as catholyte then chemically mobilized at +25 kV using 350 mM acetic acid instead of sodium hydroxide.

2.5% ampholytes. Similar increase in resolution with increased Pharmalyte™ 8-10.5 concentration from 2 to 6% v/v has been reported [1]. In our work, further increase in the ampholyte concentration to 5% v/v resulted in a narrower separation window and a high absorbance background. Thus 2.5% v/v ampholytes was chosen as the optimum ampholyte concentration.

4.3.2. Single-step cIEF

In single-step cIEF, the capillary is initially filled with sample-ampholyte mixture and then the high voltage is applied. Both focusing and transport of the sample components occurs simultaneously. To achieve EOF-driven transport of the sample components, a coated capillary with a moderately suppressed EOF is needed to mobilize the focused zones past the UV detection window during the focusing step [8, 9, 18]. Use of single-step cIEF rather than two-step cIEF simplifies the experimental procedure, reduces the analysis time, and minimizes the possibility of peak distortion and broadening during mobilization. Dynamically coated capillaries using additives such as methyl cellulose [18, 34], hydroxypropylmethylcellulose [19] and glycerol [35] have been used for single-step cIEF of proteins and the neutral hydrophilic polymer polyethylene glycol (PEG) has been used for the separation of microbial cells [21]. For PEG to be effective, it was dissolved in the catholyte, in the anolyte and in the injected sample [21]. Herein we introduce a semi-permanent coating for single-step cIEF which is easy to prepare and offers higher stability compared to previous dynamic coatings.

As both the focusing and mobilization steps occur within an ampholyte filled capillary in single-step cIEF, it is impossible to directly measure the EOF. However, the EOF observed in past CZE studies using DODAB/POE 40 can be used as a guide for cIEF method development. In 50 mM sodium phosphate pH 3.0 buffer, the 0.1 mM DODAB/0.075% w/v POE 40 stearate provided a moderately suppressed EOF of $-0.34 \times 10^{-4} \text{ cm}^2/\text{Vs}$ [22] that should be compatible with single step-cIEF separations. Similarly, Krylov *et al.* observed reversed moderately suppressed EOF with a DODAB/POE stearate coating using 50 mM sodium phosphate pH 3.0 buffer, and normal moderately suppressed EOF using different buffer types near physiological pH [26]. Under the cIEF experimental conditions in this manuscript, a positive polarity was required to move the sample components towards the detection window. Figure 4.3 shows the separation of 6 peptide pI markers on a DODAB/POE 40 stearate coated capillary using 2.5% v/v of pH 3-10 carrier ampholyte. Similarly, Figure 4.4 uses the narrower range 5-8 ampholytes to separate a set of 5 peptide pI markers including markers for pI 7.05 and 7.0. Resolution in cIEF is governed by [9]:

$$R_s \propto [E \cdot L / \Delta(\text{pH})_{\text{total}}]^{1/2} \quad (4.1)$$

where E is the field strength (V/cm), L is length of pH gradient (equal to total length of the separation capillary) and $\Delta(\text{pH})_{\text{total}}$ is the width of the pH gradient used, e.g. $\Delta(\text{pH})_{\text{total}}$ equals 7 for a pH 3-10 gradient and equals 3 for a pH 5-8 gradient. The use of narrower range ampholytes 5-8 in Figure 4.4 enhances the resolution and enables the separation of the two markers at pI 7.0 and 7.05. It should be noted however that these two markers are from different suppliers.

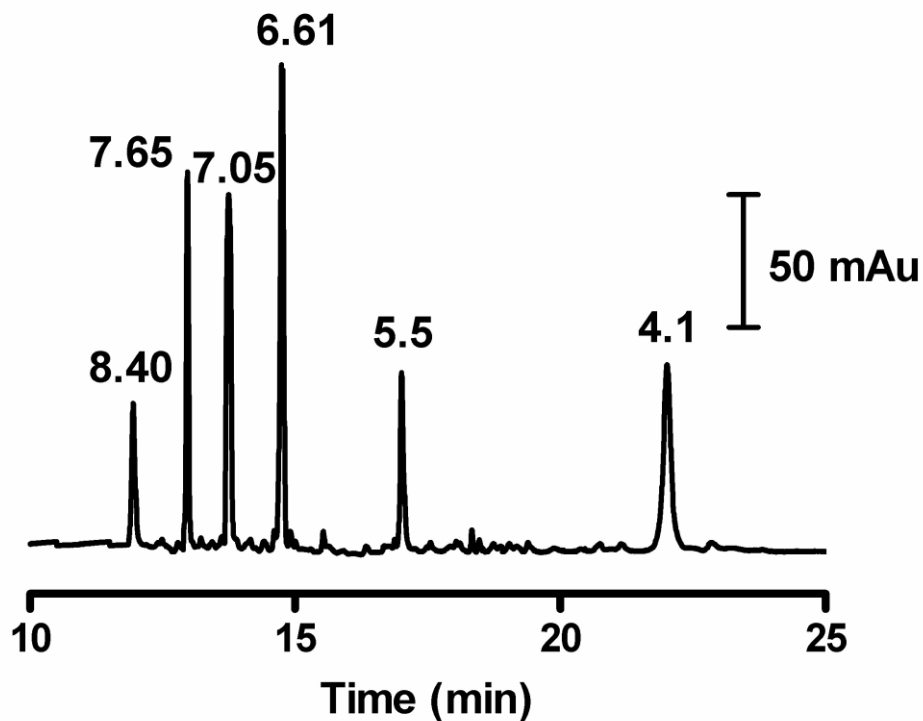


Figure 4.3: Single-step cIEF separation of 6 peptide markers on a 0.1 mM DODAB /0.075% POE 40 stearate sequentially coated capillary using 2.5% v/v of the carrier ampholytes pI 3-10.

Experimental conditions: 48.5 cm \times 50 μ m i.d. capillary (40 cm to detector); temperature, 25°C; λ , 280 nm. Samples contained 2.5% v/v of the carrier ampholytes pI 3-10; 8 μ L of 0.2 M iminodiacetic acid; 36 μ L of 0.5 M L-arginine and 6 peptide markers 8.40 (8 μ L), 7.65 (3 μ L), 7.05 (5 μ L), 6.61 (2 μ L), 5.5 (5 μ L) and 4.1 (5 μ L). Sample was diluted to a total volume of 500 μ L with cIEF gel and injected into the capillary at 2 bar pressure injection for 3 minutes. Sample was focused at +25 kV using 200 mM phosphoric acid as anolyte 300 mM sodium hydroxide as catholyte.

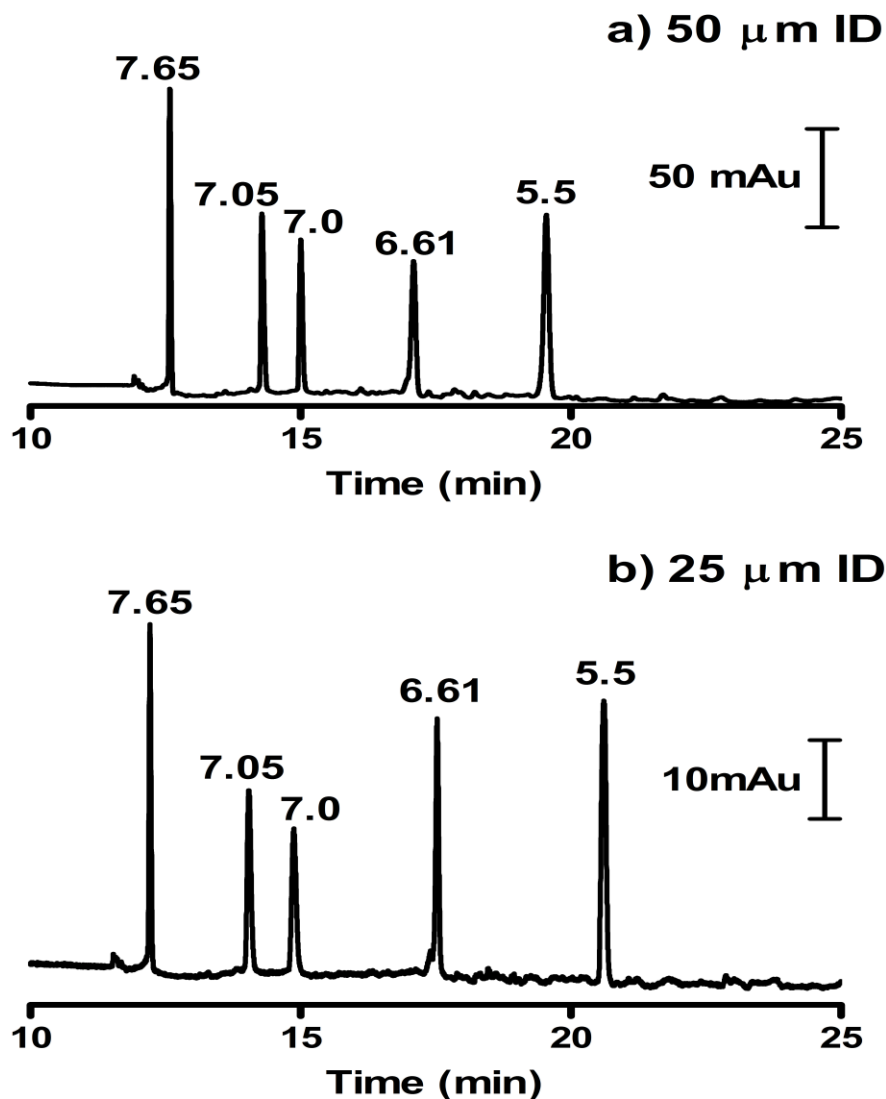


Figure 4.4: Single-step cIEF separation of 5 peptide markers on a 0.1 mM DODAB /0.075% POE 40 stearate a) 50 μm i.d. and b) 25 μm i.d. coated capillaries using 2.5% v/v of the carrier ampholytes pI 5-8.

Experimental conditions: 48.5 cm capillary (40 cm to detector); temperature, 25°C; λ , 280 nm. Samples contained 2.5% v/v of the carrier ampholytes pI 5-8; 8 μL of 0.2 M iminodiacetic acid; 36 μL of 0.5 M L-arginine and 5 peptide markers 7.65 (3 μL), 7.05 (3 μL), 7.0 (5 μL), 6.61 (2 μL) and 5.5 (5 μL). Sample was diluted to a total volume of 500 μL with cIEF gel and injected into the capillary at 2 bar pressure injection for 3 minutes. Sample was focused at +25 kV using 200 mM phosphoric acid as anolyte 300 mM sodium hydroxide as catholyte.

Their apparent ΔpI in Figure 4.4 is ≈ 0.15 pI unit. This discrepancy reflects the uncertainty associated with the pI values of standard pI markers.

Figures 4.3 and 4.4 indicate that the EOF was sufficiently suppressed to allow complete focusing but not so highly suppressed as to prevent the transport of the focused peaks to the detection window. In contrast, the 0.1 mM DODAB/0.001% w/v POE 100 stearate coating yields a more suppressed EOF ($-0.17 \times 10^{-4} \text{ cm}^2/\text{Vs}$ in 50 mM sodium phosphate pH 3.0 buffer [22]). No peaks were observed for either peptide pI marker set within 120 min at +25 kV when the DODAB/POE 100 stearate coating was used under the conditions in Figures 4.3 and 4.4. This confirms that the EOF was so highly suppressed that the residual EOF could not carry the focused peptide markers past the detection window.

The studies above (Figures 4.3 and Figure 4.4.a) were performed in 50 μm i.d. capillaries, which is the only i.d. of commercially available coated capillaries for cIEF. Availability of smaller i.d. capillaries for cIEF would enable the analysis of small volume samples which is particularly important in biological micro-environments. Also the better heat dissipation of narrow capillaries would also enable faster analysis and while maintaining the integrity of the sample protein mixture [36]. Conversely larger i.d. capillaries would be less likely to clog due to protein precipitation. One important advantage of the sequential coating is that it can be applied to different inner diameter capillaries. DODAB based coatings have been shown to be effective and stable in capillaries ranging from 5 μm [25] to 100 μm i.d. [37]. As shown in Chapter Two, the use of narrower i.d capillaries

actually enhances the stability of surfactant bilayer coatings and yields higher efficiencies for CZE separations of proteins [25, 37].

Figure 4.4.a shows the separation of peptide markers using a 50 μm i.d. DODAB/POE 40 stearate coated capillary, while Figure 4.4.b shows the comparable separation using a 25 μm i.d. coated capillary. The number of capillary volumes of coating and sample solutions flushed through the capillary were held constant for the different i.d. capillaries by controlling the pressure and time used. Comparable separations have been achieved in both capillaries indicating that the coating was effective in preventing protein adsorption even in the smaller i.d. capillary with the higher surface to volume ratio and higher potential for protein adsorption [38]. The average peak width (at 50% of peak height) of 5 peptide markers is 0.016 pH unit in both the 50 μm and 25 μm i.d. capillaries. The migration times of the peptide markers are similar in the different inner diameter capillaries. This indicates that a similar charge density coating with constant EOF is formed regardless of the inner diameter of the capillary [25, 39].

Figure 4.5 shows the single-step cIEF separation of 5 peptide markers on a 0.1 mM DODAB /0.075% POE 40 stearate coated capillary monitored at both 280 nm (Figure 4.5 a); and 420 nm (Figure 4.5. b). All pI markers absorb at 280 nm while only pI markers 7.65 and 6.61 absorb at both 280 nm and 420 nm which assists in tracking these markers.

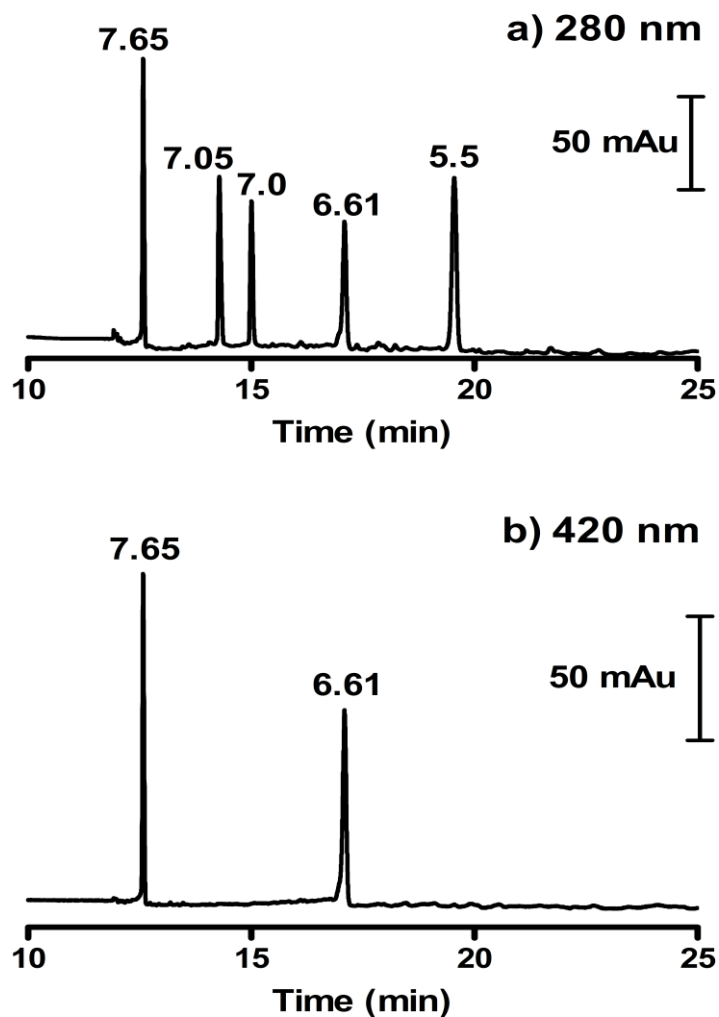


Figure 4.5: Single-step cIEF separation of 5 peptide markers on a 0.1 mM DODAB /0.075% POE 40 stearate coated capillary monitored at: a) 280 nm; and b) 420 nm.

Experimental conditions: 48.5 cm \times 50 μ m i.d. capillary (40 cm to detector); temperature, 25°C; λ , 280 or 420 nm; other experimental conditions are the same as in Figure 4.4.

The choice of the capillary length is a parameter that can be used to optimize cIEF separations. The need for rapid cIEF analysis calls for a short capillary and a high separation potential. The only restriction is that the capillary must be long enough to allow complete focusing prior to the EOF sweeping the band past the detector. This is particularly important in coatings with moderately suppressed EOF used for single-step cIEF. On the other hand, a longer capillary provides additional focusing time and a higher resolution [9, 40]. Since the pH gradient spans the entire length of the capillary, a longer capillary will result in a flatter pH gradient and higher spatial resolution. However this higher resolution comes at the expense of longer analysis time [9, 40] .

Figures 4.6 and 4.7 show the separation of 5 and 6 peptide marker mixtures using DODAB/POE 40 stearate coated capillaries of different lengths. The number of capillary volumes of coating and sample solutions flushed through the capillary were held constant for the different capillary lengths by controlling the pressure and time used for rinses. A constant voltage (+25 kV) was applied to the different length capillaries. Both the medium length capillary (48.5 cm, Figure 4.6.b) and the long capillary (65 cm, Figure 4.6.c) resolved all 5 markers with comparable resolution (average peak width = 0.016 pH units). This is consistent with equation 4.1 [9], where the use of longer capillary and a lower field strength will counterbalance one another. The shortest capillary (32 cm, Fig. 4.6.a) provides insufficient time for complete focusing resulting in low resolution (average width of 0.072 pH units) and only partial separation of the pI 7.05 and 7.0 markers.

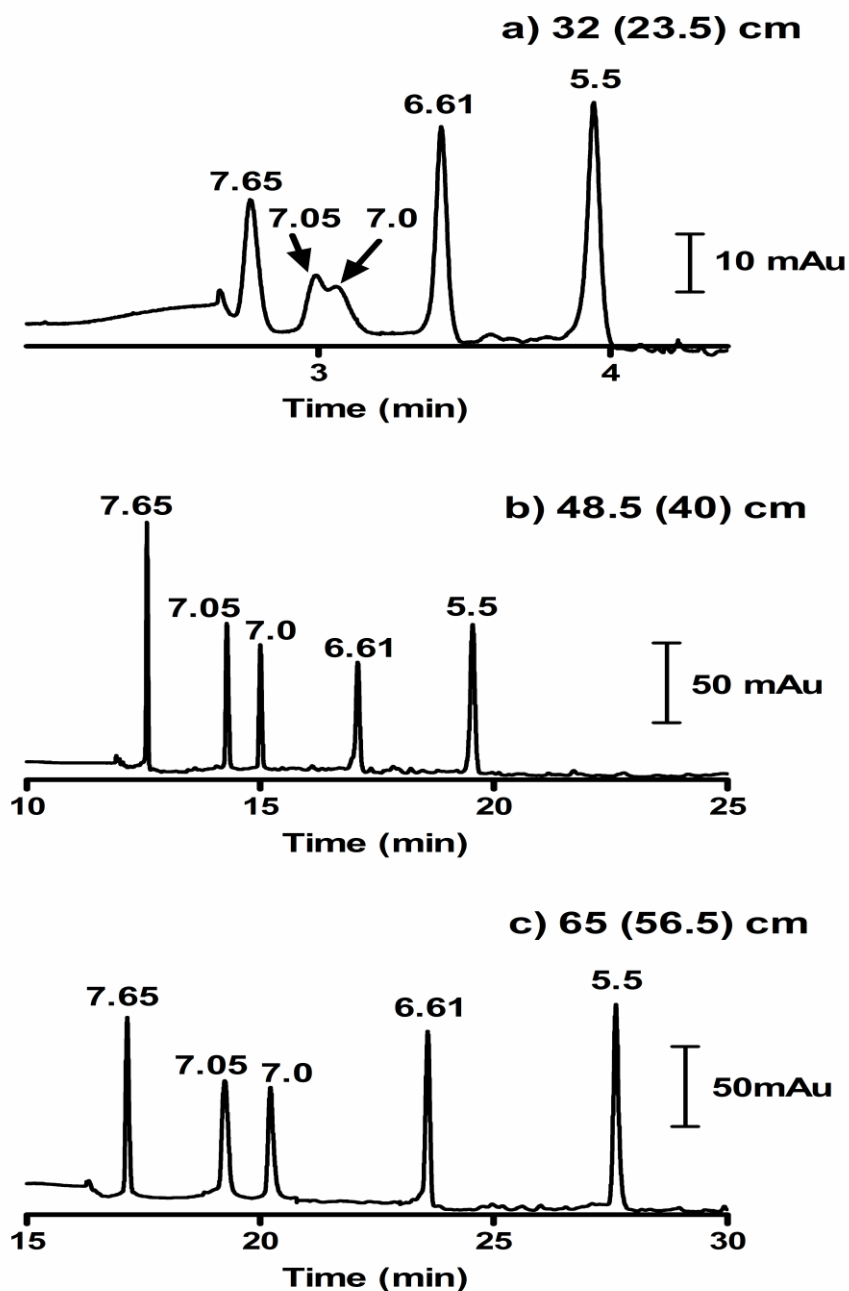


Figure 4.6: Single-step cIEF separation of 5 peptide markers on a 0.1 mM DODAB /0.075% POE 40 stearate a) 32 (23.5) cm, b) 48.5 (40) cm and 65 (56.5) cm coated capillaries using 2.5% v/v of the carrier ampholytes pI 5-8.

Experimental conditions: 50 μm i.d. capillaries; λ , 280 nm; other experimental conditions are the same as in Figure 4.4.

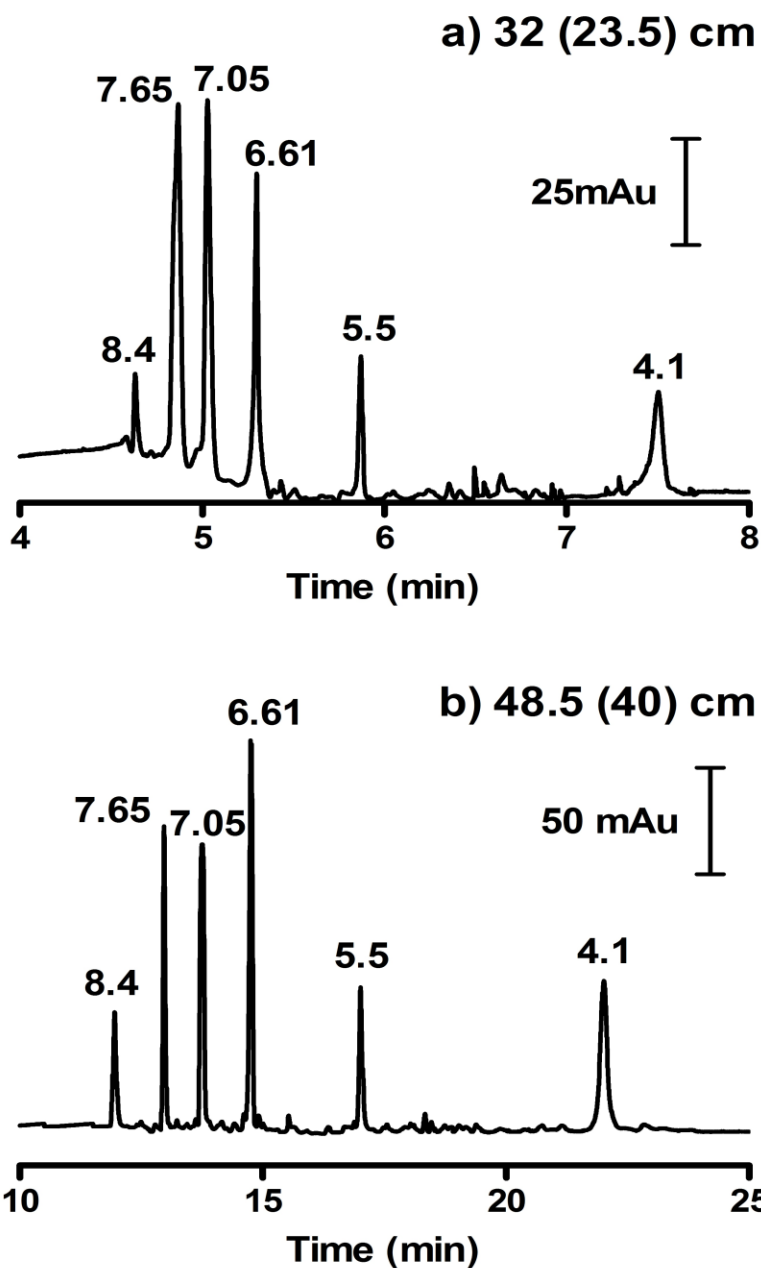


Figure 4.7: Single-step cIEF separation of 6 peptide markers on a 0.1 mM DODAB /0.075% POE 40 stearate a) 32 (23.5) cm; and b) 48.5 (40) cm coated capillaries using 2.5% v/v of the carrier ampholytes pI 3-10.

Experimental conditions: 50 μ m i.d. capillaries; λ , 280 nm; other experimental conditions are the same as in Figure 4.3.

Comparable results were observed for the separation of the 6 peptide marker mixture in DODAB/POE 40 stearate coated capillaries using 2.5% v/v carrier ampholytes pI 3-10 (Figure 4.7). Albeit in that case both capillary lengths including the shorter (32 cm total length) successfully resolved all 6 markers.

4.3.3 Two-step cIEF

Two-step cIEF separations involve both a focusing step and a mobilization step. Mobilization may be either by pressure [16, 17] or chemical [1]. Despite peak broadening during the mobilization step and the increased chance of capillary clogging, two-step cIEF offers some advantages. The strongly suppressed EOF provides better migration time reproducibility, and thus better linearity of the pH gradient which enhances the accuracy of the pI determined [14]. Covalently linked neutral hydrophilic polymer coatings such as non crosslinked acrylamide [7], hydroxypropylcellulose [15, 16] and polyvinyl alcohol [3] have been used. However, as noted above covalent coatings are time consuming, labor-intensive, difficult to reproduce, their purchase is expensive and limited to restricted capillary dimensions. Dynamic coatings based on zwitterionic surfactants [41] and hydroxypropylmethylcellulose [42] have been used for two-step cIEF. In this section, the sequential coating is used to perform two-step cIEF. The sequential coating is easy to develop, cost effective and semi-permanent. Both versions of the sequential coatings, DODAB/POE 40 stearate and DODAB/POE 100 stearate, can be used based on the degree of resolution required and the analysis time. Chemical mobilization methodology rather than

pressure mobilization was used due to parabolic hydrodynamic flow band broadening associated with the latter [17].

The EOF of the sequential coating can be tuned by varying the POE chain length. The DODAB/POE 100 stearate version of the coating provides a more suppressed EOF compared to DODAB/POE 40 stearate. Figure 4.8 shows the separation of 6 peptide markers on DODAB/POE 40 and DODAB/POE 100 coated capillaries using two-step cIEF. The focusing time was limited to 10 min to avoid eluting the peptide markers from the capillary in the case of DODAB/POE 40 stearate. The sequentially coated DODAB /POE 100 capillary results in a larger separation window compared to the DODAB/POE 40 coated capillary. The average peak width (at 50% of peak height) of the 6 peptide markers is 0.028 pH unit in DODAB/POE 40 coated capillary and 0.025 in the DODAB/POE 100 coated capillary. For replicate injections, DODAB/POE 100 stearate showed better migration time reproducibility compared to DODAB/POE 40 stearate. The DODAB/POE coatings were successfully created in all capillaries tested, but the precise peak position of the pI markers varied within-capillary and capillary-to-capillary. The EOF of freshly coated DODAB/POE 40 stearate capillaries was $-0.32 \times 10^{-4} \text{ cm}^2/\text{Vs}$ in 50 mM sodium phosphate pH 3.0 buffer. After performing a series of cIEF experiments, the EOF was comparable ($-0.13 \times 10^{-4} \text{ cm}^2/\text{Vs}$). This indicated that the coating was stable after performing cIEF experiments and was not the source of irreproducibility of migration time. Unfortunately, investigations of voltage ramping, use of fresh coating solutions, use of fresh analyte, catholyte and mobilizer solutions did not improve the

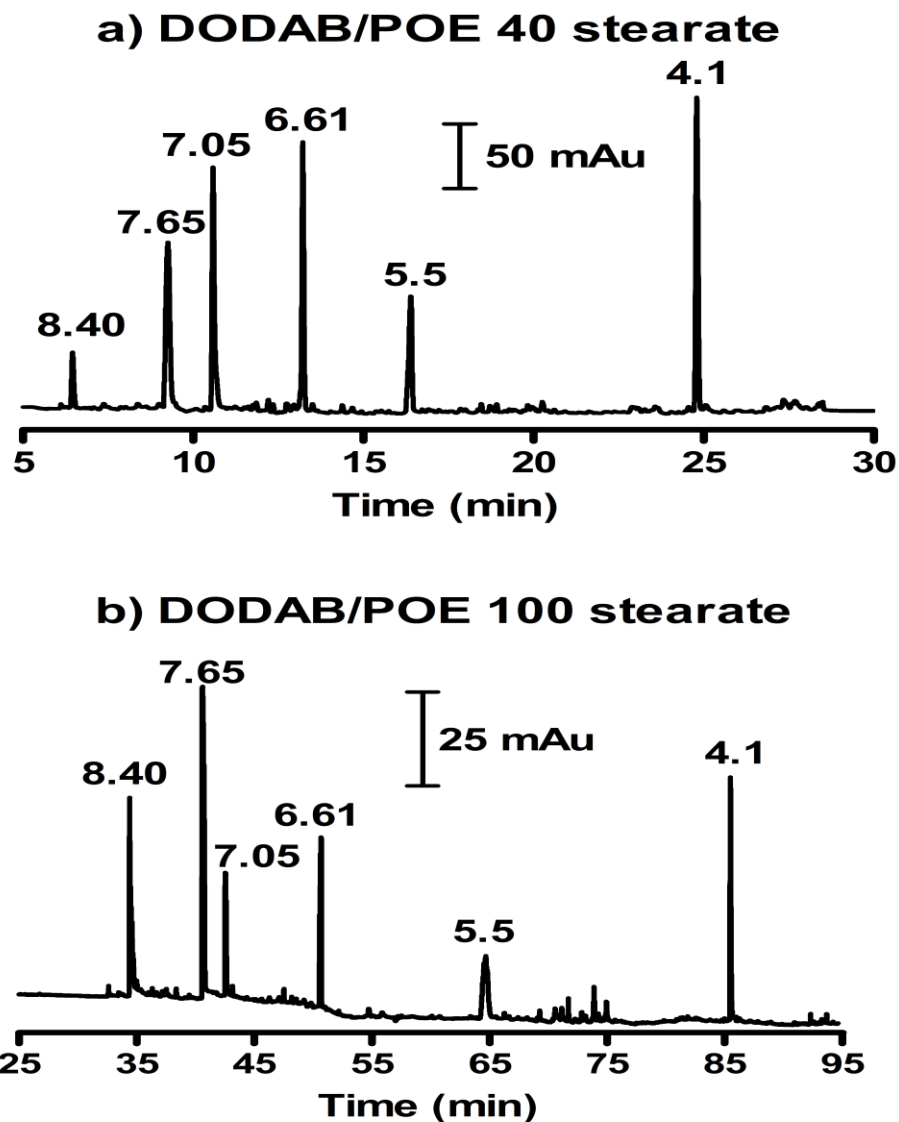


Figure 4.8: Two-step cIEF separation of 6 peptide markers on a) 0.1 mM DODAB / 0.075% POE 40 stearate and b) 0.1 mM DODAB / 0.001% POE 100 stearate sequentially coated capillaries using 2.5% v/v of the carrier ampholytes pI 3-10.

Experimental conditions: 48.5 cm \times 50 μ m i.d. capillaries (40 cm to detector); temperature, 25°C; λ , 280 nm. Samples contained 2.5% v/v of the carrier ampholytes pI 3-10; 8 μ L of 0.2 M iminodiacetic acid; 36 μ L of 0.5 M L-arginine and 6 peptide markers 8.40 (8 μ L), 7.65 (3 μ L), 7.05 (5 μ L), 6.61 (2 μ L), 5.5 (5 μ L) and 4.1 (5 μ L). Sample was diluted to a total volume of 500 μ L with cIEF gel and injected into the capillary at 2 bar pressure injection for 3 minutes. Sample was focused for 10 minutes at +25 kV using 200 mM phosphoric acid as anolyte 300 mM sodium hydroxide as catholyte then chemically mobilized at +25 kV using 350 mM acetic acid instead of sodium hydroxide.

migration time reproducibility. Thus, the inclusion of pI markers within a sample is essential.

Figure 4.9 shows a two-step cIEF separation of the 6 peptide markers under variable conditions of ampholyte concentration and POE stearate chain length. The best resolution was achieved by a combination of increasing the ampholyte concentration from 1.25% v/v to 2.5% v/v and by using DODAB/POE 100 stearate instead of DODAB/POE 40 stearate. The average peak width (at 50% of peak height) of the 6 peptide markers decreased from 0.033 pH unit in the case of 1.25% v/v ampholytes and DODAB/POE 40 stearate (Figure 4.9.a) to 0.028 in the case of 2.5% v/v ampholytes and DODAB/POE 40 stearate (Figure 4.9.b). The average peak width was further decreased to 0.025 pH unit in the case of 2.5% v/v ampholytes and DODAB/POE 100 stearate coated capillaries (Figure 4.9.c) but at the cost of much longer analysis time.

Figure 4.10 shows the two-step cIEF separation of 5 peptide markers on a DODAB/POE 40 stearate coated capillary. The 5 markers are separated within 16 min compared to 85 min on a DODAB/POE 100 stearate capillary. The two peptide markers 7.05 and 7.0 have been separated with a resolution of 7.4 using the two-step cIEF method on a DODAB/POE 40 stearate coated capillary. Comparable resolution (7.5) was observed using the two-step cIEF separation on DODAB/POE 100 stearate. In both cases, the resolution was higher than that achieved using the single-step cIEF method (Figure 4.4.a), where the resolution was 5.8.

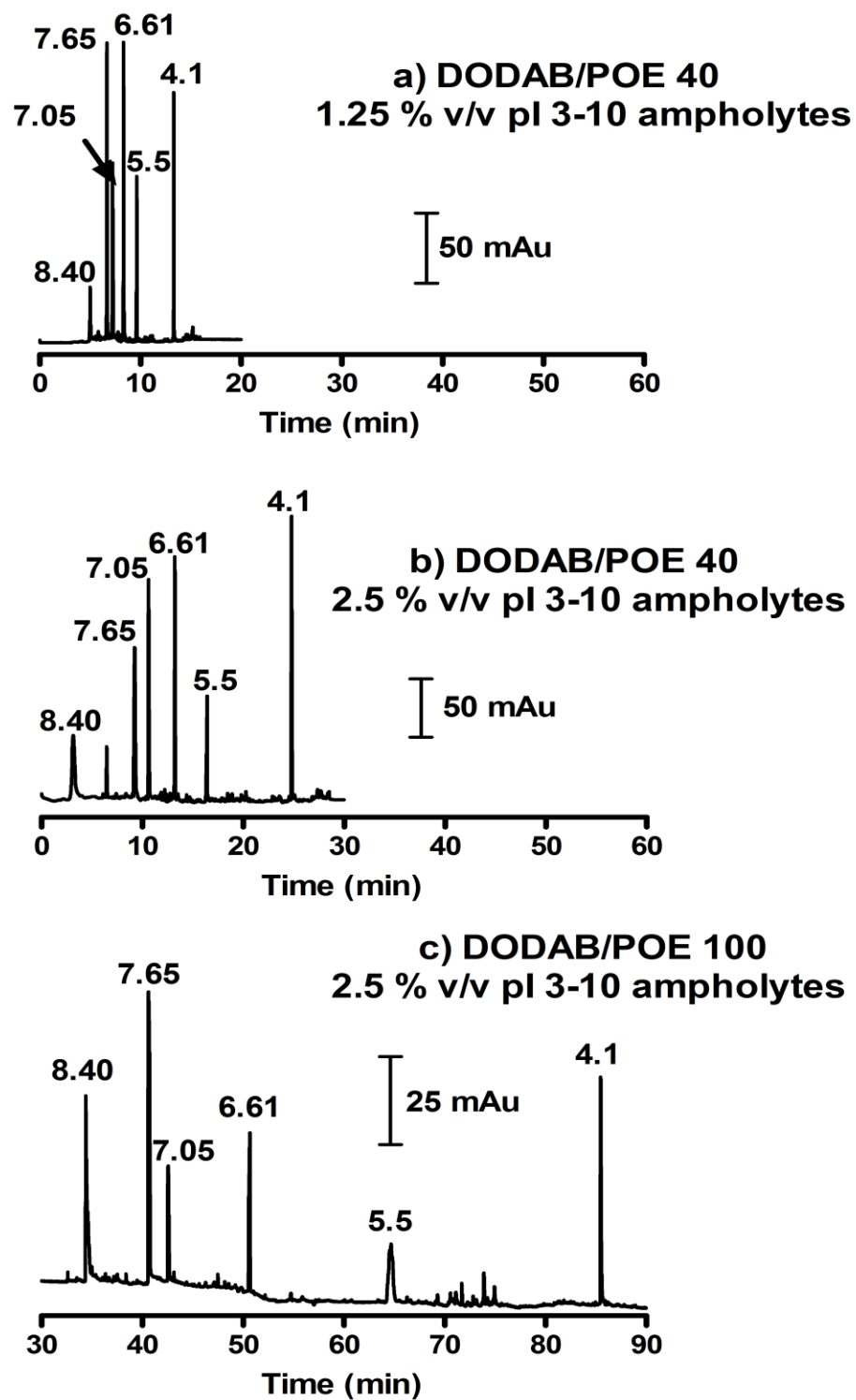


Figure 4.9: Two-step cIEF separations of 6 peptide markers using different ampholyte concentrations and different POE stearate chain lengths.

Experimental conditions: same as in Figure 4.8

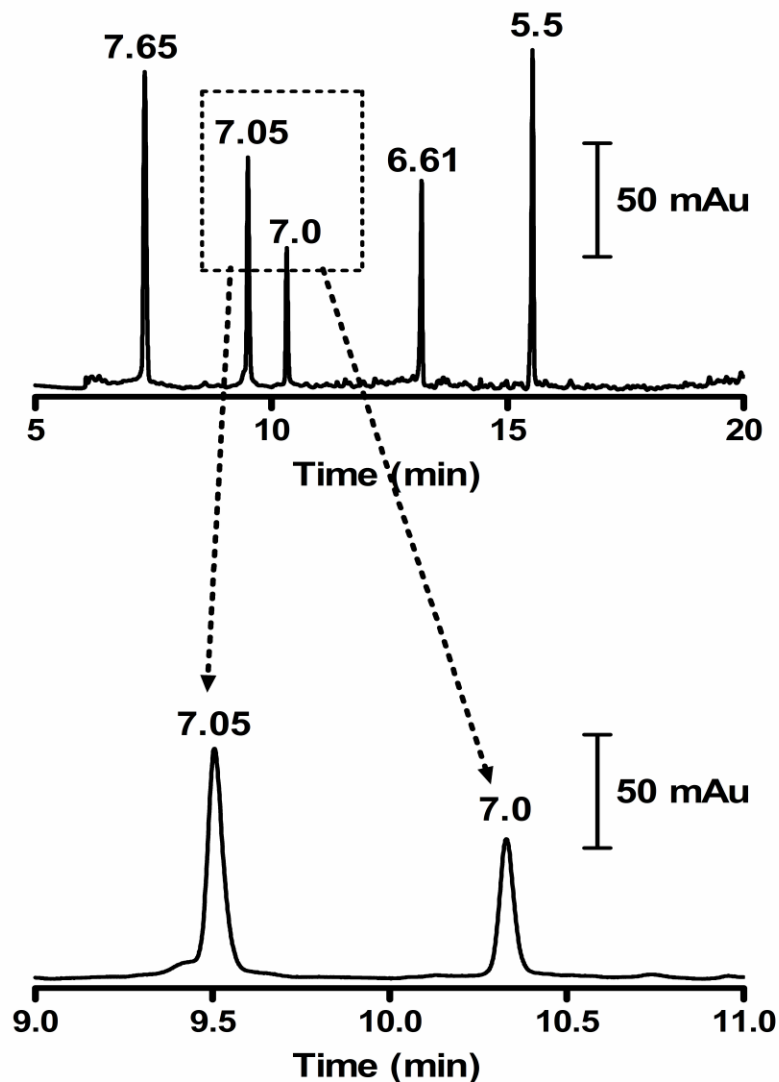


Figure 4.10: Two-step cIEF separation of 5 peptide markers on a 0.1 mM DODAB /0.075% POE 40 stearate coated capillary using 2.5% v/v of the carrier ampholytes pI 5-8. The inset shows an expanded view of the separation of the 7.05 and 7.0 pI markers.

Experimental conditions: 48.5 cm \times 50 μ m i.d. capillary (40 cm to detector); temperature, 25°C; λ , 280 nm. Samples contained 2.5 %v/v of the carrier ampholytes pI 5-8; 8 μ L of 0.2 M iminodiacetic acid; 36 μ L of 0.5 M L-arginine and 5 peptide markers 7.65 (3 μ L), 7.05 (3 μ L), 7.0 (5 μ L), 6.61 (2 μ L) and 5.5 (5 μ L). Sample was diluted to a total volume of 500 μ L with cIEF gel and injected into the capillary at 2 bar pressure injection for 3 min. Sample was focused for 10 min at +25 kV using 200 mM phosphoric acid as anolyte 300 mM sodium hydroxide as catholyte then chemically mobilized at +25 kV using 350 mM acetic acid instead of sodium hydroxide.

In both the single-step and two-step cIEF, coated capillaries have been used for more than 40 h without degradation of the capillary performance. The rinsing procedure between successive runs included flushing the capillary with 4.3 M urea for 5 min at 2 bar pressure rinse to remove any precipitated material [29].

4.3.4 Linearity of pH gradient

The pI value of a protein depends on its amino acid composition and its spatial conformation. Estimation of pI value is helpful in the identification of unknown proteins. The accuracy of the pI estimate is enhanced by the linearity of the pH gradient established along the capillary. Common causes of non linearity of the pH gradient are pressure-induced parabolic flow [43] and migration time irreproducibility associated with variable electroosmotic flow [5, 8]. The use of chemical mobilization rather than pressure mobilization [8, 43] and coated capillaries with strongly suppressed EOF rather than dynamically modified capillaries with moderate EOF overcome these limitations and improve the linearity of the pH gradient [5, 14]. In addition, the quality of the carrier ampholytes is an important contributing factor to the linearity of the pH gradient. Uneven distribution of the ampholytes over the claimed pH range of the ampholyte blend leads to uneven conductivity and buffer capacity and poor linearity of the pH gradient [5]. Studies on different commercial ampholyte blends indicated that they contain more acidic ampholytes than basic ones and their actual pH ranges are not identical to the claimed values [5, 44]. Moreover, the

markers used to construct a calibration plot should possess sharp focusing, high solubility and high purity [5].

The correlation between the pI of the peptide markers and the migration times was evaluated for verification of linearity of the pH gradient established using the sequential coating. A recta-linear relationship (Figure 4.11) was established only using two-step cIEF over 3-10 pH range in a DODAB/POE 40 coated capillary with a regression equation of [Migration time = $(40.6 \pm 2.1) - (4.1 \pm 0.3) \text{ pI}$] and a correlation coefficient of 0.977. This linearity is identical to that observed with the same ampholytes and markers on a commercial covalently modified capillary. Under different experimental conditions, no linear pH gradient was established using single-step cIEF. The increased focusing time during the single-step cIEF methodology increases the effect of both anodic and cathodic drift [29]. Consequently, poor linearity is more evident in single-step cIEF. Two-step cIEF yielded relatively linear pH gradient. Linearity of pH gradient was enhanced by increasing the ampholyte concentration from 1.25% v/v ($R^2= 0.95$) to 2.5% v/v ($R^2= 0.977$). Further increase in the carrier ampholyte concentration up to 5% v/v results in loss of linearity of the pH gradient and higher background absorbance. The linearity achieved was slightly greater using DODAB/POE 100 stearate ($R^2=0.984$) rather than DODAB/POE 40 stearate ($R^2=0.977$).

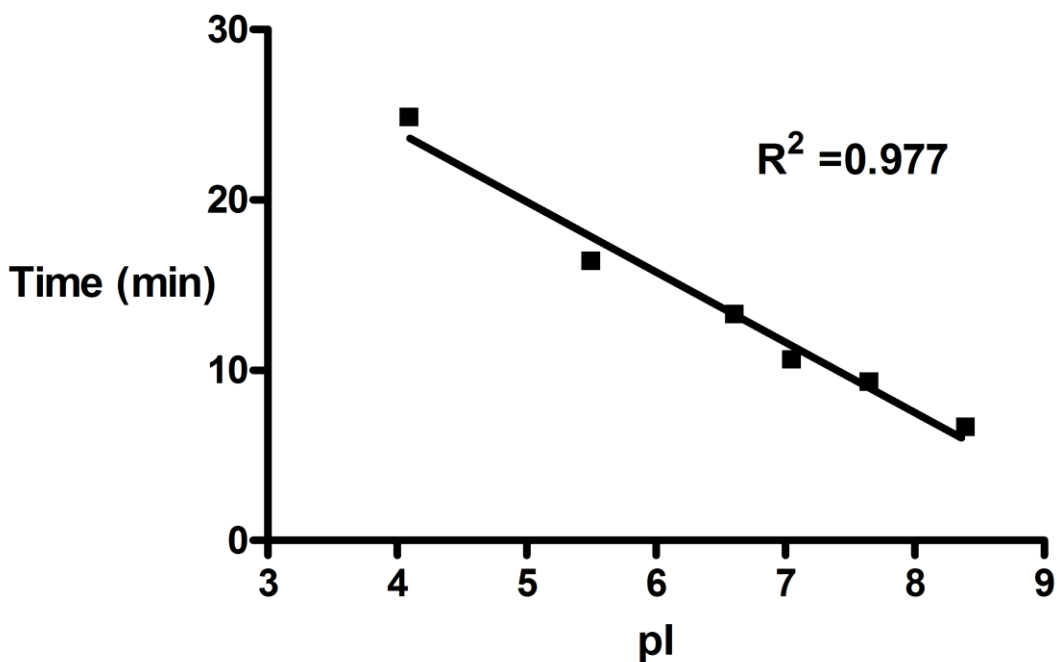


Figure 4.11: Linearity of the pH gradient established on a 0.1 mM DODAB /0.075% POE 40 stearate coated capillary using 2.5% v/v carrier ampholytes.

Experimental conditions: 48.5 cm × 50 μm i.d. capillaries (40 cm to detector); temperature, 25°C; λ, 280 nm. Samples contained 2.5% v/v of the carrier ampholytes pI 3-10; 8 μL of 0.2 M iminodiacetic acid; 36 μL of 0.5 M L-arginine and 6 peptide markers 8.40 (8 μL), 7.65 (3 μL), 7.05 (5 μL), 6.61 (2 μL), 5.5 (5 μL) and 4.1 (5 μL). Sample was diluted to a total volume of 500 μL with cIEF gel and injected into the capillary at 2 bar pressure injection for 3 minutes. Sample was focused for 10 minutes at +25 kV using 200 mM phosphoric acid as anolyte 300 mM sodium hydroxide as catholyte then chemically mobilized at +25 kV using 350 mM acetic acid instead of sodium hydroxide.

4.3.5 Separation of hemoglobin variants

The identification and determination of different hemoglobin variants are of great diagnostic and clinical importance. For instance HbA is the normal adult form of hemoglobin, while HbS is an abnormal form (the amino acid in position 6 of the β -globin chain of hemoglobin is valine instead of the glutamic acid in HbA) associated with sickle cell anemia. cIEF has been extensively utilized for monitoring hemoglobin variants [2, 45, 46]. Figure 4.12 shows the separation of HbA₀ and HbS on a DODAB/POE 40 coated capillary using 2.5% v/v of pH 3-10 Ampholyte®. Based on the linear calibration curve established using pI markers, the pI of HbS and HbA₀ are estimated to be 7.21 and 7.12, slightly higher than the literature values of 7.21 and 6.98, respectively [14, 45, 47]. The same pI values were obtained for the Hb variants using the same ampholytes and markers on a commercially available coated capillary (Figure 4.13). The slight difference between the estimated and reported pI values could be attributed to different carrier ampholytes and/or pI markers. The estimated pI value of HbA₀ ranged from 7.01 to 7.13 using different brands of the carrier ampholytes [2]. Higher resolution separations like HbA and HbF mixture ($\Delta pI \approx 0.08$) [45] or HbA and HbA1c ($\Delta pI \approx 0.04$) [2, 47] could be easily achieved by using DODAB/POE stearate in combination with a narrow (5-8) range ampholytes.

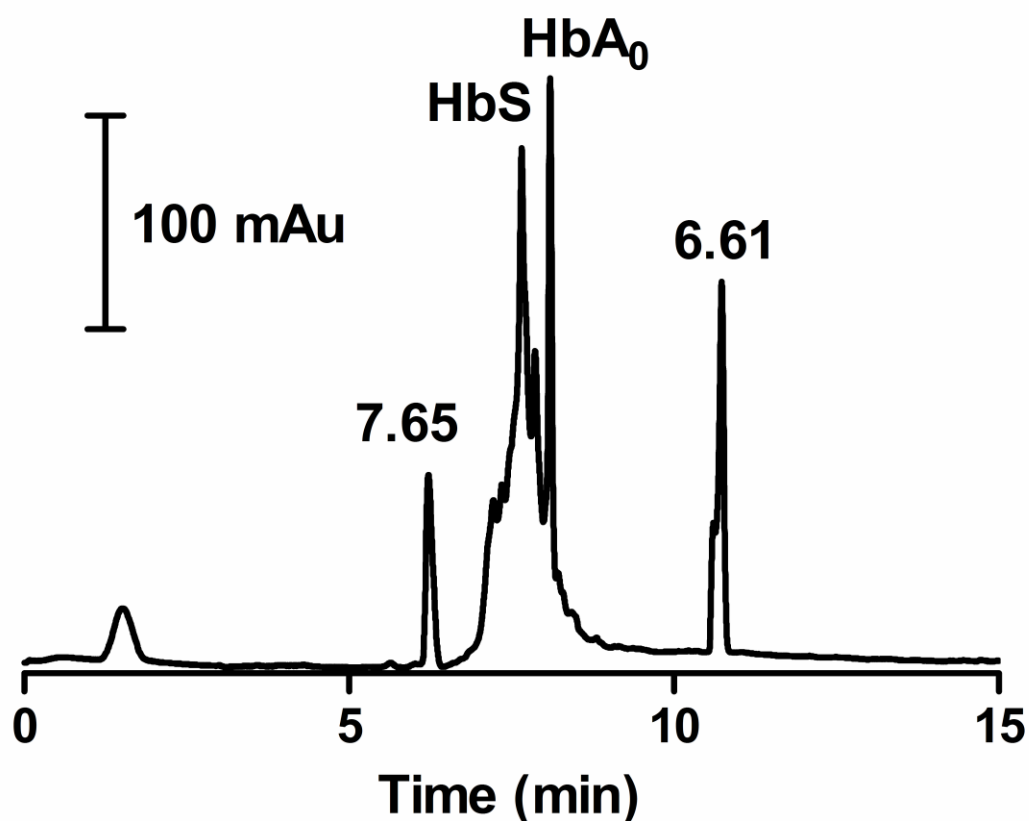


Figure 4.12: Two-step cIEF separation of two hemoglobin variants; HbA₀ and HbS on a 0.1 mM DODAB/0.075% POE 40 stearate sequentially coated capillary.

Experimental conditions: 48.5 cm × 50 μm i.d. capillary (40 cm to detector); temperature, 25°C; λ, 420 nm. Samples contained 2.5% v/v of the carrier ampholytes pI 3-10; 8 μL of 0.2 M iminodiacetic acid; 36 μL of 0.5 M L-arginine, 7.65 (3 μL), 6.61 (2 μL), HbA₀ (3 μL) and HbS (3 μL). Sample was diluted to a total volume of 500 μL with cIEF gel and injected into the capillary at 2 bar pressure injection for 3 minutes. Sample was focused for 10 min at +25 kV using 200 mM phosphoric acid as anolyte 300 mM sodium hydroxide as catholyte then chemically mobilized at +25 kV using 350 mM acetic acid instead of sodium hydroxide.

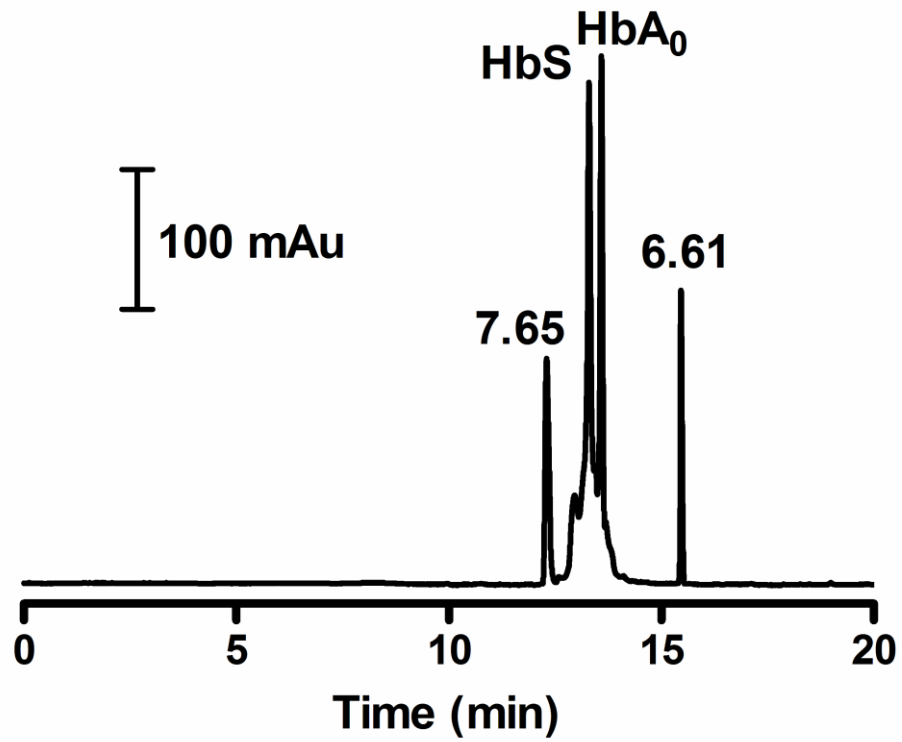


Figure 4.13: Two-step cIEF separation of two hemoglobin variants; HbA₀ and HbS on a commercially coated capillary.

Experimental conditions: same as in Figure 4.12.

4.4 Conclusions

The developed DODAB/POE stearate sequential coating offers the combined advantages of the stability of cationic surfactant coatings and the suppressed EOF of neutral polymer coatings. The sequential coating is easy to prepare, low cost, semi-permanent, and provides controllable EOF by varying the POE chain length. Single-step cIEF can be performed using the DODAB/POE 40 stearate coating. Two-step cIEF can be performed using either the DODAB/POE 40 stearate or DODAB/POE 100 stearate coating. The sequential coatings can be tailored based on the degree of resolution required and the analysis time. High resolution separations can be achieved by using, narrow pH range ampholytes, higher ampholyte concentrations, longer POE chain and longer capillaries but at the expense of longer analyses time. The sequential coating has been applied successfully to cIEF separations using different capillary lengths and inner diameters. A recta-linear pH gradient is established only in two-step CIEF methodology using 3-10 pH 2.5% v/v carrier ampholytes. Hemoglobin A₀ and S variants are successfully resolved on DODAB/POE 40 stearate sequentially coated capillaries.

4.5 References

- [1] Lin, J., Tan, Q. Q. and Wang, S. X., *J. Sep Sci.* 2011, *34*, 1696-1702.
- [2] Koval, D., Kasicka, V. and Cottet, H., *Anal. Biochem.* 2011, *413*, 8-15.
- [3] Thorne, J. M., Goetzinger, W. K., Chen, A. B., Moorhouse, K. G. and Karger, B. L., *J. Chromatogr. A* 1996, *744*, 155-165.
- [4] Lemma, T. and Pawliszyn, J., *J. Pharm. Biomed. Anal.* 2009, *50*, 570-575.
- [5] Righetti, P. G., *J. Chromatogr. A* 2004, *1037*, 491-499.
- [6] Cooper, J. W., Wang, Y. J. and Lee, C. S., *Electrophoresis* 2004, *25*, 3913-3926.
- [7] Kilar, F. and Hjerten, S., *Electrophoresis* 1989, *10*, 23-29.
- [8] Rodriguez-Diaz, R., Wehr, T. and Zhu, M. D., *Electrophoresis* 1997, *18*, 2134-2144.
- [9] Shimura, K., *Electrophoresis* 2009, *30*, 11-28.
- [10] Schure, M. R. and Lenhoff, A. M., *Anal. Chem.* 1993, *65*, 3024-3037.
- [11] Green, J. S. and Jorgenson, J. W., *J. Chromatogr.* 1989, *478*, 63-70.
- [12] Towns, J. K. and Regnier, F. E., *Anal. Chem.* 1991, *63*, 1126-1132.
- [13] Hjerten, S. and Zhu, M. D., *J. Chromatogr.* 1985, *346*, 265-270.
- [14] Huang, T. L., Shieh, P. C. H. and Cooke, N., *Chromatographia* 1994, *39*, 543-548.
- [15] Poitevin, M., Morin, A., Busnel, J. M., Descroix, S., Hennion, M. C. and Peltre, G., *J. Chromatogr. A* 2007, *1155*, 230-236.
- [16] Lecoecur, M., Goossens, J. F., Vaccher, C., Bonte, J. P. and Foulon, C., *Electrophoresis* 2011, *32*, 2857-2866.
- [17] Minarik, M., Groiss, F., Gas, B., Blaas, D. and Kenndler, E., *J. Chromatogr. A* 1996, *738*, 123-128.
- [18] Mazzeo, J. R. and Krull, I. S., *Anal. Chem.* 1991, *63*, 2852-2857.
- [19] Thormann, W., Caslavská, J., Molteni, S. and Chmelik, J., *J. Chromatogr.* 1992, *589*, 321-327.
- [20] Wu, J. Q. and Pawliszyn, J., *Anal. Chem.* 1992, *64*, 2934-2941.

- [21] Horka, M., Ruzicka, F., Hola, V. and Slais, K., *Anal. Bioanal. Chem* 2006, 385, 840-846.
- [22] MacDonald, A. M., Bahnasy, M. F. and Lucy, C. A., *J. Chromatogr. A* 2011, 1218, 178-184.
- [23] MacDonald, A. M. and Lucy, C. A., *J. Chromatogr. A* 2006, 1130, 265-271.
- [24] Barylá, N. E., Melanson, J. E., McDermott, M. T. and Lucy, C. A., *Anal. Chem.* 2001, 73, 4558-4565.
- [25] Gulcev, M. D., McGinitie, T. M., Bahnasy, M. F. and Lucy, C. A., *Analyst* 2010, 135, 2688-2693.
- [26] de Jong, S., Epelbaum, N., Liyanage, R. and Krylov, S. N., *Electrophoresis* 2012, 33, 2584-2590.
- [27] Shimura, K., Wang, Z., Matsumoto, H. and Kasai, K., *Electrophoresis* 2000, 21, 603-610.
- [28] Yassine, M. M. and Lucy, C. A., *Anal. Chem.* 2005, 77, 620-625.
- [29] Mack, S., Cruzado-Park, I., Chapman, J., Ratnayake, C. and Vigh, G., *Electrophoresis* 2009, 30, 4049-4058.
- [30] Cruzado-Park, I., Mack, S. and Ratnayake, C., "Identification of System Parameters Critical for High-Performance cIEF." *Beckman Coulter, Inc., Application information Bulletin* 2008.
- [31] Lacunza, I., Kremmer, T., Diez-Masa, J. C., Sanz, J. and de Frutos, M., *Electrophoresis* 2007, 28, 4447-4451.
- [32] Kremser, L., Bruckner, A., Heger, A., Grunert, T., Buchacher, A., Josic, D., Allmaier, M. and Rizzi, A., *Electrophoresis* 2003, 24, 4282-4290.
- [33] Silvertand, L. H. H., Torano, J. S., de Jong, G. J. and van Bennekom, W. P., *Electrophoresis* 2008, 29, 1985-1996.
- [34] Kilar, F., Vegvari, A. and Mod, A., *J. Chromatogr. A* 1998, 813, 349-360.
- [35] Busnel, J. M., Varenne, A., Descroix, S., Peltre, G., Gohon, Y. and Gareil, P., *Electrophoresis* 2005, 26, 3369-3379.
- [36] Fonslow, B. R., Kang, S. A., Gestaut, D. R., Graczyk, B., Davis, T. N., Sabatini, D. M. and Yates, J. R., *Anal. Chem.* 2010, 82, 6643-6651.
- [37] Yassine, M. M. and Lucy, C. A., *Anal. Chem.* 2004, 76, 2983-2990.

- [38] Woods, L. A., Roddy, T. P., Paxon, T. L. and Ewing, A. G., *Anal. Chem.* 2001, *73*, 3687-3690.
- [39] Knox, J. H. and Grant, I. H., *Chromatographia* 1987, *24*, 135-143.
- [40] Mazzeo, J. R. and Krull, I. S., *J. Microcol. Sep.* 1992, *4*, 29-33.
- [41] Yeung, K. K. C., Atwal, K. K. and Zhang, H. X., *Analyst* 2003, *128*, 566-570.
- [42] Kubach, J. and Grimm, R., *J. Chromatogr. A* 1996, *737*, 281-289.
- [43] Schwer, C., *Electrophoresis* 1995, *16*, 2121-2126.
- [44] Silvertand, L. H. H., Torano, J. S., van Bennekom, W. P. and de Jong, G. J., *J. Chromatogr. A* 2008, *1204*, 157-170.
- [45] Jenkins, M. A. and Ratnaike, S., *Clin. Chim. Acta* 1999, *289*, 121-132.
- [46] Hempe, J. M. and Craver, R. D., *Electrophoresis* 2000, *21*, 743-748.
- [47] Hempe, J. M., Granger, J. N. and Craver, R. D., *Electrophoresis* 1997, *18*, 1785-1795.

Chapter Five: Polyoxyethylene diblock copolymer coatings for capillary electrophoresis

5.1 Introduction

Capillary electrophoresis (CE) can provide fast, high efficiency separations of biomolecules with minimal sample consumption [1]. However, proteins may adsorb onto the capillary surface [2]. Adsorption leads to band broadening [3], EOF instability [4] and low sample recovery [5]. Different approaches have been used to minimize protein adsorption, including: extreme buffer pH [6]; high ionic strength [2]; and most commonly capillary coatings [7-9]. An ideal coating for CE should be stable, minimize analyte adsorption [7] and allow for control of the EOF [9]. Although covalent coatings can be effective at minimizing protein adsorption, they are difficult and time consuming to prepare [8]. In contrast, physically adsorbed polymer coatings are easy to prepare, can be regenerated and are cost effective [7].

Physically adsorbed cationic polymer coatings for CE include polyethyleneimine (PEI) [10], polybrene [11] and poly(diallyldimethylammonium chloride) PDADMAC [11]. These coatings adsorb to the negatively charged capillary inner surface through electrostatic interactions. However, the resultant strong anodic EOF may limit the resolution [9]. Successive multiple ionic-polymer layer (SMIL) coatings have been utilized for CE to prevent protein adsorption. In a typical SMIL, a polycationic polymer is adsorbed onto the capillary, followed by adsorption of a polyanionic polymer to yield a strong cathodic EOF that is independent of the pH [12]. However, the strongly cathodic

EOF of the SMIL still limits the resolution. Lower EOF can be achieved using physically adsorbed neutral polymer coatings such as polyethylene oxide (PEO) [13] or polyvinyl alcohol (PVA). These hydrophilic neutral coatings adsorb to the capillary wall through hydrogen bonding. They reduce analyte adsorption and suppress the EOF, but can be easily desorbed from the capillary [14]. Other neutral hydrophobic polymer coatings, such as polydimethylacrylamide (PDMA), fail to prevent irreversible adsorption of proteins [15]. Obviously, it is not easy to find a homo-polymer with all the required features of a coating (i.e., strong adsorption onto the silica surface, and biologically silent surface extended into solution) for electrophoretic separations.

As a result, several copolymers have been developed as capillary coatings. These copolymers are designed to have: an anchoring block which provides strong interaction with the capillary surface; and an anti-biofouling block to minimize adsorption. Different classes of diblock copolymers have been reported. Poly (4-vinylpyridine) poly-(ethylene oxide) [16] and cationized hydroxyethylcellulose (Cat-HEC) [17] are cationic-hydrophilic neutral copolymers. The cationic block adsorbs to the capillary wall through electrostatic interactions while the hydrophilic neutral block suppresses the EOF and minimizes analyte adsorption. Similarly, PEGMA-DMA has *N,N*-dimethylacrylamide (DMA) as the hydrophobic anchor component and the neutral poly(ethylene glycol) methyl ether methacrylate (PEGMA) as the hydrophilic block [18]. In such copolymers, synthesis of the diblock copolymers and extensive characterization were required. To tailor the EOF, synthesis and

purification of a series of copolymers with different ratios of the homopolymers was required [19].

In this chapter, polyoxyethylene (POE) based coatings are used as the neutral hydrophilic coating to prevent protein adsorption [13, 20]. Traditional adsorbed POE coatings rely on hydrogen bonding to anchor the POE to the capillary wall [13]. With adsorbed POE coatings, many operating conditions must be optimized for the coating to be effective. For example, a change in the HCl concentration used to condition the capillary, the use of a lower mass POE or a high BGE pH all destabilize the coating [13, 14]. Thus, a different approach is needed to form stable and robust POE capillary coatings.

As described in Chapter Three, we recently developed a surfactant-diblock copolymer sequential coating (Figure 3.1B) which combined the stability of a cationic surfactant bilayer and the suppressed EOF of a diblock copolymer [21]. This coating was formed by first rinsing the capillary with the two-tailed cationic surfactant dioctadecyldimethyl ammonium bromide (DODAB) which forms a stable semi-permanent bilayer coating [22, 23] anchored by electrostatic interactions. Next, a neutral diblock copolymer with a hydrophilic polyoxyethylene block and a hydrophobic (stearate) block was rinsed through the capillary. The hydrophobic block inserts into the DODAB bilayer through hydrophobic interactions [24]. This leaves the hydrophilic POE moiety protruding into the surrounding solution. The hydrophilic POE block controls the magnitude of EOF. A tunable EOF was achieved by varying the POE chain length from 8 to 100 oxyethylene units [21]. The suppressed EOF achieved using POE 40 stearate

allowed for high resolution CZE separations of acidic, basic and histone proteins [21]. The sequential coating has also been applied successfully to kinetic CE analysis [25] and capillary isoelectric focusing (Chapter Four) [26].

An advantage of this approach is that the diblock copolymer component of the sequential DODAB/diblock coating can be selected easily from a series of commercially available copolymers. Chapter Three showed that control of the EOF was achieved simply by selecting a different POE copolymer length [21] rather than by synthesizing a new copolymer. In this chapter, we explore the effect of other variables on the EOF magnitude and coating stability of DODAB/diblock copolymer coatings.

5.2 Experimental

5.2.1 Apparatus

All CE experiments were performed on a Hewlett Packard ^{3D}CE equipped with a UV absorbance detector. Data acquisition was at 10 Hz using HP ^{3D}CE ChemStation software. Untreated silica capillaries (Polymicro Technologies, Phoenix, AZ, USA) with an i.d. of 50 μm , o.d. of 360 μm , and total length of 32 cm (23.5 cm to the detector) were used. The cartridge aperture was 100 μm \times 200 μm and the capillary was thermostated at 25 ° C. All pressure rinses were at 1 bar.

5.2.2 Chemicals

The cationic surfactant DODAB and the following diblock copolymers were obtained from Sigma (Oakville, ON, Canada): POE 8 stearate (product no. P3315); POE 40 stearate (P3440); POE 100 stearate (P3690); POE 10

monododecyl ether (P9769), POE 10 tridecyl ether (P2393); POE 10 cetyl ether, also known as Brij® C10 (388858); POE 10 stearyl ether, also known as Brij® S10 (388890); and POE 100 stearyl ether, also known as Brij® S100 (466387). The neutral EOF markers benzyl alcohol (2 mM) and mesityl oxide (2 mM) were used as received from Sigma. All solutions were prepared in Nanopure 18 M Ω water (Barnstead, Chicago, IL, USA).

5.2.3 Buffer preparation

To study the ion retention characteristics of POE (Section 5.3.3), the following buffers were prepared: 50 mM Tris HCl pH 7.0, 50 mM Tris HClO₄ pH 7.0, 50 mM Tris HCl pH 9.0, 50 mM Tris HClO₄ pH 9.0 were prepared from ultrapure tris (hydroxyl-methyl) amino methane (Tris; Schwarz/Mann Biotech, Cleveland, OH, USA) and the pH was adjusted using HCl or perchloric acid.

To study the effect of pH on the coating performance (Section 5.3.4), the following buffers of constant ionic strength of 44 mM were used: phosphate buffers at pH 3.0 (50 mM), 7.0 (20 mM) and 11.5 (11 mM) were prepared from phosphoric acid, sodium monohydrogen phosphate and sodium dihydrogen phosphate (BDH, Toronto, ON, Canada), respectively. Acetate buffer at pH 5.0 (65 mM) was prepared from acetic acid (Caledon Laboratories LTD., ON, Canada). Tetraborate buffer at pH 10.0 (14 mM) was prepared from sodium tetraborate (Sigma, USA). Sodium hydroxide was used for pH adjustments.

5.2.4 Coating procedure

DODAB (0.1 mM) was dissolved in water and sonicated for 30 min at 60 °C and then stirred for 15 min. The sonication/stir cycle was repeated until a clear

solution was obtained [27]. Typically, two cycles were needed. The diblock copolymer of interest was dissolved in water (concentrations indicated in the figure captions) and prepared separately using the same sonicate/stir procedure. New capillaries were preconditioned with a 0.1 M NaOH rinse for 3.5 min and then flushed with water for 3.5 min. The capillary was then rinsed with 0.1 mM DODAB for 10 min; followed by a 10 min rinse with the diblock copolymer of interest. Finally, a 2 min buffer rinse was performed to remove any unadsorbed coating solution from the capillary.

5.2.5 Coating stability

The stability of capillary coatings was evaluated by monitoring the EOF during electrokinetic rinsing [28]. Consecutive EOF determinations were performed by successive injections of the neutral marker and application of voltage. Strongly suppressed EOF ($< 1 \times 10^{-4} \text{ cm}^2/\text{Vs}$) were measured using the three injection method [29]. A new capillary was used for each new buffer.

Coating stability under mixed aqueous-organic conditions (Section 5.3.5) was assessed by subjecting the coated capillaries to successive pressure rinses [28] with BGE containing 10 to 40% v/v acetonitrile (ACN). Capillaries were coated, the EOF was determined, and then the capillaries were rinsed for 1 min with BGE containing ACN. Finally, the capillary was pressure rinsed for 1 min with ACN free BGE and the EOF was determined. This cycle was repeated 10 times for each capillary.

5.3 Results and Discussion

Capillary coatings are commonly used to minimize undesirable analyte adsorption in CE [7-9]. Moreover, control of the EOF during electrophoretic separations is needed to optimize the resolution [9, 30]. A coating that both prevents analyte adsorption and provides EOF control is highly desirable. Diblock copolymers which combine desirable properties of their individual homopolymers have been used successfully as capillary coatings [16-19, 31]. Generally speaking, these copolymers include either a cationic block [16] or a hydrophobic block [18] that interacts with the capillary surface and serves as an anchor layer. The second block which is in contact with the bulk solution is usually hydrophilic in nature. The EOF of coated capillaries may be either highly suppressed when the second block is neutral [18] or strongly anodic when the second block is cationic [31]. Further control of the EOF calls for the synthesis of copolymers with different ratios of the homopolymers within the diblock copolymer [19].

The sequential DODAB/diblock copolymer coating offers simplicity and flexibility in altering the capillary coating [21, 26]. The DODAB cationic surfactant forms a stable bilayer coating with strongly reversed EOF [23, 27]. As detailed in Section 5.2.2, numerous POE alkyl diblock copolymers with various lengths of both the POE and the alkyl block are commercially available. Below we study the impact of this wide selection of commercial diblock copolymers on coating stability and magnitude of the EOF of the sequential DODAB/diblock copolymer coating. The selection of buffer pH and counter ion also aid in the control of the EOF, and so are also studied.

5.3.1 Effect of the hydrophobic block

POE has been used directly as a capillary coating. Such coatings are retained only via hydrogen bonding and so have poor stability and are easily washed off [13, 14]. The use of POE 10 stearyl ether as a direct capillary coating was compared to the DODAB/POE 10 stearyl ether coating. In Figure 5.1, twenty successive EOF determinations (total run time of 60 min) were performed with no rinses between the runs. With the POE 10 stearyl alone, the EOF was partially suppressed but showed significant upward drift (13.1% RSD). In contrast, with DODAB/POE 10 stearyl ether the EOF was more suppressed with less drift (5.0 %RSD). The enhanced stability of DODAB/ POE 10 stearyl ether can be attributed to the stability of the DODAB anchor layer and the strong hydrophobic interactions between the hydrophobic portion of the bilayer and the hydrophobic block of the diblock copolymer.

Drummond *et al.* studied the uptake of POE 100 stearate as an example of diblock copolymer interacting with the two-tailed cationic surfactant didodecyldimethylammonium bromide (DDAB) adsorbed layers on mica surface [24]. Their atomic force microscopy and dynamic surface forces studies indicated that the adsorption of POE 100 stearate occurs mainly by tethering of the hydrophobic moiety into the adsorbed surfactant layer. The hydrophobic stearate block inserts into the DODAB bilayer through hydrophobic interactions, leaving the hydrophilic POE moieties protruding into the surrounding solution.

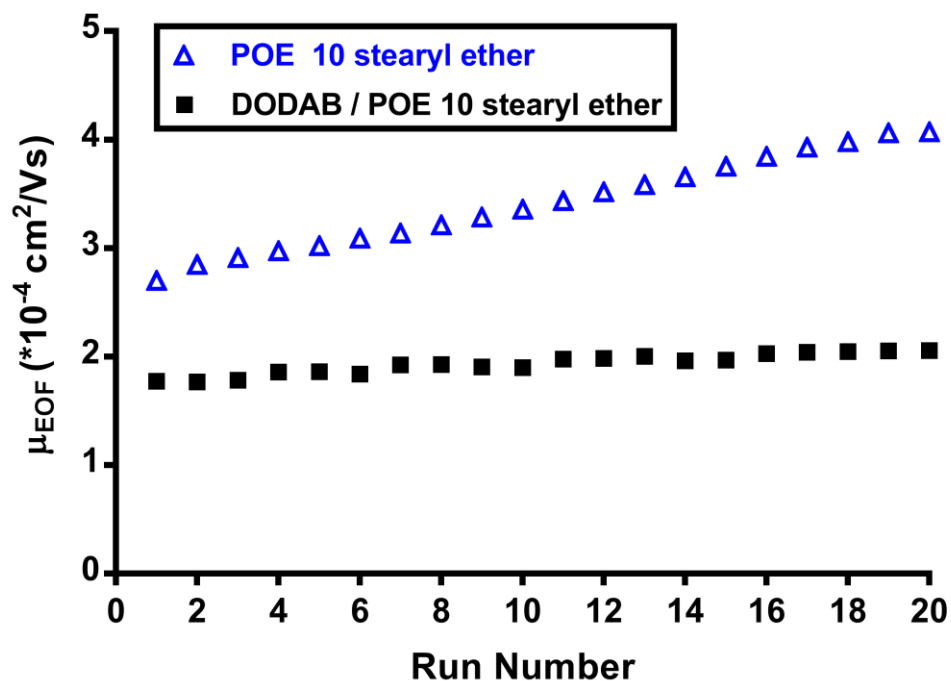


Figure 5.1: Stability of DODAB/POE diblock copolymer constructs vs. POE diblock copolymer alone coating.

Successive EOF determination were performed using 0.1 mM DODAB/0.03% POE 10 stearyl ether (■), and 0.03% POE 10 stearyl ether (△).

Experimental conditions: 50 mM Tris HCl pH 9.0; voltage, +15 kV; 32 cm × 50 μm id capillary (23.5 cm to detector); 2 mM mesityl oxide (λ , 254 nm) injected for 3 s at 50 mbar; temperature, 25°C.

To investigate the effect of varying the hydrophobic chain length of the diblock copolymers, we used a series of diblock copolymers (Figure 5.2.A) with a constant hydrophilic block of 10 polyoxyethylene units and alkyl chain length of $n=12, 16$ and 18 carbon. Figure 5.3 shows that the short 10 polyoxyethylene units partially suppresses the EOF (i.e., EOF is about 45% of that of a DODAB coated capillary). Increasing the length of hydrophobic block from lauryl ($n=12$) to stearyl ($n=18$) results in a more stable EOF. The shorter hydrophobic block ($n=12$) initially gave slightly stronger anodic EOF of $-3.3 \times 10^{-4} \text{ cm}^2/\text{Vs}$ which decreased in magnitude by 10% over ten successive runs. The stearyl ($n=18$) block yielded a more stable EOF with a RSD of 2.5% with slight random fluctuations rather than any drift. Consequently, the diblock copolymers with the longer hydrophobic block ($n=18$) will be used thereafter as it provides the most stable EOF.

5.3.2 Effect of the hydrophilic block

Previous studies [21] of the effect of varying the hydrophilic POE chain length found: 1) the magnitude of the EOF depends inversely on the length of the POE block; 2) the EOF can be fine-tuned using mixtures of two POE stearate copolymers, such as POE 8 stearate and POE 40 stearate; and 3) for a given molar concentration, the EOF stabilizes more quickly (smaller rinse volume) with longer POE polymers than their shorter ones.

The results in Figure 5.3 are consistent with these previous findings. The 0.1 mM DODAB/0.001% POE 100 stearyl ether strongly suppressed the EOF (to ~10% of the EOF of a DODAB coated capillary). In contrast, the 0.1 mM

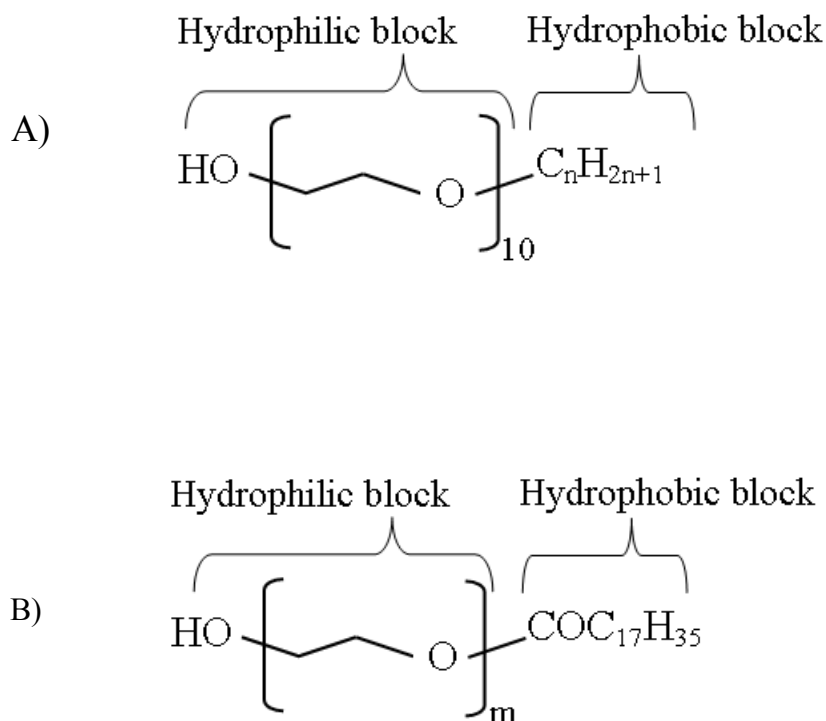


Figure 5.2: Structure of diblock copolymers used to study the effect of A) hydrophobic block and B) hydrophilic block.

n=12: Decaethylene glycol monododecyl ether; also known as polyoxyethylene (10) lauryl ether, **n=16:** Polyethylene glycol hexadecyl ether; also known as polyoxyethylene (10) cetyl ether or Brij® C10, **n=18:** Polyethylene glycol octadecyl ether; also known as polyoxyethylene (10) stearyl ether or Brij® S10

m=8: POE 8 stearate, **m=40:** POE 40 stearate, **m=100:** POE 100 stearate

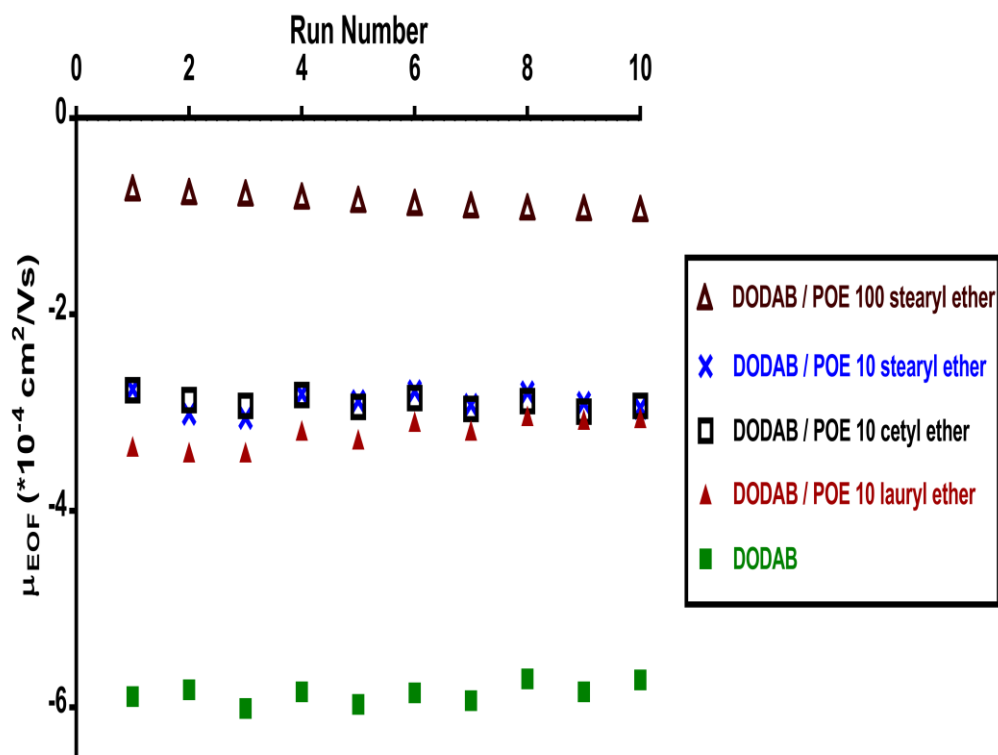


Figure 5.3: Effect of hydrophobic chain length of the diblock copolymer on EOF. 0.1 mM DODAB (■), 0.1 mM DODAB/0.1% POE 10 lauryl ether (▲), 0.1 mM DODAB/0.1% POE 10 cetyl ether (□), 0.1 mM DODAB/0.1% POE 10 stearyl ether (×) and 0.1 mM DODAB/ 0.001% POE 100 stearyl ether (△).

Experimental conditions: voltage, -15 kV; 32 cm × 50 μm id capillary (23.5 cm to detector); 50 mM sodium phosphate buffer, pH 3.0; λ , 214 nm; 2 mM benzyl alcohol injected for 3 s at 50 mbar; temperature, 25°C.

DODAB/POE 10 stearyl ether only partially suppressed the EOF (to ~ 45% of DODAB coating).

In Section 5.3.1, a series of diblock copolymers with ether linkages were used, while in Section 5.3.2 diblock copolymers with an ester linkage were used. To determine if there was an impact due to the different functional group, we compared the coating performance of the POE 100 stearyl ether (Brij® S100) and POE 100 stearate (ester). Using 50 mM sodium phosphate pH 3.0, both coatings suppressed the EOF to the same extent and showed similar EOF stability: 0.1 mM DODAB/0.001% w/v POE 100 stearyl ether yielded EOF of $-0.41 \times 10^{-4} \text{ cm}^2/\text{Vs}$ and RSD=9.7% (n=10); and 0.1 mM DODAB/0.001% w/v POE 100 stearate yielded EOF of $-0.52 \times 10^{-4} \text{ cm}^2/\text{Vs}$ and RSD=10.1% (n=10).

5.3.3 Ionic retention characteristics of POE

Despite not having any ion exchange functionality, ion chromatographic separations of inorganic have been achieved using electrically neutral stationary phases such as diol phases [32] and polyoxyethylene [33, 34]. The interaction of inorganic anions such as Br^- , I^- , BrO_3^- , IO_3^- , ClO_4^- and SCN^- with POE has been attributed to partitioning into the POE phase [33] or counter cations coordinated by the POE (through ion-dipole interaction with oxygen atoms) acting as anion exchange sites [32-34]. In these examples, anions elute in order of increasing chaotropic character in accordance with the Hofmeister series. Large ionic radius and weakly hydrated chaotropic anions such as ClO_4^- and SCN^- were retained most strongly on the POE phases [32-34]. The interaction of POE with inorganic

anions has also been reported in CE. For instance, POE has been used as a BGE additive to enhance the electrophoretic separation of Br⁻ and I⁻ [35].

Herein, we investigate the effect of anions in the buffer on the magnitude of the EOF. Capillaries were sequentially coated with 0.1 mM DODAB and then 0.03% POE 10 stearyl ether (Brij® S10). The EOF was determined for successive runs for: 50 mM Tris-HCl pH 7.0 and 50 mM Tris-HClO₄ pH 7.0 (Figure 5.4.A). A suppressed anodic EOF of -0.31×10^{-4} cm²/Vs was observed with 50 mM Tris-HCl pH 7.0. Using ClO₄⁻ as the buffer counter ion resulted in the suppressed EOF becoming cathodic ($+0.45 \times 10^{-4}$ cm²/Vs), reflecting a negative zeta potential. Presumably the chaotropic ClO₄⁻ is retained onto the POE coating to a higher extent compared to Cl⁻ as was observed in ion chromatographic studies [32-34].

Similarly at pH 9.0 (Figure 5.4.B) on the same 0.1 mM DODAB/0.03% POE 10 stearyl ether (Brij® S10) coating a cathodic suppressed EOF was observed using both 50 mM Tris-HCl pH 9.0 and 50 mM Tris HClO₄ pH 9.0 as the BGE. The magnitude of EOF was stronger in the case of Tris HClO₄ ($+2.0 \times 10^{-4}$ cm²/Vs) compared to Tris HCl ($+1.6 \times 10^{-4}$ cm²/Vs), but was much smaller than that of a bare capillary ($+8.2 \times 10^{-4}$ cm²/Vs). Similarly, with a 0.1 mM DODAB/0.001% POE 100 stearate coating the EOF was $+0.34 \times 10^{-4}$ cm²/Vs in 50 mM Tris-HCl pH 9.0 and $+1.0 \times 10^{-4}$ cm²/Vs in 50 mM Tris HClO₄ pH 9.0. These observations indicate that anion adsorption onto the POE can alter the observed EOF. However the range of effect is relatively mild ($+0.4$ to $+0.8 \times 10^{-4}$ cm²/Vs) even when shifting from a kosmotropic anion such as Cl⁻ to a highly chaotropic anion such as ClO₄⁻. Thus, the nature of the buffer anion must be

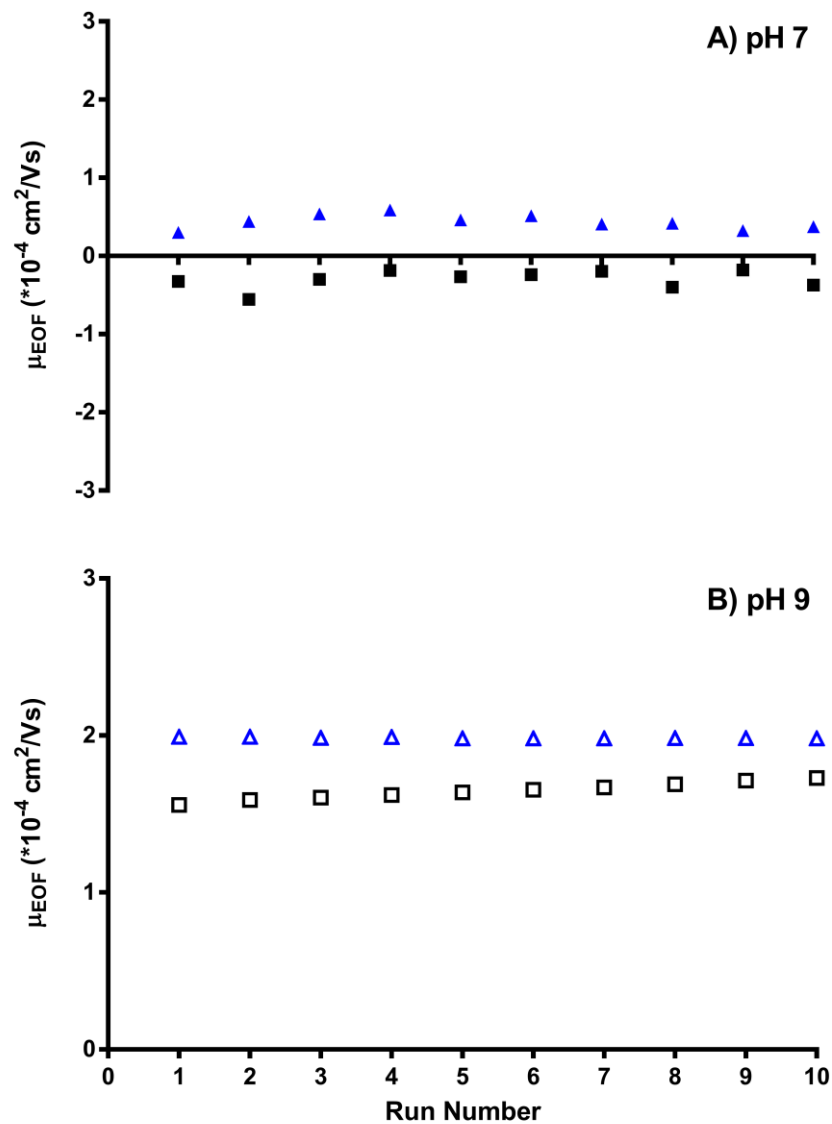


Figure 5.4: Effect of buffer anion on EOF of DODAB/diblock copolymer coatings.

Successive EOF determination at (A) pH 7 and (B) pH 9 using the following buffers: 50 mM Tris HCl pH 7 (■), 50 mM Tris HClO₄ pH 7 (▲), 50 mM Tris HCl pH 9 (□), 50 mM Tris HClO₄ pH 9 (△)

Experimental conditions: 0.1 mM DODAB/0.03% POE 10 stearyl ether; voltage, -15 kV or +15 kV; 32 cm × 50 μm id capillary (23.5 cm to detector); 2 mM mesityl oxide (λ , 254 nm) injected for 3 s at 50 mbar; temperature, 25°C.

considered to achieve reproducible EOF, but the effect of buffer anion is much less than that of the POE length (Section 5.3.2) or BGE pH (Section 5.3.4).

5.3.4 Effect of pH on the coating performance

DODAB/POE stearate coatings have been used under a variety of pH conditions. The coating has been applied to protein separations at low pH [21], kinetic CE analysis at neutral pH [25] and to capillary isoelectric focusing over the pH range 3-10 [26]. However, the influence of the pH on the EOF and coating performance has not previously been investigated. This is despite radically different EOF being reported at low [21] and neutral pH [25]. Herein, the performance of the sequential coating was investigated at pH ranging from 3.0 to 11.5 under constant ionic strength conditions.

Figure 5.5 shows the EOF as a function of pH on bare and coated capillaries. At $\text{pH} \leq 5$, all DODAB/POE stearate coated capillaries yielded suppressed anodic EOF. Crosslinked POE coatings have resulted in both suppressed anodic [36] and suppressed cathodic EOF [37]. In this study, POE copolymer coatings always yielded suppressed cathodic EOF (Figure 5.1 for pH 9, and not shown for pH 5.0 and 7.0). Thus, the anodic EOF observed at $\text{pH} \leq 5$ can be related to the positive charge of the underlying DODAB layer. As the pH increases in Figure 5.5 there is a general trend in the EOF such that at $\text{pH} \geq 10$ the EOF was still suppressed but now cathodic. This reversal in EOF is consistent with the literature. For instance, Krylov and coworkers observed moderately suppressed anodic EOF with a DODAB/POE 8 stearate coating at pH 3.0 and a

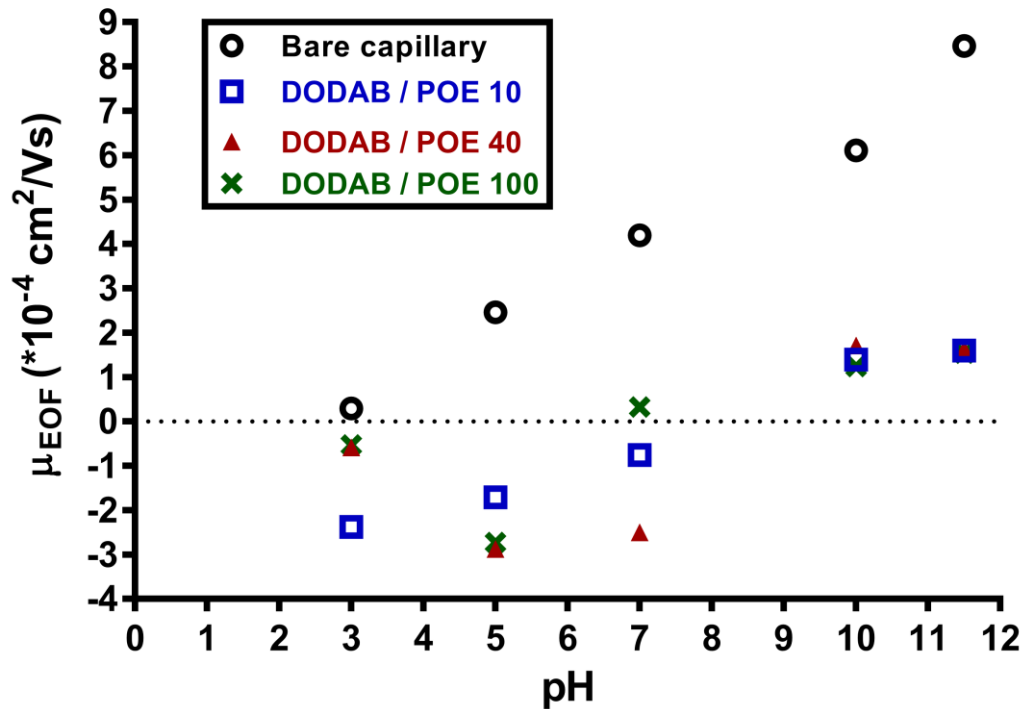


Figure 5.5: Effect of pH on the EOF of DODAB/POE diblock copolymer coated capillaries.

EOF was measured using the following buffers: 50 mM sodium phosphate pH 3.0; 65 mM sodium acetate pH 5.0; 20 mM sodium phosphate pH 7.0; 14 mM sodium tetraborate pH 10.0; and 11 mM sodium phosphate pH 11.5 in bare capillaries (○), and capillaries coated with 0.1 mM DODAB/0.03% w/v POE 10 stearyl ether (□), 0.1 mM DODAB/0.075% w/v POE 40 stearate (▲) and 0.1 mM DODAB/0.001% w/v POE 100 stearate (×).

Experimental conditions: voltage, -15 kV or +15 kV; 32 cm × 50 μm id capillary (23.5 cm to detector; 2 mM benzyl alcohol (λ , 214 nm) or 2 mM mesityl oxide (λ , 254 nm) injected for 3 s at 50 mbar; temperature, 25°C.

moderately suppressed cathodic EOF using various buffers near physiological pH [25]. Similarly, Kawai et al. [38] observed a steady transition in EOF for a DODAB/POE 40 stearate coating from $-0.96 \times 10^{-4} \text{ cm}^2/\text{Vs}$ at pH 3.0 to $+0.16 \times 10^{-4} \text{ cm}^2/\text{Vs}$ at pH 7.0 for 20 mM phosphate buffers. A similar trend in the EOF was observed with DODAB alone coated capillaries. The EOF changed from strongly anodic at acidic pH to suppressed and cathodic at basic pH [39].

The sequential DODAB/POE diblock copolymer coatings offered good stability over a wide range of pH. Figure 5.6 shows that a stable EOF was obtained over 10 successive determinations at pH range 3.0-11.5. Interestingly, DODAB alone coating does not coat the capillary effectively at pH 7.0 using phosphate buffers due to the dramatic increase in DODAB vesicle size [40]. Whereas, using the same buffer, DODAB/POE stearate forms a stable coating with a suppressed EOF (Figure 5.6). The hydrophobic interaction between DODAB alkyl chains and the hydrophobic block of the diblock copolymer may play a factor in this additional stability.

In Chapter Three, we observed that at pH 3.0 longer POE chains yielded more suppressed EOF [21]. However, this observation is not universally true. For instance, at pH 5, DODAB/POE 10 yielded an EOF of $-1.7 \times 10^{-4} \text{ cm}^2/\text{Vs}$, compared to $-2.7 \times 10^{-4} \text{ cm}^2/\text{Vs}$ for both the POE 40 and 100 stearates (Figure 5.5). Under basic conditions (pH 10.0 and 11.5), all three coatings yielded moderately suppressed cathodic EOF ($+1.6 \times 10^{-4} \text{ cm}^2/\text{Vs}$), regardless of the POE chain length.

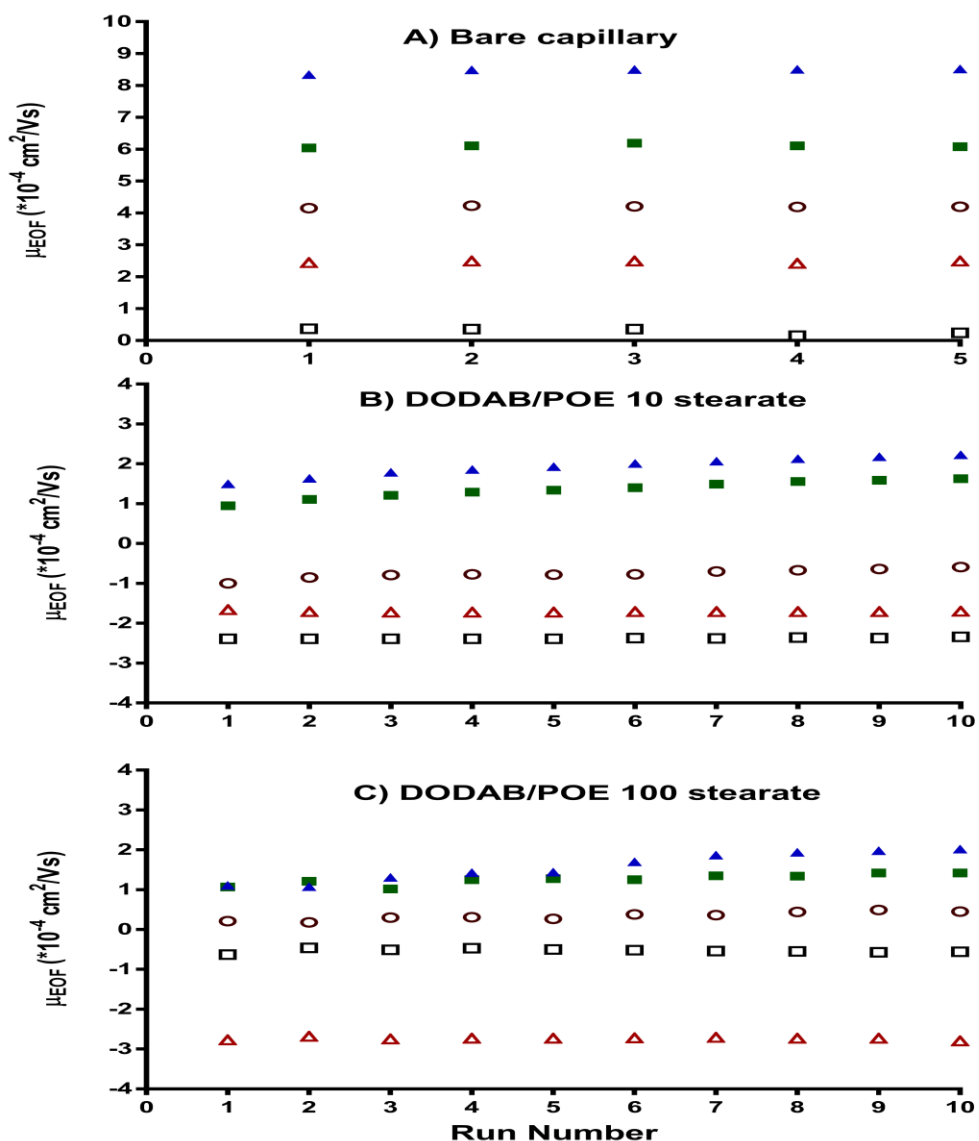


Figure 5.6: EOF stability of the DODAB/POE diblock copolymers vs. pH.

50 mM sodium phosphate pH 3 (□), 65 mM sodium acetate pH 5 (△), 20 mM sodium phosphate pH 7 (○), 14 mM sodium tetraborate pH 10 (■) and 11 mM sodium phosphate pH 11.5 (▲) in bare capillary (A), 0.1 mM DODAB/ 0.03 % w/v POE 10 stearyl ether (B) and 0.1 mM DODAB/ 0.001 % w/v POE 100 stearate (C)

Experimental conditions: voltage, -15 kV or +15 kV; 32 cm × 50 μm i.d. capillary (23.5 cm to detector; 2 mM benzyl alcohol (λ, 214 nm) or 2 mM mesityl oxide (λ, 254 nm) injected for 3 s at 0.5 psi; temperature, 25°C.

Thus, in all cases and pH the DODAB/POE stearate coatings yield suppressed EOF. However, no prediction regarding the effect of POE chain length on EOF can be made. The reason is unclear but different orientations of the adsorbed diblock copolymers at different pH may be involved. A highly dense orientation of the adsorbed polymer (*e.g.* mushroom or brush) is more effective at reducing EOF than a less dense flat orientation [41]. Polymer chain length, solvent and surface conditions are all factors that control the orientation of adsorbed polymers at solid-liquid interfaces [24, 42].

In summary, all DODAB/POE 10, 40 and 100 stearate yielded suppressed EOF over the pH range 3-11.5. The sequential coating was stable at acidic, neutral and basic pH. The coating stability and the suppressed EOF over this wide range of pH enabled a variety of applications of the sequential coating [21, 25, 26].

5.3.5 Stability of the coating under mixed aqueous-organic conditions

Non-aqueous CE can be used to enhance the analyte solubility and alter the separation selectivity [43]. However, analyte adsorption is still a problem. Capillary coatings can be used to minimize analyte adsorption and control the EOF. However, most of these coatings have been developed for aqueous CE separations. DODAB alone was used under mixed aqueous-organic conditions and displayed good stability for BGE containing up to 40-60% v/v organic solvent [44]. Similarly, thermally crosslinked PEG coatings have been used with methanolic and ACN/water BGE [45]. Herein we investigate the utility of DODAB/POE diblock copolymer as a semi-permanent coating under mixed aqueous-organic conditions.

Figure 5.7 shows that the effect of ACN on the stability of a DODAB/0.03% w/v POE 10 stearyl ether. The coating was stable when rinsed with BGE containing up to 20% v/v ACN. BGE with 30% ACN resulted in gradual loss of the coating as indicated by the cathodic drift in the EOF. BGE with 40% v/v ACN resulted in rapid loss of the coating, as indicated by the cathodic EOF comparable to that of a bare capillary ($+2.5 \times 10^{-4} \text{ cm}^2/\text{Vs}$).

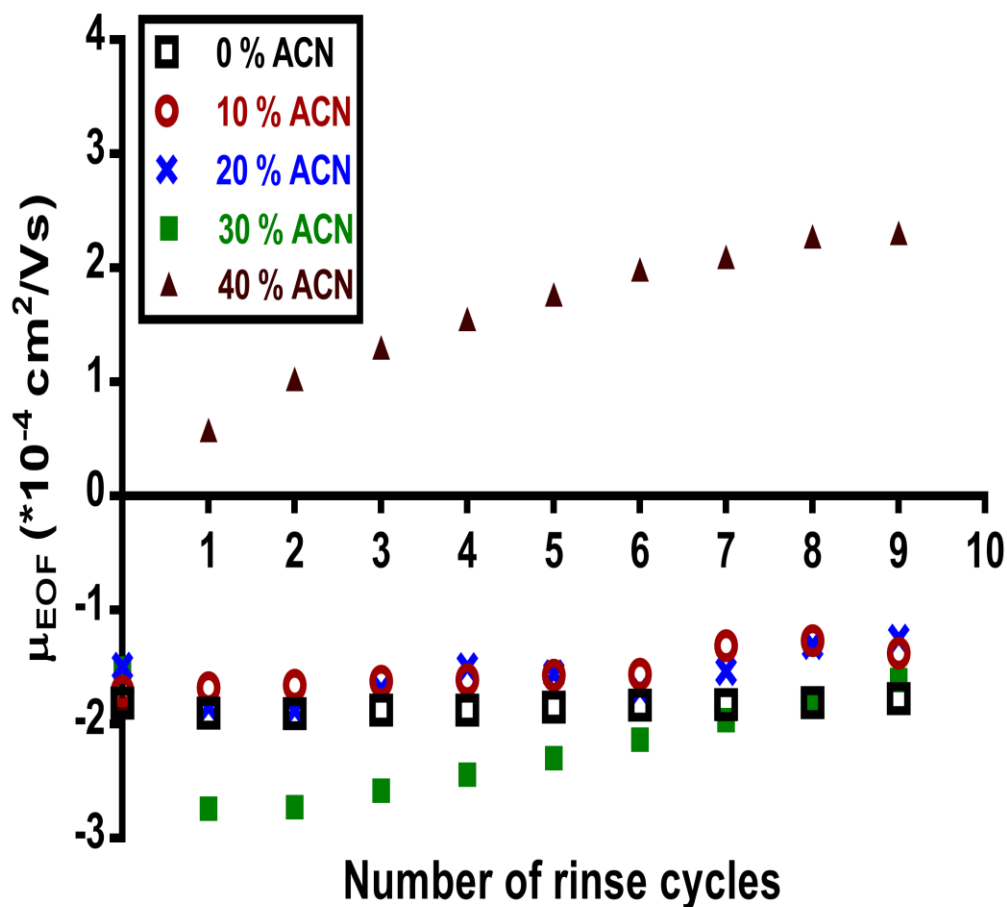


Figure 5.7: Stability of the coating under mixed aqueous-organic conditions.

Capillaries were coated with 0.1 mM DODAB/0.03% w/v POE 10 stearyl ether, and then rinsed with BGE containing 0% ACN (□), 10% v/v ACN (○), 20% v/v ACN (×), 30% v/v ACN (■) and 40% v/v ACN (▲). EOF was determined using 65 mM sodium acetate pH 5.0 containing no acetonitrile.

Experimental conditions: -15 kV or +15 kV; 32 cm × 50 μm id capillary (23.5 cm to detector; 2 mM mesityl oxide (λ, 254 nm) injected for 3 s at 50 mbar; temperature, 25°C.

5.4 Conclusions

Polyoxyethylene diblock copolymers coupled with DODAB bilayers have previously been shown to effectively prevent protein adsorption and suppress the EOF. The commercial availability of wide selection of polyoxyethylene diblock copolymers offers flexibility of the analytical method and eliminates the need for tedious synthetic procedure. The length of the hydrophobic block impacts that stability of the coating, but does not affect the magnitude or direction of the EOF. Suppressed EOF is obtained regardless of the length of the polyoxyethylene chain, but the direction and magnitude of the EOF depend on the POE chain length in a complex fashion. The sequential DODAB/POE diblock copolymer suppressed the EOF and showed good stability over a wide range of pH 3.0-11.5. The suppressed EOF gradually becomes more cathodic as the pH increases, with the polyoxyethylene displaying some ion retention characteristics. Thus, careful selection of the buffer ions is important to achieve reproducible EOF. The sequential coating shows a good stability in buffers containing up to 20% v/v acetonitrile.

5.5 References

- [1] Dovichi, N. J. and Zhang, J. Z., *Angew. Chem., Int. Ed.* 2000, 39, 4463.
- [2] Green, J. S. and Jorgenson, J. W., *J. Chromatogr.* 1989, 478, 63-70.
- [3] Schure, M. R. and Lenhoff, A. M., *Anal. Chem.* 1993, 65, 3024-3037.
- [4] Towns, J. K. and Regnier, F. E., *Anal. Chem.* 1992, 64, 2473-2478.
- [5] Baryla, N. E., Melanson, J. E., McDermott, M. T. and Lucy, C. A., *Anal. Chem.* 2001, 73, 4558-4565.
- [6] McCormick, R. M., *Anal. Chem.* 1988, 60, 2322-2328.
- [7] Lucy, C. A., MacDonald, A. M. and Gulcev, M. D., *J. Chromatogr. A* 2008, 1184, 81-105.
- [8] Doherty, E. A. S., Meagher, R. J., Albarghouthi, M. N. and Barron, A. E., *Electrophoresis* 2003, 24, 34-54.
- [9] Huhn, C., Ramautar, R., Wuhrer, M. and Somsen, G. W., *Anal. Bioanal. Chem.* 2010, 396, 297-314.
- [10] Spanila, M., Pazourek, J. and Havel, J., *J. Sep. Sci.* 2006, 29, 2234-2240.
- [11] Cordova, E., Gao, J. M. and Whitesides, G. M., *Anal. Chem.* 1997, 69, 1370-1379.
- [12] Katayama, H., Ishihama, Y. and Asakawa, N., *Anal. Chem.* 1998, 70, 2254-2260.
- [13] Iki, N. and Yeung, E. S., *J. Chromatogr. A* 1996, 731, 273-282.
- [14] Preisler, J. and Yeung, E. S., *Anal. Chem.* 1996, 68, 2885-2889.
- [15] Albarghouthi, M. N., Stein, T. M. and Barron, A. E., *Electrophoresis* 2003, 24, 1166-1175.
- [16] Liu, H., Shi, R., Wan, W., Yang, R. and Wang, Y., *Electrophoresis* 2008, 29, 2812-2819.
- [17] Yang, R., Shi, R., Peng, S., Zhou, D., Liu, H. and Wang, Y., *Electrophoresis* 2008, 29, 1460-1466.
- [18] Zhou, D., Tan, L., Xiang, L., Zeng, R., Cao, F., Zhu, X. and Wang, Y., *J. Sep. Sci.* 2011, 34, 1738-1745.

- [19] Bernal, J., Rodriguez-Meizoso, I., Elvira, C., Ibanez, E. and Cifuentes, A., *J. Chromatogr. A* 2008, *1204*, 104-109.
- [20] Ostuni, E., Chapman, R. G., Holmlin, R. E., Takayama, S. and Whitesides, G. M., *Langmuir* 2001, *17*, 5605-5620.
- [21] MacDonald, A. M., Bahnasy, M. F. and Lucy, C. A., *J. Chromatogr. A* 2011, *1218*, 178-184.
- [22] Mohabbati, S. and Westerlund, D., *J. Chromatogr. A* 2006, *1121*, 32-39.
- [23] Gulcey, M. D., McGinitie, T. M., Bahnasy, M. F. and Lucy, C. A., *Analyst* 2010, *135*, 2688-2693.
- [24] Blom, A., Drummond, C., Wanless, E. J., Richetti, P. and Warr, G. G., *Langmuir* 2005, *21*, 2779-2788.
- [25] de Jong, S., Epelbaum, N., Liyanage, R. and Krylov, S. N., *Electrophoresis* 2012, *33*, 2584-2590.
- [26] Bahnasy, M. F. and Lucy, C. A., *J. Chromatogr. A* 2012, *1267*, 89-95.
- [27] Yassine, M. M. and Lucy, C. A., *Anal. Chem.* 2005, *77*, 620-625.
- [28] Yassine, M. M. and Lucy, C. A., *Anal. Chem.* 2004, *76*, 2983-2990.
- [29] Williams, B. A. and Vigh, C., *Anal. Chem.* 1996, *68*, 1174-1180.
- [30] Yeung, K. K. C. and Lucy, C. A., *J. Chromatogr. A* 1998, *804*, 319-325.
- [31] Erny, G. L., Elvira, C., San Roman, J. and Cifuentes, A., *Electrophoresis* 2006, *27*, 1041-1049.
- [32] Arai, K., Mori, M., Kozaki, D., Nakatani, N., Itabashi, H. and Tanaka, K., *J. Chromatogr. A* 2012, *1270*, 147-152.
- [33] Lim, L. W., Rong, L. and Takeuchi, T., *Anal. Sci.* 2012, *28*, 205-213.
- [34] Linda, R., Lim, L. W. and Takeuchi, T., *J. Chromatogr. A* 2013, *1294*, 117-121.
- [35] Okada, T., *J. Chromatogr. A* 1999, *834*, 73-87.
- [36] Huang, M. X., Vorkink, W. P. and Lee, M. L., *J. Microcol. Sep.* 1992, *4*, 135-143.
- [37] Schulze, M. and Belder, D., *Electrophoresis* 2012, *33*, 370-378.

- [38] Kawai, T., Ito, J., Sueyoshi, K., Kitagawa, F. and Otsuka, K., *J. Chromatogr. A* 2012, *1267*, 65-73.
- [39] Bahnasy, M. F., *Ph.D. Thesis* 2014, Chemistry, University of Alberta, Edmonton.
- [40] Gulcev, M. D. and Lucy, C. A., *Anal. Chim. Acta* 2011, *690*, 116-121.
- [41] Österberg, E., Bergström, K., Holmberg, K., Riggs, J. A., Van Alstine, J. M., Schuman, T. P., Burns, N. L. and Harris, J. M., *Colloids Surf., A* 1993, *77*, 159-169.
- [42] Milner, S. T., *Science* 1991, *251*, 905-914.
- [43] Geiser, L. and Veuthey, J. L., *Electrophoresis* 2007, *28*, 45-57.
- [44] Diress, A. G., Yassine, M. M. and Lucy, C. A., *Electrophoresis* 2007, *28*, 1189-1196.
- [45] Belder, D., Husmann, H. and Warnke, J., *Electrophoresis* 2001, *22*, 666-672.

Chapter Six: Cationic surfactant bilayer capillary coatings under alkaline conditions

6.1 Introduction

Buffer pH is a powerful variable in optimizing selectivity in CE. However the separation of weakly acidic compounds with high pK_a requires the use of high pH. For instance, the optimum separation of dichlorinated phenols ($pK_a = 6.7-8.6$) was achieved at pH 9.0 [1], and a mixture of three aromatic amino acids ($pK_{a2} \sim 9.19 - 9.33$) was best at pH 10 [1]. One challenge is that the EOF is strongly cathodic under such alkaline conditions. This strong EOF significantly increases the average apparent electrophoretic mobilities of the analytes relative to the differences in their electrophoretic mobilities, resulting in reduced resolution (Equation 1.18). Thus, there is an interest in the development of capillary coatings with high pH stability that would allow suppression or control of the EOF at high pH.

Although covalent coatings can be effective at minimizing analyte adsorption and suppression of EOF, many covalent coatings have poor stability at basic pH [2]. The silane chemistry introduced by Hjertén [3] for covalent capillary coatings suffers from hydrolysis of the Si-O bonds at high pH. Similarly polyacrylamide based covalent coatings are susceptible to hydrolysis at high pH [1]. Such a hydrolysis results in the destruction of the coating.

Physically adsorbed coatings are easy to prepare, regenerable, and cost effective [4]. Polybrene (HDMB) has been used to reverse the EOF at pH 13.1

(130 mM NaOH) for the separation of carbohydrates [5]. The reversed EOF yielded a faster separation, but the polybrene coating had to be regenerated after every run due to the high pH. Successive multi-ion layer (SMIL) coatings have also been explored for global separations of anionic metabolites from urine using pH 9 BGE [6]. A polybrene-dextran sulfate-polybrene coating yielded reasonable separations of anionic species such as orotic acid, uric acid, hippuric acid and tyrosine, but broad peaks of FAD and no peak for NADPH due to electrostatic interactions with the positively charged capillary wall. The use of a polybrene-polyvinyl sulfate coating eliminated adsorption of the multivalent anionic compounds, but the counter-EOF was insufficiently strong to sweep fast moving analytes such as citric acid to the detector [6]. Hence, while there is interest in performing CE separations at high pH using semi-permanent adsorbed coatings, to date a stable and effective coating is lacking.

The sequential DODAB/POE diblock copolymer coatings showed good stability and suppressed EOF over a wide range of pH 3.0-11.5 (Chapter Five). Thus, DODAB/POE diblock copolymer coatings can be used for CE applications at high pH. The sequential coating has been applied to CE separations at acidic pH [7], neutral pH [8] and cIEF separations pH 3-10 [9]. The EOF was suppressed and anodic at low pH. As the pH increased, the EOF was still suppressed but now cathodic (Chapter Five). This reversal in EOF of the sequential coating is consistent with the reported applications of the sequential coating [8, 10]. To explore if the anchor DODAB layer is responsible for this

reversal, the EOF of the DODAB alone coating capillaries vs. pH is studied in this chapter.

As discussed in previous chapters, coatings prepared from two-tailed cationic surfactants are easy to form and produce stable physically adsorbed semi-permanent coatings [11-13]. DODAB forms a bilayer on the capillary wall through electrostatic interactions between the cationic surfactant vesicles and the anionic fused silica wall. Given this electrostatic interactions, we assumed that the DODAB bilayer coating would be stable or more stable at high pH where the silanols on the capillary wall are essentially fully deprotonated. Thus a strong anodic EOF was expected for DODAB capillaries at high pH. To our surprise, suppressed anodic and even cathodic EOF were observed at $\text{pH} > 9$. This chapter explores the cause of this unexpected behavior.

6.2 Experimental

6.2.1 Apparatus

All capillary electrophoresis experiments were conducted on a Hewlett Packard ^{3D}CE instrument equipped with a UV absorbance detector. Data acquisition at 10 Hz was carried out on a Pentium II HP personal computer running HP ^{3D}CE ChemStation software. Untreated fused-silica capillaries (Polymicro Technologies, Phoenix, AZ, USA) of total length 32 cm (23.5 cm to the detector), i.d. of 50 μm and o.d. of 365 μm were used. The cartridge aperture was 100 μm \times 200 μm and the capillary was thermostated at 25°C. High pressure rinses were at 2 bar.

6.2.2 Chemicals

All solutions were prepared using Nanopure 18-M Ω ultrapure water (Barnstead, Dubuque, IA, USA). The cationic surfactant DODAB was used as received from Sigma (Oakville, ON, Canada). The neutral EOF markers benzyl alcohol (2 mM; λ , 214 nm) and mesityl oxide (2 mM; λ , 254 nm) were used as received from Sigma.

To study the effect of pH on the coating performance, the following buffers were used (Table 6.1): phosphate buffers at pH 3.0 (50 mM), 7.0 (20 mM) and 11.5 (11 mM) were prepared from phosphoric acid, sodium monohydrogen phosphate and sodium dihydrogen phosphate (BDH, Toronto, ON, Canada), respectively. Acetate buffers were prepared from acetic acid (Caledon Laboratories Ltd., ON, Canada). Sodium hydroxide was used for pH adjustment. Tris HCl buffers were prepared from ultrapure tris (hydroxyl-methyl) amino methane (Tris; Schwarz/Mann Biotech, Cleveland, OH, USA) and the pH was adjusted using HCl. Buffer pH was measured using a Corning digital pH meter model 445 (Corning, Acton, MA, USA).

6.2.3 Surfactant preparation and coating procedure

Surfactant coating solutions were prepared using the sonicate/stir method [13]. DODAB solution was prepared by dissolving the surfactant in water. The solution was sonicated for 30 min at 60°C and then stirred for 15 min. This sonication/stir cycle was repeated until a clear solution was obtained. Typically 2

cycles were needed. The surfactant solution was then allowed to cool to room temperature before use. Fresh surfactant solutions were prepared daily.

New capillaries were preconditioned with a 0.1 M NaOH rinse for 3.5 min at 2 bar and then flushed with water for 3.5 min. The capillary was then rinsed with 0.1 mM DODAB for 10 min. Finally, a 1 min buffer rinse was performed to remove any unadsorbed coating solution from the capillary.

6.2.4 Coating stability

The stability of capillary coatings was evaluated by monitoring the EOF during electrokinetic rinsing [14]. Consecutive EOF determinations were performed by successive injections of the neutral marker and application of voltage. Strongly suppressed EOF ($< 1 \times 10^{-4} \text{ cm}^2/\text{Vs}$) were measured using the 3 injection method of Williams and Vigh [15]. A new capillary was used for each new buffer. Buffer inlet and outlet vials were used up to a maximum of three runs then replaced with fresh buffer vials.

6.2.5 ESI-MS

To test for chemical instability of DODAB at basic pH, 0.1 mM DODAB was prepared according to procedure in Section 6.2.3. An aliquot of DODAB was treated with 0.1 M NH_4OH to a pH ~ 10 (at 25°C for 24 h). High resolution ESI-MS analyses of both untreated DODAB and DODAB/ NH_4OH were performed to determine the molecular mass of the compound. ESI-MS analyses were performed on an Agilent Technologies 6220 TOF-ESI-MS (Santa Clara, CA, USA) by direct injection.

6.2.6 Dynamic light scattering measurements

Mean vesicle diameters (size) and polydispersity indices (PDIs) were determined at 25°C by dynamic light scattering (DLS) using a Malvern Zetasizer Nano-ZS Sizer (Worcestershire, U.K.) equipped with a 4 mW He–Ne laser (633 nm). Values obtained were based on 15 runs for each sample (150 s per sample). 0.1 mM DODAB in water was prepared using the sonicate stir method detailed in Section 6.2.3. DODAB was then diluted 19:1 with 1.0 M NaCl or 1.0 M NaOH to yield solutions of 50 mM ionic strength. The vesicle size was determined at 0 h (immediately after dilution), after 1 h and after 24 h.

6.3 Results and Discussion

Surfactants can form capillary coatings which enable efficient protein separations [13, 16]. Two-tailed surfactants such as DDAB and DODAB possess the correct packing factor (i.e., a cylindrical geometry) to form a supported bilayer on a flat surface [12]. The stability of the surfactant cationic bilayer is affected by the carbon chain length [13], capillary i.d. [13, 17], buffer ionic strength and buffer anion [18]. Herein, we investigate the performance of cationic bilayer surfactant coating under alkaline conditions.

6.3.1 DODAB stability at pH 3-7

The quaternary ammonium surfactant; DODAB forms a semipermanent coating on the capillary inner surface. The positively charged surfactant bilayer adsorbed to the capillary surface effectively prevents the adsorption of basic proteins [13, 16-18]. Phosphate pH 3.0 [18], formate pH 3.0-4.5 [13] and acetate

pH 5.0 [17] buffers have all been used with DODAB coated capillaries to yield high efficiency separations of model basic proteins.

The buffer anion has been observed to have a profound effect on the DODAB vesicle size and coating stability [18]. Conditions which promote smaller unilamellar vesicles (SUVs) should be utilized. Weakly associating buffer anions such as phosphate pH 3.0 ($\text{H}_3\text{PO}_4/\text{H}_2\text{PO}_4^-$), acetate and chloride resulted in smaller vesicles and should be used for DODAB coating solutions [18]. In contrast, strongly associated anions such as bromide and phosphate pH 7.0 ($\text{H}_2\text{PO}_4^-/\text{HPO}_4^{2-}$) resulted in larger vesicles and poor coatings particularly at high ionic strength [18].

DODAB coated capillaries exhibit strongly anodic EOF [13, 17]. Such coatings are termed semi-permanent since, as shown in Chapter Two, multiple runs may be performed on the coated capillaries with little change in the EOF [13, 17]. The decrease in the anodic EOF results in an increase in migration time from run to run, and reflects the instability of the coating. A series of buffers of constant ionic strength ($I_s = 44 \text{ mM}$) was used to assess the stability of DODAB coatings at pH 3-7 (Table 6.1 and Figure 6.1). Acetate buffer ($\text{pK}_a = 4.76$) was used at up to pH 7.0 to keep the same buffer anion while varying the pH. As a limited number of runs were performed, the limited buffer capacity of these solutions was not of great concern. Buffer inlet and outlet vials were used up to a maximum of three runs then replaced with fresh buffer vials to avoid buffer depletion.

Figure 6.1 shows the successive EOF determinations for DODAB coated capillaries using the buffers indicated in Table 6.1. Buffers with weakly associated anions such as phosphate pH 3.0, acetate pH (4.0-7.0) and Tris-HCl pH 7.0 yield stable strongly anodic EOF (-5.8 to -4.9×10^{-4} cm²/Vs). The RSD of the EOF was 0.35-4.5% over 10 successive runs (n=10), and displayed only random fluctuations. These results indicate that DODAB forms a stable coating over the pH range 3-7, consistent with previously reported results [13, 17, 18]. However, careful selection of buffer anion is still crucial [18] to obtain stable EOF. For instance, 10 mM sodium citrate pH 6.0 and 20 mM sodium phosphate pH 7 (Table 6.1) deteriorated the performance of DODAB coated the capillary and resulted in irreproducible suppressed cathodic EOF ($+0.5$ to $+1.5 \times 10^{-4}$ cm²/Vs).

The influence of buffer anion on DDOAB coating observed above is consistent with previous work of Gulcev *et al.* [18]. The use of acetate, chloride or H₂PO₄⁻ (i.e., phosphate pH 3.0) resulted in small DODAB vesicle size < 100 nm and effective coating [18]. In contrast, HPO₄²⁻ (i.e., phosphate pH 7.0, ≥ 10 mM) resulted in DODAB solution with a vesicle size of 1100 nm which did not form effective capillary coating. Thus, weakly associating buffer anions which provide small DODAB vesicle size should be used for an effective coating.

6.3.2 DODAB stability at pH ≥ 7.0

The stability of the DODAB bilayer coating at pH ≥ 7.0 was studied using Tris-HCl buffers for pH 7-10 (Table 6.1). At both pH 7.0 and pH 8.0, 0.1 mM

Table 6.1: Buffers used to study pH stability of DODAB coated capillaries

pH	Buffer	I _s (mM)	EOF ^a × 10 ⁻⁴ cm ² /V·s (%RSD)
3.0	50 mM sodium phosphate	44	-5.82 (1.1)
4.0	250 mM sodium acetate	44	-4.94 (6.0)
5.0	65 mM sodium acetate	44	-5.69 (2.2)
6.0	46 mM sodium acetate	44	-5.17 (0.4)
6.0	10 mM sodium citrate	44	----- ^b
7.0	44 mM sodium acetate	44	-5.05 (1.3)
7.0	20 mM sodium phosphate	44	----- ^b
7.0	50 mM Tris-HCl	44	-5.05 (5.4)
8.0	50 mM Tris-HCl	28	-4.94 (2.3)
9.0	50 mM Tris-HCl	5	----- ^b
9.0	50 mM Tris-HCl+ NaCl	44	----- ^b
10.0	50 mM Tris-HCl		----- ^b
11.5	11 mM sodium phosphate	44	----- ^b

Experimental conditions: 32 cm × 50 μm i.d. (23.5 cm to detector); 2 mM benzyl alcohol (λ, 214 nm) or 2 mM mesityl oxide (λ, 254 nm) injected for 3 s at 50 mbar; temperature, 25°C.

^a average of 10 determinations

^b Irreproducible EOF

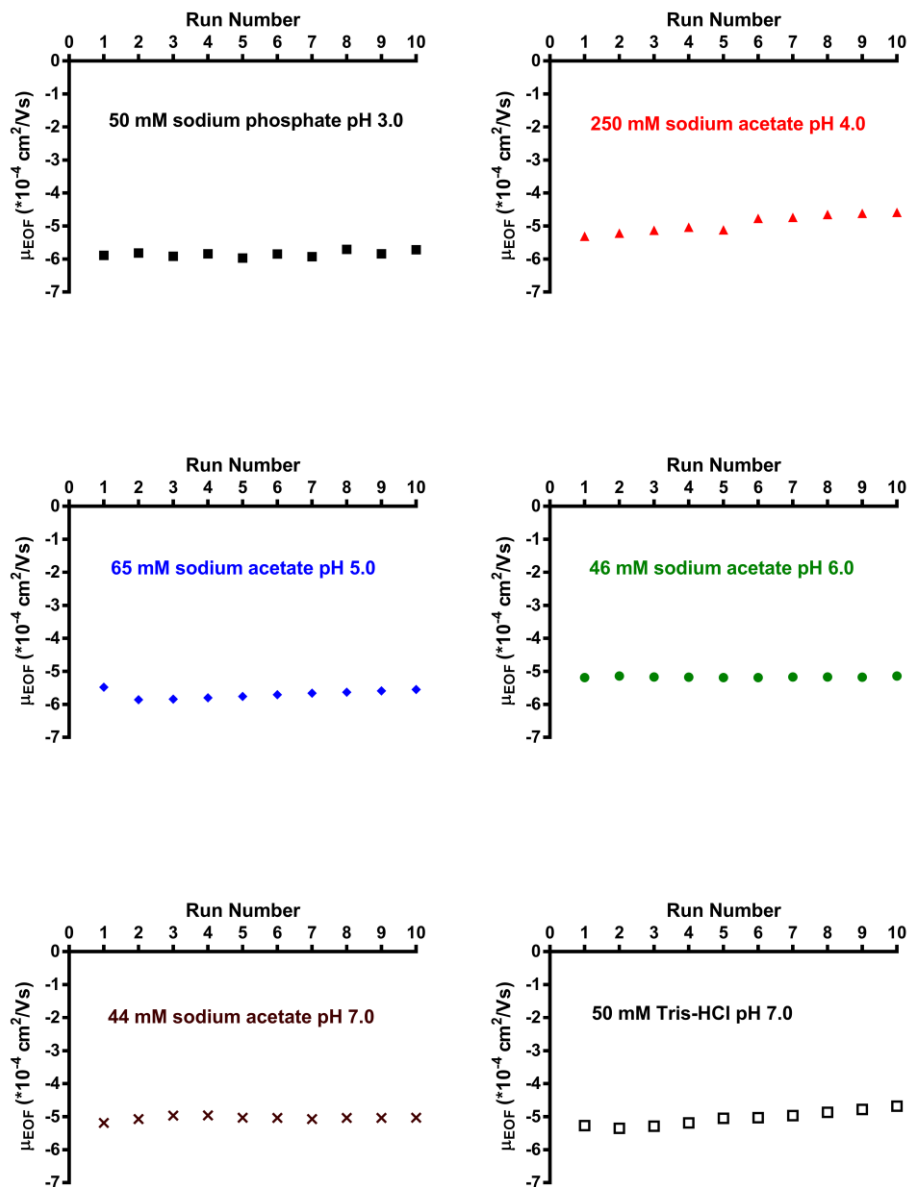


Figure 6.1: Stability of 0.1 mM DODAB coated capillaries at pH 3-7 in various buffers of constant (44 mM) ionic strength. 50 mM sodium phosphate pH 3.0 (■), 250 mM sodium acetate pH 4.0 (▲), 65 mM sodium acetate pH 5.0 (◆), 46 mM sodium acetate pH 6.0 (●), 44 mM sodium acetate pH 7.0 (×) and 50 mM Tris-HCl pH 7.0 (□).

Experimental conditions: 32 cm × 50 μm i.d. capillary (23.5 cm to detector); 2 mM benzyl alcohol (λ, 214 nm) or 2 mM mesityl oxide (λ, 254 nm) injected for 3 s at 50 mbar; temperature, 25°C.

DODAB yielded stable capillary coatings with strongly anodic EOF (Figure 6.2). However at pH 9.0, capillaries coated with 0.1 mM DODAB exhibited unpredictable and irreproducible EOF. Figure 6.2 illustrates the various types of behavior that were observed. For some trials at pH 9.0 (e.g., ● in Figure 6.2), the EOF was initially anodic and then gradually drifted to a steady state suppressed cathodic EOF. In other trials, the EOF was already cathodic from the first injection (● in Figure 6.2). Regardless, after a series of injections the EOF at pH 9.0 reached a steady state that was cathodic, but suppressed ($\leq 2 \times 10^{-4} \text{ cm}^2/\text{Vs}$) compared to the EOF of a bare capillary under the same buffer conditions ($+8.0 \times 10^{-4} \text{ cm}^2/\text{Vs}$). The same EOF trend was observed using 50 mM Tris-HCl pH 10.0 (Figure 6.2). DODAB coated capillaries equilibrated with Tris buffers pH 9-10 for 15 min or longer (i.e. in contact with buffer, neither voltage nor rinse was applied) always resulted in suppressed and cathodic EOF without any gradual transition.

Previous studies have shown that low ionic strength and weakly associating buffer anions are needed to form smaller DODAB vesicle size and more stable coatings [18]. Despite the low ionic strength of 50 mM Tris-HCl pH 9.0, ($I_s=5 \text{ mM}$) and weakly associating nature of the buffer anion Cl^- , the resultant EOF indicated instability of the cationic surfactant bilayer. This behavior suggests that high pH of the separation buffer destabilizes the DODAB coating possibly by desorption at the higher pH or by chemical degradation due to the alkaline conditions.

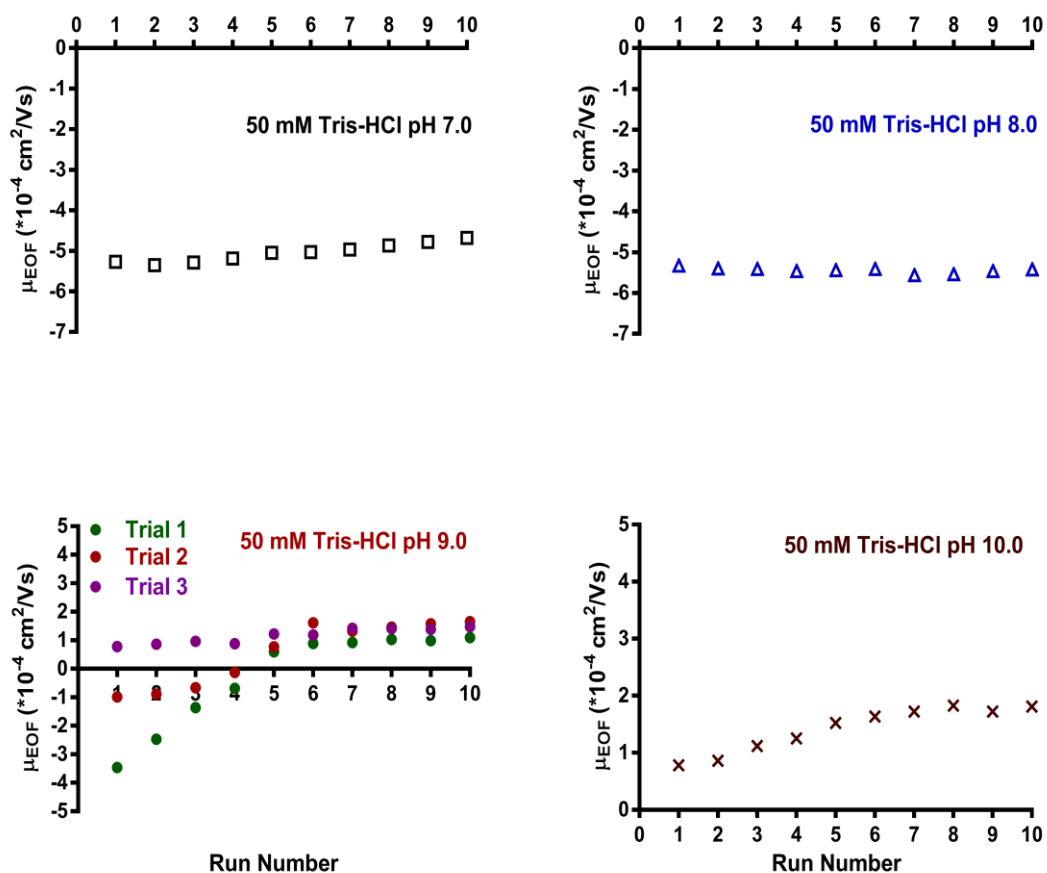


Figure 6.2: Stability of 0.1 mM DODAB coated capillaries at $\text{pH} \geq 7.0$.

50 mM Tris-HCl pH 7.0 (\square), 50 mM Tris-HCl pH 8.0 (Δ), 50 mM Tris-HCl pH 9.0 (\bullet \bullet \bullet) and 50 mM Tris-HCl pH 10.0 (\times).

Experimental conditions: 32 cm \times 50 μm i.d. capillary (23.5 cm to detector); 2 mM benzyl alcohol (λ , 214 nm) or 2 mM mesityl oxide (λ , 254 nm) injected for 3 s at 50 mbar; temperature, 25°C.

6.3.3 pH switching of DODAB coated capillaries

To test whether the DODAB was desorbed or chemically degraded by the high pH, a capillary was coated with DODAB at pH 3.0 and then EOF were determined under pH conditions that alternated between pH 3.0 (where the coating was stable) and 9.0 (where the capillary transitions to a cathodic suppressed EOF). Figure 6.3 shows the initial EOF at pH 3.0 was strong and anodic ($-5.7 \times 10^{-4} \text{ cm}^2/\text{Vs}$). After the capillary was flushed with pH 9.0 buffer, the EOF was $+1.5 \times 10^{-4} \text{ cm}^2/\text{Vs}$, consistent with Section 6.3.2. Switching the BGE back to pH 3.0, resulted in an EOF that was again anodic but lower in magnitude than originally observed at this pH (Figure 6.3). This indicates that DODAB layer was still adsorbed to the capillary inner surface but now with a lower positive zeta potential. Repeating the switch between pH 3.0 and 9.0 buffers a second time resulted in similar behavior. These results indicate that DODAB is still adsorbed on the capillary surface after exposure to alkaline buffers (as indicated by the renewed anodic EOF at low pH).

Figure 6.4 shows a similar experiment using pH switches between pH 3.0 and pH 11.5 phosphate buffers. The EOF trend observed for the first cycle of pH switching was the same as in Figure 6.3. However, with the second cycle, there was a further increase in the magnitude of cathodic EOF at pH 11.5 and a further decrease in the magnitude of anodic EOF at pH 3.0 compared to first cycle. Thus again the high pH does not fully desorb the DODAB from the capillary, but does cause substantial changes to the coating. These observations may be explained

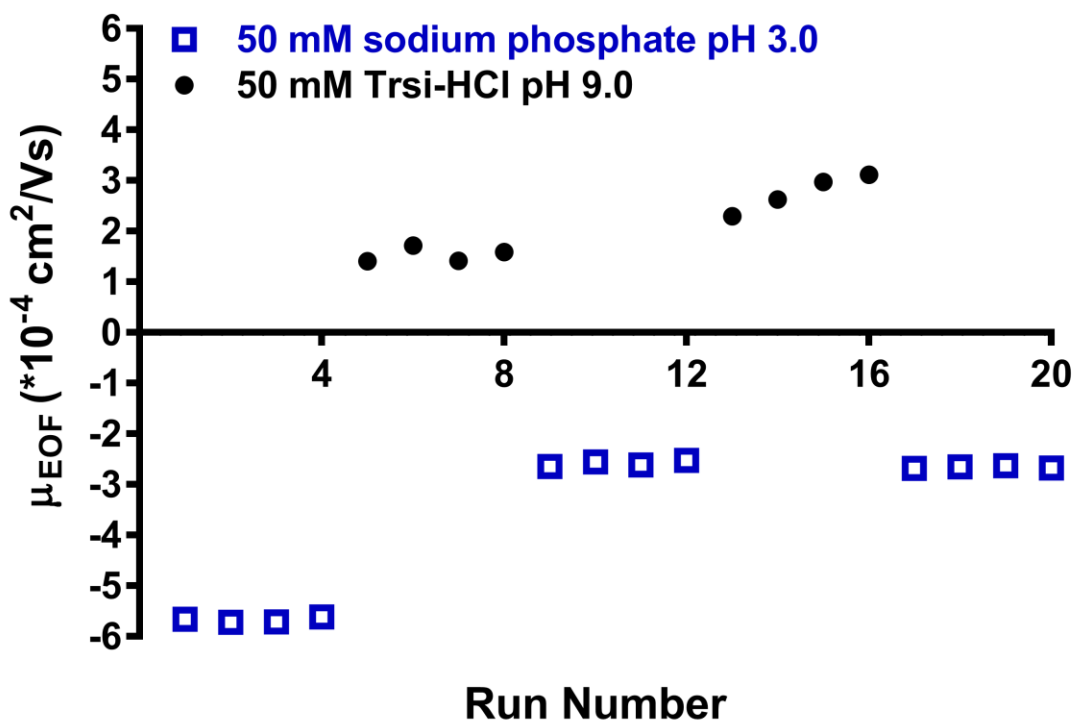


Figure 6.3: EOF of 0.1 mM DODAB coated capillary switched between pH 3.0 and pH 9.0.

50 mM sodium phosphate pH 3.0 (□) and 50 mM Tris HCl pH 9.0 (●). Before each switch, the capillary was rinsed with water for 1 min then with buffer for 1 min then equilibrated with buffer for 15 min.

Experimental conditions: ± 15 kV; 32 cm × 50 μm i.d. (23.5 cm to detector); 2 mM benzyl alcohol (λ, 214 nm) injected for 3 s at 50 mbar; temperature, 25°C.

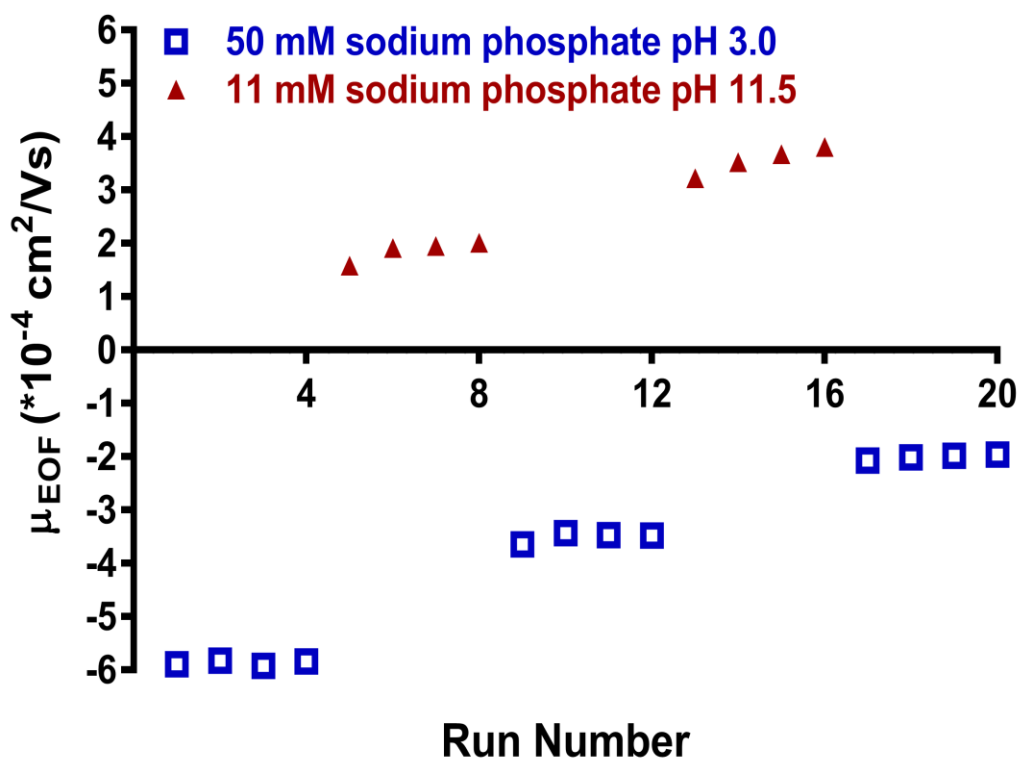


Figure 6.4: EOF of 0.1 mM DODAB coated capillary switched between pH 3.0 and pH 11.5.

50 mM sodium phosphate pH 3.0 (□) and 11 mM sodium phosphate pH 11.5 (▲). Before each switch, capillary was rinsed with water for 1 min then with buffer for 1 min then equilibrated with buffer for 15 min.

Experimental conditions: ± 15 kV; 32 cm \times 50 μm i.d. (23.5 cm to detector); 2 mM benzyl alcohol (λ , 214 nm) injected for 3 s at 50 mbar; temperature, 25°C.

by either: 1) chemical change in the coating when exposed to $\text{pH} \geq 9.0$; 2) Physical instability of DODAB bilayer; or 3) partial desorption of the DODAB coating. The following sections explore these hypotheses.

6.3.4 Alkaline reactions of DODAB

Tetraalkyl ammonium cations can react under alkaline conditions to form a tertiary amine and a side product. Different mechanisms of attack by hydroxide have been suggested for the degradation reaction [19, 20]. As shown in Equation 6.1, the quaternary amine may experience an SN^2 nucleophilic substitution leading to alcohol formation. Alternately, Hofmann elimination (Equation 6.2) might occur resulting in alkene formation.



Regardless of the mechanism, the degradation reaction results in the formation of a trialkyl tertiary amine. Such an amine would have a pK_a of ~ 9 . Thus, if a tertiary amine were formed, the tertiary amine would be protonated at $\text{pH} 3.0$ and an anodic EOF would be expected at low pH . At $\text{pH} \geq 9.0$, the tertiary amine would be partially to fully deprotonated and so the capillary inner surface would be slightly cationic to neutral which accounts for the suppressed cathodic EOF observed at $\text{pH} 9$ (Figure 6.3) and 11.5 (Figure 6.4).

Both the SN^2 and Hoffman elimination decomposition mechanisms involve the formation of a side product resulting in the formation of a trialkyl amine of lower mass than DODAB. Electrospray mass spectrometric analysis of DODAB and DODAB in NH_4OH was conducted (Section 6.2.5). The m/z of DODAB/ NH_4OH was the same as untreated DODAB (Figure 6.5). This result indicated that DODAB did not undergo chemical degradation under the mild alkaline conditions used in this chapter. Thus, the behavior of DODAB coated capillary exposed to pH 9.0 can not be explained by chemical instability.

The lack of chemical decomposition under our experimental conditions is consistent with the literature. Decomposition under alkaline conditions has previously only been observed under highly alkaline conditions at elevated temperature [19, 20]. Anion exchange columns containing quaternary amine anion exchange sites are routinely run in NaOH eluents in ion chromatography without capacity loss or loss in performance. Conversion of the quaternary amine exchange sites to tertiary amines has only been observed at column temperatures in excess of 60°C [21]. Similarly, studies of DODAB aggregation behavior has been studied in solutions of up to 0.5 M NaOH, with no discussion of decomposition.

Hence both direct chemical analysis and frequent usage of quaternary amines under comparable or more harsh alkaline conditions indicate that conversion of the quaternary amine in DODAB to a tertiary amine is unlikely. Thus, there must be an alternate cause for the EOF behavior observed at high pH.

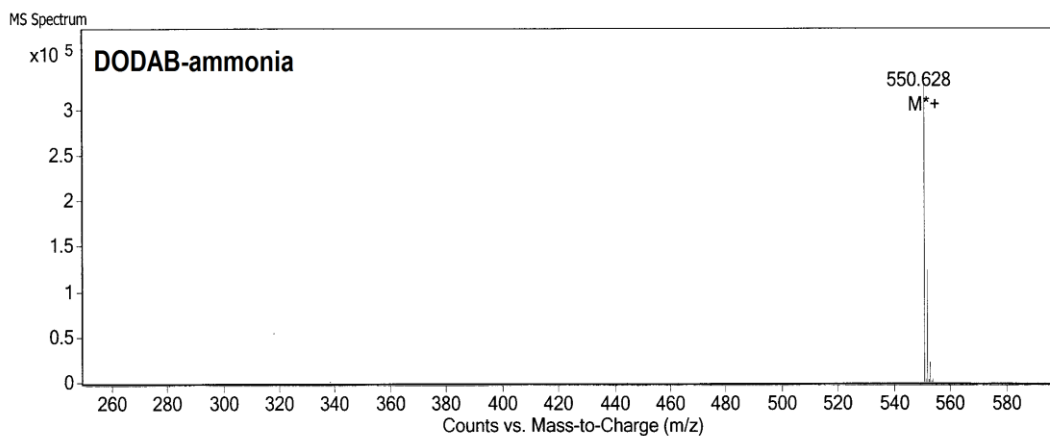
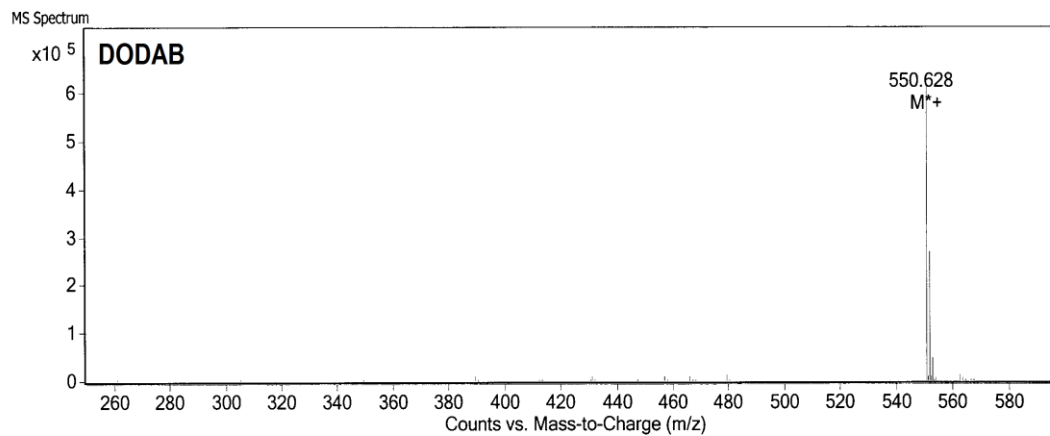


Figure 6.5: ESI Mass spectra of DODAB and DODAB treated with ammonia.

0.1 mM DODAB was prepared in water as per Section 6.2.3. An aliquot of DODAB was treated with 0.1 M NH₄OH to a pH ~ 10 (at 25°C for 24 h).

6.3.5 Aggregation behavior of DODAB under alkaline conditions

Two-tailed surfactants aggregate to form vesicles in solution. When the capillary is rinsed with the surfactant solution, vesicles adsorb to the capillary surface, and then fuse and/or rupture to form a supported bilayer on the capillary inner surface [22, 23]. Vesicle size affects the rate of formation of the coating and the coating performance [24]. Both sonicated aqueous dispersions of DODAB are metastable for several months after preparation [25]. The metastability of the dispersion is manifested by the slow increase in the vesicle size and polydispersity with time [25]. When DODAB is prepared in buffer solution, the vesicle size of DODAB and its effectiveness to form a stable capillary coating are sensitive to the buffer conditions. Increase in the buffer ionic strength results in increased DODAB vesicle size [26, 27] and ineffective capillary coating [18].

Dynamic light scattering (DLS) enables study of such molecular aggregation. With DLS, the vesicle aggregation (i.e., vesicle size) can be monitored as a function of time [18, 25]. The polydispersity index (PDI) is also useful in monitoring such solutions, as it provides information on the range of vesicle sizes present. PDI values range from 0 to 1. A PDI value close to zero indicates a monodisperse system. The higher the PDI, the broader the distribution of the vesicle size.

Using the sonicate /stir method detailed in Section 6.2.3, 0.1 mM DODAB prepared in nano pure water yielded vesicles with a mean diameter of 65 nm and a PDI of 0.27 (Table 6.2). After 24 h, the average vesicle diameter increased to 200 nm and the PDI increased slightly to 0.31. DODAB vesicles in NaOH increased from 79 nm at zero time (time when NaOH was added) to 1350 nm after 24 h. This represents a 17 fold increase in the vesicle size – much greater than was observed for DODAB in distilled water. In addition, the PDI increased from 0.35 to 0.79 after 24 h. After 24 h, the DODAB solution treated with NaOH turned cloudy while the untreated DODAB solution remained clear.

The vesicle size of DODAB increases with increasing the ionic strength [18, 26, 27]. To confirm that the increased vesicle size observed above is due to the effect of pH rather than the effect of ionic strength, DLS measurements were performed for DODAB in NaOH and NaCl solutions of same ionic strength. After 24 h, the vesicle size of DODAB in NaCl increased only to 360 nm. This is comparable to the behavior observed for DODAB vesicles in 50 mM sodium phosphate pH 3.0 ($I_s= 44$ mM) and 50 mM NaCl ($I_s= 50$ mM) where the vesicle sizes were < 250 nm and 400 nm, respectively after 24 hours [18]. These results demonstrate the effect of OH^- on the increased vesicle size of DODAB and the broad distribution of vesicle size is due to pH effects and not solely ionic strength. This is consistent with the literature, where an aggregation number of 63 was observed for DODA-Cl in 0.05 M NaCl and 6,000 for DODA-OH in 0.05 M NaOH [28].

Table 6.2: DODAB vesicle size behavior in water, NaOH and NaCl^a

	0 h		1 h		24 h	
	Mean vesicle size (nm)	PDI	Mean vesicle size (nm)	PDI	Mean vesicle size (nm)	PDI
DODAB	65	0.27	119	0.33	200	0.31
DODAB-NaOH ^b	79	0.35	470	0.65	1350	0.79
DODAB-NaCl ^b	----- ^c	---- ^c	140	0.27	360	0.38

^a Determined by dynamic light scattering (DLS), as per Section 6.2.6.

^b 0.1 mM DODAB was prepared in water as per Section 6.2.3, and then diluted 19:1 with 1.0 M NaOH or 1.0 M NaCl to yield solutions of 50 mM ionic strength.

^c Not measured.

Solution conditions which favour the formation of large vesicles of a capillary coating solution result in poor coatings [18, 24]. However, in this chapter, the DODAB solution was prepared in water according to the procedure in Section 6.2.3 which should form small unilamellar vesicles (confirmed by the vesicle size of 65 nm in Table 6.2). This SUV solution was then used as a coating solution to form the cationic bilayer on the capillary inner surface. The effectiveness of this DODAB bilayer coating procedure was also confirmed by the strong and stable anodic EOF observed at pH 2-8. However, at pH ≥ 9.0 the EOF was suppressed and cathodic (Section 6.3.2). Based on the DLS results above, a condition that promotes large vesicle formation was established inside the coated capillary when the background electrolyte was at pH ≥ 9.0 . Thus, changes in the morphology of the bilayer might be expected at higher pH. However, given the low binding constant of OH⁻ for DODA⁺ [29, 30], changes were not expected at pH as low as 9.0.

DODAB coated capillaries exhibited strong anodic EOF at pH 2.0-8.0 (Figures 6.1 and 6.2). Unexpectedly, the EOF of DODAB coated capillaries was suppressed and cathodic at $\text{pH} \geq 9.0$ (Figures 6.2, 6.3 and 6.4). The colloid literature can help explain the observed suppressed cathodic EOF at $\text{pH} \geq 9.0$. As discussed in Chapter Two, the stability of the bilayer coatings depends on the desorption of the surfactant from the bilayer to saturate the background electrolyte. The degree of this desorption correlates with the critical vesicle concentration (CVC) - the higher the CVC, the lower the stability [13]. The CVC of dioctadecyldimethylammonium hydroxide (DODAOH) is more than an order of magnitude higher than that of dioctadecyldimethylammonium bromide (DODAB) [28]. Accelerated desorption of the DODA^+ layer when exposed to $\text{pH} \geq 9.0$ driven by the increase in CVC may explain the EOF behaviour. The presence of a residual DODA^+ bilayer on the capillary surface would result in a lower surface negative potential and lower cathodic EOF compared to that of a bare capillary at pH 9.0. When the pH is switched to 3.0 (Section 6.3.3) where silanols are protonated, the residual DODA^+ would result in weakly anodic EOF. The presence of residual adsorbed surfactant is consistent with previous studies of surfactant desorption [14, 31]. This finding was supported by the presence of moderate residual EOF after extensive washing of DDAB coated capillary [14].

6.3.6 Protein separation

To test for the utility of DODAB coated capillaries after alkaline exposure, protein separations were performed in a manner similar to the pH switching experiments described in Section 6.3.3. A binary mixture of Ribonuclease A and

Lysozyme was first separated on freshly DODAB coated capillary at pH 3.0 (Figure 6.6a). The BGE was switched to pH 9.0 and then back to pH 3.0 for a second protein separation (Figure 6.6b). A second cycle of pH switching followed by protein separation was performed (Figure 6.6c).

The EOF of freshly coated DODAB capillary was strongly anodic ($-5.4 \times 10^{-4} \text{ cm}^2/\text{Vs}$) at pH 3.0. The two cationic proteins were separated successfully on the freshly DODAB coated capillary (Figure 6.6a). After the first cycle of pH switching (i.e. BGE was changed up to pH 9.0 and the back to pH 3.0), the EOF became moderately anodic ($-2.5 \times 10^{-4} \text{ cm}^2/\text{Vs}$), consistent with Section 6.3.3. The weak counter EOF necessitated the application of voltage associated with pressure to move the protein peaks towards the detector. After the first cycle of pH switching, the protein corrected peak areas were 30-50 % of the values obtained using freshly DODAB coated capillaries. The decrease in peak areas and baseline not returning to its original value after alkaline exposure (Figure 6.6b) indicate that irreversible protein adsorption to the capillary wall is now occurring [4]. After a second cycle of pH switching, protein adsorption was more severe as demonstrated by baseline not even partially recovered (Figure 6.6c). These results indicate degradation of the cationic bilayer after alkaline exposure.

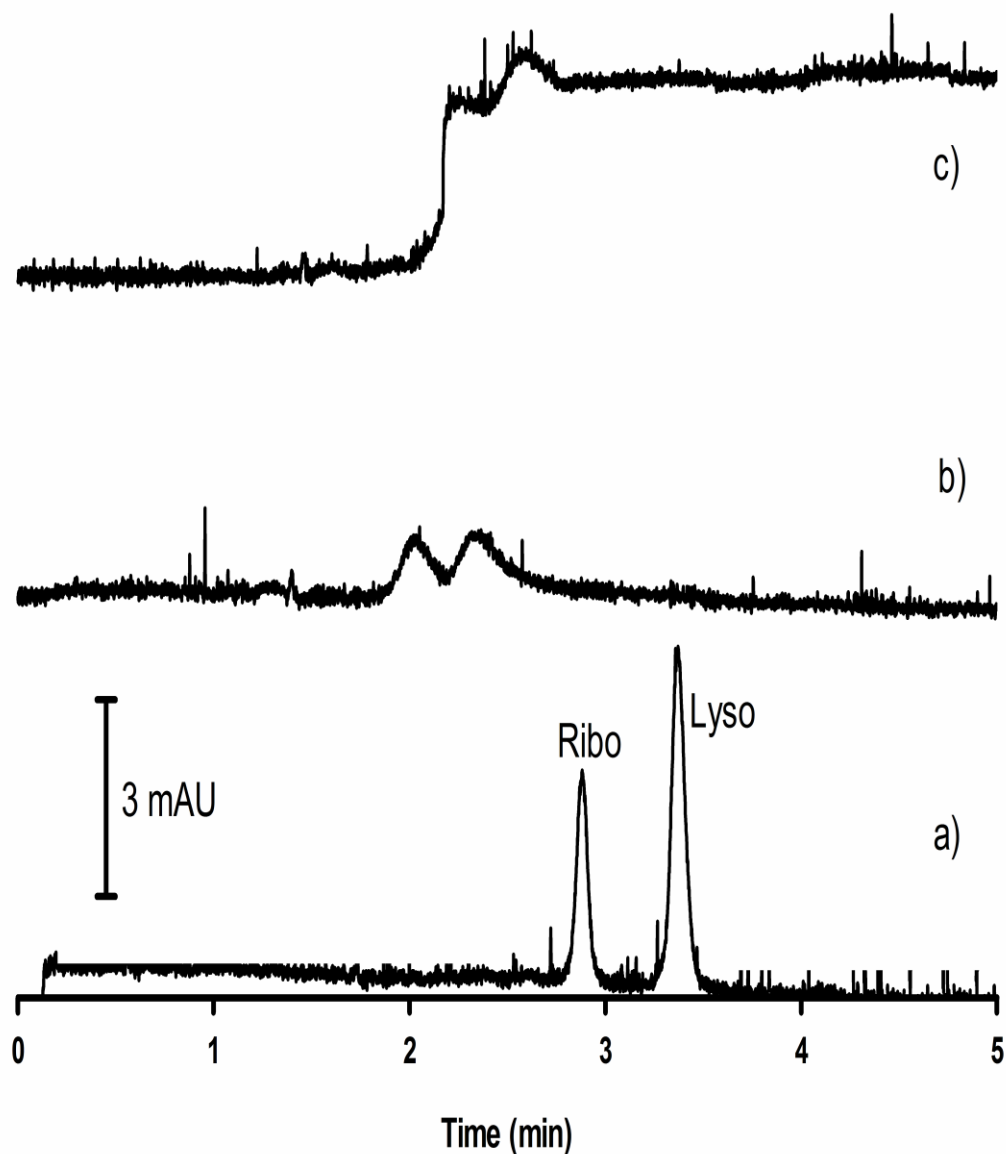


Figure 6.6: Separation of two basic proteins on 0.1 mM DODAB coated capillaries: a) before, b) after one cycle and c) after two cycles of switching between pH 3.0 and 9.0.

Each cycle means that the BGE was changed to pH 9.0 then back to pH 3.0. Before each switch, the capillary was rinsed with water for 1 min, then with buffer for 1 min, and equilibrated with buffer for 15 min.

Experimental conditions: -15 kV (a) or -15 kV and 50 mbar (b and c); 32 cm × 50 μm i.d. capillary (23.5 cm to detector); separation buffer, 50 mM sodium phosphate pH 3.0; λ, 214 nm; 0.1 mg/mL protein sample injected for 3 s at 50 mbar; temperature, 25°C.

6.4 Conclusions

Past studies such as Chapter Two have shown that two-tailed cationic surfactants such as DODAB form stable semipermanent capillary coatings. Being a quaternary ammonium compound, changing the buffer pH was expected to have no effect on the charge. However, experimentally DODAB coating showed good stability and strong anodic EOF only up to pH 8. Even in this range careful selection of the buffer anion was crucial for stable DODAB coatings. Weakly associated buffer anions such as dihydrogenphosphate, acetate and chloride form stable DODAB coatings. Strongly associating counter-ions such as monohydrogen phosphate and citrate create coating instability.

The stability of DODAB coating dropped significantly at $\text{pH} \geq 9.0$. The EOF of DODAB coated capillary drifted gradually or abruptly from anodic to cathodic and suppressed at $\text{pH} \geq 9.0$. The reason for the EOF behavior observed at high pH is uncertain. Chemical degradation at alkaline pH was excluded. The increase in vesicle size of DODAB at high pH could be a potential reason for the instability observed possibly through altered bilayer structure. Alkaline induced increase in CVC would result in accelerated desorption of the bilayer. Degradation of the cationic bilayer after exposure to $\text{pH} \geq 9.0$ was demonstrated by irreversible adsorption of the proteins to the capillary surface.

6.5 References

- [1] Chun, M. S. and Chung, D. S., *Anal. Chim. Acta* 2003, 491, 173-179.
- [2] Doherty, E. A. S., Meagher, R. J., Albarghouthi, M. N. and Barron, A. E., *Electrophoresis* 2003, 24, 34-54.
- [3] Hjertén, S., *J. Chromatogr.* 1985, 347, 191-198.
- [4] Lucy, C. A., MacDonald, A. M. and Gulcev, M. D., *J. Chromatogr. A* 2008, 1184, 81-105.
- [5] Sarazin, C., Delaunay, N., Costanza, C., Eudes, V., Mallet, J.-M. and Gareil, P., *Anal. Chem.* 2011, 83, 7381-7387.
- [6] Ramautar, R., Torano, J. S., Somsen, G. W. and de Jong, G. J., *Electrophoresis* 2010, 31, 2319-2327.
- [7] MacDonald, A. M., Bahnasy, M. F. and Lucy, C. A., *J. Chromatogr. A* 2011, 1218, 178-184.
- [8] de Jong, S., Epelbaum, N., Liyanage, R. and Krylov, S. N., *Electrophoresis* 2012, 33, 2584-2590.
- [9] Bahnasy, M. F. and Lucy, C. A., *J. Chromatogr. A* 2012, 1267, 89-95.
- [10] Kawai, T., Ito, J., Sueyoshi, K., Kitagawa, F. and Otsuka, K., *J. Chromatogr. A* 2012, 1267, 65-73.
- [11] Melanson, J. E., Baryla, N. E. and Lucy, C. A., *Anal. Chem.* 2000, 72, 4110-4114.
- [12] Baryla, N. E., Melanson, J. E., McDermott, M. T. and Lucy, C. A., *Anal. Chem.* 2001, 73, 4558-4565.
- [13] Yassine, M. M. and Lucy, C. A., *Anal. Chem.* 2005, 77, 620-625.
- [14] Yassine, M. M. and Lucy, C. A., *Anal. Chem.* 2004, 76, 2983-2990.
- [15] Williams, B. A. and Vigh, C., *Anal. Chem.* 1996, 68, 1174-1180.
- [16] Mohabbati, S. and Westerlund, D., *J. Chromatogr. A* 2006, 1121, 32-39.
- [17] Gulcev, M. D., McGinitie, T. M., Bahnasy, M. F. and Lucy, C. A., *Analyst* 2010, 135, 2688-2693.
- [18] Gulcev, M. D. and Lucy, C. A., *Anal. Chim. Acta* 2011, 690, 116-121.

- [19] Chempath, S., Boncella, J. M., Pratt, L. R., Henson, N. and Pivovar, B. S., *J. Phys. Chem. C* 2010, *114*, 11977-11983.
- [20] Long, H., Kim, K. and Pivovar, B. S., *J. Phys. Chem. C* 2012, *116*, 9419-9426.
- [21] Chong, J., Hatsis, P. and Lucy, C. A., *J. Chromatogr. A* 2003, *997*, 161-169.
- [22] Zhdanov, V. P. and Kasemo, B., *Langmuir* 2001, *17*, 3518-3521.
- [23] Reimhult, E., Hook, F. and Kasemo, B., *Langmuir* 2003, *19*, 1681-1691.
- [24] Gulcev, M. D. and Lucy, C. A., *Anal. Chem.* 2008, *80*, 1806-1812.
- [25] Feitosa, E. and Brown, W., *Langmuir* 1997, *13*, 4810-4816.
- [26] Nascimento, D. B., Rapuano, R., Lessa, M. M. and Carmona-Ribeiro, A. M., *Langmuir* 1998, *14*, 7387-7391.
- [27] Carmonaribeiro, A. M. and Chaimovich, H., *Biophys. J.* 1986, *50*, 621-628.
- [28] Clancy, S. F., Steiger, P. H., Tanner, D. A., Thies, M. and Paradies, H. H., *J. Phys. Chem.* 1994, *98*, 11143-11162.
- [29] Yusof, N. S. M. and Khan, M. N., *Adv. Colloid Interface Sci.* 2013, *193*, 12-23.
- [30] Bravo, C., Herves, P., Leis, J. R. and Pena, M. E., *J. Colloid Interface Sci.* 1992, *153*, 529-536.
- [31] Tiberg, F., Jonsson, B. and Lindman, B., *Langmuir* 1994, *10*, 3714-3722.

Chapter Seven: Summary and Future work

7.1 Summary

The thesis focuses on the development of capillary coatings to prevent protein adsorption in CE. Two-tailed cationic surfactants such as DODAB were primarily used as they are cost effective, regenerable and readily forms semi-permanent bilayer coatings in CE capillaries. Factors that affect DODAB coating stability such as capillary i.d. and pH have been studied. A new DODAB/POE stearate coating has been developed which offers the advantages of combined stability of cationic surfactant coatings and the suppressed EOF of neutral polymer coatings. The coating has been applied to CZE and cIEF separations. Different factors that affect the stability and performance of the developed coating have been studied.

7.1.1 Chapter Two

Cationic surfactants such as DDAB and DODAB readily form semi-permanent bilayer coatings in CE capillaries. Chapter Two studies the impact of using small i.d. capillary ($\leq 25 \mu\text{m}$) on the stability of surfactant bilayer coatings and efficiency of separations of model cationic proteins. Five, 10 and 25 μm i.d. DDAB coated capillaries were used for the study. Both 5 and 10 μm i.d. capillaries provided exceptionally high separation efficiencies for the basic model proteins. The coating stability improved with decreasing the capillary i.d. as demonstrated by improved migration time reproducibility over 40 runs with smaller i.d. capillaries. The bilayer stability is further enhanced by increasing the

length of the surfactant alkyl chain. The DODAB coated 5 μm capillary offered both high short and long term stability. Two hundreds and ten consecutive protein separations (1050 minute total run time) were performed without regeneration of the coating. The separation efficiency was 1.4 to 2.0 millions plates/m with migration time repeatability of 1.7-1.9 %RSD. In the long term stability study, the capillary maintained high performance for 300 injections performed over a 30 day period without any regeneration of the coating. The migration time reproducibility over this period was 6.8 %RSD. The 5 μm DODAB coated capillary was applied to the separation of cationic transmitters with separation efficiency $>470\ 000$ plates/m.

7.1.2 Chapter Three

The DODAB bilayer coatings in Chapter Two provided high stability and high separation efficiency of proteins. However, the DODAB coating results in a strong anodic EOF, which can overwhelm the differences in electrophoretic mobilities of the analytes, and thereby yield reduced resolution. The need for a stable coating with a suppressed EOF was the motivation to develop a new versatile coating in Chapter Three. The new coating was formed by flushing the capillary with the two-tailed cationic surfactant DODAB, followed by flushing the capillary with a solution of the neutral diblock copolymer POE stearate. The DODAB/POE stearate sequential coating offers the advantages of the stability of cationic surfactant coatings and the suppressed EOF of neutral polymer coatings. The coating was demonstrated to effectively prevent protein adsorption and enable tuning of the EOF. A sequential rather than mixed method for coating

preparation produces a more predictable EOF and can separate basic proteins with higher average efficiency. Coatings formed using the sequential method were more stable over a larger number of runs (%RSD for migration times: 0.7–1.0% over 30 runs) than those formed using the mixed method (%RSD: 2.4–4.6% over 14 runs). The EOF in the presence of this coating was tunable by varying the polymer chain length, and by mixing polymer chains of different lengths. A tunable EOF (-2.40 to -0.17×10^{-4} cm^2/Vs) was achieved by varying the POE chain length (8, 40 and 100 oxyethylene units). Mixtures of POE 8 and POE 40 stearate enabled continuous variation of the EOF from -2.44 to -0.42×10^{-4} cm^2/Vs . The ability to tune the EOF is important in maximizing the resolution of analytes with similar electrophoretic mobilities. Separations of basic proteins yielded efficiencies of 760 000 – 940 000 plates/m. Histone proteins can be separated with high efficiency into nine subtypes on coatings formed using the sequential method. Acidic proteins were separated on a sequentially coated capillary at pH 6.4.

7.1.3 Chapter Four

The sequential DODAB/POE stearate coating developed in Chapter Three is easy to prepare, low cost, semi-permanent, and provides controllable EOF by varying the POE chain length. In this chapter, the developed coating was applied to a different mode of CE; capillary isoelectric focusing (cIEF). Single-step cIEF is facilitated by the presence of a moderately suppressed EOF to move the analytes to the detector during the focusing step. Single-step cIEF can be performed using the DODAB/POE 40 stearate version of the sequential coating.

Two-step cIEF requires a strongly suppressed EOF to allow long-term focusing of analytes on the capillary, followed by a mobilization step. Two-step cIEF can be performed using either DODAB/POE 40 stearate or DODAB/POE 100 stearate. The sequential coatings can be tailored based on the degree of resolution required and the analysis time. A set of peptide markers was used to assess the coating performance. High resolution separations can be achieved by using, narrow pH range ampholytes, higher ampholyte concentration, longer POE chain and longer capillaries but at the expense of longer analyses time. Commercially coated capillaries for cIEF are expensive (\$ 150-250 per capillary) and available only in 50 μm i.d. formats. The need for multiple capillaries due to protein precipitation and capillary clogging lead to expensive analyses during method development. The low cost (< \$10 per capillary) and the ease of choice of capillary dimensions make the developed coating a superior alternative to commercially coated capillaries particularly during method development. A recta-linear pH gradient was established only in two-step cIEF methodology using pH 3-10 2.5% v/v carrier ampholyte. Hemoglobin A₀ and S variants were successfully resolved on DODAB/POE 40 stearate sequentially coated capillaries.

7.1.4 Chapter Five

The developed sequential DODAB/POE stearate was applied to CZE separations of acidic, basic and histone proteins (Chapter Three) and cIEF separation (Chapter Four). In this chapter, the use of other POE diblock copolymers was studied. The commercial availability of a wide selection of POE diblock copolymers eliminates the need for tedious synthetic procedures.

Attempts to coat capillaries with the POE diblock copolymers alone resulted in less stable capillary coatings compared to the DODAB/POE diblock copolymer coatings. Increasing the length of hydrophobic block from lauryl (n=12) to stearyl (n=18) resulted in a more stable EOF. Diblock copolymers with ester or ether functional group suppressed the EOF to the same extent and showed similar EOF stability. A suppressed EOF was obtained regardless of the length of the polyoxyethylene chain, but the direction and magnitude of the EOF was dependent on the POE chain length and the pH in a complex fashion. Also, the polyoxyethylene showed ion retention characteristics. Chaotropic anions such as ClO_4^- are retained onto the capillary coating. Thus, the selection of the buffer ions is important as this may influence the magnitude and even the direction of EOF of the coated capillary. The sequential DODAB/POE diblock copolymer suppressed the EOF and showed good stability over a wide range of pH 3-11.5. Interestingly, the suppressed EOF was anodic at low pH and cathodic at high pH. The sequential coating shows good stability in buffers containing up to 20% v/v acetonitrile.

7.1.5 Chapter Six

The quaternary ammonium surfactant DODAB forms a stable semipermanent capillary coating. Changing the buffer pH should have no effect on the charge of DODAB. However, DODAB coatings exhibited a strong anodic and stable EOF only up to pH 8. Care had to be taken to use weakly associated buffer anions. At $\text{pH} \geq 9.0$, the EOF was cathodic and suppressed. The reason for the EOF behavior at high pH is uncertain. Chemical degradation at alkaline pH

was excluded. The increase in vesicle size of DODAB at high pH could be a potential reason for observed EOF trend. The increased vesicle size may result in an altered bilayer structure or accelerated desorption of the bilayer or both.

Interestingly, despite this variation in the EOF of the underlying DODAB bilayer, the DODAB/POE coatings studied in Chapters Four and Five maintained a suppressed EOF and prevented protein adsorption up to pH 11.5.

7.2 Future work

7.2.1 Gemini cationic surfactants as capillary coatings

Gemini surfactants consist of two hydrophobic alkyl chains and two polar headgroups covalently attached by a spacer group. They share the same general structure *m-s-m* (Figure 7.1) where *m* stands for the surfactant monomer and *s* stands for the spacer group. Gemini surfactants differ in the chemical composition of the spacer group and hydrocarbon tail length. Gemini surfactants show many superior features to their single-tailed analogs, such as enhanced water solubility and remarkably lower CMC [1]. The CMC of a gemini surfactant is one to two orders of magnitude lower than those for the corresponding monomeric surfactants [2]. The spacer group is of great importance in determining the solution properties of gemini surfactants [2].

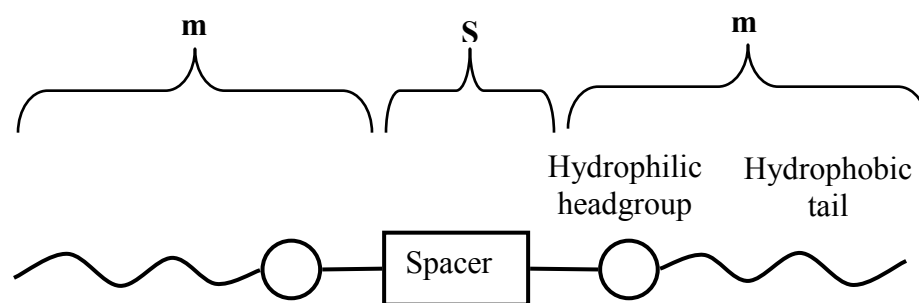


Figure 7.1: General structure of gemini surfactants.

Based on the work of Lucy and co-workers [3-5] who used two-tailed cationic surfactants as semipermanent capillary coatings, gemini di-quaternary ammonium surfactants were introduced as capillary coating for CE separation of proteins and control of the EOF [6-8]. Gemini surfactants have also been used in an aqueous organic system for CE separations of inorganic anions [9]. Self-assembly of cationic gemini surfactants on the capillary surface was the basis of capillary coating in all cases. The coating stability increased with the alkyl chain length C_m [6], consistent with the results of Chapter Two. The double long chains of gemini surfactants ($C_m \geq 14$) yielded good coating stability with the best stability achieved when $C_m = 18$. The use of long-chained gemini surfactants further reduced the CMC and enhanced the stability of the self-assembled coating. The length of the spacer group affected both the coating stability and the magnitude of EOF [6]. The enhanced water solubility of gemini surfactants

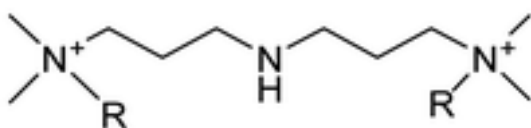
allowed for ease of preparation of surfactant solution by sonication at lower temperatures and shorter times [6].

Gemini di-quaternary ammonium surfactants could be a potential alternative for DODAB as a capillary coating at high pH. The instability of DODAB at high pH was attributed to alkaline induced increase in the CVC. The CVC of gemini surfactant is one to two orders of magnitude lower than those for the corresponding monomeric surfactants [2]. As the coating stability improves with using lower CVC [5], a gemini surfactant is expected to yield a more stable coating than DODAB. The two quaternary ammonium centers in a gemini surfactant molecule might make better attachment and stability at high pH compared to the single quaternary center in DODAB.

Recently, the synthesis of pH sensitive gemini surfactant derivatives have been reported [10, 11]. The incorporation of a pH active amino group in the spacer enabled the synthesis of pH sensitive gemini surfactants. The pKa values for the amine-substituted m-7NH-m surfactants were determined to be 4.99–5.06 [10]. It is envisioned that this new class of gemini surfactants could be very promising semipermanent capillary coating, particularly at acidic pH. At low pH, the amino functional group in the spacer will be protonated. A single gemini surfactant molecule will possess three cationic centers (two quaternary nitrogens and a protonated amino group in the spacer). This allows for multiple point attachment of the gemini surfactant to the capillary. Thus, enhanced coating stability is expected. Although the amino group in the spacer will be unprotonated

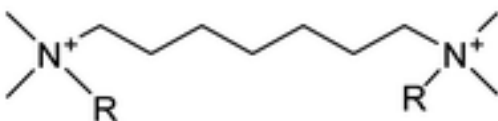
at basic pH, the gemini surfactant will still possess two cationic centers; enough to impart good coating stability. In addition, varying the pH results in varying the positive charge on the capillary inner surface by protonation or deprotonation of the amino group in the spacer. This allows for tuning of the EOF magnitude.

The enhanced water solubility of gemini surfactants allows for ease of preparation of surfactant vesicles solution. The Krafft temperature (minimum temperature at which surfactants form micelles) of a gemini surfactant is further reduced when a hydrophilic spacer is used. Thus, the presence of the amino substituted spacer group further enhances the water solubility of the gemini surfactant and facilitates solution preparation. Figure 7.2 shows the structures for a series of gemini surfactants with amino substituted spacer group m-7NH-m) and a corresponding series with non-substituted spacers. Synthesis and characterization of the surfactants are detailed in reference [10]. Within the same series, the use of longer alkyl chain length (higher C_m) results in lower CMC value and thus is expected to produce a more stable capillary coating.



a) m-7NH-m series

$C_m (R) = C_{12}, C_{16}, C_{18}$



b) m-7-m series

$C_m (R) = C_{12}, C_{16}, C_{18}$

Figure 7.2 Examples for di-quaternary cationic gemini surfactants a) with amino substituted spacer group and b) with non-substituted spacer group. Adopted from Table 1 in Reference [10].

7.2.2 Capillary coatings for in-capillary derivatization

Derivatization is a modification of the analytes of interest to introduce more desirable characteristics to the analyte. The most common reason for sample derivatization is to improve detectability. Other reasons include enhancement of stability and improved separation selectivity. Capillary electrophoresis is a powerful separation technique due to its speed, high efficiency separations and minimal sample volumes. Using conventional UV detection, some analytes encounter detection problems either due to absence of an intrinsic chromophore or low detection sensitivity due to the limited optical pathlength offered by narrow capillaries.

Derivatization reactions can be performed before (pre-capillary), during (in-capillary) or after (post-capillary) the electrophoretic separation. The pros and cons of each approach is detailed in reference [12]. In-capillary derivatization allows for automation of the whole procedure and does not require changing the setup of the commercially available CE devices. The small volume of the reaction chamber makes in-capillary derivatization useful when only small sample volumes are available.

With in-capillary derivatization, the capillary is not only used as a separation chamber, but also as a micro-reactor. The reactants (derivatizing reagents and unreacted analytes) and products (derivatized analytes) are separated based on differences in their electrophoretic mobilities. The sample and reagent plugs are introduced at the capillary inlet. When an electric field is applied, the

analyte migrates and mixes with the reagent, allowing the derivatization reaction to occur [13]. The order of sample and reagent introduction must be determined based on the magnitude and sign of the mobility.

My goal here is to utilize the capillary coatings developed in our group to develop a method for in-capillary derivatization. The use of capillary coatings allows for control of the EOF to optimize both the reaction and separation conditions. A model reaction (Figure 7.3) will be the derivatization of amino acids with 9-fluorenylmethyl chloroformate (FMOC-Cl). FMOC reacts rapidly with primary and secondary amine functions under mild condition. The derivatization reaction enables both UV and laser-induced fluorescence detection of the amino acids.

FMOC has a limited solubility in water but is easily soluble in 1:1 water:acetonitrile. Thus, the capillary coating must be stable under mixed aqueous-organic conditions to be compatible with FMOC derivatization. The DODAB/POE diblock copolymer coatings was shown to be stable in solution containing $\leq 20\%$ v/v ACN (Chapter Five). This makes DODAB/POE diblock copolymer coating unsuitable for in-capillary derivatization using FMOC. Injection of an ACN plug destabilized the coating which in turns lead to irreproducible EOF. In contrast, the polymerized lipid 1,2-bis(10,12-tricosadiynoyl)-sn-glycero-3-phosphocholine (Diyne PC, Figure 7.4) developed by a colleague in my group was strongly resistant to organic solvent rinses [14]. The EOF of the polymerized Diyne PC coated capillary remained unchanged after

600 capillary volumes of pure ACN rinse [14]. Thus, polymerized Diyne PC is anticipated to be a better option as a capillary coating for in-capillary derivatization.

Figure 7.5 shows a schematic of the proposed derivatization reaction for an amino acid mixture with FMOC. The capillary is filled with BGE and then a plug of FMOC, followed by a plug of amino acid mixture are introduced at the capillary inlet. Under alkaline conditions pH 8-10, the amino acids are negatively charged while the derivatizing reagent is neutral. When a negative polarity is applied (i.e. the anode is at the detection window side), the negatively charged amino acids migrate towards the anode driven by their electrophoretic mobilities. The amino acids mix with the FMOC and derivatization occurs. The derivatized FMOC-amino acids are then separated according to differences in their electrophoretic mobilities. The use of capillary coating to suppress the EOF would enable the electrophoretic mobility to overcome the EOF. The counter EOF (i.e. EOF is in opposite direction to electrophoretic mobility) maximizes the resolution of derivatized amino acid mixture. The EOF will carry the derivatizing reagent FMOC away from the detection window towards the cathode.

It is envisioned that the use of capillary coatings can play an important role in optimization of in-capillary derivatization. The availability of variety of capillary coatings with different criteria *e.g.* pH stability and non aqueous stability is crucial to meet the requirements of different derivatization reactions.

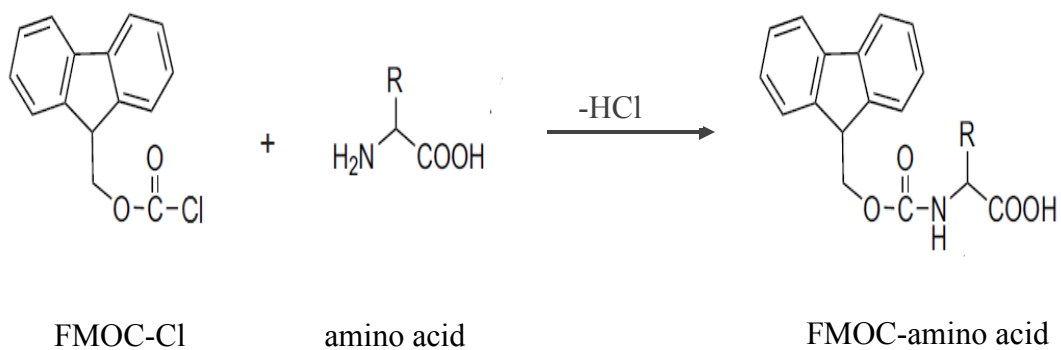


Figure 7.3: Derivatization of an amino acid with Fmoc-Cl.

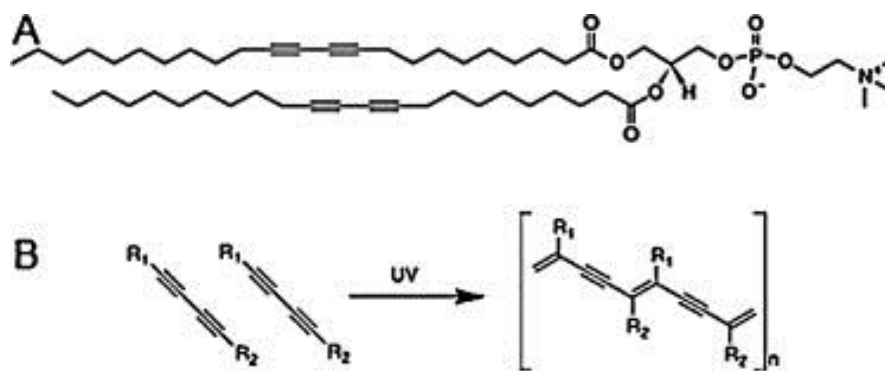


Figure 7.4: The structure (A) and the polymerization reaction (B) of 1,2-bis(10,12-tricosadiynoyl)-sn-glycero-3-phosphocholine (Diyne PC). Reprinted with permission from reference [14]. Copyright (2012) Elsevier.

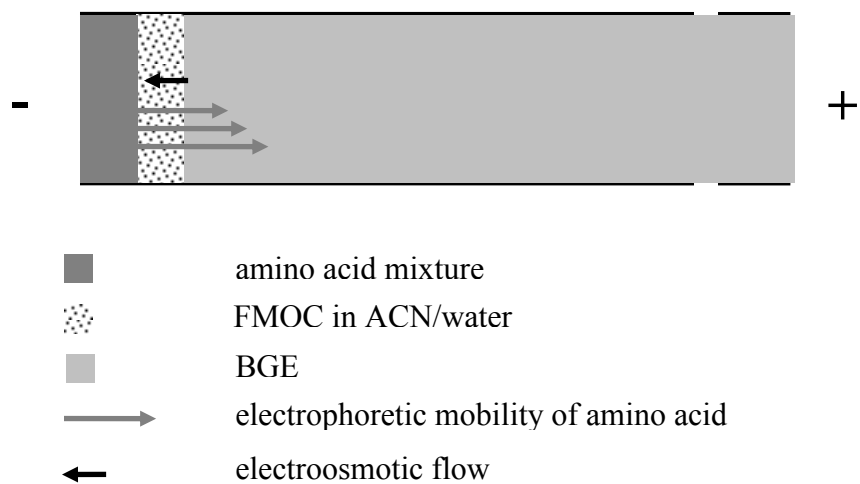


Figure 7.5: Schematic for the proposed in-capillary derivatization of amino acid mixture with FMOC.

7.3 References

- [1] Menger, F. M. and Keiper, J. S., *Angew. Chem., Int. Ed.* 2000, 39, 1907-1920.
- [2] Zana, R., *J. Colloid Interface Sci.* 2002, 248, 203-220.
- [3] Melanson, J. E., Baryla, N. E. and Lucy, C. A., *Anal. Chem.* 2000, 72, 4110-4114.
- [4] Baryla, N. E., Melanson, J. E., McDermott, M. T. and Lucy, C. A., *Anal. Chem.* 2001, 73, 4558-4565.
- [5] Yassine, M. M. and Lucy, C. A., *Anal. Chem.* 2005, 77, 620-625.
- [6] Liu, Q., Yuan, J. B., Li, Y. Q. and Yao, S. Z., *Electrophoresis* 2008, 29, 871-879.
- [7] Liu, Q., Li, Y., Yang, Y. and Yao, S., *Sci. China, Ser. B: Chem.* 2009, 52, 1666-1676.
- [8] Liu, Q., Li, Y., Tang, F., Ding, L. and Yao, S., *Electrophoresis* 2007, 28, 2275-2282.
- [9] Liu, Q., Li, Y., Yao, L. and Yao, S., *J. Sep. Sci.* 2009, 32, 4148-4154.
- [10] Donkuru, M., Wettig, S. D., Verrall, R. E., Badea, I. and Foldvari, M., *J. Mater. Chem.* 2012, 22, 6232-6244.
- [11] Wettig, S. D., Wang, C., Verrall, R. E. and Foldvari, M., *Phys. Chem. Chem. Phys.* 2007, 9, 871-877.
- [12] Bardelmeijer, H. A., Lingeman, H., de Ruiter, C. and Underberg, W. J. M., *J. Chromatogr. A* 1998, 807, 3-26.
- [13] Zhang, J., Hoogmartens, J. and Van Schepdael, A., *Electrophoresis* 2008, 29, 56-65.
- [14] Pei, L. and Lucy, C. A., *J. Chromatogr. A* 2012, 1267, 80-88.

Bibliography

- Aguilar, C., Hofte, A. J. P., Tjaden, U. R. and van der Greef, J., *J. Chromatogr. A* 2001, *926*, 57-67.
- Albarghouthi, M. N., Stein, T. M. and Barron, A. E., *Electrophoresis* 2003, *24*, 1166-1175.
- Altria, K., Marsh, A. and Sanger-van de Griend, C., *Electrophoresis* 2006, *27*, 2263-2282.
- Arai, K., Mori, M., Kozaki, D., Nakatani, N., Itabashi, H. and Tanaka, K., *J. Chromatogr. A* 2012, *1270*, 147-152.
- Bahnasy, M. F. and Lucy, C. A., *J. Chromatogr. A* 2012, *1267*, 89-95.
- Bahnasy, M. F., *Ph.D. Thesis* 2014, Chemistry, University of Alberta, Edmonton.
- Bard, A. J. and Faulkner, L. R., *Electrochemical Methods : Fundamentals and Applications*, John Wiley & Sons, Inc., New York 2001.
- Bardelmeijer, H. A., Lingeman, H., de Ruiter, C. and Underberg, W. J. M., *J. Chromatogr. A* 1998, *807*, 3-26.
- Barron, A. E. and Blanch, H. W., *Sep. Purif. Methods* 1995, *24*, 1-118.
- Baryla, N. E. and Lucy, C. A., *Anal. Chem.* 2000, *72*, 2280-2284.
- Baryla, N. E., Melanson, J. E., McDermott, M. T. and Lucy, C. A., *Anal. Chem.* 2001, *73*, 4558-4565.
- Belder, D., Husmann, H. and Warnke, J., *Electrophoresis* 2001, *22*, 666-672.
- Bergquist, J., Tarkowski, A., Ekman, R. and Ewing, A., *Proc. Natl. Acad. Sci. U. S. A.* 1994, *91*, 12912-12916.
- Bernal, J., Rodriguez-Meizoso, I., Elvira, C., Ibanez, E. and Cifuentes, A., *J. Chromatogr. A* 2008, *1204*, 104-109.
- Blom, A., Drummond, C., Wanless, E. J., Richetti, P. and Warr, G. G., *Langmuir* 2005, *21*, 2779-2788.
- Bossi, A., Gelfi, C., Orsi, A. and Righetti, P. G., *J. Chromatogr. A* 1994, *686*, 121-128.
- Bravo, C., Herves, P., Leis, J. R. and Pena, M. E., *J. Colloid Interface Sci.* 1992, *153*, 529-536.

- Buchberger, W. and Haddad, P. R., *J. Chromatogr. A* 1994, 687, 343-349.
- Bushey, M. M. and Jorgenson, J. W., *J. Chromatogr.* 1989, 480, 301-310.
- Carmonaribeiro, A. M. and Chaimovich, H., *Biophys. J.* 1986, 50, 621-628.
- Chempath, S., Boncella, J. M., Pratt, L. R., Henson, N. and Pivovar, B. S., *J. Phys. Chem. C* 2010, 114, 11977-11983.
- Chervet, J. P., Vansoest, R. E. J. and Ursem, M., *J. Chromatogr.* 1991, 543, 439-449.
- Chiu, R. W., Jimenez, J. C. and Monnig, C. A., *Anal. Chim. Acta* 1995, 307, 193-201.
- Chong, J., Hatsis, P. and Lucy, C. A., *J. Chromatogr. A* 2003, 997, 161-169.
- Chun, M. S. and Chung, D. S., *Anal. Chim. Acta* 2003, 491, 173-179.
- Cifuentes, A., Diez-Masa, J. C., Fritz, J., Anselmetti, D. and Bruno, A. E., *Anal. Chem.* 1998, 70, 3458-3462.
- Clancy, S. F., Steiger, P. H., Tanner, D. A., Thies, M. and Paradies, H. H., *J. Phys. Chem.* 1994, 98, 11143-11162.
- Cooper, J. W., Wang, Y. J. and Lee, C. S., *Electrophoresis* 2004, 25, 3913-3926.
- Cordova, E., Gao, J. M. and Whitesides, G. M., *Anal. Chem.* 1997, 69, 1370-1379.
- Corradini, D., Bevilacqua, L. and Nicoletti, I., *Chromatographia* 2005, 62, S43-S50.
- Cretich, M., Chiari, M., Pirri, G. and Crippa, A., *Electrophoresis* 2005, 26, 1913-1919.
- Cruces-Blanco, C., Gamiz-Gracia, L. and Garcia-Campana, A. M., *TrAC, Trends Anal. Chem.* 2007, 26, 215-226.
- Cunliffe, J. M., Baryla, N. E. and Lucy, C. A., *Anal. Chem.* 2002, 74, 776-783.
- de Jong, S., Epelbaum, N., Liyanage, R. and Krylov, S. N., *Electrophoresis* 2012, 33, 2584-2590.
- Desiderio, C., Rossetti, D. V., Iavarone, F., Messana, I. and Castagnola, M., *J. Pharm. Biomed. Anal.* 2010, 53, 1161-1169.
- Deyl, Z., Miksik, I., Charvátová, J. and Eckhardt, A., *J. Chromatogr. A* 2003, 1013, 233-238.

- Dickerson, J. A., Ramsay, L. M., Dada, O. O., Cermak, N. and Dovichi, N. J., *Electrophoresis* 2010, *31*, 2650-2654.
- Diress, A. G., Yassine, M. M. and Lucy, C. A., *Electrophoresis* 2007, *28*, 1189-1196.
- Doherty, E. A. S., Berglund, K. D., Buchholz, B. A., Kourkine, I. V., Przybycien, T. M., Tilton, R. D. and Barron, A. E., *Electrophoresis* 2002, *23*, 2766-2776.
- Doherty, E. A. S., Meagher, R. J., Albarghouthi, M. N. and Barron, A. E., *Electrophoresis* 2003, *24*, 34-54.
- Donkuru, M., Wettig, S. D., Verrall, R. E., Badea, I. and Foldvari, M., *J. Mater. Chem.* 2012, *22*, 6232-6244.
- Dovichi, N. J. and Zhang, J. Z., *Angew. Chem., Int. Ed.* 2000, *39*, 4463.
- Drummond, C., In, M. and Richetti, P., *Eur. Phys. J. E* 2004, *15*, 159-165.
- Elbashir, A. A. and Aboul-Enein, H. Y., *Biomed. Chromatogr.* 2010, *24*, 1038-1044.
- Emmer, A. and Roeraade, J., *J. Liq. Chromatogr.* 1994, *17*, 3831-3846.
- Ermakov, S. V., Zhukov, M. Y., Capelli, L. and Righetti, P. G., *J. Chromatogr. A* 1995, *699*, 297-313.
- Erny, G. L., Elvira, C., San Roman, J. and Cifuentes, A., *Electrophoresis* 2006, *27*, 1041-1049.
- Fang, N., Zhang, H., Li, J. W., Li, H. W. and Yeung, E. S., *Anal. Chem.* 2007, *79*, 6047-6054.
- Feitosa, E. and Brown, W., *Langmuir* 1997, *13*, 4810-4816.
- Feitosa, E., Jansson, J. and Lindman, B., *Chem. Phys. Lipids* 2006, *142*, 128-132.
- Foley, J. P. and Dorsey, J. G., *Anal. Chem.* 1983, *55*, 730-737.
- Fu, S. L. and Lucy, C. A., *Anal. Chem.* 1998, *70*, 173-181.
- Garza, S., Chang, S. and Moini, M., *J. Chromatogr. A* 2007, *1159*, 14-21.
- Gas, B., Stedry, M. and Kenndler, E., *J. Chromatogr. A* 1995, *709*, 63-68.
- Gas, B., Stedry, M. and Kenndler, E., *Electrophoresis* 1997, *18*, 2123-2133.
- Gilges, M., Kleemiss, M. H. and Schomburg, G., *Anal. Chem.* 1994, *66*, 2038-2046.

- Gilman, S. D., Jeremy, J. P. and Andrew, G. E., *J. Microcol. Sep.* 1994, 6, 373-384.
- Giordano, B. C., Muza, M., Trout, A. and Landers, J. P., *J. Chromatogr. B* 2000, 742, 79-89.
- Gostkowski, M. L., McDoniel, J. B., Wei, J., Curey, T. E. and Shear, J. B., *J. Am. Chem. Soc.* 1998, 120, 18-22.
- Gostkowski, M. L., Wei, J. and Shear, J. B., *Anal. Biochem.* 1998, 260, 244-250.
- Graf, M., Garcia, R. G. and Watzig, H., *Electrophoresis* 2005, 26, 2409-2417.
- Graul, T. W. and Schlenoff, J. B., *Anal. Chem.* 1999, 71, 4007-4013.
- Green, J. S. and Jorgenson, J. W., *J. Chromatogr.* 1989, 478, 63-70.
- Greif, D., Galla, L., Ros, A. and Anselmetti, D., *J. Chromatogr. A* 2008, 1206, 83-88.
- Grossman, P. D. and Colburn, J. C., *Capillary Electrophoresis, Theory and Practice*, Academic Press, Inc., San Diego, CA 1992.
- Grushka, E. and McCormick, R. M., *J. Chromatogr. A* 1989, 471, 421-428.
- Gulcev, M. D. and Lucy, C. A., *Anal. Chem.* 2008, 80, 1806-1812.
- Gulcev, M. D., McGinitie, T. M., Bahnasy, M. F. and Lucy, C. A., *Analyst* 2010, 135, 2688-2693.
- Gulcev, M. D. and Lucy, C. A., *Anal. Chim. Acta* 2011, 690, 116-121.
- Guo, Y., Imahori, G. A. and Colon, L. A., *J. Chromatogr. A* 1996, 744, 17-29.
- Gurley, L. R., London, J. E. and Valdez, J. G., *J. Chromatogr.* 1991, 559, 431-443.
- Hardy, W. B., *J. Physiol.* 1905, 33, 251-337.
- Harris, D. C. (Ed.), *Quantitative Chemical Analysis* New York 2007.
- Heiger, D. (Ed.), *An Introduction High Performance Capillary Electrophoresis*, Agilent Technologies, Germany 2000.
- Heiger, D. N., Kaltenbach, P. and Sievert, H. J. P., *Electrophoresis* 1994, 15, 1234-1247.
- Hellmich, W., Regtmeier, J., Duong, T. T., Ros, R., Anselmetti, D. and Ros, A., *Langmuir* 2005, 21, 7551-7557.

- Hinshaw, J. V., *Lc Gc North America* 2001, 19, 1136.
- Hjertén, S., *Chromatogr. Rev.* 1967, 9, 122-219.
- Hjertén, S., *J. Chromatogr.* 1985, 347, 191-198.
- Hogan, B. L. and Yeung, E. S., *Anal. Chem.* 1992, 64, 2841-2845.
- Hsieh, Y. Y., Lin, Y. H., Yang, J. S., Wei, G. T., Tien, P. and Chau, L. K., *J. Chromatogr. A* 2002, 952, 255-266.
- Huang, M. X., Vorkink, W. P. and Lee, M. L., *J. Microcol. Sep.* 1992, 4, 135-143.
- Huang, X. H., Coleman, W. F. and Zare, R. N., *J. Chromatogr.* 1989, 480, 95-110.
- Huhn, C., Ramautar, R., Wuhrer, M. and Somsen, G. W., *Anal. Bioanal. Chem.* 2010, 396, 297-314.
- Hult, E. L., Emmer and Roeraade, J., *J. Chromatogr. A* 1997, 757, 255-262.
- Iki, N. and Yeung, E. S., *J. Chromatogr. A* 1996, 731, 273-282.
- Israelachvili, J. N., *Intermolecular and Surface Forces*, Academic Press, London 1992.
- Jacobson, S. C., Moore, A. W. and Ramsey, J. M., *Anal. Chem.* 2002, 67, 2059-2063.
- Jiang, W., Awasum, J. N. and Irgum, K., *Anal. Chem.* 2003, 75, 2768-2774.
- Jorgenson, J. W. and Lukacs, K. D., *Anal. Chem.* 1981, 53, 1298-1302.
- Kami, K., Fujimori, T., Sato, H., Sato, M., Yamamoto, H., Ohashi, Y., Sugiyama, N., Ishihama, Y., Onozuka, H., Ochiai, A., Esumi, H., Soga, T. and Tomita, M., *Metabolomics* 2013, 9, 444-453.
- Karger, B. L., Chu, Y. H. and Foret, F., *Annu. Rev. Biophys. Biomed.* 1995, 24, 579-610.
- Katayama, H., Ishihama, Y. and Asakawa, N., *Anal. Chem.* 1998, 70, 2254-2260.
- Kawai, T., Ito, J., Sueyoshi, K., Kitagawa, F. and Otsuka, K., *J. Chromatogr. A* 2012, 1267, 65-73.
- Knox, J. H. and Grant, I. H., *Chromatographia* 1987, 24, 135-143.
- Landers, J. P. (Ed.), *Handbook of Capillary and Microchip Electrophoresis and Associated Microtechniques*, CRC Press, Boca Raton 2008.

- Lauer, H. H. and McManigill, D., *Anal. Chem.* 1986, 58, 166-170.
- Lim, L. W., Rong, L. and Takeuchi, T., *Anal. Sci.* 2012, 28, 205-213.
- Lin, J., Tan, Q. and Wang, S., *J. Sep. Sci.* 2011, 34, 1696-1702.
- Linda, R., Lim, L. W. and Takeuchi, T., *J. Chromatogr. A* 2013, 1294, 117-121.
- Lindberg, P., Stjernström, M. and Roeraade, J., *Electrophoresis* 1997, 18, 1973-1979.
- Linden, M. V., Wiedmer, S. K., Hakala, R. M. S. and Riekkola, M. L., *J. Chromatogr. A* 2004, 1051, 61-68.
- Lindner, H., Helliger, W., Dirschlmaier, A., Talasz, H., Wurm, M., Sarg, B., Jaquemar, M. and Puschendorf, B., *J. Chromatogr.* 1992, 608, 211-216.
- Liu, H., Shi, R., Wan, W., Yang, R. and Wang, Y., *Electrophoresis* 2008, 29, 2812-2819.
- Liu, J., Dolnik, V., Hsieh, Y. Z. and Novotny, M., *Anal. Chem.* 1992, 64, 1328-1336.
- Liu, Q., Li, Y., Tang, F., Ding, L. and Yao, S., *Electrophoresis* 2007, 28, 2275-2282.
- Liu, Q., Yang, Y. M. and Yao, S. Z., *J. Chromatogr. A* 2008, 1187, 260-266.
- Liu, Q., Yuan, J. B., Li, Y. Q. and Yao, S. Z., *Electrophoresis* 2008, 29, 871-879.
- Liu, Q., Li, Y., Yang, Y. and Yao, S., *Sci. China, Ser. B: Chem.* 2009, 52, 1666-1676.
- Liu, Q., Li, Y., Yao, L. and Yao, S., *J. Sep. Sci.* 2009, 32, 4148-4154.
- Liu, S., Gao, L., Pu, Q., Lu, J. J. and Wang, X., *J. Proteome Res.* 2006, 5, 323-329.
- Liu, S., Pu, Q., Gao, L. and Lu, J., *Talanta* 2006, 70, 644-650.
- Liu, Y., Foote, R. S., Culbertson, C. T., Jacobson, S. C., Ramsey, R. S. and Ramsey, J. M., *J. Microcol. Sep.* 2000, 12, 407-411.
- Long, H., Kim, K. and Pivovar, B. S., *J. Phys. Chem. C* 2012, 116, 9419-9426.
- Lucy, C. A., Yeung, K. K. C., Peng, X. J. and Chen, D. D. Y., *LC-GC* 1998, 16, 26-32.

- Lucy, C. A., MacDonald, A. M. and Gulcev, M. D., *J. Chromatogr. A* 2008, *1184*, 81-105.
- MacDonald, A. M. and Lucy, C. A., *J. Chromatogr. A* 2006, *1130*, 265-271.
- Macdonald, A. M., *Ph.D. Thesis* 2008, Chemistry, University of Alberta, Edmonton.
- MacDonald, A. M., Bahnasy, M. F. and Lucy, C. A., *J. Chromatogr. A* 2011, *1218*, 178-184.
- Malá, Z., Gebauer, P. and Boček, P., *Electrophoresis* 2013, *34*, 19-28.
- McClain, M. A., Culbertson, C. T., Jacobson, S. C., Allbritton, N. L., Sims, C. E. and Ramsey, J. M., *Anal. Chem.* 2003, *75*, 5646-5655.
- McCormick, R. M., *Anal. Chem.* 1988, *60*, 2322-2328.
- Melanson, J. E., Baryla, N. E. and Lucy, C. A., *Anal. Chem.* 2000, *72*, 4110-4114.
- Mellors, J. S., Gorbounov, V., Ramsey, R. S. and Ramsey, J. M., *Anal. Chem.* 2008, *80*, 6881-6887.
- Menger, F. M. and Keiper, J. S., *Angew. Chem., Int. Ed.* 2000, *39*, 1907-1920.
- Mikkers, F. E. P., Everaerts, F. M. and Verheggen, T., *J. Chromatogr.* 1979, *169*, 11-20.
- Milner, S. T., *Science* 1991, *251*, 905-914.
- Minarik, M., Gas, B., Rizzi, A. and Kenndler, E., *J. Cap. Elec.* 1995, *2*, 89-96.
- Mohabbati, S. and Westerlund, D., *J. Chromatogr. A* 2006, *1121*, 32-39.
- Mohabbati, S., Hjerten, S. and Westerlund, D., *Anal. Bioanal. Chem.* 2008, *390*, 667-678.
- Nascimento, D. B., Rapuano, R., Lessa, M. M. and Carmona-Ribeiro, A. M., *Langmuir* 1998, *14*, 7387-7391.
- Norde, W. and Haynes, C. A., *Proteins at Interfaces II: Fundamentals and Applications*, American Chemical Society, Washington, DC 1995.
- Okada, T., *J. Chromatogr. A* 1999, *834*, 73-87.
- Olefirowicz, T. M. and Ewing, A. G., *Anal. Chem.* 1990, *62*, 1872-1876.

- Österberg, E., Bergström, K., Holmberg, K., Riggs, J. A., Van Alstine, J. M., Schuman, T. P., Burns, N. L. and Harris, J. M., *Colloids Surf., A* 1993, 77, 159-169.
- Ostuni, E., Chapman, R. G., Holmlin, R. E., Takayama, S. and Whitesides, G. M., *Langmuir* 2001, 17, 5605-5620.
- Otsuka, K. and Terabe, S., *J. Chromatogr.* 1989, 480, 91-94.
- Pei, L. and Lucy, C. A., *J. Chromatogr. A* 2012, 1267, 80-88.
- Peterson, C. L. and Laniel, M. A., *Curr. Biol.* 2004, 14, R546-R551.
- Phillips, K. S., Kottegoda, S., Kang, K. M., Sims, C. E. and Allbritton, N. L., *Anal. Chem.* 2008, 80, 9756-9762.
- Pinero, M. Y., Bauza, R. and Arce, L., *Electrophoresis* 2011, 32, 1379-1393.
- Preisler, J. and Yeung, E. S., *Anal. Chem.* 1996, 68, 2885-2889.
- Puerta, A., Axén, J., Söderberg, L. and Bergquist, J., *J. Chromatogr. B* 2006, 838, 113-121.
- Quigley, W. W. C. and Dovichi, N. J., *Anal. Chem.* 2004, 76, 4645-4658.
- Ramautar, R., Torano, J. S., Somsen, G. W. and de Jong, G. J., *Electrophoresis* 2010, 31, 2319-2327.
- Raymond, S. and Weintraub, L., *Science* 1959, 130, 711.
- Reimhult, E., Hook, F. and Kasemo, B., *Langmuir* 2003, 19, 1681-1691.
- Robelin, C., Duval, F. P., Richetti, P. and Warr, G. G., *Langmuir* 2002, 18, 1634-1640.
- Rundlett, K. L. and Armstrong, D. W., *Anal. Chem.* 1996, 68, 3493-3497.
- Runmiao, Y., Ronghua, S., Shuhua, P., Dan, Z., Hang, L. and Yanmei, W., *Electrophoresis* 2008, 29, 1460-1466.
- Sakai-Kato, K., Kato, M., Nakajima, T., Toyo'oka, T., Imai, K. and Utsunomiya-Tate, N., *J. Chromatogr. A* 2006, 1111, 127-132.
- Sanders, J. C., Breadmore, M. C., Kwok, Y. C., Horsman, K. M. and Landers, J. P., *Anal. Chem.* 2003, 75, 986-994.
- Sarazin, C., Delaunay, N., Costanza, C., Eudes, V., Mallet, J.-M. and Gareil, P., *Anal. Chem.* 2011, 83, 7381-7387.

Schulze, M. and Belder, D., *Electrophoresis* 2012, 33, 370-378.

Schure, M. R. and Lenhoff, A. M., *Anal. Chem.* 1993, 65, 3024-3037.

Schwarz, M. A. and Hauser, P. A., *Anal. Chem.* 2003, 75, 4691.

Schwer, C. and Kenndler, E., *Anal. Chem.* 1991, 63, 1801-1807.

Simal-Gandara, J., *Crit. Rev. Anal. Chem.* 2004, 34, 85-94.

Simo, C., Elvira, C., González, N., San Román, J., Barbas, C. and Cifuentes, A., *Electrophoresis* 2004, 25, 2056-2064.

Sloss, S. and Ewing, A. G., *Anal. Chem.* 1993, 65, 577-581.

Smith, J. T. and El Rassi, Z., *HRC-J. High Res. Chromatogr.* 1992, 15, 573-578.

Smoluchowski, M. V., *Bull. Int. Acad. Sci. Cracovie* 1903, 184.

Spanila, M., Pazourek, J. and Havel, J., *J. Sep. Sci.* 2006, 29, 2234-2240.

Sternberg, J. C., *Adv. Chromatogr.* 1966, 2, 206-270.

Svitova, T. F., Smirnova, Y. P., Pisarev, S. A. and Berezina, N. A., *Colloids Surf., A* 1995, 98, 107-115.

Swinney, K. and Bornhop, D. J., *Electrophoresis* 2000, 21, 1239-1250.

Terabe, S., Otsuka, K., Ichikawa, K., Tsuchiya, A. and Ando, T., *Anal. Chem.* 1984, 56, 111-113.

Tiberg, F., Jonsson, B. and Lindman, B., *Langmuir* 1994, 10, 3714-3722.

Tien, P., Chau, L. K., Shieh, Y. Y., Lin, W. C. and Wei, G. T., *Chem. Mater.* 2001, 13, 1124-1130.

Tiselius, A., *Trans. Faraday Soc.* 1937, 33, 524-530.

Towns, J. K. and Regnier, F. E., *J. Chromatogr.* 1990, 516, 69-78.

Towns, J. K. and Regnier, F. E., *Anal. Chem.* 1991, 63, 1126-1132.

Towns, J. K. and Regnier, F. E., *Anal. Chem.* 1992, 64, 2473-2478.

Ullsten, S., Zuberovic, A., Wetterhall, M., Hardenborg, E., Markides, K., E. and Bergquist, J., *Electrophoresis* 2004, 25, 2090-2099.

Virtanen, R., *Acta Polytech. Scand.* 1974, 123, 1-67.

- von Holt, C., *BioEssays* 1985, 3, 120-124.
- Walbroehl, Y. and Jorgenson, J. W., *J. Chromatogr.* 1984, 315, 135-143.
- Wang, C. Z. and Lucy, C. A., *Electrophoresis* 2004, 25, 825-832.
- Waters, L. C., Jacobson, S. C., Kroutchinina, N., Khandurina, J., Foote, R. S. and Ramsey, J. M., *Anal. Chem.* 1998, 70, 158-162.
- Wei, W. and Ju, H., *Electrophoresis* 2005, 26, 586-592.
- Wettig, S. D., Wang, C., Verrall, R. E. and Foldvari, M., *Phys. Chem. Chem. Phys.* 2007, 9, 871-877.
- White, C. M., Luo, R., Archer-Hartmann, S. A. and Holland, L. A., *Electrophoresis* 2007, 28, 3049-3055.
- Williams, B. A. and Vigh, C., *Anal. Chem.* 1996, 68, 1174-1180.
- Woods, L. A., Roddy, T. P., Paxon, T. L. and Ewing, A. G., *Anal. Chem.* 2001, 73, 3687-3690.
- Woods, L. A. and Ewing, A. G., *Chem Phys Chem* 2003, 4, 207-211.
- Xu, X., Kok, W. T. and Poppe, H., *J. Chromatogr. A* 1996, 742, 211-227.
- Xue, Y. J. and Yeung, E. S., *Anal. Chem.* 1994, 66, 3575-3580.
- Yang, R., Shi, R., Peng, S., Zhou, D., Liu, H. and Wang, Y., *Electrophoresis* 2008, 29, 1460-1466.
- Yao, Y. and Lenhoff, A. M., *Anal. Chem.* 2004, 76, 6743-6752.
- Yassine, M. M. and Lucy, C. A., *Anal. Chem.* 2004, 76, 2983-2990.
- Yassine, M. M. and Lucy, C. A., *Anal. Chem.* 2005, 77, 620-625.
- Yassine, M. M. and Lucy, C. A., *Electrophoresis* 2006, 27, 3066-3074.
- Yeung, K. K. C. and Lucy, C. A., *Anal. Chem.* 1997, 69, 3435-3441.
- Yeung, K. K. C. and Lucy, C. A., *J. Chromatogr. A* 1998, 804, 319-325.
- Yusof, N. S. M. and Khan, M. N., *Adv. Colloid Interface Sci.* 2013, 193, 12-23.
- Zana, R., *J. Colloid Interface Sci.* 2002, 248, 203-220.
- Zhang, J., Hoogmartens, J. and Van Schepdael, A., *Electrophoresis* 2008, 29, 56-65.

- Zhang, Z. X., Du, X. Z. and Li, X. M., *Anal. Chem.* 2011, 83, 1291-1299.
- Zhao, Z. X., Malik, A. and Lee, M. L., *Anal. Chem.* 1993, 65, 2747-2752.
- Zhdanov, V. P. and Kasemo, B., *Langmuir* 2001, 17, 3518-3521.
- Zhou, D., Tan, L., Xiang, L., Zeng, R., Cao, F., Zhu, X. and Wang, Y., *J. Sep. Sci.* 2011, 34, 1738-1745.
- Zhou, M. X. and Foley, J. P., *Anal. Chem.* 2006, 78, 1849-1858.
- Zhu, Z., Lu, J. J. and Liu, S., *Anal. Chim. Acta* 2012, 709, 21-31.